**School of Science**
**Department of Environment and Agriculture**

# The integration and validation of precision management tools in mixed farming systems

**Peter John McEntee**

**This thesis is presented for the Degree of**

**Doctor of Philosophy**
**of**
**Curtin University**

**October 2016**

**DECLARATION**

To the best of my knowledge and belief, this thesis contains no material previously published by any other person except where due acknowledgment has been made.

This thesis contains no material which has been accepted for the award of any other degree or diploma in any university.

Peter John McENTEE

PhD Candidate

Date: 4 October 2016

**ACKNOWLEDGMENTS**

Firstly, I would like to acknowledge my four supervisors, principal supervisor Dr Sarita Bennett and co-supervisors Professor Bob Belford, Dr John Harper and Dr Mark Trotter. Special thanks to Bob (even in retirement) and Sarita for their patience and perseverance when paid employment distracted me from this thesis. It has been an interesting journey, with many thesis progress meetings being held on Skype while I sat on the side of the Great Northern Highway near Fitzroy Crossing WA, using my mobile as a hotspot, as road trains rumbled past.

A special thank you to the two farming families that hosted my research and welcomed me into their lives: Murray and Kris Hall and family at "Milroy", Brookton, WA and Adam Inchbold at "Grandview", Yarrawonga, Vic. No question was too stupid nor request too large. Murray and Kris welcomed me into their house on many occasions over the years of field work. Thanks also for the use of workshops and equipment as needed. Both Adam's and Murray's enthusiasm for farming knows no bounds. I sincerely hope that this research will be of value to them.

I would also like to acknowledge the early support of Dr Roger Mandel as I started on this journey. The never-ending mad humour and support of Dr John Harper has been invaluable to get through the tough times.

There are so many others to thank:

Roger Lawes and Mike Robertson from CSIRO Floreat for the initial idea for this research.

Gonz Mata from CSIRO Floreat for background on Pastures from Space over coffees in the Floreat staff room.

Richard Stovold and Norm Santich from Landgate Floreat for MODIS data and advice on remote sensing.

Graham Donald for sharing his extraordinary wealth of remote sensing experience.

Dez Schneider at PARG, UNE for advice on setting up and using a CropCircle, JMP and ArcGIS and answering lots of stupid questions.

Deanna Duffy from SPAN at CSU Thurgoona for patient advice over the years on finding my way around ArcGIS.

Simon McDonald from SPAN at CSU Thurgoona for his insightful statistical and ArcGIS advice.

Roger Weise and Colin Booth at Fairport Farm Software for their generous provision of PAM, gpMapper and PastureWatch software and support.

Frank D'Emden from Precision Agronomics Australia.

Wes Lefroy from Precision Soil Tech.

James Easton at CSBP for support with soil testing.

Dr Christine Davies of Tweak Editing for her invaluable assistance in formatting and proofreading the final version of the thesis.

Special thanks to life-long best buddy Andy Pearce for providing a home away from home (and many bottles of red) on my ventures to Perth. Without Andy's generous support this thesis would never have come to fruition.

I would also like to acknowledge Curtin University for their ongoing support, and to the Grains Research and Development Corporation for providing a Grains Research Scholarship. This work would not have happened without their support.

And finally to my darling wife Robyn and my daughter Eva. Thank you for the sacrifices you have made, for persevering with and believing in your missing husband/dad, whether down in the 'dungeon' or across in the west, you never lost faith in what I was doing. It has finally come to an end and now we can have some weekends together. To my mum Jean, who is so proud that I have completed this, thanks for being there for me.

## TERMS AND ABBREVIATIONS

| | |
|---|---|
| AGB | Above Ground Biomass |
| AG | Asymmetric Gaussian |
| ANCOVA | Analysis of Covariance |
| APAR | Absorbed Photosynthetically Active Radiation |
| APSIM | Agricultural Production Systems Simulator |
| AR | Annual Rainfall |
| AVHRR | Advanced Very High Resolution Radiometer |
| BOM | Bureau of Meteorology |
| CSIRO | Commonwealth Scientific and Industrial Research Organisation |
| CV | Coefficient of Variation |
| DEM | Digital Elevation Model |
| DL | Double Logistic |
| DM | Dry Matter |
| DWR | Dry Weight Ranking |
| EC | Electrical Conductivity |
| ECa | Apparent Electrical Conductivity |
| ECe | Electrical Conductivity of Saturated Soil Extract |
| EM | ElectroMagnetic |
| EMI | ElectroMagnetic Induction |
| EVI | Enhanced Vegetation Index |
| *f*APAR | Fraction of Absorbed Photosynthetically Active Radiation |
| FOO | Feed on Offer |
| GC | Ground Cover |
| GI | Growth Index |
| GIS | Geographic Information System |
| GPS | Global Positioning System |
| GPP | Gross Primary Production |
| GR | Gamma Radiometric |
| GSR | Growing Season Rainfall |
| HS | High and Stable |
| HUS | High and Unstable |
| Landsat ETM+ | Landsat Enhanced Thematic Mapper Plus |
| LAI | Leaf Area Index |

| | |
|---|---|
| LOOCV | Leave One Out Cross Validation |
| LS | Low and Stable |
| LUE | Light Use Efficiency |
| LUS | Low and Unstable |
| MODIS | Moderate Resolution Imaging Spectroradiometer |
| MNLI | Modified Non-Linear Index |
| MVC | Maximum Value Composite |
| NDVI | Normalised Difference Vegetation Index |
| NIR | Near-InfraRed |
| NLI | Non-Linear Index |
| NPP | Net Primary Productivity |
| OC | Organic Carbon |
| PAR | Photosynthetically Active Radiation |
| PfS | Pastures from Space |
| PGR | Pasture Growth Rate |
| RF | Rainfall |
| RMSE | Root Mean Square Error |
| RPM | Rising Plate Meter |
| RTK | Real-Time Kinematic |
| SAVI | Soil-Adjusted Vegetation Index |
| SLC | Scan Line Corrector |
| SG | Savitzky-Golay |
| SR | Simple Ratio |
| SSM | Site Specific Management |
| TGDM | Total Green Dry Matter |
| USGS | United States Geological Survey |
| VI | Vegetation Index |
| VIC | Victoria |
| WA | Western Australia |

**ABSTRACT**

While precision agriculture (PA) technologies are widely used in cropping systems, the use of these technologies as a whole-of-farm management strategy in mixed farming systems has received far less attention. Relatively little is known about the nature, extent, or temporal stability of spatial variability of pasture production in mixed farming systems and whether it is feasible to manage this variability in a site-specific way. Given that, in a mixed farming system, somewhere between 20 and 40% of the farm area is in pasture at any time, there is significant potential for PA technologies to enhance mixed farm management practices.

The research described in this thesis was conducted in selected paddocks on two farms in southern Australia—"Milroy" located near Brookton in the south-west of Western Australia and "Grandview" near Yarrawonga in north-eastern Victoria. The owners of both farms were long-term users of PA technologies for their cropping enterprises. The intention in the research methodology was to use existing PA technologies which were available to farmers at an affordable cost. The work fell into three phases. The first phase was essentially a 'desk-top' exercise, to see if there were relationships, on both farms, between sub-paddock spatial variation in biomass production in the crop and pasture phases. This was done using the Moderate Resolution Imaging Spectroradiometer (MODIS) normalised difference vegetation index (NDVI) as an indirect measure of crop and pasture productivity. The results indicated that relationships appeared to exist between individual MODIS pixels in both cropping and pasture phases of paddock rotations over time. However, the relatively large size of MODIS pixels (6.25 ha) ultimately became a limiting factor in the analysis in terms of interpretive value, as the removal of contaminated pixels meant using fewer data samples which affected the statistical analysis. The second phase involved extensive field work to obtain, process and map geo-referenced, high-resolution data about the nature of spatial variability in crop and pasture growth and the variations in soil chemical and physical properties at "Milroy" and "Grandview". A CropCircle™ active optical sensor was used to measure pasture NDVI, which was correlated to pasture total green dry matter (TGDM) with in-field pasture calibration sampling. Electromagnetic induction (EMI)

sensing of soils using the EM38 instrument was undertaken, as well as gamma radiometric sensing at “Milroy”. Overall, there was a general trend for apparent electrical conductivity (ECa) to increase linearly with increasing clay content across all paddocks. There were also generally strong correlations between ECa and salinity. The most robust relationships with agronomic significance at “Milroy” were between ECa and soil texture (clay content), phosphorus buffering index (PBI), exchangeable sodium percentage (ESP), chloride, cation exchange capacity (CEC) and organic carbon. At “Grandview”, the results were less consistent, but the combined data for both paddocks again demonstrated robust relationships between ECa and soil texture (clay content) and organic carbon. However, in some instances, the relationships between ECa and agronomic factors of importance were negative or showed no relationship. Prediction of pasture TGDM from the Crop Circle™ NDVI scans revealed strong correlations between NDVI and the harvested pasture biomass, with $R^2$ values between 0.72 and 0.85 across both properties. Depending on the paddock, the root mean square prediction errors ranged from 157–533 kg/ha, which compared favourably to more time-consuming traditional pasture measurement methods using devices such as rising plate meters. Potential zones for differential management across crop and pasture phases were created using *k*-means clustering of plant yield and soil data. The defined zones revealed important differences between management classes, irrespective of whether the paddock was in crop or pasture.

The third phase integrated the high-resolution data to create a single spatial and temporal index of production for paddock. Crop grain yields and pasture TGDM data were reduced to a single stability index (SI) for each paddock, creating four productivity zones: high and stable, high and unstable, low and stable, and low and unstable. The index has the potential to be used by farmers to manage from a whole-of-farm perspective.

The research described here has been successful in working towards providing both researchers and producers with a methodology and information to incorporate pasture phase information into a mixed farming precision management system.

# TABLE OF CONTENTS

## LIST OF FIGURES

## LIST OF TABLES

## LIST OF APPENDICES

# CHAPTER 1. GENERAL INTRODUCTION

## 1.1 THE ADOPTION OF PRECISION AGRICULTURE IN MIXED FARMING SYSTEMS

Precision agriculture (PA) has become a major driver for productivity within farming systems (Banhazi et al., 2012; Blumenthal et al., 2008; Chen et al., 2009; Hedley, 2015; Kingwell and Pannell, 2005; Robertson et al., 2012). Precision agriculture aims to vary production inputs such as fertiliser and seeding rates, both spatially and temporally at the sub-paddock scale for cost efficiencies, productivity improvements and environmental benefits.

Several factors have facilitated the adoption of PA technologies in Australia:

- The advent of low-cost global positioning systems (GPS) linked to yield monitors on grain harvesters (Bramley and Janik, 2005).
- Differential GPS with 2 cm accuracy and auto-steer fitted to tractors has allowed the sowing of a crop between the rows of a previous crop and enabled differential management of contrasting zones within variable paddocks.
- Farmers have recognised opportunities to improve input efficiency and maximise profitability by optimising decisions around inputs within large heterogeneous paddocks.
- Affordable GPS-linked remote sensing technologies have enabled the monitoring of within-paddock biomass and/or nitrogen status of crops at high resolutions during the growing season.
- These same technologies have enabled the identification and mapping of variable soil properties such as soil texture and salinity using electromagnetic induction (EMI) and gamma radiometric (GR) sensors.

Despite PA technologies in Australia being readily available, their use has been largely confined to cropping systems. In contrast to their adoption for cropping, few producers have applied these tools—which they have often already acquired—to improve the production efficiency of their pasture phases and livestock enterprises.

There appear to have been few attempts to use spatial monitoring technologies to investigate livestock and pasture interactions in the pasture phase and to follow the after-effects of different management strategies into a subsequent cropping phase. For the most part, pasture paddocks tend to be managed as single units, ignoring the existence of productivity gradients across the landscape (Hill et al., 1999). There have been no published studies into a grazing system that matches the management of land, soil types and selection of pasture cultivars to site-specific management zones, and the effects of such a system on the productivity of pasture–crop systems. As a consequence, the uniform application of inputs to variable-yielding paddocks may result in economic losses and contribute to environmental degradation (Chen et al., 2009). Factors such as soil type and depth, botanical composition, livestock grazing preferences and aspect (Murray et al., 2007; Virgona and Hackney, 2008), and the location of watering points and shade (Mathews et al., 1999) can all create nutrient gradients across a landscape. Research has also shown that grazing livestock create specific spatial patterns of pasture biomass utilisation which affects the spatial heterogeneity of the paddock and brings about significant nutrient redistribution (Laca, 2009; Rook et al., 2004; Schellberg et al., 2008; Schnyder et al., 2010; Trotter et al., 2010).

## 1.2 OBJECTIVES

The primary objective of this thesis was to explore the nature of sub-paddock scale spatial variation in both the cropping and pasture phases of mixed farming enterprises in southern Australia using readily available PA technologies. This is an aspect of precision farming technology that has not been previously explored to any extent.

Secondary objectives were to:

1. Quantify spatial and temporal crop and pasture yield variability using in-paddock high-resolution proximal sensing.
2. Explore the spatio-temporal relationships between crop and pasture production using the high-resolution data obtained.

There is a significant amount of high-resolution data which has been gathered and is available for analysis from cropping phases in the form of geo-referenced yield monitor data and, to varying degrees, soil chemical/conductivity analysis. Most farmers have historical records about spatial variability in grain yields, but have little information about the spatial variability of pasture productivity from those same paddocks.

By and large, pasture–livestock phases are 'set and forget' exercises, where livestock and the pastures they graze are managed in the most basic manner. This practice is a missed opportunity to improve whole-farm management by taking advantage of precision farming systems, especially as most farmers are already familiar with and using some form of precision technology in their cropping enterprises. Many farmers who actively use PA in their cropping phases have pondered the very same questions (pers. comm.):

- "How can I use PA to find out what is going on in pasture–livestock phases?"
- "Can I integrate this knowledge into my overall farming system to minimise the cost and risks of moving between cropping and livestock phases?"

Meeting these objectives will provide valuable insights into the capacity of PA technologies to be used as an integrated, whole-farm management system, rather than in cropping phases alone.

## 1.3 OVERVIEW OF THESIS STRUCTURE AND CHAPTERS

This thesis consists of a series of investigations linked by underlying considerations around the potential use of PA technologies in both the crop and pasture phases of mixed farming systems in southern Australia. The thesis is organised according to the general order in which the research was undertaken.

**Chapter 2** provides an overview of past and current research literature in the use of remote sensing in crop and pasture systems and the role of vegetation indices in measuring crop and pasture biomass. This is then extended to include the use of high-resolution active proximal sensors for the measurement of crop and pasture biomass and soil characteristics.

**Chapter 3** describes a preliminary analysis using eight consecutive years of low-resolution Moderate Resolution Imaging Spectroradiometer (MODIS) NDVI data to investigate the relationship, if any, between biomass production across the crop and pasture phases on two properties. The limitations of using low-resolution remotely sensed data for identifying sub-paddock scale spatial variation are discussed. The findings of Chapter 3 were presented at the 16th Australian Agronomy Conference, 14–18 October 2012 in Armidale, NSW in a paper entitled "*The integration and validation of precision management tools in mixed farming systems*".

**Chapter 4** extends the analysis of Chapter 3 by using TIMESAT software to create a series of metrics that characterise vegetation phenology from the MODIS NDVI data. The phenology metrics were analysed to test the utility of the low-resolution MODIS data in exploring the variability of within-paddock biomass production between the crop and pasture phases. The findings of Chapter 4 were presented at the 9th European Conference on Precision Agriculture in Lleida, Catalonia, Spain, July 2013 in a paper entitled "*Sub-paddock scale spatial variability between the pasture and cropping phases of mixed farming systems in Australia*".

**Chapter 5** describes the acquisition, processing, spatial mapping and preliminary analysis of high-resolution soil textural, 'on-the-go' proximal sensing methods using soil electromagnetic induction and gamma radiometrics. The proximally sensed data is supported by traditional soil sampling and chemical testing.

**Chapter 6** describes methodology for the acquisition of high-resolution pasture NDVI data from a Crop Circle™ active optical sensor, calibrated with *in situ* pasture sampling. The data were processed and used to identify the extent of spatial variability in pasture dry matter production over a two-year period within the experimental paddocks.

The soil ECa and gamma radiometric data, soil chemistry and paddock elevation data acquired in Chapter 5 were used, in combination with existing crop yield data for those paddocks and the pasture dry matter data derived from Crop Circle™ sensing, to delineate potential whole-of-rotation management classes that integrate both the pasture and cropping phases.

**Chapter 7** describes the process of calculating spatial and temporal trends in the variability of crop grain and pasture green dry matter over time and their spatio-temporal relationships using the data acquired and developed in Chapters 5 and 6. A paddock production stability index (SI) was created to identify and combine the spatial and temporal variation for both crop and pasture phases on selected paddocks from each property and to divide a paddock into four productivity zones: high and stable, high and unstable, low and stable, and low and unstable.

A component of the methodology and results from Chapter 7 were presented at the 13th International Conference on Precision Agriculture, St Louis, Missouri, 31 July 2016, in a paper entitled "*Mapping the stability of spatial production in integrated crop and pasture systems: towards zonal management that accounts for both yield and livestock–landscape interactions*".

**Chapter 8** summarises the results, discusses the implications of the research, and presents the overall conclusions for the management of mixed farming systems. It also discusses research limitations and areas for further research.

The **Appendices** provide the supplementary information in relation to particular chapters.

## 1.4 REFERENCES

Banhazi, T. M., Lehr, H., Black, J. L., Crabtree, H., Schofield, P., Tscharke, M., & Berckmans, D. (2012). Precision livestock farming: an international review of scientific and commercial aspects. *International Journal of Agricultural and Biological Engineering*, *5*(3), 1–9.

Blumenthal, M., Umbers, A., & Day, P. (2008). A responsible lead: an environmental plan for the Australian grains industry: Grains Research and Development Corporation.

Bramley, R. G. V., & Janik, L. J. (2005). Precision agriculture demands a new approach to soil and plant sampling and analysis–examples from Australia. *Communications in Soil Science & Plant Analysis*, *36*(1–3), 9–22.

Chen, W., Bell, R. W., Brennan, R. F., Bowden, J., Dobermann, A., Rengel, Z., & Porter, W. (2009). Key crop nutrient management issues in the Western Australia grains

industry: a review. *Australian Journal of Soil Research*, *47*(1), 1–18. doi: 10.1071/SR08097

Hedley, C. (2015). The role of precision agriculture for improved nutrient management on farms. *Journal of the Science of Food and Agriculture*, *95*(1), 12–19. doi: 10.1002/jsfa.6734

Hill, M. J., Vickery, P. J., Furnival, E. P., & Donald, G. E. (1999). Pasture land cover in eastern Australia from NOAA-AVHRR NDVI and classified Landsat TM. *Remote Sensing of Environment*, *67*(1), 32–50.

Kingwell, R. S., & Pannell, D. J. (2005). Economic trends and drivers affecting the wheatbelt of Western Australia to 2030. *Australian Journal of Agricultural Research*, *56*(6), 553–561.

Laca, E. A. (2009). New approaches and tools for grazing management. *Rangeland Ecology & Management*, *62*(5), 407–417. doi: 10.2111/08-104.1

Mathews, B. W., Tritschler, J. P., Carpenter, J. R., & Sollenberger, L. E. (1999). Soil macronutrient distribution in rotationally stocked kikuyu grass paddocks with short and long grazing periods. *Communications in Soil Science and Plant Analysis*, *30*(3), 557–571.

Murray, R. I., Yule, I. J., & Gillingham, A. G. (2007). Developing variable rate application technology: modelling annual pasture production on hill country. *New Zealand Journal of Agricultural Research*, *50*(1), 41–52.

Robertson, M. J., Llewellyn, R. S., Mandel, R., Lawes, R., Bramley, R. G. V., Swift, L., . . . O'Callaghan, C. (2012). Adoption of variable rate fertiliser application in the Australian grains industry: status, issues and prospects. *Precision Agriculture*, *13*(2), 181–199.

Rook, A. J., Dumont, B., Isselstein, J., Osoro, K., WallisDeVries, M. F., Parente, G., & Mills, J. (2004). Matching type of livestock to desired biodiversity outcomes in pastures–a review. *Biological Conservation*, *119*(2), 137–150. doi: 10.1016/j.biocon.2003.11.010

Schellberg, J., Hill, M. J., Gerhards, R., Rothmund, M., & Braun, M. (2008). Precision agriculture on grassland: applications, perspectives and constraints. *European Journal of Agronomy*, *29*(2–3), 59–71.

Schnyder, H., Locher, F., & Auerswald, K. (2010). Nutrient redistribution by grazing cattle drives patterns of topsoil N and P stocks in a low-input pasture ecosystem. *Nutrient Cycling in Agroecosystems*, *88*(2), 188–195.

Trotter, M. G., Lamb, D. W., Hinch, G. N., & Guppy, C. N. (2010). Global navigation satellite system livestock tracking: system development and data interpretation. *Animal Production Science*, *50*(6), 616–623. doi:10.1071/AN09203

Virgona, J., & Hackney, B. (2008). *Within-paddock variation in pasture growth: landscape and soil factors*. Paper presented at the 14th Australian Agronomy Conference, "Global Issues, Paddock Action", Adelaide, South Australia.

# CHAPTER 2. LITERATURE REVIEW

## 2.1 MIXED FARMING SYSTEMS IN AUSTRALIA

Mixed farming systems that combine grain cropping and pasture-based livestock enterprises dominate the dryland farming regions of Australia. In southern Australia, the mixed farming zone lies between the 300 and 600 mm average annual rainfall isohyets and is highly seasonal, encompassing temperate climates with cool, wet winters and hot, dry summers. The combination of highly variable rainfall (Love, 2004) and volatile commodity prices faced by Australian farmers in these regions has favoured a diversified farming system. Having a flexible mix of crop and livestock options to even out fluctuations in income over time, in response to price and/or climate signals, moderates the risks to the farm enterprise (Bell and Moore, 2011).

The main pastures sown are self-regenerating annual legumes—mainly subterranean clover (*Trifolium subterraneum* L.) and annual medics (*Medicago* spp.). Where rainfall is sufficient to support perennial species, lucerne (*Medicago sativa* L.) is often sown in mixtures with annuals such as subterranean clover (Hayes et al., 2010; Kirkegaard et al., 2011). The use of lucerne and other perennials is limited to areas receiving more than 450 mm of annual rainfall (Fillery and Poulter, 2006; White et al., 2003).

Incorporating a pasture–livestock phase provides a number of important benefits including:

- Improving soil nitrogen for subsequent crops: estimates of atmospheric N-fixation for legumes range between 20 and 25 kg N/ha per tonne of legume dry matter produced (Herridge et al., 2008). Angus and Peoples (2013) observed that a mixed farming system with legume-dominant pasture phases occupying ~40% of the farmed area can sustain a stable N balance. In contrast, much of the biologically fixed N in a grain legume rotation is removed in the grain (Peoples et al., 2012).

- Rebuilding soil organic matter and improving soil structure: pasture phases are an effective way of building soil organic matter, especially in conjunction with grasses (Angus et al., 2006).
- Control and management of weeds through competition and grazing by livestock, particularly where herbicide-resistant weeds are an issue (Doole and Pannell, 2008).
- Crop disease and pest control (Doole and Pannell, 2008).
- Improving livestock production: legume-based pastures can maintain higher carrying capacities (Bathgate and Pannell, 2002; Fisher et al., 2012).
- Provide management flexibility: the length of pasture or crop phases can be varied as a management response to climate or commodity price variations (Verburg et al., 2008).

By international standards, Australian mixed farms are large and becoming larger (Figure 2.1). This has occurred to capture economies of scale and allow farmers to offset diminishing terms of trade. The increased size of farms has meant that properties often encompass different soil types of varying productivity. This has occurred concurrently with a reduction in available farm labour, placing pressure on farm owners and managers to simplify their farming systems, often at the expense of a pasture–livestock phase.

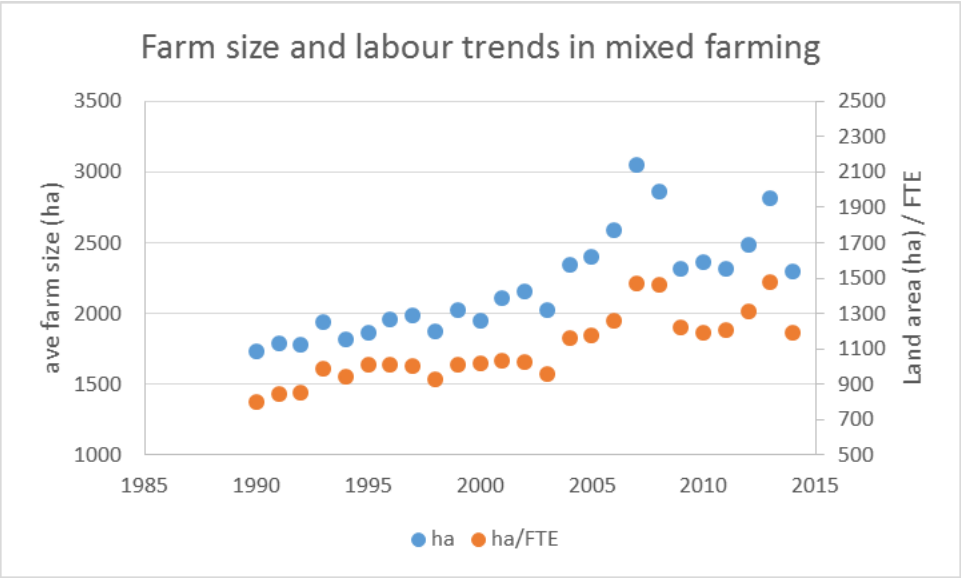


**FIGURE 2.1:** TRENDS IN THE SIZE OF FARMS (BLUE) AND LAND AREA PER UNIT OF LABOUR (ORANGE) ACROSS THE SOUTHERN AUSTRALIAN MIXED FARMING ZONE BETWEEN 1990 AND 2014. SOURCE: AUSTRALIAN BUREAU OF AGRICULTURAL AND RESOURCE ECONOMICS (2016).

### *2.1.1 DIMINISHED ADOPTION OF PASTURE–LIVESTOCK PHASES IN AUSTRALIAN MIXED FARMING SYSTEMS*

Notwithstanding the advantages of pasture–livestock phases described in the literature, there has been a trend over the past 20 years towards increased cropping intensity within mixed farming zones and a shift towards higher proportions of cropping (Figure 2.2). In some cases, this has involved the complete removal of livestock and associated infrastructure, and a change to continuous cropping using cereal and broadleaf crops, herbicides for weed control and higher rates of nitrogen fertiliser. The higher relative prices received for grain products compared to livestock in recent years, and the associated decline in returns to grazing enterprises, has contributed to this trend (Bell and Moore, 2012). There have also been significant technical changes to cropping systems over this period that have led to longer cropping rotations and the declining importance of pasture phases in crop rotations. These include:

- The replacement of pasture phases with canola as a break crop and grain legumes for nitrogen fixation.

- The introduction of herbicide-tolerant crops which have facilitated the adoption of no-till/conservation agriculture, allowing the intensification of cropping. Additionally, residual herbicides used in cropping (e.g. sulfonylureas (Group B), triazine (Group C)) have severely affected the capacity for pasture legumes to regenerate and persist during pasture phases (Nichols et al., 2007; Peoples et al., 2012).
- Labour supply shortages that have favoured increased cropping activity over more labour-intensive livestock activities (Doole et al., 2009). There has been an ongoing trend towards less labour per hectare farmed (Figure 2.1).
- Crop residues retained under no-till cropping systems have reduced the variability in cereal yields (D'Emden and Llewellyn, 2006).
- The economics of fertiliser nitrogen has been seen as more financially attractive and flexible than biologically fixed N from pastures (Angus and Peoples, 2013).
- The increasing trend towards no-till and controlled-traffic cropping systems (Tullberg et al., 2007) has led to a belief among some producers that soil structural damage by livestock could adversely affect the following crop yields (Flower et al., 2008; Rainbow and Derpsch, 2011). However, experimental evidence indicates that the effects of soil compaction by livestock on following crop yields are unlikely to be significant (Bell et al., 2011).

Ironically, increased herbicide use under a no-till, controlled-traffic farming system can increase the rate of herbicide resistance in weeds (Farooq et al., 2011; Owen et al., 2014, 2015), requiring either cultivation or a pasture–livestock phase to enable adequate weed control (Kirkegaard et al., 2014; Renton and Flower, 2015).

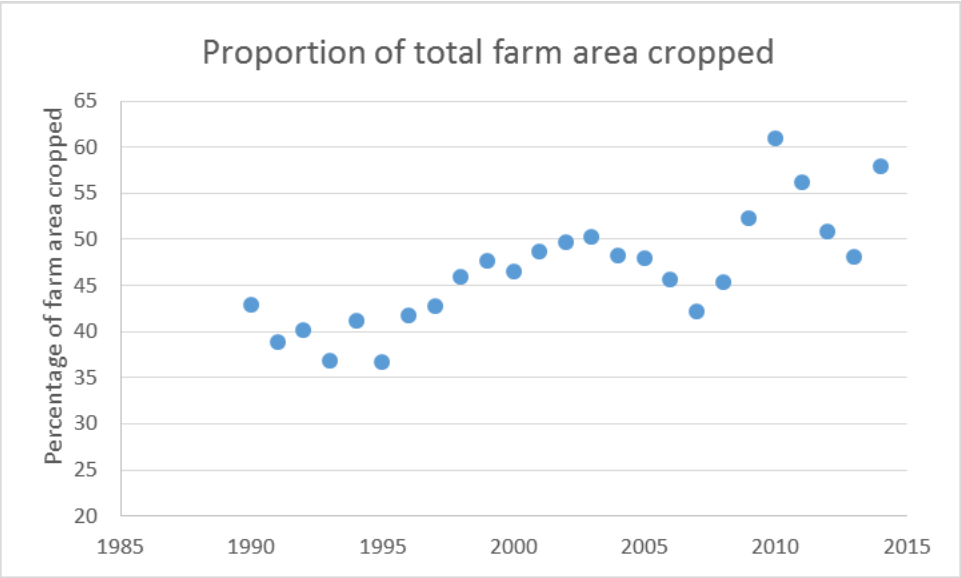


**FIGURE 2.2:** TREND IN THE PROPORTION OF FARM AREA CROPPED ACROSS THE SOUTHERN AUSTRALIAN MIXED FARMING ZONE BETWEEN 1990 AND 2014. SOURCE: AUSTRALIAN BUREAU OF AGRICULTURAL AND RESOURCE ECONOMICS (2016).

## 2.2 PRECISION AGRICULTURE IN MIXED FARMING SYSTEMS

Precision agriculture collects and processes high-resolution data about crops, pastures, livestock and soils, in time and space, to improve the efficiency of farm input use, productivity and environmental outcomes (Chen et al., 2009; Mulla, 2013; Robertson et al., 2012). Historically, PA has been largely confined to cropping systems, with much lower levels of adoption in pasture, livestock and viticulture (Bramley, 2009; Schellberg et al., 2008).

The widespread availability of high-resolution, low-cost global navigation satellite systems such as GPS has been a key enabling technology of PA, making technological advances such as machinery auto-steer/guidance (through real-time kinematic technology) possible. Further advances have included variable rate fertiliser application, section control on spray units and, more recently, robotics based on sensor networks and proximal sensing, allowing enhanced real-time decision making (Banhazi et al., 2012; Dong et al., 2013; Hedley, 2015; Robertson et al., 2012).

These technologies have significant potential for adoption across both the pasture and crop phases of mixed farming systems. The near real-time monitoring of pastures, as well as crops by remote sensing applications, has the capacity to allow high-resolution management of pasture–crop systems, without the need for extensive, labour-intensive and expensive field sampling. Additionally, technologies such as real-time livestock tracking through the use of GPS collars or eartags, and the control of stock with virtual fencing are now being brought to the market at an affordable cost (http://agersens.com/).

Monitoring livestock behaviour with the use of tracking devices has become widespread in the last ten years (Barnes et al., 2011; Handcock et al., 2009; Schellberg et al., 2008; Trotter et al., 2010b). The precision of modern GPS technology allows the position of individual animals to be determined within 10 m or better (Laca, 2009). The development of lightweight tracking collars has allowed cost-effective monitoring of stock movements, tracking the times and locations of peak grazing activity (Freire et al., 2012; Trotter et al., 2010c). This data can be imported into a geographic information system (GIS) to evaluate livestock behaviour and herd inter-relationship characteristics, pasture utilisation and nutrient redistribution (Finger et al., 2014; Trotter et al., 2010c). Analysing the total time spent by animals in a particular area can help to visualise the spatial variability in grazing pressure, by producing maps that indicate the preferred grazing areas (Trotter and Lamb, 2008). Research to date has shown that grazing livestock create specific spatial patterns of pasture biomass utilisation that affect the spatial heterogeneity of the paddock and brings about significant nutrient redistributions (Laca, 2009; Rook et al., 2004; Trotter et al., 2010b).

The development of virtual fences has been ongoing over recent decades. Bishop-Hurley et al. (2007) found virtual fencing to be a viable technology for managing livestock. Unlike conventional fencing, virtual fences are not fixed in time and space. The most common virtual fencing systems work on the basis of an audible warning and electric stimulation as negative reinforcements (Umstatter, 2011). A significant advantage of virtual fencing is the flexibility it offers in managing stocking densities and the time spent grazing particular areas of a paddock (Anderson, 2007).

Although beyond the scope of this research, both GPS-mapped livestock activity and virtual fencing are technologies that can provide an additional means of validating the observed spatial variability in pasture growth from NDVI imaging, soil characteristics and landscape factors.

### *2.2.1 THE USE OF REMOTE SENSING IN PRECISION AGRICULTURE*

Remote sensing refers to technologies for measuring object properties on the Earth's surface using data acquired at a distance, rather than *in situ*, for example from aircraft and satellites. It is done by recording the electromagnetic radiation (EMR) that emanates from the Earth's land surfaces, oceans or atmosphere (Jones and Vaughan, 2010). There are many types of EMR, of which visible light is just one form. An important criterion of EMR is its wavelength, which ranges from fractions of a nanometre to several metres. The properties of objects or areas on the Earth's surface can be identified and delineated in terms of their associated levels of electromagnetic energy. Areas observed are referenced in a geographic coordinate system so that they can be located on a map.

Remote sensing systems can be categorised into two types, passive or active, based on the energy source. Passive remote sensing systems do not have their own light energy source and rely on the detection of electromagnetic (EM) energy from the sun or reflected from the Earth's surface. Passive sensing of visible light is therefore limited to daytime. Satellite-based optical sensors are an example of passive sensors. Active remote sensing systems have their own energy source. These systems send bursts of EM energy in the direction of the target and measure the energy returning from the target to the sensor. This means they can be used at night. Radar and lasers are examples of active sensors.

Most remote sensing in PA uses optical imagery to record the spatial variability in soil and crops by measuring the reflected radiation from plant or soil surfaces. The underlying premise of monitoring crop and pasture condition by remote sensing is that key vegetation parameters related to growth and yield have distinguishing reflectance signatures in the visible and/or non-visible EM spectrum (Bauer, 1985). Remote sensing in agriculture using satellites has occurred since the early 1970s (Bauer and Cipra, 1973; Doraiswamy et al., 2003; Jewel, 1989). As precision

agriculture has increased in adoption, satellite remote sensing has been incorporated within the suite of PA technologies and tools. Information about many vegetation and soil characteristics is linked to the amount of energy reflected, transmitted or emitted in these areas of the EM spectrum. Depending on the spatial resolution of the sensor, variability in these characteristics can be analysed over time at the paddock, farm or regional scale by making use of the different bands of information captured by the sensors.

Satellite-based sensors range from relatively low resolution (100 m to 1 km) multispectral platforms such as the Advanced Very High Resolution Radiometer (AVHRR) and MODIS to medium-resolution sensors (10–30 m) such as Landsat and SPOT, through to modern high-resolution (1–5 m) sensors like IKONOS, Quickbird and Rapideye. However, high-resolution imagery is very expensive.

Two satellite systems in particular have been fundamental to the use of remote sensing in precision agriculture: Landsat and the earth observing system's (EOS) Aqua and Terra platforms. Because MODIS and Landsat imagery is free, they provide a low-cost means of assessing variability in crop and pasture characteristics at the paddock scale. These two satellite-based sensor systems will now be discussed briefly.

### *2.2.2 LANDSAT*

A series of Landsat satellites have been launched since 1972. Landsat 4 and Landsat 5 were the fourth and fifth satellites of the series, respectively. Landsat 4 and 5 are sun synchronous, polar orbiting satellites travelling around the Earth from pole to pole at an altitude of 705 km. Landsat 4, launched on 16 July 1982, was equipped with the Multiple Spectral Scanner (MSS); Landsat 5, launched on 1 May 1984, was equipped with both the MSS and Thematic Mapper (TM) sensors (Headley, 2012; Markham et al., 2004).

Landsats 4 and 5 offered images at 30 m resolution. Landsats 1 to 5 have now been decommissioned. In October 1993, Landsat 6 failed at launch after not reaching the velocity necessary to obtain orbit.

Landsat 7 carried the Enhanced Thematic Mapper Plus (ETM+) and was launched on 15 April 1999. ETM+ replicated the capabilities of the TM sensors with additional features such as a panchromatic band with 15 m spatial resolution, full aperture diffuser calibration system, a thermal IR channel with 60 m spatial resolution and an on-board data recorder (Headley, 2012). The TM sensor has seven spectral bands (see Table 2.1). The Scan Line Corrector (SLC), which compensates for the forward motion of Landsat 7, failed in May 2003. Attempts to recover the SLC were unsuccessful. This now results in around 22% of any given scene being lost (Markham et al., 2004). Landsat 8 was launched in February 2013 and covers the entire globe every 16 days in an 8-day offset from Landsat 7 (Headley, 2012).

**TABLE 2.1:** LANDSAT 7 SENSITIVITY AND RESOLUTION.

| Landsat 7 | Wavelength (micrometres) | Resolution (metres) |
|---|---|---|
| Band 1–Blue | 0.45–0.52 | 30 |
| Band 2–Green | 0.52–0.60 | 30 |
| Band 3–Red | 0.63–0.69 | 30 |
| Band 4–Near-Infrared (NIR) | 0.77–0.90 | 30 |
| Band 5–SWIR 1 | 1.55–1.75 | 30 |
| Band 6–Thermal Infrared 1 | 10.40–12.50 | 60 (30) |
| Band 7–SWIR 2 | 2.09–2.35 | 30 |
| Band 8–Panchromatic | 0.52–0.90 | 15 |

Source: US Geological Survey. http://landsat.usgs.gov/band_designations_landsat_satellites.php

Although Landsat offers high-resolution imagery that is ideal for pasture biomass assessment, the lack of regular coverage in the southern hemisphere and long revisit times reduce the opportunities to monitor reflectance from crop and soil. If cloud cover interferes, the observation windows decrease further, resulting in few images during the growing season.

### *2.2.3 TERRA (EOS AM) AND AQUA (EOS PM)*

The Terra (EOS AM) and Aqua (EOS PM) satellites carry the Moderate Resolution Imaging Spectroradiometer (MODIS) instrument. MODIS is part of the National Aeronautics and Space Administration's (NASA) Earth Observing System program which has provided continuous global data on the Earth's biosphere since the sensor was first launched aboard the Terra satellite in December 1999. It was complemented by a second sensor launched aboard the Aqua satellite in May 2002 and subsequently both the Terra and Aqua MODIS sensors have provided nearly complete Earth coverage on a daily basis. Temporal compositing (usually on a weekly basis) is used to remove clouds, aerosols and cloud-shadow contamination. The composited vegetation indices are produced at 10-day intervals. The suite of MODIS land products includes three vegetation-focused product series: i) MOD13—vegetation indices (VIs): normalised difference vegetation index (NDVI) and enhanced vegetation index (EVI), ii) MOD15—leaf area index (LAI) and fraction of absorbed photosynthetically active radiation (fAPAR), and iii) MOD17—gross primary production (GPP), net primary production (NPP) and net photosynthesis (Justice et al., 2002).

### *2.2.4 PLANT/SOIL/LIGHT INTERACTIONS*

For remote sensing of vegetation, the most common EM bands used are the red and near-infrared (NIR) bands because they are specifically related to plant physiology. Between wavelengths of 400 and 2500 nm, the incident radiation on a vegetation surface is influenced by three main elements (Dorigo et al., 2007):

- the optical properties of the vegetative material itself
- the arrangement of the materials in the vegetation canopy
- the optical properties of the soil beneath the canopy.

The quality of the signal received is also affected by atmospheric conditions as well as the viewing and illumination angles (Cierniewski and Verbrugghe, 1997; Roujean and Breon, 1995). Depending on the wavelength, the radiance flux can be affected by atmospheric scattering or pass through without impact. Atmospheric scattering is more significant at low angles of solar elevation and high levels of atmospheric turbidity (Jensen, 2005).

Chlorophyll pigments inside leaf cell chloroplasts provide energy for photosynthesis by absorbing sunlight in the visible blue and red wavelengths (~400–480 nm; 620–700 nm, respectively), resulting in dominant reflectance in the green wavelengths (~500–580 nm). The chloroplast pigments are transparent to higher wavelength near-infrared (NIR) radiation (>700 nm) in healthy, actively growing plants. Combined with scattering within the leaf mesophyll layer, this results in very strong NIR reflectance (Gates et al., 1965; Jones and Vaughan, 2010; Trotter et al., 2010b). Green light (500–600 nm) is largely reflected by all plants, so a healthy, actively photosynthesising plant appears green, due to the reduced amounts of red and blue light reflected.

Healthy, actively growing plants will present a large difference between the levels of absorbed red and NIR reflectance. In contrast, the lower levels of chlorophyll in stressed plants absorb much less red light (red reflectance rises) and reduced NIR reflectance as the internal structure of the leaf collapses. As a result, the combination of red and NIR wavelengths, or the 'red-edge' region between the Red and NIR wavebands (around 700 nm), can be good indicators of plant type, species composition, biomass, LAI, phenological stage, and disease or nutritional status (Devadas et al., 2009; Flowers et al., 2001; Haboudane et al., 2004; Huete et al., 1999; Lamb et al., 2002; Moges et al., 2005). Bare soil can be differentiated from actively growing vegetation because it typically has a higher red and lower NIR reflectance.

### *2.2.5 SPECTRAL INDICES*

Spectral indices are created by combining two or more spectral bands mathematically in such a way that the index created is more clearly related to parameters of interest such as photosynthetic activity or plant canopy LAI. Deriving spectral indices is a widely adopted practice in remote sensing, particularly in the use of vegetation indices (VIs) for studying vegetation cover (Bannari et al., 1995; Glenn et al., 2008; Huete et al., 2011; Ji and Peters, 2007; Zwiggelaar, 1998). Indices were developed to reduce 'noise' from the data, introduce corrections for atmospheric distortions and to normalise results. Although there are many indices, most provide a ratio between light reflected in the red and NIR parts of the EM

spectrum (Table 2.1) to separately identify water, soil and vegetation effects (Glenn et al., 2008). Most vegetation indices are related to the Simple Ratio (SR) (Jordan, 1969):

$$SR = \rho NIR/\rho Red$$

where ρNIR and ρRed are the reflectance values of red and near-infrared light received at the sensors.

According to Huete et al. (1994; p. 226), a vegetation index should:

- maximise sensitivity to plant biophysical parameters
- normalise or model external effects such as sun angle, viewing angle and atmosphere
- minimise canopy ground contamination caused by canopy background variations for consistent spatial and temporal comparisons
- be a global product that allows for spatial and temporal assessments of vegetation conditions, and
- be correlated to key biophysical parameters such as biomass, LAI or *f*APAR for validation and quality control.

Over the years, different vegetation indices have been derived to take advantage of the relationship between red and near-infrared reflectance and healthy vegetation (Thenkabail et al., 2000). These vegetation indices have been positively correlated with a wide range of functionally useful variables that tend to vary together, including biomass, LAI, chlorophyll content, leaf nitrogen content, photosynthesis and *f*APAR (Atzberger, 2013; Bannari et al., 1995; Carlson and Ripley, 1997; Dorigo et al., 2007; Lamb et al., 2002; Rembold et al., 2013; Schellberg et al., 2008; Zwiggelaar, 1998).

The NDVI is the most widely used index (Ollinger, 2011; Rouse et al., 1973; Tucker, 1979). The advantage of NDVI is that it can be calculated from sensors which have a database of images acquired over a long period of time. These extensive datasets provide a means to monitor vegetation characteristics such as GPP and feed on offer (FOO) (Edirisinghe et al., 2004, 2011; Hill et al., 2004). Canopy architecture strongly influences NIR reflectance (Gitelson et al., 2002). This includes the

distribution of vegetation and the amount of light reflected from the soil beneath the plant canopy, leaf angle distribution, localised chlorosis, and the LAI of the canopy (Huete, 1988; Verhoef, 1984). Lamb et al. (2002) reported that the NDVI and, in particular, the NIR band tended to plateau as the number of leaf layers increased because NIR was unable to infiltrate past the top 3–5 leaves. In comparison, the enhanced vegetation index (EVI) and the red-edge position (REP) do not saturate as quickly at higher levels of canopy closure (Huete et al., 2002).

*The normalised difference vegetation index (NDVI)*

The NDVI is the most widely used mathematical combination of red and NIR wavelengths for remote monitoring of vegetation in agriculture (Tucker, 1979).

It is expressed as: $$\mathrm{NDVI} = \frac{\rho(\mathrm{NIR}) - \rho(\mathrm{Red})}{\rho(\mathrm{NIR}) + \rho(\mathrm{Red})}$$

The NDVI was first expressed by Rouse et al. (1973) and in the ensuing years used in a wide range of remote sensing studies and applications (Balaghi et al., 2008; Beck et al., 2006; Tucker, 1979; Tucker and Sellers, 1986; Tucker et al., 2001; Wall et al., 2008; Xu et al., 2014; Zhao et al., 2009).

The SR and NDVI are based on the strong absorption of light in the red wavelengths by chlorophylls a and b in green leaves, which reaches a maximum ~690 nm, whereas plant cell walls scatter light in NIR wavelengths (~850 nm) (Tucker, 1979). This absorption contrast across the 650–850 nm bandwidth is captured by the NDVI and other vegetation indices. The NDVI normalises values between –1 and +1. Dense, actively photosynthesising vegetation has a high NDVI value, while soil values have a low, positive NDVI value and water has negative NDVI values because of strong absorption in NIR wavelengths.

Various combinations of the red, NIR and green bands were tested by Tucker (1979) for the prediction of plant green biomass, chlorophyll content and leaf moisture content. He found that NDVI was strongly correlated with these parameters.

Advantages of the NDVI include (Huete et al., 2002):

- It allows changes in seasonal and inter-annual vegetation growth to be monitored at local and global scales.

- The use of a ratio-based index minimises the effects of multiplicative noise such as solar illumination differences, low viewing angles, atmospheric attenuation and cloud shadows that can be present in multi-band imagery taken over extended time periods.

Disadvantages of the NDVI include (Huete et al., 2002):

- It is non-linear and can be affected by additive noise influences such as atmospheric path radiance and viewing angles.
- The index has scaling issues in high biomass conditions where the NDVI signal saturates.
- The index is highly sensitive to background 'noise' such as bare soil and gives high NDVI values with darker-coloured plant canopies.

Many alternative formulations have been developed to correct for specific deficiencies of the basic NDVI. The alternatives incorporate modifications aimed at minimising the effects of noise caused by variation in the underlying soil reflectance or by atmospheric absorption. They include the enhanced vegetation index (EVI) (Huete et al., 1999) and the soil-adjusted vegetation index (SAVI) (Huete, 1988). The value of SAVI for reducing the background soil noise intrinsic to the NDVI has been established in several studies (Bannari et al., 1995; Bausch, 1993; Rondeaux et al., 1996). Several modifications to SAVI to optimise the reduction in soil background effects have been reported (Broge and Leblanc, 2001). The EVI was developed for MODIS and corrects for canopy background and atmospheric influences. It does not saturate as readily as the NDVI at high biomass values. Several studies have shown the EVI to be strongly correlated with photosynthesis and plant transpiration (Huete et al., 2011; Ponce et al., 2011; Wagle et al., 2014). A few of the most widely adopted vegetation indices based primarily on red/infrared wavelengths are shown in Table 2.2.

### *2.2.6 REMOTE SENSING OF CROPS*

Low-resolution imagery from the AVHRR and MODIS sensors has been widely used for more than 30 years in crop monitoring and yield prediction (Atzberger, 2013; Tucker and Sellers, 1986). High temporal frequency, wide coverage and low cost per unit area have made satellite imagery an important management tool for

monitoring agricultural vegetation. The most common vegetation index used for these analyses is the NDVI (Labus et al., 2002; Quarmby et al., 1993; Wall et al., 2008) because the nearly linear relationship with *f*APAR means it can be used as an indirect measure of primary productivity (Baret and Guyot, 1991).

The simplest form of crop monitoring using remotely sensed information is to compare current crop status with real-time in-paddock measurements or with imagery from previous years, or the average of a run of previous years. Differences are then used to identify possible yield limitations for the current drop (Aase and Siddoway, 1981; Baret et al., 1989; Tucker et al., 1980, 1981).

The size of individual MODIS pixels (250 m square) is relatively large for use on an individual farm. Pixels can, therefore, include non-crop and other vegetation, rocky outcrops, buildings, etc. Image masking (Kastens et al., 2005) is used to limit the analysis to a subset of yield-correlating pixels.

More quantitative approaches to yield prediction have included various correlation or regression approaches using yield monitor data in conjunction with AVHRR, MODIS (Wall et al., 2008) and higher resolution Landsat IKONOS and SPOT imagery (Fisher et al., 2009; Meroni et al., 2013; Thenkabail, 2003). More sophisticated approaches have included agronomic and/or meteorological data and achieved high correlation for certain crops (Balaghi et al., 2008; Prasad et al., 2007; Reynolds et al., 2000).

**TABLE 2.2:** COMMON VEGETATION INDICES USED IN REMOTE BIOMASS SENSING.

| Abbreviation | Name | Formula | Parameter measured | Reference |
|---|---|---|---|---|
| NDVI | Normalised difference vegetation index | (NIR–Red)/(NIR+Red) | Green biomass | Rouse et al. (1973) |
| NDRE | Normalised difference red-edge | $(NIR_{790nm}–Red_{720nm})/(NIR_{790nm}+Red_{720nm})$ | Chlorophyll content | Clarke et al. (2001) |
| SR | Simple ratio | NIR/Red | Chlorophyll content | Birth and McVey (1968) |
| SAVI | Soil-adjusted vegetation index | [(NIR–Red)/(NIR+Red+L)]x(1+L) | Green biomass when vegetation cover is low | Huete (1988) |
| EVI | Enhanced vegetation index | 2.5x[(NIR–Red)/((NIR+6xRed–7.5xBlue)+1)] | Green biomass corrected for certain atmospheric distortions | Huete et al. (2002) |
| NLI | Non-linear index | $(NIR^2–Red)/(NIR^2+Red)$ | Green biomass | Goel and Qin (1994) |
| MNLI | Modified non-linear vegetation index | $[(NIR^2–Red)x1.5)]/[(NIR^2+Red)+1.5)]$ | Green biomass | Gong et al. (2003) |

### *2.2.7 REMOTE MONITORING OF PASTURES*

Compared to spatial variation of yields in cropping phases, far less is known about the extent of within-paddock spatial variation during the pasture–livestock phase in mixed farming systems. Most of the reported research in this regard has been undertaken on international grassland farming systems (Edirisinghe et al., 2012; Lee et al., 2011; Marques Da Silva et al., 2008; Serrano et al., 2010, 2011a; Suzuki et al., 2012; Zhao et al., 2007), with a much smaller body of work relevant to Australian dryland pasture systems (Trotter, 2010; Trotter et al., 2008, 2010a; Virgona and Hackney, 2008). None of this research has been conducted on mixed farming systems.

There are relatively few reports in the literature relating to the spatial variation in pasture biomass, its underlying causes and how it compares to grain harvest yield variation during the cropping phase. This knowledge could significantly enhance the capacity for a manager to implement highly effective site-specific management strategies in a continuous sequence across pasture and cropping phases.

Historically, grazing management in most mixed farming systems has been low-input, using conservative, set-stocking systems which result in under-utilisation of pasture. More intensive grazing systems such as rotational and cell grazing enable greater utilisation of pastures and can lead to higher levels of productivity and profitability (Warn et al., 2003). Intensive rotational systems involve controlled movement of livestock, grazing for short periods through small paddocks based on regular, quantitative assessment of biomass/feed budgeting (Laca, 2009). Whichever grazing system is used, the regular measuring and mapping of pasture herbage mass can provide producers with information on the current condition of their pastures which can be used to calculate forage demand and supply. This can then be used to develop spatially-effective grazing management strategies (Bell et al., 2008).

The estimation of paddock pasture biomass during the growing period has traditionally been based on direct measurement by harvesting from numerous, relatively small quadrats and the subsequent sorting and weighing of pasture

samples (Haydock and Shaw, 1975). The method is highly labour-intensive, expensive and time-consuming. A variety of alternative point sampling biomass estimation methods exist, including visual assessments (Campbell and Arnold, 1973; Cayley and Bird, 1996), pasture height measurers (Ganguli et al., 2000; Hutchings, 1991), plate meters (Earle and McGowan, 1979; Gourley and McGowan, 1991), electrical capacitance probes (Vickery et al., 1980) and 'on-the-go' point sampling strategies such as dry weight ranking (Cayley and Bird, 1996; Haydock and Shaw, 1975; Tsutsumi and Itano, 2005). Each method has advantages and disadvantages, but all are labour intensive, expensive, difficult to use on a regular basis, and prone to error when practised by unskilled operators.

The only extensive application of satellite remote sensing to pastures as a co-ordinated service is 'Pastures from Space' (PfS). Pastures from Space is a remote sensing based pasture monitoring and evaluation service which uses satellite imaging as a basis for providing estimates of pasture growth rate (PGR) and FOO (Donald et al., 2010; Edirisinghe et al., 2011). It is available commercially as Pasture Watch™ (Fairport Farm Software, Perth WA). The model includes components detailed by Fitzpatrick and Nix (1970), where a growth index is derived from soil moisture, temperature and light indices. It also takes advantage of NDVI's strong relationship to LAI (Baret and Guyot, 1991; Edirisinghe et al., 2011; Gower et al., 1999; Hill et al., 2004) to provide the spatial fraction of absorbed photosynthetic active radiation (*f*APAR) (Edirisinghe et al., 2004; Hill et al., 2004). The growth index, combined with local climate data, is used to calculate estimates of PGR and FOO. Research carried out in Western Australia has indicated that the sub-paddock spatial distribution of pasture biomass is strongly related to spatial variability in NDVI (Donald et al., 2010; Edirisinghe et al., 2011; Hill et al., 2004). The ability for remote sensing technology such as PfS to provide timely pasture availability data at a paddock scale to accurately assess pasture biomass on a regular basis is a significant management breakthrough for maximising pasture utilisation.

The information from PfS has the potential to enable growers to:

- optimise PGR, quality and utilisation
- better manage the whole-farm system such as pasture–crop rotations

- better match land and soil types to management and selection of pasture cultivars
- monitor the effect of long-term regional climate shifts.

The spatial resolution of PfS is limited to that of the MODIS sensor, providing a resolution of approximately 250 metres square (equivalent to a pixel size of 6.25 ha). However, at the sub-paddock scale, a spatial resolution of 6 ha means a significant number of MODIS pixels in a particular paddock may be 'mixed', i.e. containing data from neighbouring paddocks, rocky outcrops, trees, etc. Fairport Farm Software has discontinued the PastureWatch service. A new version of PfS has recently been released, 'Pastures from Space Plus'. It is largely a research and teaching tool at this stage.

## 2.3 SUMMARY

The amount of solar radiation absorbed by plants is a function of the intensity and duration of incoming radiation and the crop or pasture's PAR interception capacity. Interception capacity is largely determined by plant leaf area/LAI. Monteith (1972, 1977) suggested that the net gain, by plant photosynthetic tissues, in dry matter production per unit time (net primary productivity–NPP) was linearly related to the amount of incident solar energy plants received, moderated with a number of independent efficiency terms, including the amount of solar radiation absorbed over a season and a vegetation light use efficiency (LUE) term. Because of its close relationship to LAI and *f*APAR (Myneni et al., 1997; Wang et al., 2003), NDVI can be used as an indirect measure of primary productivity. NDVI was chosen for this study because, as well as providing a measure of the relative use of photosynthetically active radiation (PAR) by plant canopies, it is cheaply and readily available from sensors such as MODIS and Landsat. MODIS imagery is available on a daily basis, composited to weekly images, thereby minimising data loss due to cloud events.

While there are a large number of vegetation indices available for monitoring the Earth's surface (Thenkabail et al., 2000), the NDVI is widely used because of its simplicity and low-cost availability. The NDVI can be easily obtained from satellite sensors such as NOAA-AVHRR, MODIS and Landsat, and provides a measure of PAR

from plant canopies (Edirisinghe et al., 2011). Despite the issues of noise and error in NDVI datasets, and the presence of numerous alternative vegetation indices designed to reduce some of these effects, the NDVI remains particularly popular for the remote sensing of vegetation phenology. In particular, MODIS vegetation indices, which are produced daily and composited at 16-day intervals and multiple spatial resolutions, can provide reliable spatial and temporal assessments of vegetation canopy greenness.

## 2.4 PADDOCK MANAGEMENT ZONES AND SITE-SPECIFIC MANAGEMENT

Precision agriculture uses the gathering, processing and analysis of high-resolution, spatially-dense, geo-referenced datasets to better inform decision making for improved management of crop and pasture production (Harmon et al., 2005). The most common approach to managing spatial variability in crops is to define and use 'management zones' in a system known as 'site-specific management' (SSM) (Plant, 2001; Taylor et al., 2007; Whelan and McBratney, 2003). SSM aims to better quantify and delineate the causes of yield variability between different parts of a paddock by creating management zones (Buttafuoco et al., 2010; Farid et al., 2016; Moral et al., 2010). Management zones are defined as areas within a paddock to which a particular management action can be applied. In general, the delineation of management zones is based on factors such as soil electrical conductivity, soil chemistry, elevation, slope and organic matter content, in combination with historical crop or pasture yields (Taylor et al., 2007; Whelan and Taylor, 2013). Using this data, paddocks can be partitioned into management classes so that each homogeneous zone receives inputs tailored to the particular soil types, landscape position and management history. A strong focus of SSM has been on improving nutrient use efficiency (Aggelopoulou et al., 2011; McCormick et al., 2009; Robertson et al., 2012; Serrano et al., 2011b, 2014). There are several data sources available to a producer that can be used to help delineate management zones. Examples in the literature range from farmer 'mud maps' (Oliver et al., 2010), yield and soil survey data (Oliver and Robertson, 2009; Simeoni et al., 2009; Sudduth et al., 2010), proximal soil sensors (Pullanagari et al., 2012; Schirrmann et al., 2011;

Serrano et al., 2010; Sun et al., 2012), and combinations of these (Castrignanò et al., 2012; Wong et al., 2010).

Several approaches have been developed using yield data coupled to remotely sensed soil and elevation information to more accurately delineate site-specific management zones. These include the use of EMI sensors which measure the capacity of the soil to conduct an electrical current and gamma radiometric emissions which provide information on soil parent materials which can be associated with changes in soil types and textures across a paddock (De Benedetto et al., 2013; Farid et al., 2016; Hedley et al., 2004; Moral et al., 2010; Rodrigues Jr et al., 2015; Song et al., 2009).

Field studies have indicated that in-season SSM-based variation of fertiliser inputs to account for differences in yield potential across a paddock can significantly improve nitrogen use efficiency (Diacono et al., 2013; Song et al., 2009). Although SSM has been largely restricted to crop management, its application in the pasture phases of mixed farming systems could be advantageous over traditional methods in terms of optimising fertiliser efficiency and pasture productivity, given that there is significant variation in pasture productivity across a paddock (Virgona and Hackney, 2008). Anderson et al. (2012) reported strong responses in biomass production and pasture quality to nitrogen differentially applied to SSM zones. The authors expected that the responses would become more evident as the season unfolded, as a result of soil moisture variation across the paddock.

## 2.5 PROXIMAL SENSING SYSTEMS

Yield monitor data or remotely sensed data sets such as the NDVI and other vegetation indices discussed above can show the variability of biomass or crop production at the sub-paddock scale at a range of resolutions (Blackmore, 2003; Robertson et al., 2008, 2009). However, determining sub-paddock scale management zones from yield maps or remotely sensed satellite data alone is problematic, as these data sets give little indication about the reasons for differences in crop performance. Biomass production within a zone over time is affected by a range of interactions between climate, biotic and abiotic factors.

Remotely sensed imagery needs to be used carefully for management zone identification because it provides only a within-season snapshot and may not relate to final crop yield.

Given the limitations of satellite remote sensing described earlier, the use of proximal sensors to monitor crop growth and crop stress has been increasing. Both grain and pasture production in Australia is often strongly dependent on soil type, particularly the capacity for the soil to retain water and subsequently release it to the plant. Therefore, defining within-field management zones based on estimates of plant available water capacity (PAWC) can be of value.

A better understanding of the spatial patterns in soil properties that cause yield/quality variation can be achieved with maps of soil variability. The use of high-accuracy GPS receivers enables geo-referencing of sensor data and permits the simultaneous collection of elevation data, which influences water movement and soil development in the local environment. Traditionally, geo-referenced manual soil sampling and laboratory analysis has involved sampling at a relatively small number of sites across a paddock due to the cost and labour intensiveness of such surveys. The relatively few sampling sites make it difficult to quantify the degree of variability in soil properties at a sufficiently high resolution for site-specific management. This in turn can make it hard to identify relationships between soil properties of agronomic interest and crop and pasture yields.

The advent of relatively low cost, proximal soil sensing technologies such as EMI, which measures the ability of the soil to conduct electricity, and gamma radiometrics, which measures naturally occurring gamma ray emitting isotopes of potassium (K), uranium (U) and thorium (Th) as they decay (Wilford, 2008), are enabling technologies for high-resolution soil mapping.

### *2.5.1 SOIL ELECTRICAL CONDUCTIVITY*

When an electrical current is applied to soil, it can be conducted via three pathways (Corwin and Lesch, 2005b):

1. A liquid phase pathway through pore-connected soil solution of water and ions.

2. A solid–liquid phase pathway primarily through exchangeable cations that are bound to the surface of clay particles.
3. A solid pathway via solid soil particles that are in direct and continuous contact with one another.

As a consequence, the soil's ability to conduct electricity is affected by soil texture (particularly clay content), mineralogy, soil moisture and drainage, the soil's cation exchange capacity (CEC), subsoil characteristics, soil organic matter, ions of dissolved salts, and soil temperature (Kitchen et al., 2005; McBratney et al., 2005). The higher the level of each of these attributes, the greater the electrical conductivity of the soil. Higher electrical conductivity values generally translate into higher fertility and hence higher yield potential. Excessively high readings tend to indicate salinity (Brevik et al., 2006; Corwin and Lesch, 2003; Kitchen et al., 2005).

Apparent soil electrical conductivity (ECa) is a depth-weighted measure of a soil's ability to conduct electricity to a specified depth (Greenhouse and Slaine, 1983). It is reported in milliSiemens per metre (mS/m). Changes in the electrical conductivity of the soil are reflected in variations in ECa.

Since an EMI sensor is measuring ECa rather than directly measuring salinity, the ECa readings must be calibrated to the traditional laboratory estimate of salinity, which is the electrical conductivity of the saturation paste extract (ECe). To convert ECa to ECe, regression of measured ECa values against laboratory ECe standards are used (Bennett et al., 2009; Corwin and Lesch, 2005a).

There are two main 'on-the-go' technologies for measuring bulk soil ECa: electromagnetic induction (EMI) and electrical resistivity (ER). Soil EC measurement by either method reportedly produces similar results (Sudduth et al., 1998). The use of electromagnetic induction instruments is the more common practice in Australia. EMI instruments such as the Geonics EM31 and EM38 (Geonics Inc., Mississauga, Ontario, Canada) use pairs of transmitting and receiving induction coils at opposite ends of the instrument.

EMI has been used to map soil properties such as salinity, water and clay content (Brevik et al., 2006; Corwin and Lesch, 2005a; Kitchen et al., 2005; Llewellyn et al.,

2010), to estimate the soil depth to underlying clay hardpans (Doolittle et al., 1994), elevation, soil pH and pasture dry matter yield (Serrano et al., 2010), and for irrigation scheduling (Hedley et al., 2013).

The variations in soil properties identified using ECa are often used to define management zones. For agricultural applications, soil properties that correlate strongly with ECa are soil salinity, clay content and soil water. However, temperature (air and soil), mineral content and clay type will affect any calibration (McBratney et al., 2005).

**FIGURE 2.3:** GEONICS EM38.

### *2.5.2 GAMMA RADIOMETRICS*

Gamma ray spectrometry is a soil sensing technique that can be performed from the air or a ground-based platform. Gamma rays are part of the natural radioactive decay process and are emitted as high-energy short wavelength electromagnetic radiation. Potassium (K), uranium (U) and thorium (Th) are the three main elements in the soil that have naturally occurring isotopes which emit gamma rays as they decay (Wilford, 2008). The rays can be detected by remote sensors because they can travel a reasonable distance in the air. Gamma radiometers measure natural emissions such as 40K, the daughter radionuclides of 238U and 232Th, and total emissions from all elements primarily from the top 40 cm of soil or rock. Emissions from the radionuclides have been used to estimate soil properties across a paddock such as clay content, topsoil texture, soil depth, soil pH, plant available potassium,

organic carbon levels and iron content (Viscarra-Rossel et al., 2007; Wong et al., 2008, 2009; Wong and Harper, 1999).

**FIGURE 2.4:** A GAMMA RADIOMETER.

### *2.5.3 COMBINING EMI AND GR SENSING*

In certain landscapes, the use of EMI sensing alone for measuring soil properties can be problematic. The occurrence of salt in the landscape can make it difficult to differentiate between clay soils and saline sandy soils since both give high ECa readings. Additionally, EMI sensing cannot distinguish sandy soils from gravels because both materials give low ECa readings. This makes it difficult to estimate soil depth and PAWC from EMI sensor outputs in landscapes containing shallow soils over gravel (Wong et al., 2009). Similarly, GR sensing cannot discriminate between soils of varying gravel and clay content as they both give strong signals. These limitations can be overcome by combining EMI sensing with gamma radiometry as complementary technologies for soil mapping and interpretation. Wong et al. (2008, 2010) used both EMI and GR sensors to map the soil properties of a West Australian cropping paddock that contained sands, clays, gravels and saline soils. By combining the ECa and GR paddock survey data, Wong et al. (2010) predicted soil characteristics in the highly weathered sands and gravel soils in the Western Australian wheatbelt using a rule-based method and derived a set of rules for

combining the interpretation of dual EM38 and GR sensor data. These rules are summarised in Table 2.3.

**TABLE 2.3:** RULES FOR INTERPRETATION OF DUAL EM38 AND GAMMA RADIOMETRIC SENSOR DATA.

| Rule number and description | $EC_a$ (mS/m) | $^{40}K$ counts (100/s) | Grower's description of soil type |
|---|---|---|---|
| 1. High–medium | >20 | <80 | Good sand |
| 2. Low–high | <15 | >80 | Shallow gravelly |
| 3. Low–low | <10 | <40 | Poor sand |
| 4. Low–medium | <15 | 40–80 | Medium sand |
| 5. High–high | >20 | >80 | Red clayey |

Source: Wong et al. (2010)

### *2.5.4 ACQUISITION OF HIGH-RESOLUTION MEASUREMENTS OF PASTURE BIOMASS USING AN NDVI PROXIMAL SENSOR*

Recently, a range of relatively low cost 'on-the-go' optical sensors for collecting geo-referenced, high-resolution data about biomass in the paddock has become available that overcome many of the constraints and drawbacks of manual measurement or estimation described above. Unlike satellite-based sensors, these devices are 'self-contained', having their own light source. The Crop Circle™ and Greenseeker® sensors are examples of these LED-based active sensors. A single LED provides both red (~650 nm) and near-infrared (NIR) (~880 nm) output (Holland et al., 2004). The NDVI, produced from these 'active optical sensors', has been extensively used in crop nitrogen management (Holland et al., 2004; Inman et al., 2005; Lamb et al., 2009; Tremblay et al., 2009). There has been considerably less research investigating the use of these sensors for measuring and managing pastures (Trotter et al., 2010a).

### *2.5.5 OTHER PROXIMAL SENSING TECHNOLOGIES*

While proximal sensors are widely used to identify potential management zones and to map soil properties such as salinity, clay and soil water content, the development of sensing technologies that can measure soil fertility and pH status for agronomic management are still in the development stage (Adamchuk et al., 2004). Recently, Veris Technologies (Salina, Kansas, USA) released a sensor to log soil organic matter, EC and CEC values 'on-the-go'. To calibrate the sensor, 'traditional' soil sampling is carried out with sample locations guided by the results from the sensor for calibrating the sensor output to laboratory-tested organic matter and CEC values. Field testing has shown the unit to have variable accuracy at this stage (Cho and Sudduth, 2016; Kweon et al., 2013; Schirrmann et al., 2011).

## 2.6 CONCLUSIONS

The continued integration of crop and legume-based pasture–livestock phases in a mixed farming system offers great benefits to Australian dryland farming systems into the future. Legume pastures are one of the few reliable means for building soil organic matter, and the emerging threat of herbicide-resistant weeds will increase the need for animals in the system in the future.

The ongoing run-down in soil fertility and soil carbon under cropping rotations (Keating and Carberry, 2010) is also likely to constrain the extent of continuous cropping rotations. The balance between crop and pasture–livestock enterprises is highly sensitive to price differentials between grain and livestock products.

Increased climate variability being observed in many of Australia's mixed crop–livestock regions will require flexible production options. In the longer term, energy prices and consequently nitrogen fertiliser prices will continue to rise, making the economics of obtaining a greater proportion of nitrogen from legumes, particularly pasture legumes, attractive.

The use of precision agriculture (PA) on a whole-of-farm basis provides farmers with the opportunity to take advantage of technologies that can improve farm efficiency and productivity through the flexible use of resources between enterprises that are facilitated by mixed farming systems. The use of PA technologies has the potential

to enable pasture–livestock phases to improve the sustainable productivity of cropping systems. However, at this stage, there is no evidence in the literature that explores the effects within a paddock through multiple cropping and pasture phases. At the moment, many producers have a significant bank of data on the cropping phase of a rotation, but virtually no data on what is happening during the pasture rotation and certainly none at the sub-paddock scale. There is no data on how livestock use a paddock over time and no data on nutrient transfers. During pasture phases, the paddock and livestock generally receive only minimal management attention. There are no measurements, at the sub-paddock scale, of the relationships between production during the cropping phase and the pasture phase.

For example, do areas of high crop production correlate with areas of high pasture production? These are significant knowledge gaps. The research described in this thesis explores some of these knowledge gaps by using readily available PA technologies to monitor and explore the relationships between crop and pasture productivity at the sub-paddock scale.

The following hypotheses were tested:

**HYPOTHESIS 1:** *Spatial variation in biomass production over time is correlated between the cropping and pasture phases of mixed farming enterprises*.

If Hypothesis 1 is proven from a preliminary analysis of remotely sensed satellite data in Chapters 3 and 4, then two further hypotheses will be tested. These are:

**HYPOTHESIS 2:** *Spatial variation of production in the crop and pasture phases of a mixed farming system can be identified and quantified at high resolution using PA technologies*.

**HYPOTHESIS 3:** *Data acquired using PA technologies can be used to create a single index of paddock productivity that describes the spatial variation in, and temporal stability of, crop and pasture production over time*.

## 2.7 REFERENCES

Aase, J., & Siddoway, F. (1981). Assessing winter wheat dry matter production via spectral reflectance measurements. *Remote Sensing of Environment*, *11*, 267–277.

Adamchuk, V. I., Hummel, J. W., Morgan, M. T., & Upadhyaya, S. K. (2004). On-the-go soil sensors for precision agriculture. *Computers and Electronics in Agriculture*, *44*(1), 71–91.

Aggelopoulou, K. D., Pateras, D., Fountas, S., Gemtos, T. A., & Nanos, G. D. (2011). Soil spatial variability and site-specific fertilization maps in an apple orchard. *Precision Agriculture*, *12*(1), 118–129.

Anderson, D. M. (2007). Virtual fencing–past, present and future. *The Rangeland Journal*, *29*(1), 65–78. doi:10.1071/RJ06036

Anderson, S., Trotter, M., Haling, R., Edwards, C., Guppy, C., & Lamb, D. (2012). *Exploring the potential for site specific nitrogen management in grazing systems*. Paper presented at the Proceedings of the 3rd Australian and New Zealand spatially enabled livestock management symposium, Lincoln University, Lincoln, New Zealand.

Angus, J. F., Bolger, T. P., Kirkegaard, J. A., & Peoples, M. B. (2006). Nitrogen mineralisation in relation to previous crops and pastures. *Soil Research*, *44*(4), 355–365. doi:10.1071/SR05138

Angus, J. F., & Peoples, M. B. (2013). Nitrogen from Australian dryland pastures. *Crop and Pasture Science*, *63*(9), 746–758.

Atzberger, C. (2013). Advances in remote sensing of agriculture: context description, existing operational monitoring systems and major information needs. *Remote Sensing*, *5*(2), 949–981.

Australian Bureau of Agricultural and Resource Economics. (2016). Retrieved 21.05.16, from http://apps.daff.gov.au/AGSURF/

Balaghi, R., Tychon, B., Eerens, H., & Jlibene, M. (2008). Empirical regression models using NDVI, rainfall and temperature data for the early prediction of wheat grain yields in Morocco. *International Journal of Applied Earth Observation and Geoinformation*, *10*(4), 438–452.

Banhazi, T. M., Lehr, H., Black, J. L., Crabtree, H., Schofield, P., Tscharke, M., & Berckmans, D. (2012). Precision livestock farming: an international review of scientific and commercial aspects. *International Journal of Agricultural and Biological Engineering*, *5*(3), 1–9.

Bannari, A., Morin, D., Bonn, F., & Huete, A. (1995). A review of vegetation indices. *Remote Sensing Reviews*, *13*(1–2), 95–120.

Baret, F., & Guyot, G. (1991). Potentials and limits of vegetation indices for LAI and APAR assessment. *Remote Sensing of Environment*, *35*(2–3), 161–173.

Baret, F., Guyot, G., & Major, D. (1989). Crop biomass evaluation using radiometric measurements. *Photogrammetria*, *43*(5), 241–256.

Barnes, P., Wilson, B. R., Trotter, M. G., Lamb, D. W., Reid, N., Koen, T., & Bayerlein, L. (2011). The patterns of grazed pasture associated with scattered trees across an Australian temperate landscape: an investigation of pasture quantity and quality. *The Rangeland Journal*, *33*(2), 121–130. doi: http://dx.doi.org/10.1071/RJ10068

Bathgate, A., & Pannell, D. J. (2002). Economics of deep-rooted perennials in western Australia. *Agricultural Water Management*, *53*(1–3), 117–132.

Bauer, M. E. (1985). Spectral inputs to crop identification and condition assessment. *Proceedings of the IEEE*, *73*(6), 1071–1085.

Bausch, W. C. (1993). Soil background effects on reflectance-based crop coefficients for corn. *Remote Sensing of Environment*, *46*(2), 213–222.

Beck, P. S. A., Atzberger, C., Høgda, K. A., Johansen, B., & Skidmore, A. K. (2006). Improved monitoring of vegetation dynamics at very high latitudes: a new method using MODIS NDVI. *Remote Sensing of Environment*, *100*(3), 321–334.

Bell, L. W., Kirkegaard, J. A., Swan, A., Hunt, J. R., Huth, N. I., & Fettell, N. A. (2011). Impacts of soil damage by grazing livestock on crop productivity. *Soil and Tillage Research*, *113*(1), 19–29. doi: 10.1016/j.still.2011.02.003

Bell, L. W., & Moore, A. D. (2011). *Mixed crop–livestock businesses reduce price- and climate-induced variability in farm returns: a model-derived case study*. Paper presented at the 5th World Congress of Conservation Agriculture incorporating 3rd Farming Systems Design Conference Brisbane, Australia.

Bell, L. W., & Moore, A. D. (2012). Integrated crop–livestock systems in Australian agriculture: trends, drivers and implications. *Agricultural Systems*, *111*, 1–12. doi: http://dx.doi.org/10.1016/j.agsy.2012.04.003

Bell, L. W., Robertson, M. J., Revell, D. K., Lilley, J. M., & Moore, A. D. (2008). Approaches for assessing some attributes of feed-base systems in mixed farming enterprises. *Australian Journal of Experimental Agriculture*, *48*(7), 789–798.

Bennett, S. J., Barrett-Lennard, E. G., & Colmer, T. D. (2009). Salinity and waterlogging as constraints to saltland pasture production: a review. *Agriculture, Ecosystems & Environment*, *129*(4), 349–360. doi: http://dx.doi.org/10.1016/j.agee.2008.10.013

Birth, G. S., & McVey, G. R. (1968). Measuring the color of growing turf with a reflectance spectrophotometer. *Agronomy Journal*, *60*(6), 640–643.

Bishop-Hurley, G. J., Swain, D. L., Anderson, D. M., Sikka, P., Crossman, C., & Corke, P. (2007). Virtual fencing applications: Implementing and testing an automated cattle control system. *Computers and Electronics in Agriculture*, *56*(1), 14–22. doi: http://dx.doi.org/10.1016/j.compag.2006.12.003

Blackmore, S. (2003). *The role of yield maps in precision farming*. (PhD), Cranfield University, Silsoe.

Bramley, R. G. V. (2009). Lessons from nearly 20 years of Precision Agriculture research, development, and adoption as a guide to its appropriate application. *Crop and Pasture Science*, *60*(3), 197–217. doi:10.1071/CP08304

Brevik, E., Fenton, T., & Lazari, A. (2006). Soil electrical conductivity as a function of soil water content and implications for soil mapping. *Precision Agriculture*, *7*(6), 393–404. doi: 10.1007/s11119-006-9021-x

Broge, N. H., & Leblanc, E. (2001). Comparing prediction power and stability of broadband and hyperspectral vegetation indices for estimation of green leaf area index and canopy chlorophyll density. *Remote Sensing of Environment*, *76*(2), 156–172.

Buttafuoco, G., Castrignanò, A., Colecchia, A. S., & Ricca, N. (2010). Delineation of management zones using soil properties and a multivariate geostatistical approach. *Italian Journal of Agronomy*, *5*(4), 323–332.

Campbell, N. A., & Arnold, G. W. (1973). The visual assessment of pasture yield. *Australian Journal of Experimental Agriculture and Animal Husbandry*, *13*(62), 263–267.

Carlson, T. N., & Ripley, D. A. (1997). On the relation between NDVI, fractional vegetation cover, and leaf area index. *Remote Sensing of Environment*, *62*(3), 241–252. doi: http://dx.doi.org/10.1016/S0034-4257(97)00104-1

Castrignanò, A., Wong, M. T. F., Stelluti, M., De Benedetto, D., & Sollitto, D. (2012). Use of EMI, gamma-ray emission and GPS height as multi-sensor data for soil characterisation. *Geoderma*, *175–176*(0), 78–89. doi: 10.1016/j.geoderma.2012.01.013

Cayley, J. W. D., & Bird, P. R. (1996). Techniques for measuring pastures: Pastoral and Veterinary Institute Hamilton, Victoria, Australia.

Chen, W., Bell, R. W., Brennan, R. F., Bowden, J., Dobermann, A., Rengel, Z., & Porter, W. (2009). Key crop nutrient management issues in the Western Australia grains industry: a review. *Australian Journal of Soil Research*, *47*(1), 1–18. doi: 10.1071/SR08097

Cho, Y., & Sudduth, K. A. (2016). *Estimation of soil properties using a VIS-NIR-EC-force probe*. Paper presented at the 13th International Conference on Precision Agriculture, St Louis, Missouri, USA.

Cierniewski, J., & Verbrugghe, M. (1997). Influence of soil surface roughness on soil bidirectional reflectance. *International Journal of Remote Sensing*, *18*(6), 1277–1288. doi: 10.1080/014311697218412

Clarke, T. R., Moran, M. S., Barnes, E. M., Pinter Jr, P. J., & Qi, J. (2001). *Planar domain indices: a method for measuring a quality of a single component in two-component pixels*. Paper presented at the International Geoscience and Remote Sensing Symposium, Sydney Australia.

Corwin, D. L., & Lesch, S. M. (2003). Application of soil electrical conductivity to precision agriculture: theory, principles, and guidelines. *Agronomy Journal*, *95*(3), 455.

Corwin, D. L., & Lesch, S. M. (2005a). Apparent soil electrical conductivity measurements in agriculture. *Computers and Electronics in Agriculture*, *46*(1–3), 11–43.

Corwin, D. L., & Lesch, S. M. (2005b). Characterizing soil spatial variability with apparent soil electrical conductivity: I. Survey protocols. *Computers and Electronics in Agriculture*, *46*(1–3), 103–133.

D'Emden, F. H., & Llewellyn, R. S. (2006). No-tillage adoption decisions in southern Australian cropping and the role of weed management. *Animal Production Science*, *46*(4), 563–569.

De Benedetto, D., Castrignanò, A., Rinaldi, M., Ruggieri, S., Santoro, F., Figorito, B., . . . Tamborrino, R. (2013). An approach for delineating homogeneous zones by using multi-sensor data. *Geoderma*, *199*, 117–127. doi: http://dx.doi.org/10.1016/j.geoderma.2012.08.028

Devadas, R., Lamb, D., Simpfendorfer, S., & Backhouse, D. (2009). Evaluating ten spectral vegetation indices for identifying rust infection in individual wheat leaves. *Precision Agriculture*, *10*(6), 459–470.

Diacono, M., Rubino, P., & Montemurro, F. (2013). Precision nitrogen management of wheat. A review. *Agronomy for Sustainable Development*, *33*(1), 219–241.

Donald, G. E., Gherardi, S. G., Edirisinghe, A., Gittins, S. P., Henry, D. A., & Mata, G. (2010). Using MODIS imagery, climate and soil data to estimate pasture growth rates on farms in the south-west of Western Australia. *Animal Production Science*, *50*(6), 611–615. doi:10.1071/AN09159

Dong, X., Vuran, M., & Irmak, S. (2013). Autonomous precision agriculture through integration of wireless underground sensor networks with center pivot irrigation systems. *Ad Hoc Networks*, *1*1(7), 1975–1987.

Doole, G. J., Bathgate, A. D., & Robertson, M. J. (2009). Labour scarcity restricts the potential scale of grazed perennial plants in the Western Australian wheatbelt. *Animal Production Science*, *49*(10), 883–893. doi:10.1071/EA08284

Doole, G. J., & Pannell, D. J. (2008). Role and value of including lucerne (*Medicago sativa* L.) phases in crop rotations for the management of herbicide-resistant *Lolium rigidum* in Western Australia. *Crop Protection*, *27*(3), 497–504.

Doolittle, J. A., Sudduth, K. A., Kitchen, N. R., & Indorante, S. J. (1994). Estimating depths to claypans using electromagnetic induction methods. *Journal of Soil and Water Conservation*, *49*(6), 572.

Dorigo, W. A., Zurita-Milla, R., de Wit, A. J. W., Brazile, J., Singh, R., & Schaepman, M. E. (2007). A review on reflective remote sensing and data assimilation techniques for enhanced agroecosystem modeling. *International Journal of Applied Earth Observation and Geoinformation*, *9*(2), 165–193. doi: 10.1016/j.jag.2006.05.003

Earle, D. F., & McGowan, A. A. (1979). Evaluation and calibration of an automated rising plate meter for estimating dry matter yield of pasture. *Australian Journal of Experimental Agriculture and Animal Husbandry*, *19*(98), 337–343.

Edirisinghe, A., Clark, D., & Waugh, D. (2012). Spatio-temporal modelling of biomass of intensively grazed perennial dairy pastures using multispectral remote sensing. *International Journal of Applied Earth Observation and Geoinformation*, *16*, 5–16.

Edirisinghe, A., Henry, D. A., Donald, G. E., & Hulm, E. (2004). Pastures from Space–assessing forage quality using remote sensing. *Animal Production in Australia*, *25*, 235.

Edirisinghe, A., Hill, M. J., Donald, G. E., & Hyder, M. (2011). Quantitative mapping of pasture biomass using satellite imagery. *International Journal of Remote Sensing*, *32*(10), 2699–2724. doi: 10.1080/01431161003743181

Farid, H. U., Bakhsh, A., Ahmad, N., Ahmad, A., & Mahmood-Khan, Z. (2016). Delineating site-specific management zones for precision agriculture. *The Journal of Agricultural Science*, *154*(02), 273–286. doi:10.1017/S0021859615000143

Farooq, M., Flower, K. C., Jabran, K., Wahid, A., & Siddique, K. H. M. (2011). Crop yield and weed management in rainfed conservation agriculture. *Soil and Tillage Research*, *117*, 172–183. doi: http://dx.doi.org/10.1016 /j.still.2011.10.001

Fillery, I. R. P., & Poulter, R. E. (2006). Use of long-season annual legumes and herbaceous perennials in pastures to manage deep drainage in acidic sandy soils in Western Australia. *Australian Journal of Agricultural Research*, *57*(3), 297–308. doi: http://dx.doi.org/10.1071/AR04278

Finger, A., Patison, K. P., Heath, B. M., & Swain, D. L. (2014). Changes in the group associations of free-ranging beef cows at calving. *Animal Production Science*, *54*(3), 270–276. doi: http://dx.doi.org/10.1071/AN12423

Fisher, J., Tozer, P., & Abrecht, D. (2012). Livestock in no-till cropping systems–a story of trade-offs. *Animal Production Science*, *52*(4), 197–214.

Fisher, P. D., Abuzar, M., Rab, M. A., Best, F., & Chandra, S. (2009). Advances in precision agriculture in south-eastern Australia. I. A regression methodology to simulate spatial variation in cereal yields using farmers' historical paddock yields and normalised difference vegetation index. *Crop and Pasture Science*, *60*(9), 844–858. doi:10.1071/CP08347

Fitzpatrick, E. A., & Nix, H. A. (1970). The climatic factor in Australian grassland ecology. In R. M. Moore (Ed.), *Australian Grasslands* (pp. 3–26). Canberra: ANU Press.

Flower, K., Crabtree, B., & Butler, G. (2008). No-till cropping systems in Australia. In T. Goddard, M. Zoebisch, Y. Gan, W. Ellis, Watson A., & S. Sombatpanit (Eds.), *No-Till Farming Systems* (Vol. 3, pp. 457–467). Bangkok, Thailand: World Association of Soil and Water Conservation.

Flowers, M., Weisz, R., & Heiniger, R. (2001). Remote sensing of winter wheat tiller density for early nitrogen application decisions. *Agronomy Journal*, *93*(4), 783–789.

Freire, R., Swain, D. L., & Friend, M. A. (2012). Spatial distribution patterns of sheep following manipulation of feeding motivation and food availability. *animal*, *6*(Special Issue 05), 846–851. doi:10.1017/S1751731111002126

Ganguli, A. C., Vermeire, L. T., Mitchell, R. B., & Wallace, M. C. (2000). Comparison of four nondestructive techniques for estimating standing crop in shortgrass plains. *Agronomy Journal*, *92*(6), 1211–1215.

Gates, D. M., Keegan, H. J., Schleter, J. C., & Weidner, V. R. (1965). Spectral properties of plants. *Applied Optics*, *4*(1), 11–20.

Gitelson, A. A., Kaufman, Y. J., Stark, R., & Rundquist, D. (2002). Novel algorithms for remote estimation of vegetation fraction. *Remote Sensing of Environment*, *80*(1), 76–87.

Glenn, E. P., Huete, A. R., Nagler, P. L., & Nelson, S. G. (2008). Relationship between remotely-sensed vegetation indices, canopy attributes and plant physiological processes: what vegetation indices can and cannot tell us about the landscape. *Sensors*, *8*(4), 2136–2160.

Goel, N. S., & Qin, W. (1994). Influences of canopy architecture on relationships between various vegetation indices and LAI and FPAR: a computer simulation. *Remote Sensing Reviews*, *10*(4), 309–347.

Gong, P., Pu, R., Biging, G. S., & Larrieu, M. R. (2003). Estimation of forest leaf area index using vegetation indices derived from Hyperion hyperspectral data. IEEE *Transactions on Geoscience and Remote Sensing*, *41*(6), 1355–1362. doi: 10.1109/TGRS.2003.812910

Gourley, C. J. P., & McGowan, A. A. (1991). Assessing differences in pasture mass with an automated rising plate meter and a direct harvesting technique. *Australian Journal of Experimental Agriculture*, *31*(3), 337–339.

Gower, S. T., Kucharik, C. J., & Norman, J. M. (1999). Direct and indirect estimation of leaf area index, f (APAR), and net primary production of terrestrial ecosystems. *Remote Sensing of Environment*, *70*(1), 29–51.

Greenhouse, J. P., & Slaine, D. D. (1983). The use of reconnaissance electromagnetic methods to map contaminant migration. *Ground Water Monitoring & Remediation*, *3*(2), 47–59. doi: 10.1111/j.1745-6592.1983.tb01199.x

Haboudane, D., Miller, J. R., Pattey, E., Zarco-Tejada, P. J., & Strachan, I. B. (2004). Hyperspectral vegetation indices and novel algorithms for predicting green LAI of crop canopies: modeling and validation in the context of precision agriculture. *Remote Sensing of Environment*, *90*(3), 337–352.

Handcock, R. N., Swain, D. L., Bishop-Hurley, G. J., Patison, K. P., Wark, T., Valencia, P., . . . O'Neill, C. J. (2009). Monitoring animal behaviour and environmental interactions using wireless sensor networks, GPS collars and satellite remote sensing. *Sensors*, *9*(5), 3586–3603.

Haydock, K. P., & Shaw, N. H. (1975). The comparative yield method for estimating dry matter yield of pasture. *Australian Journal of Experimental Agriculture and Animal Husbandry*, *15*(76), 663–670.

Hayes, R., Dear, B., Li, G., Virgona, J., Conyers, M., Hackney, B., & Tidd, J. (2010). Perennial pastures for recharge control in temperate drought-prone environments. Part 1: productivity, persistence and herbage quality of key species. *New Zealand Journal of Agricultural Research*, *53*(4), 283–302.

Headley, R. (2012). Landsat: A Global Land-Imaging Project. US Geological Survey.

Hedley, C. (2015). The role of precision agriculture for improved nutrient management on farms. *Journal of the Science of Food and Agriculture*, *95*(1), 12–19. doi: 10.1002/jsfa.6734

Hedley, C. B., Roudier, P., Yule, I. J., Ekanayake, J., & Bradbury, S. (2013). Soil water status and water table depth modelling using electromagnetic surveys for precision irrigation scheduling. *Geoderma*, *199*(0), 22–29. doi: http://dx.doi.org/10.1016/j.geoderma.2012.07.018

Hedley, C. B., Yule, I. J., Eastwood, C. R., Shepherd, T. G., & Arnold, G. (2004). Rapid identification of soil textural and management zones using electromagnetic induction sensing of soils. *Soil Research*, *42*(4), 389–400. doi: http://dx.doi.org/10.1071/SR03149

Herridge, D. F., Peoples, M. B., & Boddey, R. M. (2008). Global inputs of biological nitrogen fixation in agricultural systems. *Plant and Soil*, *311*(1), 1–18.

Hill, M. J., Donald, G. E., Hyder, M. W., & Smith, R. C. G. (2004). Estimation of pasture growth rate in the south west of Western Australia from AVHRR NDVI and climate data. *Remote Sensing of Environment*, *93*(4), 528–545.

Holland, K., Schepers, J., Shanahan, J., Horst, G., & Mulla, D. (2004). *Plant canopy sensor with modulated polychromatic light source*. Paper presented at the Proceedings of the 7th International Conference on Precision Agriculture and Other Precision Resources Management, Hyatt Regency, Minneapolis, MN, USA, 25–28 July, 2004.

Huete, A., Justice, C., & Liu, H. (1994). Development of vegetation and soil indices for MODIS-EOS. *Remote Sensing of Environment*, *49*(3), 224–234.

Huete, A. R. (1988). A soil-adjusted vegetation index (SAVI). *Remote Sensing of Environment*, *25*(3), 295–309.

Huete, A. R., Didan, K., Miura, T., Rodriguez, E. P., Gao, X., & Ferreira, L. G. (2002). Overview of the radiometric and biophysical performance of the MODIS vegetation indices. *Remote Sensing of Environment*, *83*(1–2), 195–213. doi: 10.1016/s0034-4257(02)00096-2

Huete, A. R., Didan, K., van Leeuwen, W., Miura, T., & Glenn, E. (2011). MODIS vegetation indices. In B. Ramachandran, C. O. Justice, & M. J. Abrams (Eds.), *Land Remote Sensing and Global Environmental Change* (pp. 579–602): Springer.

Huete, A. R., Justice, C., & van Leeuwen, W. (1999). MODIS vegetation index (MOD13) algorithm theoretical basis document. Retrieved from: http://modis.gsfc.nasa.gov/data/atbd/atbd_mod13.pdf

Hutchings, N. (1991). Spatial heterogeneity and other sources of variance in sward height as measured by the sonic and HFRO sward sticks. *Grass and Forage Science, 46*(3), 277–282.

Inman, D., Khosla, R., & Mayfield, T. (2005). On-the-go active remote sensing for efficient crop nitrogen management. *Sensor Review*, *25*(3), 209–214.

Jensen, J. R. (2005). *Introductory digital image processing: a remote sensing perspective* (3 ed.). Upper Saddle River: Prentice Hall.

Ji, L., & Peters, A. J. (2007). Performance evaluation of spectral vegetation indices using a statistical sensitivity function. *Remote Sensing of Environment*, *106*(1), 59–65. doi: http://dx.doi.org/10.1016/j.rse.2006.07.010

Jones, H. G., & Vaughan, R. A. (2010). *Remote Sensing of Vegetation*. Oxford: Oxford University Press.

Jordan, C. F. (1969). Derivation of leaf-area index from quality of light on the forest floor. *Ecology*, *vol*, 663–666.

Justice, C. O., Townshend, J. R. G., Vermote, E. F., Masuoka, E., Wolfe, R. E., Saleous, N., . . . Morisette, J. T. (2002). An overview of MODIS Land data processing and product status. *Remote Sensing of Environment*, *83*(1–2), 3–15. doi: 10.1016/s0034-4257(02)00084-6

Kastens, J. H., Kastens, T. L., Kastens, D. L. A., Price, K. P., Martinko, E. A., & Lee, R. Y. (2005). Image masking for crop yield forecasting using AVHRR NDVI time series imagery. *Remote Sensing of Environment*, *99*(3), 341–356.

Keating, B. A., & Carberry, P. S. (2010). Emerging opportunities and challenges for Australian broadacre agriculture. *Crop and Pasture Science*, *61*(4), 269–278. doi:10.1071/CP09282

Kirkegaard, J. A., Conyers, M. K., Hunt, J. R., Kirkby, C. A., Watt, M., & Rebetzke, G. J. (2014). Sense and nonsense in conservation agriculture: principles, pragmatism and productivity in Australian mixed farming systems. *Agriculture, Ecosystems & Environment*, *187*(0), 133–145. doi: http://dx.doi.org /10.1016/j.agee.2013.08.011

Kirkegaard, J. A., Peoples, M. B., Angus, J. F., & Unkovich, M. J. (2011). Diversity and evolution of rainfed farming systems in southern Australia. In P. Tow, I. Cooper, I. Partridge, & C. Birch (Eds.), *Rainfed Farming Systems* (pp. 715–754). Dordrecht: Springer Netherlands.

Kitchen, N. R., Sudduth, K. A., Myers, D. B., Drummond, S. T., & Hong, S. Y. (2005). Delineating productivity zones on claypan soil fields using apparent soil electrical conductivity. *Computers and Electronics in Agriculture*, *46*(1–3), 285–308.

Kweon, G., Lund, E., & Maxton, C. (2013). Soil organic matter and cation-exchange capacity sensing with on-the-go electrical conductivity and optical sensors. *Geoderma*, *199* (May), 80–89. doi: http://dx.doi.org/10.1016 /j.geoderma.2012.11.001

Labus, M., Nielsen, G., Lawrence, R., Engel, R., & Long, D. (2002). Wheat yield estimates using multi-temporal NDVI satellite imagery. *International Journal of Remote Sensing*, *23*(20), 4169–4180.

Laca, E. A. (2009). New approaches and tools for grazing management. *Rangeland Ecology & Management*, *62*(5), 407–417. doi: 10.2111/08-104.1

Lamb, D. W., Steyn-Ross, M., Schaare, P., Hanna, M. M., Silvester, W., & Steyn-Ross, A. (2002). Estimating leaf nitrogen concentration in ryegrass (*Lolium* spp.) pasture using the chlorophyll red-edge: theoretical modelling and experimental observations. *International Journal of Remote Sensing*, *23*(18), 3619–3648.

Lamb, D. W., Trotter, M. G., & Schneider, D. A. (2009). Ultra low-level airborne (ULLA) sensing of crop canopy reflectance: a case study using a CropCircle(TM) sensor. *Computers and Electronics in Agriculture*, *69*(1), 86–91.

Lee, H. J., Kawamura, K., Watanabe, N., Sakanoue, S., Sakuno, Y., Itano, S., & Nakagoshi, N. (2011). Estimating the spatial distribution of green herbage biomass and quality by geostatistical analysis with field hyperspectral measurements. *Grassland Science*, *57*(3), 142–149.

Llewellyn, R., Whitbread, A., Jones, B., & Davoren, B. (2010). *The role for EM mapping in precision agriculture in the Mallee*. Paper presented at the 15th Agronomy Conference "Food Security from Sustainable Agriculture", Lincoln, New Zealand.

Love, G. (2004). *Implications of climate change for climate variability*. Paper presented at the ABARE Outlook Conference, 2004, Canberra.

Markham, B. L., Storey, J. C., Williams, D. L., & Irons, J. R. (2004). Landsat sensor performance: history and current status. *IEEE Transactions on Geoscience and Remote Sensing*, *42*(12), 2691–2694.

Marques Da Silva, J. R., Peça, J. O., Serrano, J. M., De Carvalho, M. J., & Palma, P. M. (2008). Evaluation of spatial and temporal variability of pasture based on topography and the quality of the rainy season. *Precision Agriculture*, *9*(4), 209–229.

McBratney, A. B., Minasny, B., & Whelan, B. M. (2005). *Obtaining 'useful' high-resolution soil data from proximally sensed electrical conductivity/resistivity (PSEC/R) surveys*. Paper presented at the 5th European Conference on Precision Agriculture, ECPA 2005, Uppsala, Sweden.

McCormick, S., Jordan, C., & Bailey, J. (2009). Within and between-field spatial variation in soil phosphorus in permanent grassland. *Precision Agriculture*, *10*(3), 262–276.

Meroni, M., Marinho, E., Sghaier, N., Verstrate, M. M., & Leo, O. (2013). Remote sensing based yield estimation in a stochastic framework–case study of durum wheat in Tunisia. *Remote Sensing*, *5*(2), 539–557.

Moges, S. M., Raun, W. R., Mullen, R. W., Freeman, K. W., Johnson, G. V., & Solie, J. B. (2005). Evaluation of green, red, and near infrared bands for predicting winter wheat biomass, nitrogen uptake and final grain yield. *Journal of Plant Nutrition*, *27*(8), 1431–1441.

Monteith, J. L. (1972). Solar radiation and productivity in tropical ecosystems. *Journal of Applied Ecology*, *9*(3), 747–766.

Monteith, J. L. (1977). Climate and the efficiency of crop production in Britain. *Philosophical Transactions of the Royal Society of London, 281*(980), 277–294.

Moral, F., Terrón, J., & Silva, J. (2010). Delineation of management zones using mobile measurements of soil apparent electrical conductivity and multivariate geostatistical techniques. *Soil and Tillage Research*, *106*(2), 335–343.

Mulla, D. J. (2013). Twenty five years of remote sensing in precision agriculture: key advances and remaining knowledge gaps. *Biosystems Engineering*, *114*(4), 358–371. doi: http://dx.doi.org/10.1016/j.biosystemseng.2012.08.009

Myneni, R. B., Ramakrishna, R., Nemani, R. R., & Running, S. W. (1997). Estimation of global leaf area index and absorbed PAR using radiative transfer models. *Geoscience and Remote Sensing, IEEE Transactions on Geoscience and Remote Sensing*, *35*(6), 1380–1393.

Nichols, P. G. H., Loi, A., Nutt, B. J., Evans, P. M., Craig, A. D., Pengelly, B. C., . . . You, M. P. (2007). New annual and short-lived perennial pasture legumes for Australian agriculture –15 years of revolution. *Field Crops Research*, *104*(1–3), 10–23.

Oliver, Y. M., & Robertson, M. J. (2009). Quantifying the benefits of accounting for yield potential in spatially and seasonally responsive nutrient management in a mediterranean climate. *Australian Journal of Soil Research*, *47*(1), 114–126. doi:10.1071/SR08099

Oliver, Y. M., Robertson, M. J., & Wong, M. T. F. (2010). Integrating farmer knowledge, precision agriculture tools, and crop simulation modelling to evaluate management options for poor-performing patches in cropping fields. *European Journal of Agronomy*, *32*(1), 40–50.

Ollinger, S. V. (2011). Sources of variability in canopy reflectance and the convergent properties of plants. *New Phytologist*, *189*(2), 375–394. doi: 10.1111/j.1469-8137.2010.03536.x

Owen, M. J., Goggin, D. E., & Powles, S. B. (2015). Intensive cropping systems select for greater seed dormancy and increased herbicide resistance levels in *Lolium rigidum* (annual ryegrass). *Pest Management Science*, *71*(7), 966–971. doi: 10.1002/ps.3874

Owen, M. J., Martinez, N. J., & Powles, S. B. (2014). Multiple herbicide-resistant *Lolium rigidum* (annual ryegrass) now dominates across the Western Australian grain belt. *Weed Research*, *54*(3), 314–324. doi: 10.1111/wre.12068

Peoples, M. B., Brockwell, J., Hunt, J. R., Swan, A. D., Watson, L., Hayes, R. C., . . . Fillery, I. R. P. (2012). Factors affecting the potential contributions of $N_2$ fixation by legumes in Australian pasture systems. *Crop and Pasture Science*, *63*(9), 759–786. doi: http://dx.doi.org/10.1071/CP12123

Plant, R. (2001). Site-specific management: the application of information technology to crop production. *Computers and Electronics in Agriculture*, *30*(1), 9–29.

Ponce, G., Moran, S., Huete, A., Bresloff, C., Huxman, T., Bosch, D., . . . Heartsill, T. (2011). Convergence of dynamic vegetation net productivity responses to precipitation variability from 10 years of MODIS EVI. Paper presented at the 34th International Symposium on Remote Sensing of Environment – The GEOSS Era: Towards Operational Environmental Monitoring.

Prasad, A., Singh, R., Tare, V., & Kafatos, M. (2007). Use of vegetation index and meteorological parameters for the prediction of crop yield in India. *International Journal of Remote Sensing*, *28*(23), 5207–5235.

Pullanagari, R. R., Yule, I. J., Tuohy, M. P., Hedley, M. J., Dynes, R. A., & King, W. M. (2012). Proximal sensing of the seasonal variability of pasture nutritive value using multispectral radiometry. *Grass and Forage Science*. doi: 10.1111/j.1365-2494.2012.00877.x

Quarmby, N., Milnes, M., Hindle, T., & Silleos, N. (1993). The use of multi-temporal NDVI measurements from AVHRR data for crop yield estimation and prediction. *International Journal of Remote Sensing*, *14*(2), 199–210.

Rainbow, R., & Derpsch, R. (2011). Advances in no-till farming technologies and soil compaction management in rainfed farming systems. In P. Tow, I. Cooper, I. Partridge, & C. Birch (Eds.), *Rainfed Farming Systems* (pp. 991–1014). Dordrecht: Springer Netherlands.

Rembold, F., Atzberger, C., Savin, I., & Rojas, O. (2013). Using low resolution satellite imagery for yield prediction and yield anomaly detection. *Remote Sensing*, *5*(4), 1704–1733.

Renton, M., & Flower, K. C. (2015). Occasional mouldboard ploughing slows evolution of resistance and reduces long-term weed populations in no-till systems. *Agricultural Systems*, *139*, 66–75.

Reynolds, C., Yitayew, M., Slack, D., Hutchinson, C., Huete, A., & Petersen, M. (2000). Estimating crop yields and production by integrating the FAO Crop Specific Water Balance model with real-time satellite data and ground-based ancillary data. *International Journal of Remote Sensing*, *21*(18), 3487–3508.

Robertson, M. J., Llewellyn, R. S., Mandel, R., Lawes, R., Bramley, R. G. V., Swift, L., . . . O'Callaghan, C. (2012). Adoption of variable rate fertiliser application in the Australian grains industry: status, issues and prospects. *Precision Agriculture*, *13*(2), 181–199.

Robertson, M. J., Lyle, G., & Bowden, J. W. (2008). Within-field variability of wheat yield and economic implications for spatially variable nutrient management. *Field Crops Research*, *105*(3), 211–220.

Robinson, N. J., Rampant, P. C., Callinan, A. P. L., Rab, M. A., & Fisher, P. D. (2009). Advances in precision agriculture in south-eastern Australia. II. Spatio-temporal prediction of crop yield using terrain derivatives and proximally sensed data. *Crop and Pasture Science*, *60*(9), 859–869. doi:10.1071/CP08348

Rodrigues Jr, F. A., Bramley, R. G. V., & Gobbett, D. L. (2015). Proximal soil sensing for Precision Agriculture: simultaneous use of electromagnetic induction and gamma radiometrics in contrasting soils. *Geoderma*, *243–244*, 183–195. doi: http://dx.doi.org/10.1016/j.geoderma.2015.01.004

Rondeaux, G., et al. (1996). Optimization of soil-adjusted vegetation indices. *Remote Sensing of Environment, 55*(2), 95–107.

Rook, A. J., Dumont, B., Isselstein, J., Osoro, K., WallisDeVries, M. F., Parente, G., & Mills, J. (2004). Matching type of livestock to desired biodiversity outcomes in pastures-a review. *Biological Conservation*, *119*(2), 137–150.

Roujean, J., & Breon, F. (1995). Estimating PAR absorbed by vegetation from bidirectional reflectance measurements. *Remote Sensing of Environment*, *51*(3), 375–384. doi: 10.1016/0034-4257(94)00114-3

Rouse, J. W., Haas, R. H., Schell, J. A., & Deering, D. W. (1973). *Monitoring vegetation systems in the Great Plains with ERTS*. Paper presented at the Third Earth Resources Technology Satellite-1 Symposium, Washington, DC.

Schellberg, J., Hill, M. J., Gerhards, R., Rothmund, M., & Braun, M. (2008). Precision agriculture on grassland: applications, perspectives and constraints. *European Journal of Agronomy*, *29*(2–3), 59–71.

Schirrmann, M., Gebbers, R., Kramer, E., & Seidel, J. (2011). Soil pH mapping with an on-the-go sensor. *Sensors*, *11*(1), 573–598.

Serrano, J., Marques da Silva, J., & Shahidian, S. (2014). Spatial and temporal patterns of potassium on grazed permanent pastures–management challenges. *Agriculture, Ecosystems & Environment*, *188*, 29–39. doi: http://dx.doi.org/10.1016/j.agee.2014.02.012

Serrano, J. M., Peça, J. O., Marques da Silva, J., & Shahidian, S. (2011a). Calibration of a capacitance probe for measurement and mapping of dry matter yield in mediterranean pastures. *Precision Agriculture*, *12*(6), 860–875.

Serrano, J. M., Peça, J. O., Marques da Silva, J. R., & Shahidian, S. (2011b). Spatial and temporal stability of soil phosphate concentration and pasture dry matter yield. *Precision Agriculture*, *12*(2), 214–232.

Serrano, J. M., Peça, J. O., Marques da Silva, J. R., & Shaidian, S. (2010). Mapping soil and pasture variability with an electromagnetic induction sensor. *Computers and Electronics in Agriculture*, *73*(1), 7–16.

Simeoni, M. A., Galloway, P. D., O'Neil, A. J., & Gilkes, R. J. (2009). A procedure for mapping the depth to the texture contrast horizon of duplex soils in south-western Australia using ground penetrating radar, GPS and kriging. *Soil Research*, *47*(6), 613–621. doi:10.1071/SR08241

Song, X., Wang, J., Huang, W., Liu, L., Yan, G., & Pu, R. (2009). The delineation of agricultural management zones with high resolution remotely sensed data. *Precision Agriculture*, *10*(6), 471–487. doi: http://dx.doi.org/10.1007/s11119-009-9108-2

Sudduth, K. A., Fraisse, C. W., Drummond, S. T., & Kitchen, N. R. (1998). *Integrating spatial data collection, modeling and analysis for precision agriculture*. Paper presented at the First International Conference on Geospatial Information in Agriculture and Forestry, Lake Buena Vista, Florida.

Sudduth, K. A., Kitchen, N. R., Chung, S. O., & Drummond, S. T. (2010). *Site-specific compaction, soil physical property, and crop yield relationships for claypan soils*. Paper presented at the American Society of Agricultural and Biological Engineers Annual International Meeting 2010.

Sun, W., Whelan, B. M., Minasny, B., & McBratney, A. B. (2012). Evaluation of a local regression kriging approach for mapping apparent electrical conductivity of soil (ECa) at high resolution. *Journal of Plant Nutrition and Soil Science*, *175*(2), 212–220. doi: 10.1002/jpln.201100005

Suzuki, Y., Okamoto, H., Takahashi, M., Kataoka, T., & Shibata, Y. (2012). Mapping the spatial distribution of botanical composition and herbage mass in pastures using hyperspectral imaging. *Grassland Science*, *58*, 1–7.

Taylor, J. A., McBratney, A. B., & Whelan, B. M. (2007). Establishing management classes for broadacre agricultural production. *Agronomy Journal*, *99*(5), 1366–1376. doi: 10.2134/agronj2007.0070

Thenkabail, P. S. (2003). Biophysical and yield information for precision farming from near-real-time and historical Landsat TM images. *International Journal of Remote Sensing*, *24*(14), 2879–2904.

Thenkabail, P. S., Smith, R. B., & De Pauw, E. (2000). Hyperspectral vegetation indices and their relationships with agricultural crop characteristics. *Remote Sensing of Environment*, *71*(2), 158–182.

Tremblay, N., Wang, Z., Ma, B. L., Belec, C., & Vigneault, P. (2009). A comparison of crop data measured by two commercial sensors for variable-rate nitrogen application. *Precision Agriculture*, *10*(2), 145–161.

Trotter, M., & Lamb, D. (2008). *GPS tracking for monitoring animal, plant and soil interactions in livestock systems*. Paper presented at the 9th International Conference on Precision Agriculture, Denver, Colorado, USA.

Trotter, M. G. (2010). *Precision agriculture for pasture, rangeland and livestock systems*. Paper presented at the 15th Australian agronomy conference "Food Security from Sustainable Agriculture" Lincoln, New Zealand.

Trotter, M. G., Lamb, D. W., Donald, G. E., & Schneider, D. A. (2010a). Evaluating an active optical sensor for quantifying and mapping green herbage mass and growth in a perennial grass pasture. *Crop and Pasture Science*, *61*(5), 389–398.

Trotter, M. G., Lamb, D. W., Hinch, G. N., & Guppy, C. N. (2010b). Global navigation satellite system livestock tracking: system development and data interpretation. *Animal Production Science*, *50*(6), 616–623. doi:10.1071/AN09203

Trotter, M. G., Lamb, D. W., Hinch, G. N., & Guppy, C. N. (2010c). GNSS tracking of livestock: towards variable fertilizer strategies for the grazing industry. Paper presented at the 10th International Conference on Precision Agriculture, Denver Colorado.

Trotter, T. F., Frazier, P., Trotter, M. G., & Lamb, D. W. (2008). *Objective biomass assessment using an active plant sensor (Crop Circle), preliminary experiences on a variety of agricultural landscapes*. Paper presented at the 9th International Conference on Precision Agriculture, Denver Colorado.

Tsutsumi, M., & Itano, S. (2005). Variant of estimation method of above-ground plant biomass in grassland with gamma model 1. Use of an electronic capacitance probe. *Grassland Science*, *51*(4), 275–279.

Tucker, C., Holben, B., Elgin Jr, J., & Mcmurtrey III, J. (1980). Relationship of spectral data to grain yield variation. *Photogrammetric Engineering and Remote Sensing*, *46*, 657–666

Tucker, C. J. (1979). Red and photographic infrared linear combinations for monitoring vegetation. *Remote Sensing of Environment*, *8*(2), 127–150.

Tucker, C. J., Holben, B. N., Elgin, J. H., & McMurtrey, J. E. (1981). Remote sensing of total dry-matter accumulation in winter wheat. *Remote Sensing of Environment*, *11*, 171–189.

Tucker, C. J., & Sellers, P. J. (1986). Satellite remote sensing of primary production. *International Journal of Remote Sensing*, *7*(11), 1395–1416.

Tucker, C. J., Slayback, D. A., Pinzon, J. E., Los, S. O., Myneni, R. B., & Taylor, M. G. (2001). Higher northern latitude normalized difference vegetation index and growing season trends from 1982 to 1999. *International Journal of Biometeorology*, *45*(4), 184–190.

Tullberg, J. N., Yule, D. F., & McGarry, D. (2007). Controlled traffic farming–from research to adoption in Australia. *Soil and Tillage Research*, *97*(2), 272–281. doi: 10.1016/j.still.2007.09.007

Umstatter, C. (2011). The evolution of virtual fences: A review. Computers and *Electronics in Agriculture*, *75*(1), 10–22. doi: http://dx.doi.org/10.1016/j.compag.2010.10.005

Verburg, K., Bond, W. J., Brennan, L. E., & Robertson, M. J. (2008). An evaluation of the tactical use of lucerne phase farming to reduce deep drainage. *Crop and Pasture Science*, *58*(12), 1142–1158.

Verhoef, W. (1984). Light scattering by leaf layers with application to canopy reflectance modeling: the SAIL model. *Remote Sensing of Environment*, *16*(2), 125–141.

Vickery, P. J., Bennett, I. L., & Nicol, G. R. (1980). An improved electronic capacitance meter for estimating herbage mass. *Grass and Forage Science*, *35*(3), 247–252.

Virgona, J., & Hackney, B. (2008). *Within-paddock variation in pasture growth: landscape and soil factors*. Paper presented at the 14th Australian Agronomy Conference, "Global Issues, Paddock Action", Adelaide, South Australia.

Viscarra-Rossel, R. A., Taylor, H. J., & McBratney, A. B. (2007). Multivariate calibration of hyperspectral γ-ray energy spectra for proximal soil sensing. *European Journal of Soil Science*, *58*(1), 343–353.

Wagle, P., et al. (2014). Sensitivity of vegetation indices and gross primary production of tallgrass prairie to severe drought. *Remote Sensing of Environment*, *152,* 1–14.

Wall, L., Larocque, D., & Léger, P.-M. (2008). The early explanatory power of NDVI in crop yield modelling. *International Journal of Remote Sensing*, *29*(8), 2211–2225.

Wang, P., Zhu, Q., Wu, M., Liu, S., & Shuai, X. (2003). Research on the relationships among FAPAR, LAI, Vis in the winter wheat canopy. *Remote Sensing Information*, *3*, 19–22.

Warn, L. K., McViegh, P., Semmler, A., McLarty, G. R., Sale, P., Frame, H. R., . . . Jones, L. (2003). *Grazing management for productive hill country pastures: The Broadford grazing experiment 1998–2002*. Melbourne: Department of Primary Industries.

Whelan, B., & Taylor, J. (2013). *Precision Agriculture for Grain Production Systems*: CSIRO Publishing.

Whelan, B. M., & McBratney, A. B. (2003). *Definition and interpretation of potential management zones in Australia*. Paper presented at the 11th Australian Agronomy Conference: "Solutions for a better environment", Geelong, Victoria.

White, R., Christy, B., Ridley, A., Okom, A., Murphy, S., Johnston, W., . . . Johnson, I. (2003). SGS Water Theme: influence of soil, pasture type and management on water use in grazing systems across the high rainfall zone of southern Australia. *Animal Production Science*, *43*(8), 907–926.

Wilford, J. (2008). Remote sensing with gamma-ray spectrometry. In N. J. McKenzie, M. J. Grundy, R. Webster, & A. J. Ringrose-Voase (Eds.), *Guidelines for surveying soil and land resources* (pp. 189–202). Collingwood, Victoria, Australia: CSIRO Publishing.

Wong, M. T. F., Asseng, S., Robertson, M. J., & Oliver, Y. M. (2008). Mapping subsoil acidity and shallow soil across a field with information from yield maps, geophysical sensing and the grower. *Precision Agriculture*, *9*(1), 3–15. doi: 10.1007/s11119-008-9052-6

Wong, M. T. F., & Harper, R. J. (1999). Use of on-ground gamma-ray spectrometry to measure plant-available potassium and other topsoil attributes. *Australian Journal of Soil Research*, *37*(2), 267–278. doi:10.1071/S98038

Wong, M. T. F., Oliver, Y. M., & Robertson, M. J. (2009). Gamma radiometric assessment of soil depth across a landscape not measurable using electromagnetic surveys. *Soil Science Society of America Journal*, *73*(4), 1261–1267.

Wong, M. T. F., Wittwer, K., Oliver, Y. M., & Robertson, M. J. (2010). Use of EM38 and gamma ray spectrometry as complementary sensors for high-resolution soil property mapping. In R. Viscarra-Rossel (Ed.), *Proximal Soil Sensing* (pp. 343–349): Springer Science.

Xu, Q., Yang, G., Long, H., Wang, C., Li, X., & Huang, D. (2014). Crop information identification based on MODIS NDVI time-series data. *Nongye Gongcheng*

*Xuebao/Transactions of the Chinese Society of Agricultural Engineering*, *30*(11), 134–144. doi: 10.3969/j.issn.1002-6819.2014.11.017

Zhao, D., Starks, P. J., Brown, M. A., Phillips, W. A., & Coleman, S. W. (2007). Assessment of forage biomass and quality parameters of bermudagrass using proximal sensing of pasture canopy reflectance. *Grassland Science*, *53*(1), 39–49.

Zhao, H., Yang, Z., Di, L., Li, L., & Zhu, H. (2009). *Crop phenology date estimation based on NDVI derived from the reconstructed MODIS daily surface reflectance data*. Paper presented at the 17th International Conference on Geoinformatics.

Zwiggelaar, R. (1998). A review of spectral properties of plants and their potential use for crop/weed discrimination in row-crops. *Crop Protection*, *17*(3), 189–206.

# CHAPTER 3. TEMPORAL AND SPATIAL CORRELATION OF PASTURE AND CROP BIOMASS WITHIN PADDOCKS USING MODIS NDVI

## 3.1 INTRODUCTION

As discussed in Chapter 2, there is little information available regarding the relationships between the spatial variation of biomass production in both the cropping and pasture phases of a paddock rotation in Australian mixed farming systems, particularly at the sub-paddock scale. For the most part, paddocks in the pasture phase tend to be managed as single units, ignoring the existence of productivity gradients across the landscape (Hill et al., 1999).

While historical data on spatial variation in crop yields is available from producers who use properly calibrated yield monitors during harvest, there are no long-term records of paddock pasture 'yields', particularly at the sub-paddock scale, held by producers. Measurements of pasture productivity have historically relied on harvesting, drying and weighing samples from quadrats, which is a time-consuming and expensive task.

An alternative approach to measuring crop and pasture yield is to use the spatial variation in remotely sensed biomass as a surrogate for yield. In an Australian context, the agronomic basis to using remote sensing of biomass to forecast crop yields has been discussed by Smith et al. (1995), Perry et al. (2013) and Schutt et al. (2009) and for pasture yields by Hill et al. (2004), Donald et al. (2010a) and Edirisinghe et al. (2011). The advantage of this approach is that remotely sensed spectral reflectance indices can be used to estimate crop and pasture biomass. The NDVI itself (like other remotely sensed vegetation indices) is not an intrinsic physical quality of plants. It is an optical measure of canopy greenness, being comprised of a mathematical combination of spectral bands. While a platform such as Landsat 7 TM/ETM+ (30 m spatial resolution) provides higher resolution data than MODIS (Headley, 2012), the temporal coverage (every 16 days) combined with the higher probability of cloud contamination (Ju and Roy, 2008) can restrict the availability of

Landsat images to just a few scenes each year. This would have limited the analysis. Additionally, there have been image quality issues with Landsat 7 since 2003, due to an irreparable fault in the satellite's sensors (Chapter 2, p. 17). MODIS NDVI data was therefore chosen as a proxy measure of biomass production.

The objective described in this and the following chapter was to investigate the nature of the relationship in spatial variation between pasture and crop yields using MODIS NDVI as an indirect measure of changes in biomass at the sub-paddock scale in two different regions of Australia and across a range of seasons. Having many years of historical MODIS satellite images available meant that sufficient seasons of data could be obtained to describe paddock performance.

This chapter tested Hypothesis 1 (Chapter 2, p. 36) that, "*spatial variation in biomass production over time is correlated between the cropping and pasture phases of mixed farming enterprises*". This chapter describes the study sites and the initial testing of the hypothesis using low-resolution MODIS NDVI data.

## 3.2 MATERIALS AND METHODS

### *3.2.1 STUDY SITES*

Two properties were used for the study: "Milroy", a 1900 ha sheep and cropping enterprise located at Brookton (32.22$^{o}$S, 116.57$^{o}$E), 120 km east of Perth, WA and "Grandview", a 2250 ha cattle and cropping enterprise located 10 km south of Yarrawonga (36.05$^{o}$S, 145.60$^{o}$E) in north-eastern Victoria (Figure 3.1). Wheat (*Triticum* spp.) and canola (*Brassica napus* L.) are the main crops grown on both properties.

"Milroy" has a mean annual and growing season (April–October) rainfall of 437 mm and 357 mm, respectively (Australian Bureau of Meteorology (BOM), Brookton patched-point data 1970–2000). Rainfall is winter dominant. The mean daily maximum temperature is 24.1°C and the mean daily minimum temperature is 9.8°C. Growing season temperatures range from a mean maximum of 20.2°C to a mean minimum of 7.0°C. "Grandview" has a mean annual and growing season (April–October) rainfall of 539 mm and 359 mm, respectively (BOM Yarrawonga data-drill 1970–2000). Rainfall is winter dominant. The mean daily maximum

temperature is 22.0°C and the mean daily minimum temperature is 8.9°C. Growing season temperatures range from a mean maximum of 17.8°C to a mean minimum of 5.9°C.

Detailed rainfall data is shown in Table 3.1.

On each property, three paddocks were identified that had historically been in pasture/crop rotations. Pastures on "Milroy" are predominantly self-sown and dominated by subterranean clover (*Trifolium subterraneum* L.) and capeweed (*Arctotheca calendula* L.) with some serradella (*Ornithopus sativus* Brot.), barley grass (*Hordeum glaucum* Steud.) and annual ryegrass (*Lolium rigidum* Gaud.). After a continuous cropping rotation (three years or more), annual pastures at "Milroy" are generally re-sown. At "Grandview", the crop and pasture phases are each of six years' duration. Pastures comprise lucerne (*Medicago sativa* L.), subterranean clover and chicory (*Chicorium intybus* L.), and are established by undersowing with the crop in the last cropping year. Pasture and crop rotations across the three selected paddocks at each property are described in Table 3.2.

At "Milroy", soil landscapes fall within the Pingelly subsystems Pn_1 and Pn_3u. Pn_1 is described as "gravelly hill crests and upper slopes with sandy gravels and small areas of pale deep sands and loamy gravels". Pn_3u is described as "mainly sandy and loamy duplexes with some loamy earths, coarse granitic sands, doleritic clay loams and shallow gravelly rises. Mainly York Gum, Jam and Wandoo woodland" (Verboom and Galloway 2004). Soils at "Grandview" comprise brown sodosols and patches of vertosols (Isbell 2016) with surface soils of stony sandy loams and sandy clay loams.

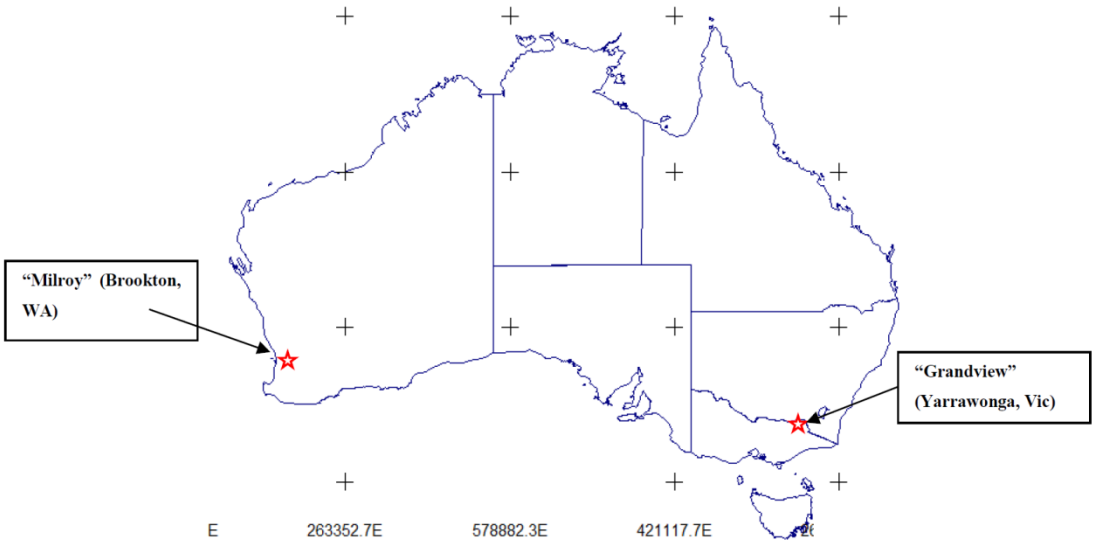


**FIGURE 3.1:** LOCATION OF THE TWO STUDY SITES IN AUSTRALIA. "MILROY" FARMING ENTERPRISES ARE CROPPING AND CROSS-BRED SHEEP ON AN ANNUAL PASTURE SYSTEM, WITH SUBTERRANEAN CLOVER, CAPEWEED AND SERRADELLA. "GRANDVIEW" FARMING ENTERPRISES ARE CROPPING AND CATTLE ON A PERENNIAL PASTURE SYSTEM, WITH LUCERNE, SUBTERRANEAN CLOVER AND CHICORY.

**TABLE 3.1:** ACTUAL RAINFALL RECEIVED 2004–2011 AS GROWING SEASON RAINFALL (GSR) AND ANNUAL RAINFALL, AND AS A PERCENTAGE OF LONG-TERM AVERAGE GSR AND ANNUAL RAINFALL FOR "MILROY" AND "GRANDVIEW".

| | 2004 | 2005 | 2006 | 2007 | 2008 | 2009 | 2010 | 2011 | Ave |
|---|---|---|---|---|---|---|---|---|---|
| **"MILROY"** | | | | | | | | | |
| GSR | 263.9 | 428.4 | 227.9 | 360.8 | 416.3 | 327.7 | 161.7 | 330.8 | 381.0 |
| % of average GSR | 74% | 120% | 64% | 104% | 117% | 92% | 45% | 93% | |
| Annual rainfall | 303.7 | 501.3 | 391.7 | 391.5 | 494.2 | 439.2 | 256.4 | 466.7 | 405.6 |
| % of average annual rainfall | 70% | 115% | 90% | 90% | 113% | 100% | 59% | 107% | |
| **"GRANDVIEW"** | | | | | | | | | |
| GSR | 260 | 333.5 | 148 | 190 | 155 | 245 | 406.5 | 242.5 | 338.3 |
| % of average GSR | 72% | 93% | 41% | 53% | 43% | 68% | 113% | 67% | |
| Annual rainfall | 365 | 567.5 | 217 | 355 | 334 | 293 | 794 | 687.5 | 517.5 |
| % of average annual rainfall | 68% | 105% | 40% | 66% | 62% | 54% | 147% | 127% | |

**TABLE 3.2:** PADDOCK ROTATIONS FOR "MILROY" AND "GRANDVIEW". THE PADDOCK NOTATION (E.G. M25) IS THE SYSTEM USED BY THE FARM OWNER TO IDENTIFY INDIVIDUAL PADDOCKS.

| Paddock | 2004 | 2005 | 2006 | 2007 | 2008 | 2009 | 2010 | 2011 |
|---|---|---|---|---|---|---|---|---|
| **"MILROY"** | | | | | | | | |
| M25 (53 ha) | wheat | pasture | pasture | barley | pasture | wheat | pasture | pasture |
| M41 (70 ha) | lupins | barley | pasture | pasture | canola | wheat | pasture | pasture |
| M45 (67 ha) | wheat | lupin | pasture | canola | wheat | pasture | barley | pasture |
| **"GRANDVIEW"** | | | | | | | | |
| GV4 (63 ha) | pasture | wheat | oaten | canola | wheat | canola | wheat | pasture |
| GV8 (38 ha) | pasture | canola | wheat | wheat | canola | wheat | wheat | pasture |
| GV39 (60 ha) | pasture | canola | wheat | canola | wheat | wheat | barley | pasture |

### *3.2.2 MODIS SATELLITE DATA*

The NDVI data sets for 2004–2011 used in this study were derived from composite images of daily MODIS NDVI from the radiometers carried on the Terra and Aqua satellites, and were provided by Landgate's Satellite Remote Sensing Services unit in Perth, Western Australia. The NDVI data was calculated from calibrated, top-of-atmosphere reflectances. The daily NDVI images were composited into weekly images using the Maximum Value Composite (MVC) process described by Holben (1986) to minimise atmospheric effects and to remove cloud and cloud-shadow pixels. Any pixels in the resulting composite that had a 'no data' value due to cloud cover were filled by using the value from the previous week's NDVI composite at the same location. The MODIS images have a ground resolution of approximately 250 metres square with an ortho-rectification accuracy of approximately ±50 m (Smith et al., 2011). The datasets contained 52 or 53 NDVI observations per pixel per year, depending on the annual starting date. The dataset values were located to pixel centres using ArcGIS 10.2 (ESRI Redlands, California, USA) so that pixels lying within the study paddocks boundaries could be identified. MODIS pixels for each paddock are shown at Appendices 1 and 2.

*Selection of MODIS pixels for use in the analysis*

MODIS pixel spatial resolution of 6.25 ha in paddocks of 60–100 ha can mean that a significant number of the pixels for a paddock may contain 'corrupted' data values, e.g. pixels that straddle paddock boundaries, areas containing rocky outcrops, or contaminated by other types of vegetation such as forested areas. This limited the number of pixels that could be used in the analysis. Mixed pixels (those that were not predominantly crop or pasture within the nominated paddocks) were also removed from the analysis (e.g. see Figure 3.2). This comprised pixels with more than 20% of their total area not in either pasture or crop and/or lying outside the paddock boundary.

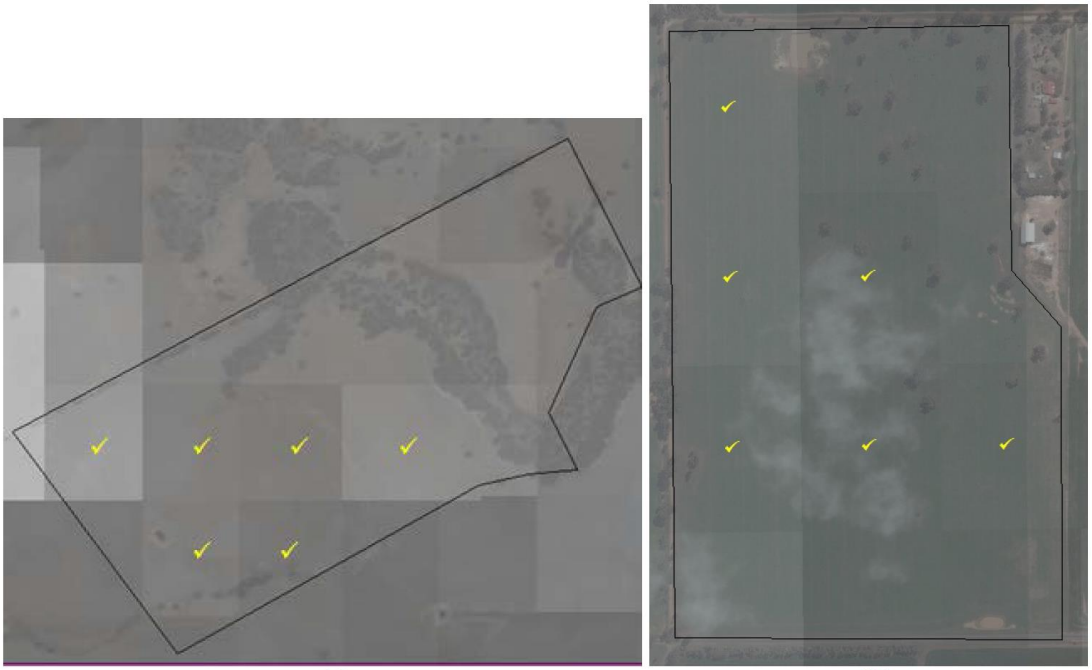


**FIGURE 3.2:** EXAMPLES OF THE DISTRIBUTION OF MODIS PIXELS (250 M X 250 M) OVER "MILROY" (WA) PADDOCK M41 (A) AND "GRANDVIEW" (VIC) PADDOCK GV39 (B). PIXELS MARKED WITH A YELLOW TICK WERE INCLUDED IN THE ANALYSIS. OTHER PIXELS WERE CONSIDERED EITHER TOO CONTAMINATED BY BUSHLAND, WATER OR ROCKY OUTCROPS OR HAD INSUFFICIENT PIXEL AREA FALLING WITHIN THE PADDOCK BOUNDARY TO BE INCLUDED.

*Data processing and analysis*

The analysis had three parts:

1. Analysing the relationships, on a year-by-year basis, between individual paddock pixels when in a cropping or pasture phase.
2. Identifying the spatial trend of annual NDVI values, over time, by calculating a mean value of each pixel for the eight years of the study.
3. Identifying the stability, over time, of NDVI values across a paddock, by pixel.

1. Comparison of annual NDVI values: For the pixels retained for analysis, weekly MODIS NDVI data values were extracted from weekly maximum value composites, over the period 2004–2011. For each year, the 52 weekly NDVI values (January to December), were summed to create a total annual NDVI value. The accumulated NDVI was used as a surrogate for green biomass growth, through continuous additions of NDVI through the year. This resulted in values between 16 and 26 for annual accumulated NDVI, depending on the pixel and the season. The use of accumulated NDVI as an estimate of annual biomass production is common in the literature, either as a summation of weekly NDVI values, or as the integral of the area under an NDVI time-series curve (Bradley et al., 2007; Ferencz et al., 2004; Hill and Donald, 2003; Jönsson and Eklundh, 2004; Reed et al., 1994, 1996). Capturing the NDVI values across the year also takes into account the variability in plant growth rates across the season, particularly in pasture phases, where different plant successions may dominate at different times of the year, e.g. sub-clover early in the season and capeweed late in the season.

Because in some years the paddocks were in pasture and other years in crop (and a variety of crops including canola), standardisation of the data was also explored using the methodology described in Blackmore (2000) and Fisher et al. (2009). However, the analysis showed no difference between using the raw NDVI values or standardising the data, so the standardising approach was not pursued.

2. Calculation of the spatial trend in NDVI pixel values: Once the accumulated annual NDVI data sets had been created, they were analysed for spatial trends.

Correlation analyses were run on the accumulated annual MODIS NDVI values for each pixel in each paddock using the JMP v.12.2.0 software package (SAS Institute Inc, Cary, North Carolina,USA) to determine if relationships existed between the pasture phase and crop phase NDVI values on a pixel-by-pixel basis over the eight years for which data were available.

3. Calculating the temporal stability of NDVI pixel values over time: The temporal stability of crop or pasture production comprises two elements. The first is the variation that occurs between the paddock mean yield from year to year. Blackmore (2000) referred to this as the 'inter-year offset' and defined it as the difference between the mean yield value between two years in the same paddock. The largest driver of this variation in temperate cropping zones is variability in annual rainfall (Turner and Asseng, 2005).

The second temporal effect involves situations in which a particular part of a paddock produces above average yield in one year and below average yield in another year, irrespective of rainfall. This alternating pattern of relative grain yield has been referred to as the 'flip-flop effect' (Nuttall and Armstrong, 2006). Blackmore et al. (2003) termed this variation the 'temporal variance at a single point'.

In terms of the MODIS NDVI analysis described here, temporal stability is measured by the between-season variability for each pixel, i.e. how stable the estimate of production from a particular part of the paddock is over time under different seasonal conditions. It was measured by calculating the standard deviation for each mean pixel NDVI value over time. The temporal standard deviation indicates the amount of change in accumulated NDVI for a particular pixel over time. If a pixel was temporally stable in regard to total NDVI, it showed a persistent relationship with the median value for a period of time. A pixel was considered temporally stable if the median relative difference was near zero and there was a small standard deviation.

## 3.3 RESULTS

### *3.3.1 ANNUAL VARIATION IN NDVI*

Tables 3.3 and 3.4 show the accumulated annual NDVI value for each MODIS pixel used, the paddock means, the associated standard deviations and GSR for "Milroy" and "Grandview", respectively.

Table 3.5 summarises the correlation analyses, showing the range of correlation coefficients for accumulated annual NDVI for crop years, pasture years, and crop x pasture years between 2004 and 2011 for each of the three paddocks at "Milroy" and "Grandview". The data sets were approximately normally distributed.

Figure 3.3 is an example of a scatterplot matrix from the cross-correlation analysis of annual accumulated NDVI values for each pixel for each year. The example is for paddock M45 based on the data from Table 3.3. Correlations are linear and positive. The effect of low rainfall in 2006 and 2010 is reflected in lower r-values. Scatterplot matrices for the remaining paddocks are in Appendices 3 and 4.

*"Milroy": Paddock M25*

In this paddock, all cropping years showed strong positive correlations for NDVI values for individual MODIS pixels with r-values between 0.78 and 0.97 (Table 3.5). This indicates that the same NDVI value pixels were consistently high over time and low NDVI value areas were consistently low. There was a similar pattern when comparing years in which the paddock was in pasture, with r-values ranging from 0.59 to 0.94, except in the 2006 drought year which had an r-value of 0.36.

When comparing pixel biomass production between crop years and pasture years (16 combinations), the correlation matrix gave strong r-values ranging from 0.71 to 0.96, with one weak value of 0.44 between 2004 (wheat) and 2008 (pasture), and two medium strength correlations of 0.55 and 0.61.

*"Milroy": Paddock M41*

For the cropping years (six combinations), there was only one strong positive r-value (0.97). Other r-values ranged between –0.37 and 0.43. These were all associated with the 2004 (lupin) or 2005 (barley) years. For years in which the

paddock was in pasture, all r-values were strong and positive, ranging from 0.70 to 0.98. Correlation between crop and pasture phases showed eight combinations with r-values between 0.61 and 0.99. The lowest r-value was –0.43, between the 2004 (lupin) and 2007 (pasture) years. There were seven other weak correlations, three associated with 2004 (lupin) and four with 2005 (barley).

*"Milroy": Paddock M45*

In this paddock, all cropping years showed strong positive correlations with r-values between 0.65 and 0.91. There was a similar pattern when comparing years in which the paddock was in pasture with r-values between 0.74 and 0.97. The interaction between crop and pasture phases showed 11 combinations with r-values between 0.84 and 0.98 and four combinations, all associated with the 2006 drought year, with r-values between 0.55 and 0.69.

*"Grandview"*

The 2006 drought season had the lowest mean NDVI value in all three paddocks. The 2006 season received 40% of average GSR. The 2010 and 2011 seasons had the highest mean NDVI values for all paddocks and received 147% and 127% of "Grandview" average annual rainfall, coinciding with the transition from a cropping phase to a new pasture phase.

*"Grandview": Paddock GV4*

Pairwise correlations for accumulated annual NDVI for paddock GV4, between all cropping years (15 combinations), were generally poor with only three r-values between 0.89 and 0.98. The remaining 12 were between –0.91 and 0.40. Nine of these were associated with either the 2007, 2008 or 2010 seasons. For the only pasture–pasture combination (2004/2011), the r-value was 0.74. Pasture–crop interactions (12 combinations) had five r-values between 0.52 and 0.98. Seven were between –0.63 and 0.33, with five of these associated with the 2008 or 2011 seasons.

*"Grandview": Paddock GV8*

Eight of the 15 combinations for crop years had r-values between 0.53 and 0.99. There were seven between –0.90 and 0.38, of which five were associated with the 2007 or 2008 years. For the two years in which the paddock was in pasture (2004 and 2011), the r-value was 0.92. Crop/pasture pairwise comparisons (12 combinations) had eight r-values between 0.56 and 0.94. There were four between –0.85 and 0.33, all associated with the 2007 or 2008 seasons.

*"Grandview": Paddock GV39*

Seven of the 15 combinations for cropping phase correlations had r-values between 0.54 and 0.96. There were seven combinations with r-values between –0.25 and 0.40, of which six were associated with 2007 or 2008. For the two years in which the paddock was in pasture (2004 and 2011), the r-value was 0.96. Crop/pasture phase comparisons (12 combinations), showed nine with r-values between 0.61 and 0.99 and four between –0.36 and 0.10. All four were associated with 2007 or 2008.

### *3.3.2 SPATIAL TREND*

Tables 3.6 and 3.7 show the temporal trends at the sub-paddock scale using the means of NDVI values for each of the MODIS pixels used and also overall paddock NDVI means for "Milroy" and "Grandview", respectively. The temporal means show the average NDVI value for each pixel in a paddock over the eight years of the study.

Values are shown for (i) all years irrespective of whether the paddock was in crop or pasture, (ii) for years when in crop, and (iii) for years when in pasture. MODIS pixels with a mean greater than the paddock mean could be expected to have higher production than the paddock average in most seasons, and *vice versa*. This is a measure of the consistency of spatial variation over time. For example, in "Milroy" paddock M25, pixels 45 and 46 consistently had the highest NDVI value whether in crop or pasture.

Similarly, in "Grandview" paddock GV4, pixels 46 and 48 had the highest mean NDVI values across all years irrespective of whether the paddock was in pasture or crop, while pixels 51 and 52 had the lowest mean values across all years and rotations.

Table 3.8 shows the results of a correlation analysis of the data in Tables 3.6 and 3.7. Spearman's correlation co-efficient was used because of the small sample size. All combinations of variables show strong and significant correlations at "Milroy" and two strong correlations at "Grandview", with one of these significant. That is, except for "Grandview" paddock GV8, over the eight years of the study, MODIS pixels with a high mean NDVI when in crop could be expected to have a high mean NDVI when in pasture, and *vice versa*.

### *3.3.3 TEMPORAL STABILITY*

Tables 3.9 and 3.10 show the standard deviations in the long term (2004–2011) NDVI for "Milroy" and "Grandview", respectively. Values are shown for each pixel for all years (s.d. all), crop years only (s.d. crop) and pasture years only (s.d. past).

The medians shown were derived from descriptive statistics for the NDVI data. Pixels with an s.d. lower than the median could be considered relatively stable in biomass production over time whereas pixels with a high value for temporal s.d. could be yielding high in some years and low in others, i.e. relatively unstable over time (Blackmore, 2000) and showing inconsistent behaviour.

*"Milroy"*

In paddock M25, for all years, the most stable pixels were 46, 51 and 58. This was also the case with pasture years. For crop years, pixels 46, 51 and 52 were the most stable. Overall, the standard deviations for pasture were significantly larger than for crop, indicating greater variation in pasture production across the paddock than for crop.

In paddock M41, for all years, pixels 3, 4 and 5 were most stable. Again, this was the case for pasture. For crop, pixels 3, 5 and 6 were most stable. In M45, for all years, pixels 24, 25, 33 and 34 were most stable. For pasture, it was pixels 25, 27, 33 and 34 and for crop years pixels 21, 23, 24 and 25.

*"Grandview"*

In paddock GV4, for all years, the most stable pixels were 46, 47 and 51. This was also the case with pasture and cropping years.

In paddock GV8, for all years, pixels 37 and 38 were most stable. Again this was the case for pasture and crop years. In GV39, for all years, pixels 1, 8 and 15 were most stable. This was also the case for pasture years. However, in cropping years, pixels 9, 16 and 17 were most stable.

**TABLE 3.3:** RAW ACCUMULATED ANNUAL NDVI VALUES AND GSR (MM), FOR "MILROY" PADDOCKS, 2004–2011.

| | Pixel | 2004 | 2005 | 2006 | 2007 | 2008 | 2009 | 2010 | 2011 |
|---|---|---|---|---|---|---|---|---|---|
| | | **wheat** | **past** | **past** | **barley** | **past** | **wheat** | **past** | **past** |
| M25 | 45 | 20.56 | 24.89 | 17.98 | 22.14 | 24.66 | 20.45 | 21.23 | 21.56 |
| | 46 | 20.94 | 24.27 | 17.58 | 21.89 | 24.19 | 20.47 | 20.97 | 22.32 |
| | 51 | 19.65 | 23.78 | 17.35 | 20.65 | 23.85 | 19.44 | 20.22 | 21.24 |
| | 52 | 20.08 | 24.38 | 17.25 | 20.81 | 24.21 | 19.57 | 20.62 | 21.51 |
| | 58 | 20.11 | 23.55 | 17.35 | 20.43 | 23.03 | 18.90 | 20.09 | 20.60 |
| | mean | 20.27 | 24.17 | 17.5 | 21.18 | 23.99 | 19.77 | 20.63 | 21.45 |
| | s.d. | 0.5 | 0.53 | 0.3 | 0.78 | 0.61 | 0.68 | 0.48 | 0.62 |
| | | **lupin** | **barley** | **past** | **past** | **canola** | **wheat** | **past** | **past** |
| M41 | 3 | 18.86 | 22.55 | 19.28 | 20.04 | 23.54 | 20.48 | 21.02 | 21.91 |
| | 4 | 19.49 | 23.55 | 17.88 | 18.80 | 22.66 | 18.42 | 20.44 | 20.09 |
| | 5 | 19.61 | 23.27 | 17.11 | 18.63 | 22.47 | 18.62 | 18.81 | 19.70 |
| | 6 | 19.70 | 22.40 | 16.38 | 18.40 | 22.26 | 18.40 | 17.46 | 19.40 |
| | 11 | 18.27 | 22.85 | 15.78 | 18.92 | 21.56 | 17.20 | 19.01 | 18.32 |
| | 12 | 18.57 | 23.29 | 16.02 | 18.84 | 21.34 | 17.36 | 18.20 | 18.23 |
| | mean | 19.08 | 22.98 | 17.08 | 18.94 | 22.31 | 18.41 | 19.16 | 19.61 |
| | s.d. | 0.6 | 0.46 | 1.32 | 0.57 | 0.8 | 1.17 | 1.35 | 1.35 |
| | | **wheat** | **lupin** | **past** | **canola** | **wheat** | **past** | **barley** | **past** |
| M45 | 20 | 17.29 | 21.48 | 14.67 | 17.97 | 20.21 | 17.99 | 18.66 | 19.20 |
| | 21 | 18.09 | 21.30 | 14.69 | 18.59 | 20.42 | 18.04 | 17.34 | 18.85 |
| | 23 | 16.23 | 20.17 | 12.85 | 16.69 | 18.02 | 16.34 | 16.80 | 17.47 |
| | 24 | 15.95 | 18.82 | 12.63 | 16.35 | 16.82 | 15.39 | 15.41 | 16.40 |
| | 25 | 16.23 | 19.24 | 14.45 | 16.30 | 18.75 | 16.46 | 15.90 | 17.16 |
| | 27 | 15.37 | 18.63 | 12.28 | 14.74 | 16.02 | 15.02 | 14.45 | 15.84 |
| | 33 | 16.45 | 19.41 | 13.88 | 15.54 | 15.24 | 15.90 | 14.67 | 17.01 |
| | 34 | 17.26 | 20.07 | 14.61 | 15.94 | 16.69 | 16.89 | 15.77 | 17.26 |
| | mean | 16.61 | 19.89 | 13.76 | 16.52 | 17.77 | 16.5 | 16.3 | 17.4 |
| | s.d. | 0.88 | 1.07 | 1.02 | 1.25 | 1.91 | 1.11 | 1.41 | 1.13 |
| | GSR | 263.9 | 428.4 | 227.9 | 360.8 | 416.3 | 327.7 | 161.7 | 330.8 |

**TABLE 3.4:** RAW ACCUMULATED ANNUAL NDVI VALUES AND GSR (MM) FOR "GRANDVIEW" PADDOCKS, 2004–2011.

| | Pixel | 2004 | 2005 | 2006 | 2007 | 2008 | 2009 | 2010 | 2011 |
|---|---|---|---|---|---|---|---|---|---|
| | | **past** | **wheat** | **oaten hay** | **canola** | **wheat** | **canola** | **wheat** | **past** |
| GV4 | 46 | 22.28 | 23.84 | 18.25 | 21.50 | 19.88 | 20.79 | 23.59 | 25.08 |
| | 47 | 22.19 | 23.82 | 18.32 | 21.20 | 19.76 | 19.25 | 23.97 | 25.11 |
| | 48 | 22.41 | 24.52 | 18.40 | 21.17 | 19.75 | 19.56 | 24.18 | 26.05 |
| | 51 | 22.00 | 22.67 | 17.66 | 20.21 | 20.15 | 19.97 | 24.44 | 24.99 |
| | 52 | 21.97 | 22.26 | 17.42 | 20.18 | 19.79 | 19.70 | 24.46 | 25.10 |
| | mean | 22.17 | 23.42 | 18.01 | 20.85 | 19.87 | 19.85 | 24.13 | 25.27 |
| | s.d. | 0.19 | 0.93 | 0.44 | 0.61 | 0.17 | 0.58 | 0.36 | 0.44 |
| | | **past** | **canola** | **wheat** | **wheat** | **canola** | **wheat** | **wheat** | **past** |
| GV8 | 37 | 22.48 | 21.81 | 18.48 | 21.56 | 19.77 | 20.87 | 22.34 | 26.09 |
| | 38 | 22.87 | 21.84 | 19.34 | 22.60 | 20.36 | 21.73 | 23.45 | 25.57 |
| | 40 | 24.31 | 22.19 | 19.72 | 22.40 | 19.34 | 22.67 | 24.68 | 28.75 |
| | 42 | 23.57 | 22.31 | 19.19 | 21.67 | 18.81 | 22.62 | 24.38 | 28.22 |
| | mean | 23.31 | 22.04 | 19.18 | 22.06 | 19.57 | 21.97 | 23.71 | 27.16 |
| | s.d. | 0.81 | 0.25 | 0.52 | 0.52 | 0.66 | 0.86 | 1.05 | 1.57 |
| | | **past** | **canola** | **wheat** | **canola** | **wheat** | **wheat** | **barley** | **past** |
| GV3 | 1 | 19.94 | 20.52 | 17.10 | 21.30 | 20.60 | 21.07 | 23.67 | 23.14 |
| | 8 | 21.71 | 21.64 | 18.11 | 21.34 | 19.87 | 20.64 | 23.60 | 25.46 |
| | 9 | 22.85 | 22.10 | 18.71 | 20.39 | 20.04 | 21.16 | 23.84 | 28.69 |
| | 15 | 22.92 | 23.24 | 19.08 | 22.41 | 20.34 | 21.11 | 24.34 | 26.89 |
| | 16 | 23.49 | 22.76 | 19.39 | 20.79 | 20.43 | 21.50 | 24.02 | 29.86 |
| | 17 | 23.66 | 23.18 | 19.72 | 21.21 | 20.68 | 21.52 | 24.40 | 29.81 |
| | mean | 22.43 | 22.24 | 18.09 | 21.24 | 20.33 | 21.17 | 22.98 | 27.31 |
| | s.d. | 1.4 | 1.05 | 0.96 | 0.68 | 0.32 | 0.32 | 0.34 | 2.67 |
| | GSR | 260 | 333.5 | 148 | 190 | 155 | 245 | 406.5 | 242.5 |

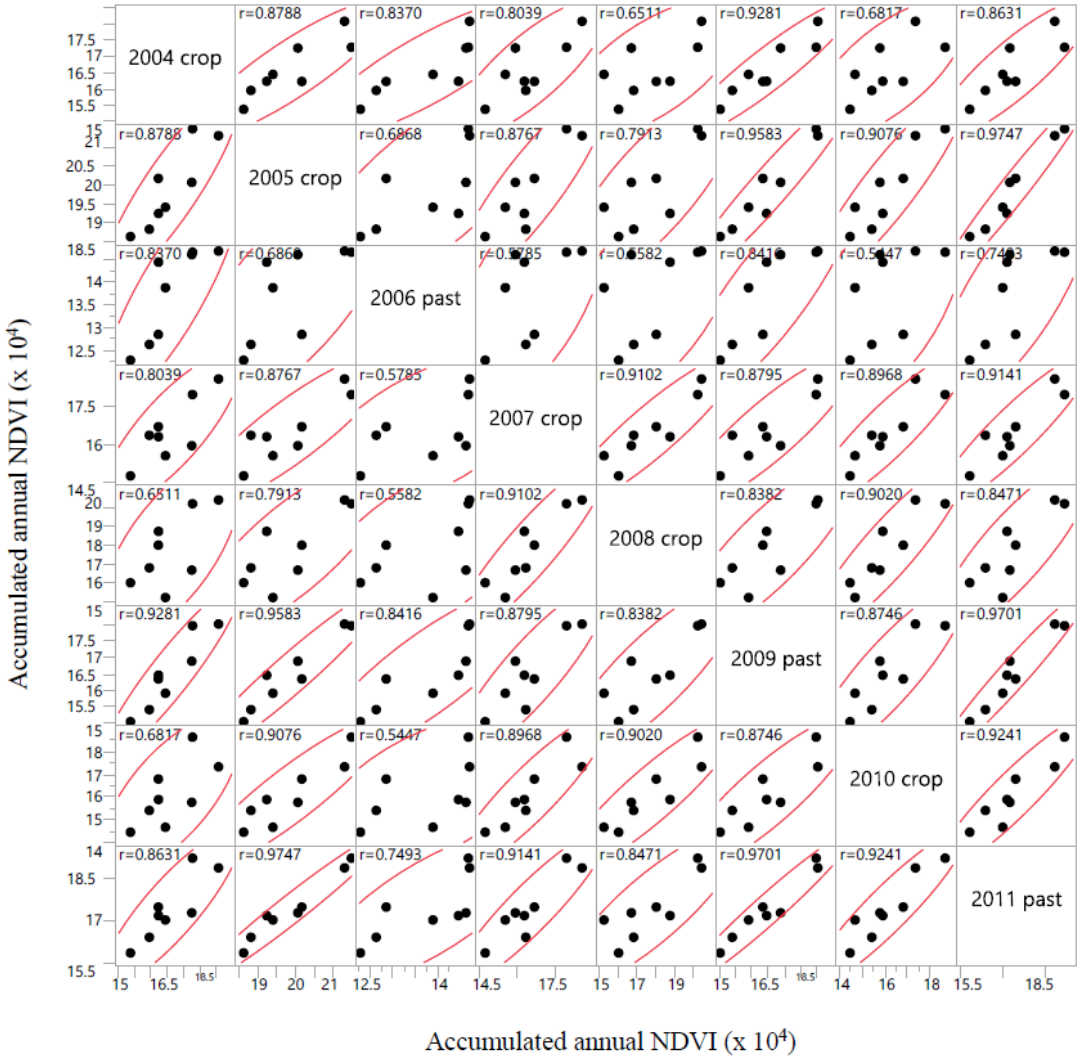


**FIGURE 3.3:** PAIRWISE SCATTERPLOTS SHOWING PEARSON CORRELATION COEFFICIENTS (R) BETWEEN ACCUMULATED ANNUAL MODIS NDVI PIXEL VALUES, 2004–2011, FOR "MILROY" PADDOCK M45. FOR EXAMPLE, THE R-VALUE BETWEEN 2005 (CROP) AND 2009 (PASTURE) IS 0.9583 (AN R-VALUE OF 1 IMPLIES PERFECT CORRELATION). THE DENSITY ELLIPSES (RED LINES) ENCLOSE APPROXIMATELY 95% OF THE POINTS.

**TABLE 3.5:** HIGHEST AND LOWEST PEARSON CORRELATION COEFFICIENTS (R-VALUES) FOR "MILROY" AND "GRANDVIEW" PADDOCKS, FROM CROSS-CORRELATION ANALYSIS OF ACCUMULATED ANNUAL NDVI BETWEEN CROPPING PHASES, PASTURE PHASES AND CROPPING X PASTURE PHASES.

| | Between: | | |
|---|---|---|---|
| | **Crop years** | **Pasture years** | **Crop & pasture years** |
| **"MILROY" M25** | | | |
| Lowest r-value | 0.78 (2004/2009) | 0.36 (2006/2011) | 0.44 (2004/2008) |
| Highest r-value | **0.97** (2007/2009) | **0.94** (2005/2008) | **0.96** (2007/2010) |
| **"MILROY" M41** | | | |
| Lowest r-value | –0.37 (2005/2009) | 0.70 (2007/2011) | –0.43 (2004/2007) |
| Highest r-value | **0.97** (2008/2009) | **0.98** (2006/2011) | **0.99** (2008/2011) |
| **"MILROY" M45** | | | |
| Lowest r-value | 0.65 (2004/2008) | **0.74** (2006/2011) | 0.55 (2006/2010) |
| Highest r-value | **0.91** (2007/2008) | **0.97** (2009/2011) | **0.98** (2005/2011) |
| **"GRANDVIEW" GV4** | | | |
| Lowest r-value | **–0.91** (2007/2010) | 0.74 (2004/2011) | –0.63 (2004/2010) |
| Highest r-value | **0.98** (2005/2006) | 0.74 (2004/2011) | **0.98** (2004/2005) |
| **"GRANDVIEW" GV8** | | | |
| Lowest r-value | –0.9 (2005/2008) | 0.92 (2004/2011) | –0.85 (2008/2011) |
| Highest r-value | **0.99** (2009/2010) | 0.92 (2004/2011) | 0.94 (2004/2010) |
| **"GRANDVIEW" GV39** | | | |
| Lowest r-value | –0.25 (2007/2009) | **0.96** (2004/2011) | –0.36 (2007/2011) |
| Highest r-value | **0.96** (2005/2006) | **0.96** (2004/2011) | **0.99** (2004/2006) |

Values in bold significant at P=0.05

**TABLE 3.6:** TEMPORAL NDVI MEANS FOR "MILROY" PADDOCKS, 2004–2011. MEANS ARE SHOWN FOR ALL CROP/PASTURE YEARS, CROP YEARS ONLY AND PASTURE YEARS ONLY.

| Paddock | Pixel | All years | Crop years | Pasture years |
|---|---|---|---|---|
| M25 | 45 | 21.69 | 21.05 | 22.07 |
| | 46 | 21.58 | 21.10 | 21.86 |
| | 51 | 20.77 | 19.91 | 21.29 |
| | 52 | 21.05 | 20.15 | 21.59 |
| | 58 | 20.51 | 19.81 | 20.92 |
| | Paddock mean | 21.12 | 20.41 | 21.55 |
| M41 | 3 | 20.96 | 21.36 | 20.56 |
| | 4 | 20.16 | 21.03 | 19.30 |
| | 5 | 19.78 | 20.99 | 18.56 |
| | 6 | 19.30 | 20.69 | 17.91 |
| | 11 | 18.99 | 19.97 | 18.01 |
| | 12 | 18.98 | 20.14 | 17.82 |
| | Paddock mean | 19.7 | 20.7 | 18.7 |
| M45 | 20 | 18.43 | 19.12 | 17.28 |
| | 21 | 18.42 | 19.15 | 17.19 |
| | 23 | 16.82 | 17.58 | 15.55 |
| | 24 | 15.97 | 16.67 | 14.81 |
| | 25 | 16.81 | 17.28 | 16.02 |
| | 27 | 15.29 | 15.84 | 14.38 |
| | 33 | 16.01 | 16.26 | 15.60 |
| | 34 | 16.81 | 17.15 | 16.26 |
| | Paddock mean | 16.82 | 17.38 | 15.89 |

**TABLE 3.7:** TEMPORAL NDVI MEANS FOR "GRANDVIEW" PADDOCKS, 2004–2011. MEANS ARE SHOWN FOR ALL CROP/PASTURE YEARS, CROP YEARS ONLY AND PASTURE YEARS ONLY.

| Paddock | Pixel | All years | Crop years | Pasture years |
|---|---|---|---|---|
| GV4 | 46 | 21.90 | 21.31 | 23.68 |
| | 47 | 21.70 | 21.05 | 23.65 |
| | 48 | 22.00 | 21.26 | 24.23 |
| | 51 | 21.51 | 20.85 | 23.50 |
| | 52 | 21.36 | 20.63 | 23.54 |
| Paddock mean | | 21.70 | 21.02 | 23.72 |
| GV8 | 37 | 21.67 | 20.80 | 24.29 |
| | 38 | 22.22 | 21.55 | 24.22 |
| | 40 | 23.01 | 21.83 | 26.53 |
| | 42 | 22.60 | 21.50 | 25.90 |
| Paddock mean | | 22.38 | 21.42 | 25.23 |
| GV39 | 1 | 20.92 | 20.71 | 21.54 |
| | 8 | 21.55 | 20.87 | 23.58 |
| | 9 | 22.22 | 21.04 | 25.77 |
| | 15 | 22.54 | 21.76 | 24.90 |
| | 16 | 22.78 | 21.48 | 26.67 |
| | 17 | 23.02 | 21.79 | 26.73 |
| Paddock mean | | 22.17 | 21.27 | 24.87 |

**TABLE 3.8:** PAIRWISE CORRELATIONS BETWEEN THE TEMPORAL MEAN PIXEL NDVI FOR "MILROY" AND "GRANDVIEW" BETWEEN CROP AND PASTURE PHASES.

| Paddock | Spearman's rho | N | P |
|---|---|---|---|
| **"Milroy"** | | | |
| M25 | 0.90 | 5 | <0.05 |
| M41 | 0.83 | 6 | <0.05 |
| M45 | 0.76 | 8 | <0.05 |
| **"Grandview"** | | | |
| GV4 | 0.80 | 5 | 0.1 |
| GV8 | 0.40 | 4 | 0.6 |
| GV39 | 0.82 | 6 | <0.05 |

**TABLE 3.9:** STANDARD DEVIATION OF NDVI PIXEL MEANS FOR "MILROY" PADDOCKS, 2004–2011.

| | | Standard deviation | | |
|---|---|---|---|---|
| **Paddock** | **Pixel** | **All years** | **Crop years** | **Pasture years** |
| M25 | 45 | 2.27 | 0.95 | 2.84 |
| | 46 | 2.16 | 0.72 | 2.76 |
| | 51 | 2.20 | 0.65 | 2.71 |
| | 52 | 2.36 | 0.63 | 2.93 |
| | 58 | 2.02 | 0.80 | 2.49 |
| | Median | 2.2 | 0.72 | 2.76 |
| M41 | 3 | 1.62 | 2.10 | 1.15 |
| | 4 | 2.01 | 2.46 | 1.18 |
| | 5 | 2.08 | 2.23 | 1.08 |
| | 6 | 2.14 | 1.97 | 1.29 |
| | 11 | 2.27 | 2.67 | 1.51 |
| | 12 | 2.30 | 2.68 | 1.24 |
| | Median | 2.11 | 2.35 | 1.21 |
| M45 | 20 | 2.04 | 1.71 | 2.34 |
| | 21 | 1.99 | 1.65 | 2.20 |
| | 23 | 2.05 | 1.59 | 2.41 |
| | 24 | 1.73 | 1.31 | 1.95 |
| | 25 | 1.55 | 1.58 | 1.41 |
| | 27 | 1.78 | 1.67 | 1.87 |
| | 33 | 1.68 | 1.87 | 1.58 |
| | 34 | 1.59 | 1.74 | 1.43 |
| | Median | 1.75 | 1.66 | 1.9 |

**TABLE 3.10:** STANDARD DEVIATION OF NDVI PIXEL MEANS FOR "GRANDVIEW" PADDOCKS 2004–2011.

| | | Standard deviation | | |
|---|---|---|---|---|
| **Paddock** | **Pixel** | **All years** | **Crop years** | **Pasture years** |
| GV4 | 46 | 2.26 | 2.16 | 1.98 |
| | 47 | 2.48 | 2.39 | 2.06 |
| | 48 | 2.74 | 2.55 | 2.58 |
| | 51 | 2.48 | 2.37 | 2.12 |
| | 52 | 2.59 | 2.43 | 2.22 |
| | Median | 2.48 | 2.39 | 2.12 |
| GV8 | 37 | 2.24 | 1.44 | 2.55 |
| | 38 | 1.90 | 1.49 | 1.91 |
| | 40 | 3.00 | 2.00 | 3.14 |
| | 42 | 2.99 | 2.13 | 3.28 |
| | Median | 2.62 | 1.75 | 2.85 |
| GV39 | 1 | 2.02 | 2.11 | 2.26 |
| | 8 | 2.24 | 1.84 | 2.65 |
| | 9 | 3.08 | 1.78 | 4.13 |
| | 15 | 2.44 | 1.94 | 2.81 |
| | 16 | 3.27 | 1.67 | 4.50 |
| | 17 | 3.17 | 1.71 | 4.35 |
| | Median | 2.76 | 1.81 | 3.47 |

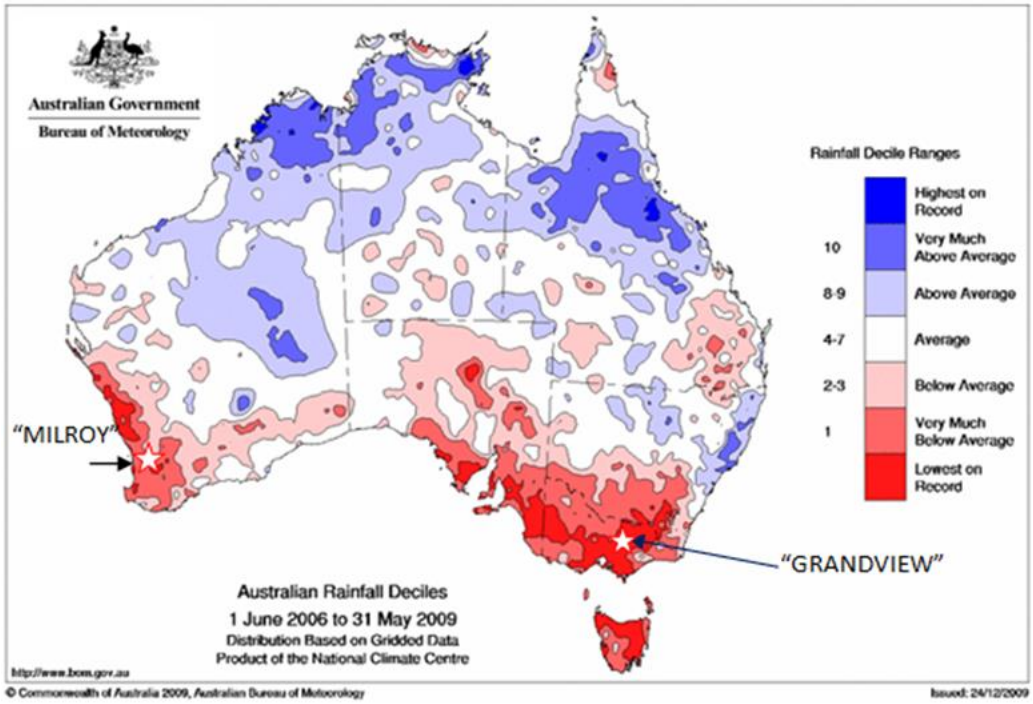


**FIGURE 3.4:** SOUTH-EASTERN AUSTRALIA SUFFERED A SEVERE DROUGHT BETWEEN 2006 AND 2009. THIS FIGURE SHOWS TOTAL RAINFALL DECILES ACROSS THE AUSTRALIAN CONTINENT FOR THE THREE YEARS FROM JUNE 2006 TO MAY 2009. THE LOCATIONS OF THE TWO PROPERTIES ARE INDICATED. DECILES ARE EXPRESSED USING LONG-TERM CLIMATOLOGY FROM 1900 TO 2009. SOURCE: AUSTRALIAN BUREAU OF METEOROLOGY.

## 3.4 DISCUSSION

The purpose of this initial analysis was to test Hypothesis 1 (Chapter 2, p. 36), that "*spatial variation in biomass production over time is correlated between the cropping and pasture phases of mixed farming enterprises*". This was done using relatively low spatial resolution MODIS NDVI data to determine if a relationship existed at the sub-paddock scale and over time, between the productivity in the pasture and cropping phases of mixed farming rotations. In the past, MODIS NDVI information has been used in conjunction with rainfall and temperature data to estimate pasture growth rates (Donald et al., 2010, 2013; Edirisinghe et al., 2011; Smith et al., 2011) and crop biomass or yield (Hu et al., 2009; Perry et al., 2013; Schut et al., 2009; Wardlow et al., 2007; Xu et al., 2014) but has not been used to test correlations between crop and pasture growth. Geerken et al. (2005) used

correlation between NDVI time-series to classify variations in rangeland vegetation; Donald et al. (2010) used it to evaluate low-resolution MODIS NDVI data against two, higher spatial resolution data sets; and Brown et al. (2007) incorporated it to assist in classifying crop types.

There is no evidence in the literature that low-resolution NDVI data has been used to explore the relationships between crop and pasture production within the same paddock(s). The results reported here indicate that the Pearson correlation coefficients for accumulated MODIS NDVI across all paddocks on "Milroy" had generally strong, positive relationships between crop, pasture and crop–pasture interactions. In other words, at "Milroy", over time, the same MODIS pixels were high yielding irrespective of whether the paddock was in a crop or pasture phase.

This provides evidence to support the hypothesis being tested here, that spatial variation in biomass production over time is correlated between the cropping and pasture phases of mixed farming enterprises.

The only periods where this consistent pattern was broken at "Milroy" were associated with the 2006 and 2010 drought years (64% and 45% of average GSR, respectively). In the case of paddock M41, which was in pasture in 2006 and 2007 and again in 2010 and 2011, the farm owner reported that the low rainfall of 2006 and 2010 caused poor subterranean clover seed-set which carried through into 2007 and 2011 (Hall, pers. comm.).

The correlation relationships at "Grandview" were not as consistent, but it must be borne in mind that this research occurred within the 'Millenium drought' that impacted all of south-eastern Australia (Figure 3.4). Growing season rainfall (GSR) for "Grandview" in 2006, 2007 and 2008 was in the first decile of long-term GSR (1970–2000). For 2009, GSR was in the first quartile of long-term averages. In fact, GSR was less than average in seven of the eight years of the study (Table 3.1).

At "Grandview", the severity of the drought between 2006 and 2008 led to restricted plant growth throughout those seasons as a result of the cumulative negative effects on stored soil moisture, which were reflected in the NDVI results in 2007 and 2008. Figure 3.4 shows the extent of the rainfall deficiency between 2006

and 2009, with “Grandview” falling within the zone delineated as ‘lowest on record’. During this period, all three “Grandview” paddocks were in crop (Table 3.2). The farm owner reported such poor crop performance in 2007 and 2008 that many crops on “Grandview” were cut for hay or grazed off, rather than harvested. The extremely poor GSR from 2006–2009 appears to have influenced the strength and direction of some MODIS NDVI pixel correlations. Additionally, pastures were only in the rotation in years 1 and 8, which presents a difficulty for meaningful statistical analysis. Crop and pasture phases at “Grandview” last for six years, so 2004 was the last of a pasture phase which was followed by six years in crop (2005–2010), with a new pasture phase commencing in 2011.

The responses of perennial pastures to seasonal climatic conditions are more complex than annuals, as they do not exhibit the distinct beginning and end of season that characterises both annual pastures and crops. The pattern of perennial pasture growth (and associated NDVI values) at “Grandview” can be affected by annual rainfall outside of the crop growing season. This is especially the case if there is a large difference between AR and GSR. This can result in longer periods of high NDVI readings and bursts of photosynthesis in response to rainfall events. As such, the mixed perennial/annual pasture swards such as at “Grandview” may fluctuate more in NDVI signal strength than at “Milroy” due to differential rates of growth between the various constituents of the pasture. This is evident in 2011, when the NDVI pixel responses to the newly established pasture varied significantly, particularly in paddocks GV8 (s.d.=1.57) and GV39 (s.d.=2.67). These standard deviations were the highest across all years for both these paddocks. The annual rainfall in 2011 was 127% of the long-term average and followed 2010 which received 147% of the long-term average rainfall, so there would have been considerable biomass growth over a long period. In contrast, 2004 (pasture year) annual rainfall was 68% of the long-term average (1970–2000) and standard deviations were 0.19, 0.81 and 1.4 for GV4, GV8 and GV39, respectively.

Notwithstanding the less-than-ideal seasonal conditions in the majority of years, there were strong and significant correlations for both spatial trend and temporal stability in the cropping rotations for the three “Grandview” paddocks. The only

exception was to temporal stability in GV8. It is not clear at this stage why this occurred with GV8, but there were only four pixels in the analysis and it is possible that there are simply too few pixels to develop a clear trend.

Although only an indirect indicator of biomass, by measuring changes in plant canopy optical properties, the MODIS NDVI pixel data in this study enabled changes in crop and pasture growth to be tracked at the sub-paddock scale. The drawback to the analysis is related to the low spatial resolution, which results in mixed pixels and small data sets of between four and eight pixels per paddock, making it difficult to draw firm conclusions about sub-paddock scale spatial variation. Nonetheless, evidence from the results in this chapter provides grounds to accept Hypothesis 1.

## 3.5 CONCLUSION

In this chapter, MODIS NDVI was used as a proxy for biomass production to investigate the nature of biomass growth in crop and pasture phases in a mixed farming system on two properties, in different climatic regions and different states, of Australia.

In the absence of any data on pasture productivity on either farm, MODIS NDVI data was used as an indirect measure of crop and pasture productivity over time. The relationship between the spectral properties of crops and pastures and their biomass/yield has long been recognised, and there is a significant body of published research on the relationship between NDVI and biomass dating back to the 1970s.

This chapter tested Hypothesis 1 (Chapter 2, p. 36), that "*spatial variation in biomass production over time is correlated between the cropping and pasture phases of mixed farming enterprises*".

The correlations between biomass growth in cropping and pasture phases at "Milroy" were encouraging and generally provided evidence in support of the hypothesis being tested. On both properties, poor correlations appear to have been primarily a reflection of periods of plant stress during drought. This may be reflecting variations in soil water availability inherent in differing soil textures and also physical/chemical constraints within a paddock. This was particularly evident in

the drought years at “Grandview” between 2006 and 2009. These possibilities will be explored further in Chapter 5 using proximal soil sensing and soil testing.

Additionally, the relatively coarse spatial resolution of MODIS data is recognised as a limiting factor to the spatial patterns that can be resolved in this analysis, particularly given the size of MODIS pixels (6.25 ha) in comparison with paddock sizes at “Milroy” and “Grandview” (65–100 ha). The relative size of MODIS pixels also means that the analysis was based on a small number of data points once pixels with mixed vegetation were removed, which is likely to introduce some bias. Despite the relatively coarse resolution data used in this initial study, the results, based on multiple paddocks over multiple years, indicate that relationships appear to exist between individual MODIS pixels between the cropping and pasture phases of paddock rotations over time.

These relationships appear to hold for both annual pasture/crop-based systems at “Milroy” and to a lesser extent in the perennial pasture/crop system at “Grandview” which was badly affected by drought between 2006 and 2008. The results are encouraging but are hampered by the low spatial resolution of MODIS NDVI.

The following chapter extends the MODIS NDVI analysis by creating a smoothed time series of the weekly NDVI composites to calculate a range of phenology metrics for each pixel between 2004 and 2011.

The relationships between these metrics and paddock behaviour are explored to see if they can enhance the MODIS NDVI analysis and help to explain some of the inconsistencies reported in this chapter.

## 3.6 REFERENCES

Blackmore, S. (2000). The interpretation of trends from multiple yield maps. *Computers and Electronics in Agriculture, 26*(1), 37–51.

Bradley, B. A., Jacob, R. W., Hermance, J. F., & Mustard, J. F. (2007). A curve fitting procedure to derive inter-annual phenologies from time series of noisy satellite NDVI data. *Remote Sensing of Environment, 106*(2), 137–145. doi: 10.1016/j.rse.2006.08.002

Brown, J. C., Jepson, W. E., Kastens, J. H., Wardlow, B. D., Lomas, J. M., & Price, K. P. (2007). Multitemporal, moderate-spatial-resolution remote sensing of modern agricultural production and land modification in the Brazilian Amazon. *GIScience & Remote Sensing, 44*(2), 117–148. doi: 10.2747/1548-1603.44.2.117

Donald, G. E., Gherardi, S. G., Edirisinghe, A., Gittins, S. P., Henry, D. A., & Mata, G. (2010a). Using MODIS imagery, climate and soil data to estimate pasture growth rates on farms in the south-west of Western Australia. *Animal Production Science, 50*(6), 611–615. doi:10.1071/AN09159

Donald, G. E., Scott, J. M., & Vickery, P. J. (2013). Satellite derived evidence of whole farmlet and paddock responses to management and climate. *Animal Production Science, 53*(8), 699–710. doi: http://dx.doi.org/10.1071/AN11179

Donald, G. E., Trotter, M., & Lamb, D. W. (2010b). *Using high resolution landscape and soils data to understand spatiotemporal variability in net pasture productivity as derived from low spatial resolution remote sensing*. Paper presented at the 15th Agronomy Conference "Food Security from Sustainable Agriculture", Lincoln, New Zealand.

Edirisinghe, A., Hill, M. J., Donald, G. E., & Hyder, M. (2011). Quantitative mapping of pasture biomass using satellite imagery. *International Journal of Remote Sensing, 32*(10), 2699–2724. doi: 10.1080/01431161003743181

Ferencz, C., Bognar, P., Lichtenberger, J., Hamar, D., Tarcsai†, G., Timar, G., . . . Szekely, B. (2004). Crop yield estimation by satellite remote sensing. *International Journal of Remote Sensing, 25*(20), 4113–4149.

Fisher, P. D., Abuzar, M., Rab, M. A., Best, F., & Chandra, S. (2009). Advances in precision agriculture in south-eastern Australia. I. A regression methodology to simulate spatial variation in cereal yields using farmers' historical paddock yields and normalised difference vegetation index. *Crop and Pasture Science, 60*(9), 844–858. doi:10.1071/CP08347

Geerken, R., Batikha, N., Celis, D., & DePauw, E. (2005). Differentiation of rangeland vegetation and assessment of its status: field investigations and MODIS and SPOT VEGETATION data analyses. *International Journal of Remote Sensing, 26*(20), 4499–4526. doi: 10.1080/01431160500213425

Headley, R. (2012). Landsat: A Global Land-Imaging Project. US Geological Survey.

Hill, M. J., & Donald, G. E. (2003). Estimating spatio-temporal patterns of agricultural productivity in fragmented landscapes using AVHRR NDVI time series. *Remote Sensing of Environment, 84*(3), 367–384. doi: 10.1016/s0034-4257(02)00128-1

Hill, M. J., Donald, G. E., Hyder, M. W., & Smith, R. C. G. (2004). Estimation of pasture growth rate in the south west of Western Australia from AVHRR NDVI and climate data. *Remote Sensing of Environment, 93*(4), 528–545.

Hill, M. J., Vickery, P. J., Furnival, E. P., & Donald, G. E. (1999). Pasture land cover in eastern Australia from NOAA-AVHRR NDVI and classified Landsat TM. *Remote Sensing of Environment, 67*(1), 32–50.

Holben, B. N. (1986). Characteristics of maximum-value composite images from temporal AVHRR data. *International Journal of Remote Sensing, 7*(11), 1417–1434. doi: 10.1080/01431168608948945

Hu, Z., Zhengwei, Y., Liping, D., Lin, L., & Haihong, Z. (2009). *Crop phenology date estimation based on NDVI derived from the reconstructed MODIS daily surface reflectance data*. Paper presented at the 17th International Conference on Geoinformatics.

Isbell, R. (2016). *The Australian soil classification*: CSIRO Publishing.

Jönsson, P., & Eklundh, L. (2004). TIMESAT-a program for analyzing time-series of satellite sensor data. *Computers & Geosciences, 30*(8), 833–845.

Ju, J., & Roy, D. P. (2008). The availability of cloud-free Landsat ETM+ data over the conterminous United States and globally. *Remote Sensing of Environment, 112*(3), 1196–1211.

Perry, E., Morse-McNabb, E., Nuttall, J., O'Leary, G., & Clark, R. (2013). *Managing wheat from space: Linking MODIS NDVI and crop models for Australian dryland wheat.* Paper presented at the International Geoscience and Remote Sensing Symposium (IGARSS).

Reed, B. C., Brown, J. F., VanderZee, D., Loveland, T. R., Merchant, J. W., & Ohlen, D. O. (1994). Measuring phenological variability from satellite imagery. *Journal of Vegetation Science, 5*(5), 703–714.

Reed, B. C., Loveland, T. R., & Tieszen, L. L. (1996). An approach for using AVHRR data to monitor US Great Plains grasslands. *Geocarto International, 11*(3), 13–22.

Schut, A. G. T., Stephens, D. J., Stovold, R. G. H., Adams, M., & Craig, R. L. (2009). Improved wheat yield and production forecasting with a moisture stress index, AVHRR and MODIS data. *Crop and Pasture Science, 60*(1), 60–70. doi:10.1071/CP08182

Smith, R. C. G., Adams, J., Stephens, D. J., & Hick, P. T. (1995). Forecasting wheat yield in a mediterranean-type environment from the NOAA satellite. *Australian Journal of Agricultural Research, 46*(1), 113–125. doi:10.1071/AR9950113

Smith, R. C. G., Adams, M., Gittins, S., Gherardi, S., Wood, D., Maier, S., . . . Allen, A. (2011). Near real-time feed on offer (FOO) from MODIS for early season grazing management of Mediterranean annual pastures. *International Journal of Remote Sensing, 32*(16), 4445–4460.

Verboom, W., & Galloway, P. (2004). Corrigin area land resources survey. *Land Resources Series*(20).

Wardlow, B. D., Egbert, S. L., & Kastens, J. H. (2007). Analysis of time-series MODIS 250 m vegetation index data for crop classification in the U.S. Central Great Plains. *Remote Sensing of Environment, 108*(3), 290–310. doi: 10.1016/j.rse.2006.11.021

Xu, Q., Yang, G., Long, H., Wang, C., Li, X., & Huang, D. (2014). Crop information identification based on MODIS NDVI time-series data. *Nongye Gongcheng Xuebao/Transactions of the Chinese Society of Agricultural Engineering, 30*(11), 134–144. doi: 10.3969/j.issn.1002-6819.2014.11.017

# CHAPTER 4. ANALYSIS OF CROP AND PASTURE PHENOLOGY WITH MODIS NDVI TIME SERIES

## 4.1 INTRODUCTION

The previous chapter described the analysis of accumulated MODIS NDVI data over an eight-year period to determine if there was any correlation, over time, in biomass production between the cropping and pasture–livestock phases in two mixed farming systems. The analysis, which used a broad metric in the form of total accumulated annual NDVI, showed a strong correlation, on a pixel-by-pixel basis, in biomass production across the experimental paddocks at "Milroy". The exceptions were due to drought effects in 2006 and 2010. The correlations for "Grandview" were less clear but were likely to have been affected by the millennium drought. In this chapter, Hypothesis 1, that "*spatial variation in biomass production over time is correlated between the cropping and pasture phases of mixed farming enterprises*", is further tested by comparing crop and pasture phenology in each paddock MODIS pixel to determine if correlations exist between crop and pasture phenology. This is done using the TIMESAT 3.1 software package developed by Jönsson and Eklundh (2004). TIMESAT was used to characterise vegetation phenology in the "Milroy" and "Grandview" paddocks by extracting numerical observations related to vegetation dynamics for each MODIS NDVI pixel in the time series of NDVI data (Henebry and de Beurs, 2013; Reed et al., 2009). The software creates and analyses smoothed time-series satellite sensor data. The temporal smoothing removes artefacts associated with atmospheric conditions, data gaps and cloud cover effects. After smoothing, extracted profiles are significantly clearer making it possible to identify phenological markers. The TIMESAT software provides three different smoothing functions to fit time-series data (Eklundh and Jönsson, 2011): asymmetric Gaussian (AG) (Jönsson and Eklundh, 2002), double logistic (DL) (Beck et al., 2006) and adaptive Savitzky-Golay (SG) filtering (Chen et al., 2004).

## 4.2 MATERIALS AND METHODS

### *4.2.1 CALCULATION OF NDVI PHENOLOGY METRICS*

The TIMESAT programme processes NDVI time-series curves to calculate a set of phenology metrics. The metrics decompose the curve into a set of statistics which are shown in Figure 4.1 and described in Table 4.1. In this analysis, all three smoothing methods contained within TIMESAT were tested by creating smoothed curves from "Milroy" paddock M25 NDVI data (Figure 4.2). All three approaches have different strengths and weaknesses. Both the AG and DL approaches are less sensitive to noise and can give a better description on the beginning and ending of the seasons (Jönsson and Eklundh, 2002) than SG (Hird and McDermid, 2009). Although the adaptive SG approach can identify subtle and rapid changes in the time series, it is sensitive to noise. Beck et al. (2006), Gao et al. (2008) and Hird et al. (2009) examined the DL and AG function approaches and found that they produced similar results, with the AG method being less sensitive to incomplete time-series data and concluding that either method was appropriate for describing vegetation dynamics. The overall advantage of the AG method is flexibility, in that it can be applied to time series at varying temporal resolutions (e.g. daily, bi-weekly, monthly values), and with scaled or unscaled NDVI values. Based on assessments of the three approaches in the literature, the AG method was selected for temporally smoothing data and estimating phenology metrics.

Smoothed time series of weekly NDVI composites for each MODIS pixel were constructed using the AG filter. The parameters applied in the TIMESAT analysis were as described in the TIMESAT 3.1 software manual, section 9.4; seasonal parameter: 0.5, number of envelope iterations: 1, number of seasons/year: 1 (setting the seasonality parameter to 1 forces the program to treat data as if there is one annual season), adaptation strength: 2, SG window size: 4, amplitude value: 0, season start: 0.1, season end: 0.1. Eight complete phenological cycles (2004–2011) were processed using the MODIS NDVI data from Chapter 3 and 11 phenology metrics were calculated for each cycle. The raw metric values for the small integral (as a proxy for annual biomass production) were also graphed against

GSR, by paddock, for each pixel, to examine within-paddock spatial and temporal variation across the study period.

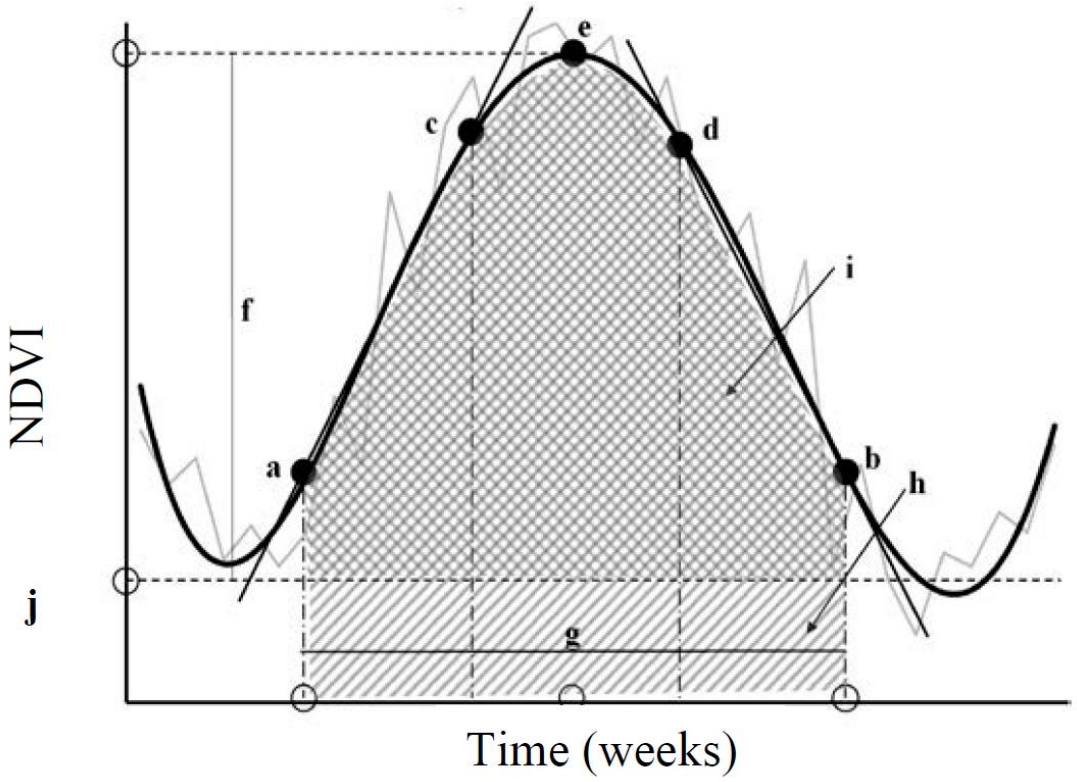


**FIGURE 4.1:** PHENOLOGY METRICS ASSOCIATED WITH THE SMOOTHED CURVE OF AN NDVI TIME SERIES. 'A' = START OF ACTIVE GROWING SEASON; 'B'=END OF ACTIVE GROWING SEASON; 'C' & 'D' = 80% POINTS FOR CALCULATING MIDDLE OF SEASON; 'E' = VALUE AT PEAK OF SEASON; 'AC' & 'DB' = RATES OF INCREASE/DECREASE (RATE OF GREEN-UP/DECLINE); 'F' = AMPLITUDE; 'G' = SEASON LENGTH; 'H' = LARGE INTEGRAL; 'I' = SMALL INTEGRAL (SEASONAL VEGETATION PRODUCTIVITY); 'J' BASE LEVEL. ADAPTED FROM TUANMU ET AL. (2010).

### *4.2.2 STATISTICAL ANALYSIS*

Data from 34 MODIS pixels were processed through TIMESAT from the three paddocks at "Milroy" and three at "Grandview" over the eight-year period (2004–2011). The paddock pixel means were then used in a correlation analysis using JMP 12.2 to explore relationships between pasture and crop phenology over the eight

years of the data set. Because of the small number of pixels per paddock, the data sets were analysed by farm rather than by paddock.

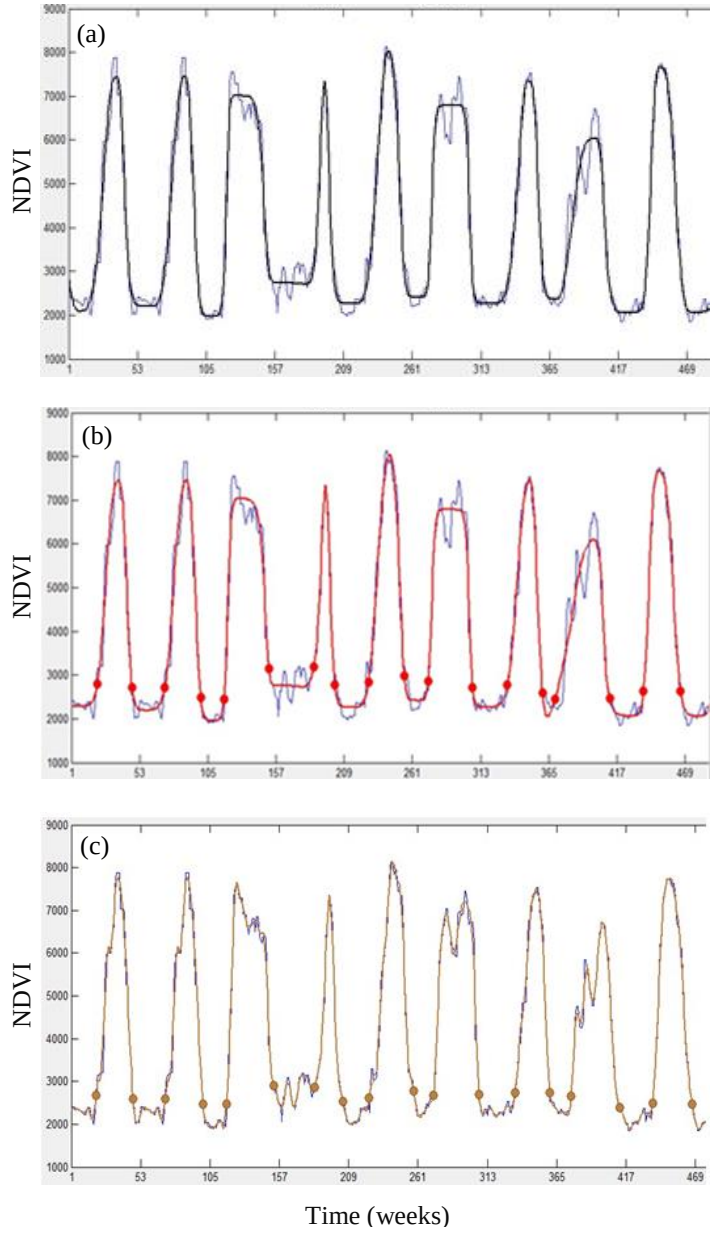


**FIGURE 4.2:** EXAMPLE OF NDVI SIGNAL SMOOTHING FROM "MILROY" PADDOCK M25 BY (A) ASYMMETRIC GAUSSIAN, (B) DOUBLE LOGISTIC AND (C) SAVITZKY-GOLAY APPROACHES USING TIMESAT 3.1.

**TABLE 4.1:** DEFINITIONS OF THE TIMESAT SEASONALITY PARAMETERS SHOWN IN FIGURE 4.1 AND THE METHOD OF CALCULATION.

| | Metric | Significance | How calculated |
|---|---|---|---|
| a | Season onset | Time at which seasonal photosynthetic activity begins | Time for which the left edge increased to 10% of the seasonal amplitude, measured from the left minimum level |
| b | Season end | Time at which seasonal photosynthetic activity ends | Time for which the right edge decreased to 10% of the seasonal amplitude, measured from the right minimum level |
| g | Season length | Period of seasonal photosynthetic activity | Time from the start to the end of the season |
| j | Base level | | Given as the average of the left and right minimum values |
| c,d | Peak time | Time at which seasonal photosynthetic activity reaches a maximum | Computed as the mean value of the times for which, respectively, the left edge increased to the 80% level, and the right edge decreased to the 80% level |
| e | Peak value | Maximum level of seasonal photosynthetic activity | Largest data value for the fitted function during the season |
| f | Seasonal amplitude | Amplitude of seasonal photosynthetic activity, measure of seasonality | Difference between the maximum value and the base level |
| a–c | Left derivative | Rate of increase at the beginning of the season | Calculated as the ratio of the difference between the left 20% and 80% levels and the corresponding time difference |
| d–b | Right derivative | Rate of decrease at the end of the season | Calculated as the absolute value of the ratio of the difference between the right 20% and 80% levels and the corresponding time difference. The rate of decrease is thus given as a positive quantity |
| i | Large seasonal integral | Accumulation of seasonal photosynthetic activity, related to biomass | Integral of the function describing the season from the season start to the season end |
| h | Small seasonal integral | Accumulation of seasonal photosynthetic activity, related to biomass | Integral of the difference between the function describing the season and the base level from season start to season end |

Source: (Tuanmu et al., 2010)

## 4.3 RESULTS

The means for the phenology metrics, by MODIS pixel for both crop and pasture phases, for each paddock at "Milroy" are shown in Tables 4.3–4.5 and for "Grandview" paddocks in Tables 4.6–4.8. The results of the correlation analysis between crop and pasture pixel means for each property are at Table 4.9.

The correlation analysis for "Milroy" showed reasonably strong and significant correlations for end of season, peak ndvi value, seasonal amplitude and small integral. At "Grandview", reasonably strong and significant correlations occurred for start of season (negative), season length (negative), timing of peak ndvi value and seasonal amplitude (negative). In both crop and pasture phases at "Milroy," there were variations in mean emergence times between pixels which ranged from two weeks for paddock M25 to five weeks for paddock M45 (Tables 4.3–4.5). The mean rate of green-up shows that pixel 52 in M25, pixel 12 in M41 and pixel 23 in M45 exhibited the fastest rates of growth, whether in crop or pasture. The slowest pixels to senesce (seasonal amplitude or rate of brown-off) were pixels 58, 3 and 25. Peak NDVI and greatest amplitude occurred at pixel 45 and 52 in M25, pixel 12 in M41 and pixel 20 in M45. In paddocks M25, M41 and M45, pixels 45, 3/4 and 20 were respectively associated with the longest mean season lengths and highest, or close to highest, total mean biomass production as measured by the small integral. At "Grandview", there was less variation evident between mean values for the start of the season for both crop and pasture, with no more than a week's variation in crop emergence and no more than two week's variation in pasture, for all pixels in all three paddocks. In paddock GV4, pixel 52 exhibited the fastest mean rate of green-up for crop and pasture and pixel 46 had the slowest mean rate of brown-off. Pixel 46 also had the longest mean growing period for crop and close to longest for pasture and highest mean biomass production for crop as measured by the small integral. In GV8, pixels 40 and 42 had the fastest mean rate of growth for crop and second fastest for pasture, and pixels 37 and 38 shared the longest mean rate of brown-off. This accorded with the longest mean growing periods for crop, but not for pasture (pixels 40 and 42 for pasture). Pixels 40 and 42 had the highest mean biomass for crop as measured by the small integral, with pixels 37 and 38 being

highest for pasture. Pixel 8 had the fastest mean rate of growth and rates of brown-off in paddock GV39. Mean growing length between pixels was similar in crop, but there was up to four-week's difference between pixels for pasture.

Figure 4.3 provides an example of the smoothed NDVI time-series curves fitted by the TIMESAT programme using the AG approach. The example is for the eight MODIS pixels (here labelled P1 to P8) in "Milroy" paddock M45. The pale blue lines are the raw NDVI signals.

Graphs showing the small integral (as a proxy of annual biomass production) plotted against GSR, by paddock, for each pixel, are in Figure 4.4 for "Milroy" paddocks and Figure 4.5 for "Grandview" paddocks. These graphs do not discriminate between crop and pasture phases; all data has been combined. It can be seen that the NDVI response generally tracks GSR. At "Milroy", there is significant spatial variation evident between pixels within a year, except in 2008 where it is less than the temporal variation (between years), demonstrating a temporal response to climate. At "Grandview", there appears to be much less spatial variation evident between pixels within a year than at "Milroy". Temporal variation is greater than spatial variation between pixels within a year, again indicating a temporal response to climate. The years 2006–2008 were drought years.

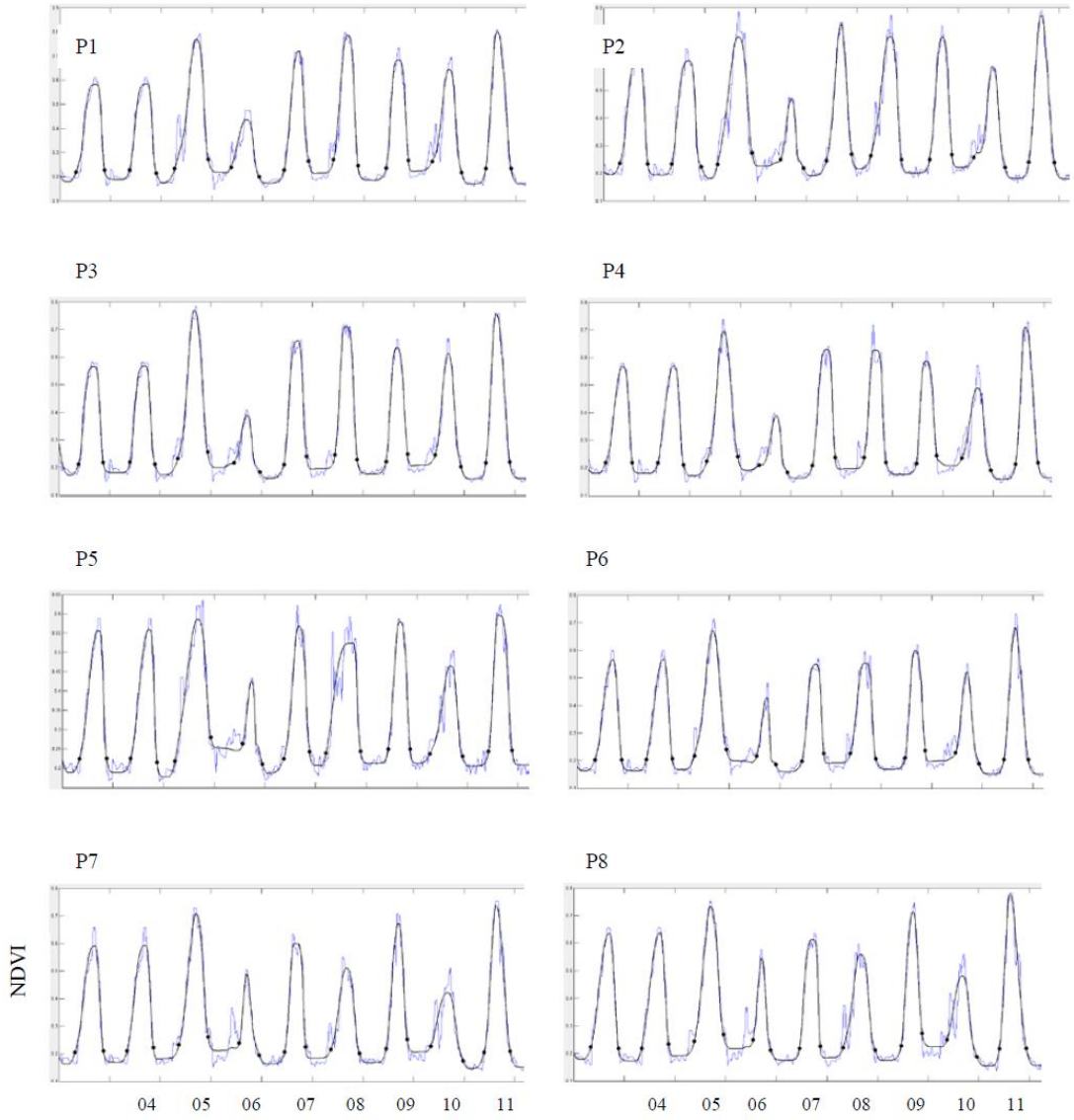


**FIGURE 4.3:** SMOOTHED NDVI TIME-SERIES CURVES FITTED BY THE TIMESAT PROGRAMME USING THE ASYMMETRIC GAUSSIAN APPROACH FOR THE EIGHT MODIS PIXELS IN "MILROY" PADDOCK M45. THE NDVI VALUES ON THE LEFT-HAND AXIS ARE IN 0.1 INCREMENTS, BEGINNING AT 0.1. THE SEQUENCE STARTS IN 2004, THE FIRST CURVE ON THE LEFT IS A 'DUMMY' CURVE REQUIRED TO FORCE TIMESAT TO PROCESS THE FULL SEQUENCE OF YEARS.

**TABLE 4.2:** AN EXAMPLE OF THE OUTPUT FROM TIMESAT, PIXEL 45 FROM "MILROY" PADDOCK M25, BETWEEN 2004 AND 2011, SHOWING VALUES FOR THE DERIVED PHENOLOGY METRICS. THE GAUSSIAN FIT WAS USED. SEASON START, SEASON END, SEASON LENGTH AND PEAK TIME ARE MEASURED IN WEEKS FROM 1 JANUARY. PEAK VALUE AND AMPLITUDE ARE NDVI VALUES, AND THE REMAINING METRICS ARE UNIT-LESS.

| Pixel ID | Rotation phase | Year | Season start (week) | Season end (week) | Season length (weeks) | Base value (NDVI) | Peak time (week) | Peak value (NDVI) | Ampli-tude (NDVI) | Rate of green-up | Rate of die-off | Large integral | Small integral |
|---|---|---|---|---|---|---|---|---|---|---|---|---|---|
| 45 | wheat | 2004 | 20.37 | 47.60 | 27.24 | 0.2092 | 35.81 | 0.7454 | 0.5362 | 0.04016 | 0.0662 | 15.34 | 9.27 |
| 45 | pasture | 2005 | 12.5 | 47.00 | 34.41 | 0.2344 | 28.60 | 0.7021 | 0.4677 | 0.0937 | 0.04785 | 21.42 | 12.98 |
| 45 | pasture | 2006 | 30.9 | 46.00 | 15.07 | 0.2483 | 38.70 | 0.7351 | 0.4867 | 0.0656 | 0.08127 | 8.35 | 4.13 |
| 45 | barley | 2007 | 19.3 | 47.10 | 27.83 | 0.2338 | 35.10 | 0.8032 | 0.5694 | 0.04219 | 0.06353 | 16.99 | 9.98 |
| 45 | pasture | 2008 | 13.2 | 47.10 | 33.87 | 0.2335 | 30.10 | 0.6797 | 0.4461 | 0.07452 | 0.07844 | 21.01 | 12.60 |
| 45 | wheat | 2009 | 21.4 | 48.20 | 26.76 | 0.2311 | 37.10 | 0.7349 | 0.5038 | 0.03919 | 0.06807 | 15.13 | 8.43 |
| 45 | pasture | 2010 | 11.5 | 47.50 | 36.01 | 0.2215 | 32.20 | 0.6104 | 0.3889 | 0.02198 | 0.04642 | 17.83 | 9.42 |
| 45 | pasture | 2011 | 20.3 | 48.70 | 28.41 | 0.2071 | 33.20 | 0.7656 | 0.5585 | 0.06845 | 0.04758 | 16.86 | 10.65 |

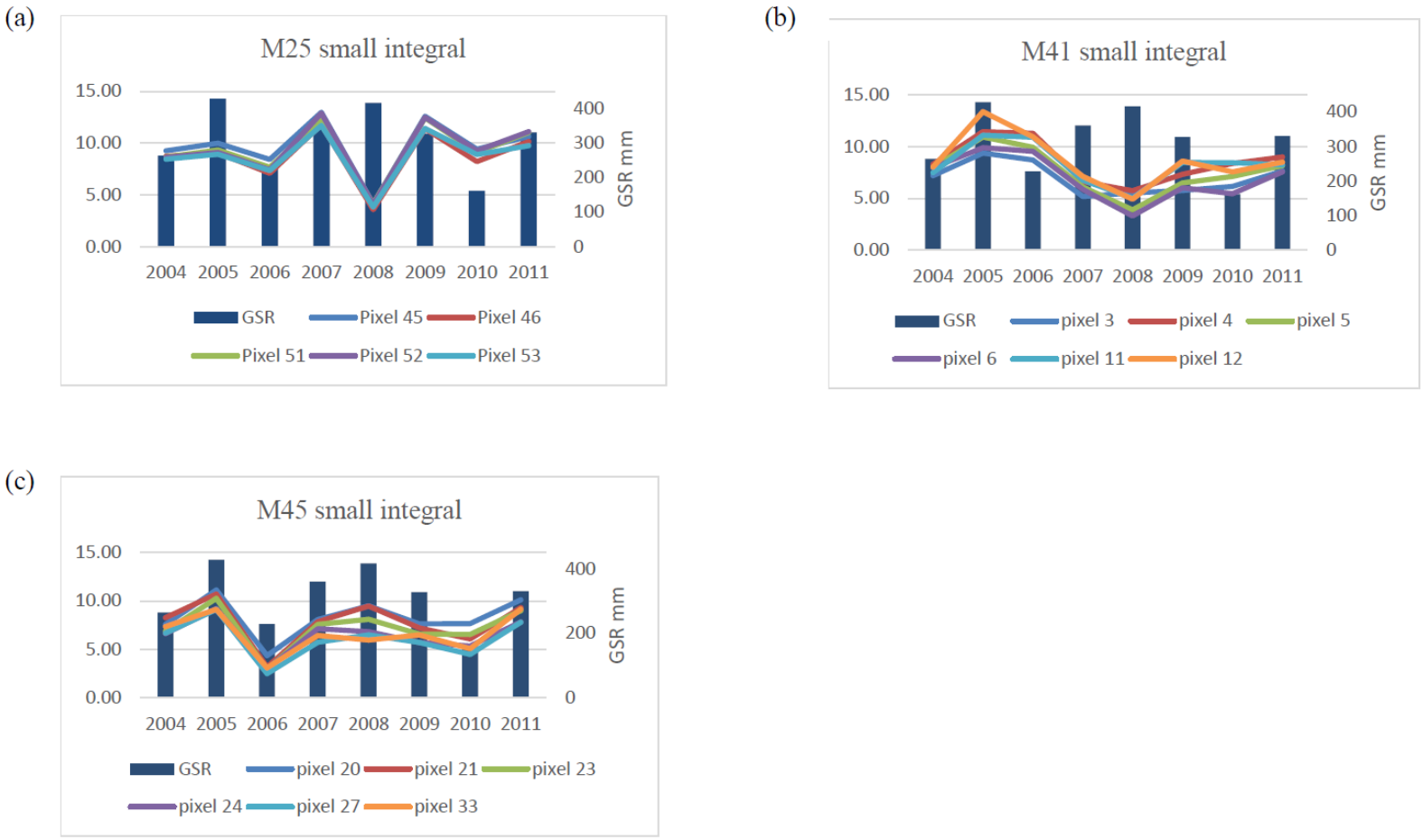


**FIGURE 4.4:** SMALL INTEGRAL (A PROXY FOR ANNUAL BIOMASS PRODUCTION) AGAINST GROWING SEASON RAINFALL (GSR) FOR MODIS PIXELS ANALYSED FROM "MILROY" PADDOCKS (A) M25, (B) M41 AND (C) M45 FROM 2004–2011.

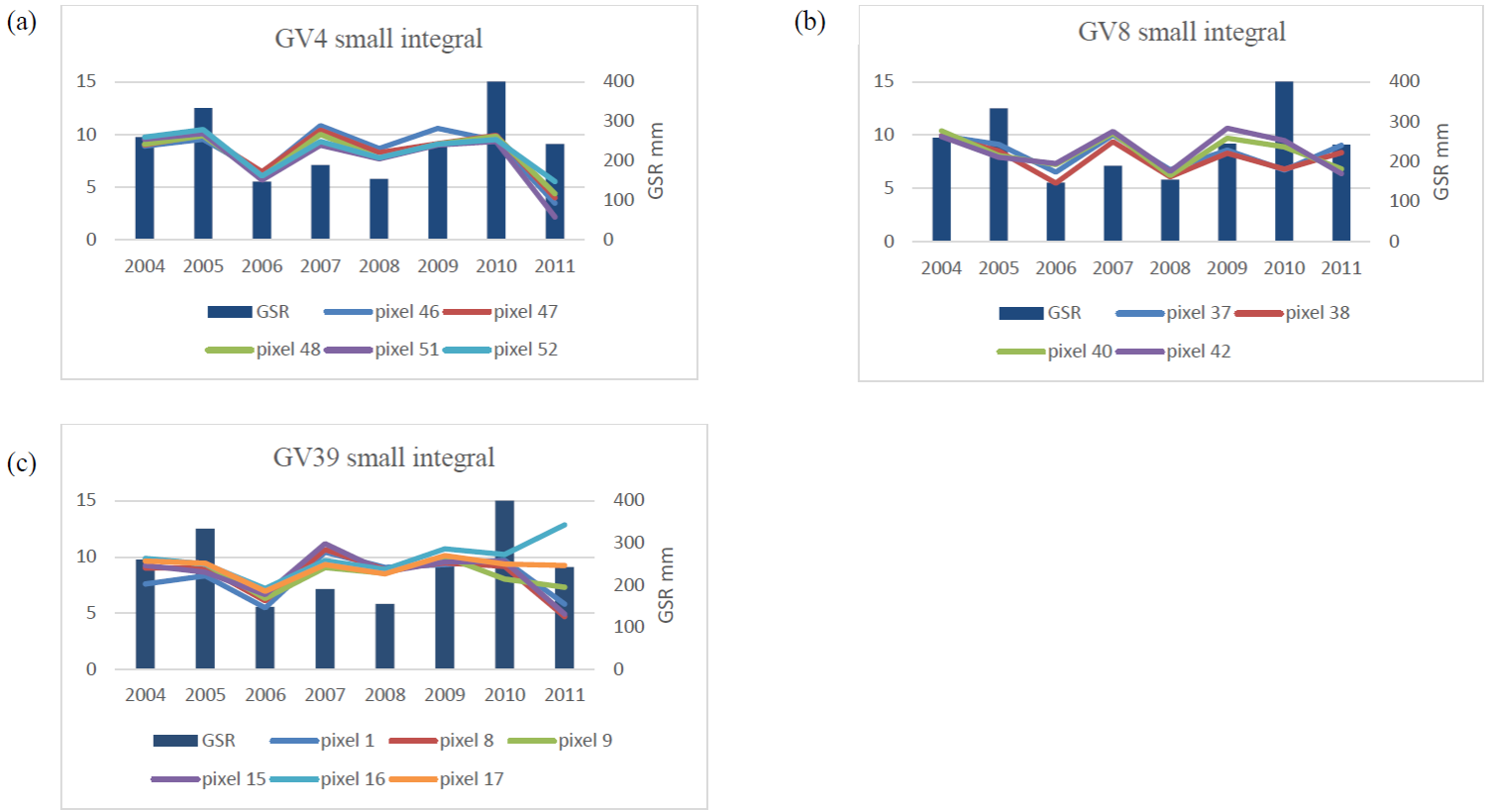


**FIGURE 4.5:** SMALL INTEGRAL (A PROXY FOR ANNUAL BIOMASS PRODUCTION) AGAINST GROWING SEASON RAINFALL (GSR) FOR MODIS PIXELS ANALYSED FROM "GRANDVIEW" PADDOCKS (A) GV4, (B) GV8 AND (C) GV39 FROM 2004–2011. PASTURE YEARS WERE 2004 (OLD PASTURE GOING INTO A NEW SIX-YEAR CROP PHASE) AND 2011 (NEW SIX-YEAR PASTURE PHASE COMING OUT OF CROP).

**TABLE 4.3:** MEANS OF PHENOLOGY METRICS FOR BOTH CROP AND PASTURE PHASES FROM TIMESAT FOR "MILROY" PADDOCK M25. SEASON START, SEASON END, SEASON LENGTH AND PEAK TIME ARE MEASURED IN WEEKS FROM 1 JANUARY. PEAK VALUE AND AMPLITUDE ARE NDVI VALUES, AND THE REMAINING METRICS ARE UNIT-LESS.

| Pixel | Season start (week) | | Season end (week) | | Season length (weeks) | | Peak time (week) | | Peak value (NDVI) | |
|---|---|---|---|---|---|---|---|---|---|---|
| | crop | pasture | crop | pasture | crop | pasture | crop | pasture | crop | pasture |
| 45 | 20.36 | 17.68 | 47.63 | 47.26 | 27.28 | 29.55 | 36.00 | 32.56 | 0.76 | 0.70 |
| 46 | 22.26 | 17.22 | 47.72 | 47.34 | 25.47 | 30.11 | 36.59 | 32.54 | 0.77 | 0.67 |
| 51 | 22.33 | 16.08 | 46.34 | 46.58 | 24.01 | 30.52 | 35.80 | 31.36 | 0.78 | 0.66 |
| 52 | 23.30 | 15.92 | 46.36 | 46.82 | 23.06 | 30.90 | 35.73 | 31.20 | 0.79 | 0.67 |
| 58 | 21.45 | 15.88 | 46.23 | 46.36 | 24.82 | 30.48 | 35.41 | 31.08 | 0.74 | 0.64 |
| | **Amplitude (NDVI)** | | **Rate of green-up** | | **Rate of die-off** | | **Large integral** | | **Small integral** | |
| | crop | pasture | crop | pasture | crop | pasture | crop | pasture | crop | pasture |
| 45 | 0.54 | 0.47 | 0.04 | 0.06 | 0.07 | 0.06 | 15.82 | 17.09 | 9.22 | 9.96 |
| 46 | 0.53 | 0.42 | 0.04 | 0.05 | 0.07 | 0.06 | 14.88 | 16.82 | 8.29 | 9.02 |
| 51 | 0.57 | 0.45 | 0.05 | 0.06 | 0.08 | 0.06 | 14.00 | 16.85 | 8.55 | 9.79 |
| 52 | 0.57 | 0.45 | 0.06 | 0.06 | 0.08 | 0.06 | 13.90 | 17.18 | 8.40 | 9.97 |
| 58 | 0.52 | 0.42 | 0.05 | 0.05 | 0.07 | 0.05 | 14.12 | 16.29 | 8.23 | 9.12 |

**TABLE 4.4:** MEANS OF PHENOLOGY METRICS FOR BOTH CROP AND PASTURE PHASES FROM TIMESAT FOR "MILROY" PADDOCK M41. SEASON START, SEASON END, SEASON LENGTH AND PEAK TIME ARE MEASURED IN WEEKS FROM 1 JANUARY. PEAK VALUE AND AMPLITUDE ARE NDVI VALUES, AND THE REMAINING METRICS ARE UNIT-LESS.

| Pixel | Season start (week) | | Season end (week) | | Season length (weeks) | | Peak time (week) | | Peak value (NDVI) | |
|---|---|---|---|---|---|---|---|---|---|---|
| | crop | pasture | crop | pasture | crop | pasture | crop | pasture | crop | pasture |
| 3 | 20.25 | 18.80 | 47.98 | 48.25 | 27.75 | 29.45 | 35.34 | 34.33 | 0.67 | 0.62 |
| 4 | 18.77 | 19.78 | 48.12 | 47.75 | 29.35 | 27.97 | 35.90 | 35.58 | 0.70 | 0.66 |
| 5 | 20.06 | 22.55 | 47.80 | 47.05 | 27.74 | 24.50 | 36.76 | 36.13 | 0.71 | 0.66 |
| 6 | 21.35 | 22.95 | 47.63 | 45.95 | 26.29 | 22.98 | 36.96 | 36.08 | 0.71 | 0.64 |
| 11 | 21.53 | 21.55 | 48.80 | 47.45 | 27.26 | 25.91 | 37.14 | 35.50 | 0.73 | 0.67 |
| 12 | 21.64 | 22.33 | 48.55 | 47.30 | 26.93 | 24.96 | 36.95 | 35.78 | 0.72 | 0.67 |
| | **Amplitude (NDVI)** | | **Rate of green-up** | | **Rate of die-off** | | **Large integral** | | **Small integral** | |
| | crop | pasture | crop | pasture | crop | pasture | crop | pasture | crop | pasture |
| 3 | 0.40 | 0.35 | 0.05 | 0.03 | 0.06 | 0.03 | 15.49 | 14.84 | 7.60 | 6.25 |
| 4 | 0.48 | 0.44 | 0.04 | 0.03 | 0.08 | 0.05 | 16.34 | 14.25 | 9.41 | 7.59 |
| 5 | 0.48 | 0.43 | 0.04 | 0.04 | 0.08 | 0.06 | 15.62 | 12.43 | 8.73 | 6.40 |
| 6 | 0.47 | 0.40 | 0.05 | 0.04 | 0.09 | 0.06 | 15.04 | 11.37 | 8.30 | 5.57 |
| 11 | 0.52 | 0.47 | 0.04 | 0.04 | 0.07 | 0.06 | 15.05 | 13.08 | 9.05 | 7.53 |
| 12 | 0.52 | 0.48 | 0.06 | 0.05 | 0.08 | 0.06 | 15.69 | 12.65 | 9.86 | 7.38 |

**TABLE 4.5:** MEANS OF PHENOLOGY METRICS FOR BOTH CROP AND PASTURE PHASES FROM TIMESAT FOR "MILROY" PADDOCK M45. SEASON START, SEASON END, SEASON LENGTH AND PEAK TIME ARE MEASURED IN WEEKS FROM 1 JANUARY. PEAK VALUE AND AMPLITUDE ARE NDVI VALUES, AND THE REMAINING METRICS ARE UNIT-LESS.

| Pixel | Season start (week) | | Season end (week) | | Season length (weeks) | | Peak time (week) | | Peak value (NDVI) | |
|---|---|---|---|---|---|---|---|---|---|---|
| | crop | pasture | crop | pasture | crop | pasture | crop | pasture | crop | pasture |
| 20 | 19.73 | 22.13 | 48.12 | 47.93 | 28.41 | 25.78 | 36.30 | 35.60 | 0.701 | 0.639 |
| 21 | 17.33 | 23.90 | 48.40 | 48.23 | 31.06 | 24.35 | 35.58 | 36.20 | 0.664 | 0.644 |
| 23 | 22.42 | 24.27 | 48.15 | 48.63 | 25.73 | 24.36 | 36.24 | 36.17 | 0.664 | 0.593 |
| 24 | 21.33 | 23.30 | 48.07 | 47.60 | 26.74 | 24.32 | 36.26 | 36.23 | 0.602 | 0.560 |
| 25 | 15.73 | 25.53 | 47.56 | 47.77 | 31.84 | 22.22 | 35.40 | 36.80 | 0.540 | 0.533 |
| 27 | 21.49 | 25.90 | 48.01 | 47.70 | 26.52 | 21.80 | 36.48 | 36.70 | 0.572 | 0.569 |
| 33 | 20.47 | 25.40 | 48.73 | 48.37 | 28.26 | 22.95 | 36.29 | 36.47 | 0.567 | 0.633 |
| 34 | 20.41 | 24.40 | 48.50 | 46.97 | 28.09 | 22.54 | 36.44 | 36.87 | 0.604 | 0.631 |
| | **Amplitude (NDVI)** | | **Rate of green-up** | | **Rate of die-off** | | **Large integral** | | **Small integral** | |
| | crop | pasture | crop | pasture | crop | pasture | crop | pasture | crop | pasture |
| 20 | 0.508 | 0.449 | 0.039 | 0.048 | 0.069 | 0.055 | 14.67 | 12.68 | 8.80 | 7.37 |
| 21 | 0.463 | 0.445 | 0.033 | 0.044 | 0.055 | 0.054 | 15.19 | 11.80 | 8.49 | 6.56 |
| 23 | 0.483 | 0.416 | 0.048 | 0.049 | 0.062 | 0.046 | 12.91 | 10.80 | 7.88 | 6.17 |
| 24 | 0.421 | 0.385 | 0.038 | 0.049 | 0.060 | 0.048 | 12.18 | 10.12 | 7.03 | 5.51 |
| 25 | 0.338 | 0.321 | 0.021 | 0.036 | 0.051 | 0.044 | 13.58 | 9.75 | 6.71 | 4.61 |
| 27 | 0.398 | 0.400 | 0.033 | 0.046 | 0.056 | 0.059 | 11.51 | 9.32 | 6.51 | 5.34 |
| 33 | 0.388 | 0.459 | 0.032 | 0.050 | 0.052 | 0.048 | 12.21 | 10.54 | 6.80 | 6.25 |
| 34 | 0.416 | 0.441 | 0.032 | 0.043 | 0.060 | 0.062 | 12.90 | 10.68 | 7.23 | 6.16 |

**TABLE 4.6:** MEANS OF PHENOLOGY METRICS FOR BOTH CROP AND PASTURE PHASES FROM TIMESAT FOR "GRANDVIEW" PADDOCK GV4. SEASON START, SEASON END, SEASON LENGTH AND PEAK TIME ARE MEASURED IN WEEKS FROM 1 JANUARY. PEAK VALUE AND AMPLITUDE ARE NDVI VALUES, AND THE REMAINING METRICS ARE UNIT-LESS.

| Pixel | Season start (week) | | Season end (week) | | Season length (weeks) | | Peak time (week) | | Peak value (NDVI) | |
|---|---|---|---|---|---|---|---|---|---|---|
| | crop | pasture | crop | pasture | crop | pasture | crop | pasture | crop | pasture |
| 46 | 22.97 | 13.08 | 47.13 | 47.69 | 24.19 | 34.61 | 36.25 | 37.97 | 0.773 | 0.742 |
| 47 | 23.32 | 13.60 | 47.17 | 47.85 | 23.88 | 34.25 | 36.50 | 37.58 | 0.773 | 0.737 |
| 48 | 23.72 | 13.24 | 47.28 | 47.61 | 23.56 | 34.38 | 36.72 | 37.40 | 0.775 | 0.733 |
| 51 | 24.02 | 13.23 | 47.05 | 48.20 | 23.03 | 34.98 | 36.90 | 38.07 | 0.778 | 0.755 |
| 52 | 23.98 | 13.31 | 47.00 | 48.40 | 23.03 | 35.10 | 36.88 | 38.23 | 0.781 | 0.759 |
| | **Amplitude (NDVI)** | | **Rate of green-up** | | **Rate of die-off** | | **Large integral** | | **Small integral** | |
| | crop | pasture | crop | pasture | crop | pasture | crop | pasture | crop | pasture |
| 46 | 0.742 | 0.406 | 0.066 | 0.042 | 0.098 | 0.086 | 15.25 | 13.90 | 9.23 | 6.19 |
| 47 | 0.737 | 0.394 | 0.063 | 0.051 | 0.112 | 0.079 | 15.05 | 19.29 | 9.03 | 6.50 |
| 48 | 0.733 | 0.393 | 0.062 | 0.055 | 0.105 | 0.089 | 14.91 | 18.79 | 8.75 | 6.74 |
| 51 | 0.755 | 0.429 | 0.062 | 0.054 | 0.112 | 0.098 | 14.44 | 11.99 | 8.46 | 5.86 |
| 52 | 0.759 | 0.433 | 0.064 | 0.066 | 0.120 | 0.098 | 14.48 | 24.88 | 8.71 | 7.64 |

**TABLE 4.7:** MEANS OF PHENOLOGY METRICS FOR BOTH CROP AND PASTURE PHASES FROM TIMESAT FOR "GRANDVIEW" PADDOCK GV8. SEASON START, SEASON END, SEASON LENGTH AND PEAK TIME ARE MEASURED IN WEEKS FROM 1 JANUARY. PEAK VALUE AND AMPLITUDE ARE NDVI VALUES, AND THE REMAINING METRICS ARE UNIT-LESS.

| Pixel | Season start (week) | | Season end (week) | | Season length (weeks) | | Peak time (week) | | Peak value (NDVI) | |
|---|---|---|---|---|---|---|---|---|---|---|
| | crop | pasture | crop | pasture | crop | pasture | crop | pasture | crop | pasture |
| 37 | 21.43 | 21.43 | 47.07 | 48.15 | 25.62 | 26.78 | 36.08 | 37.81 | 0.727 | 0.812 |
| 38 | 21.75 | 21.43 | 46.98 | 48.15 | 25.21 | 26.78 | 35.95 | 37.81 | 0.742 | 0.812 |
| 40 | 23.32 | 18.79 | 46.40 | 47.39 | 23.11 | 28.57 | 36.02 | 36.73 | 0.779 | 0.798 |
| 42 | 23.02 | 18.62 | 46.82 | 46.71 | 23.80 | 28.10 | 36.03 | 36.48 | 0.776 | 0.773 |
| | **Amplitude (NDVI)** | | **Rate of green-up** | | **Rate of die-off** | | **Large integral** | | **Small integral** | |
| | crop | pasture | crop | pasture | crop | pasture | crop | pasture | crop | pasture |
| 37 | 0.483 | 0.529 | 0.046 | 0.044 | 0.078 | 0.107 | 14.72 | 17.78 | 7.95 | 9.49 |
| 38 | 0.474 | 0.529 | 0.047 | 0.044 | 0.068 | 0.107 | 14.70 | 17.78 | 7.43 | 9.49 |
| 40 | 0.521 | 0.458 | 0.064 | 0.042 | 0.092 | 0.090 | 14.81 | 19.03 | 8.38 | 8.60 |
| 42 | 0.531 | 0.433 | 0.063 | 0.042 | 0.088 | 0.107 | 15.04 | 18.41 | 8.71 | 8.12 |

**TABLE 4.8:** MEANS OF PHENOLOGY METRICS FOR BOTH CROP AND PASTURE PHASES FROM TIMESAT FOR "GRANDVIEW" PADDOCK GV39. SEASON START, SEASON END, SEASON LENGTH AND PEAK TIME ARE MEASURED IN WEEKS FROM 1 JANUARY. PEAK VALUE AND AMPLITUDE ARE NDVI VALUES, AND THE REMAINING METRICS ARE UNIT-LESS.

| Pixel | Season start (week) | | Season end (week) | | Season length (weeks) | | Peak time (week) | | Peak value (NDVI) | |
|---|---|---|---|---|---|---|---|---|---|---|
| | crop | pasture | crop | pasture | crop | pasture | crop | pasture | crop | pasture |
| 1 | 21.28 | 24.65 | 47.20 | 46.47 | 25.92 | 21.82 | 35.28 | 37.50 | 0.718 | 0.744 |
| 8 | 21.78 | 23.46 | 47.05 | 46.09 | 25.25 | 22.66 | 35.28 | 36.78 | 0.747 | 0.767 |
| 9 | 22.30 | 21.61 | 46.95 | 47.52 | 24.64 | 37.20 | 35.85 | 36.19 | 0.758 | 0.782 |
| 15 | 21.40 | 21.64 | 47.08 | 46.15 | 25.66 | 24.50 | 35.10 | 36.58 | 0.755 | 0.771 |
| 16 | 22.10 | 20.57 | 47.22 | 47.88 | 25.11 | 36.42 | 35.85 | 36.07 | 0.782 | 0.794 |
| 17 | 22.33 | 20.82 | 47.07 | 46.19 | 24.72 | 34.55 | 35.85 | 36.29 | 0.779 | 0.801 |
| | **Amplitude (NDVI)** | | **Rate of green-up** | | **Rate of die-off** | | **Large integral** | | **Small integral** | |
| | crop | pasture | crop | pasture | crop | pasture | crop | pasture | crop | pasture |
| 1 | 0.487 | 0.462 | 0.054 | 0.046 | 0.070 | 0.094 | 15.07 | 13.41 | 8.71 | 6.69 |
| 8 | 0.514 | 0.451 | 0.059 | 0.046 | 0.071 | 0.091 | 15.19 | 14.48 | 8.88 | 6.86 |
| 9 | 0.514 | 0.458 | 0.056 | 0.038 | 0.076 | 0.099 | 15.07 | 22.16 | 8.55 | 8.56 |
| 15 | 0.510 | 0.430 | 0.059 | 0.042 | 0.072 | 0.091 | 15.84 | 15.99 | 9.04 | 7.08 |
| 16 | 0.550 | 0.491 | 0.058 | 0.028 | 0.080 | 0.089 | 15.61 | 23.54 | 9.34 | 11.36 |
| 17 | 0.534 | 0.458 | 0.059 | 0.026 | 0.080 | 0.100 | 15.51 | 22.60 | 8.94 | 9.43 |

**TABLE 4.9:** RESULTS OF CORRELATION ANALYSIS FOR "MILROY" AND "GRANDVIEW" SHOWING PEARSON'S CORRELATION CO-EFFICIENT (r) AND ASSOCIATED P-VALUE (p), BETWEEN PIXEL MEANS OF CROP AND PASTURE, FOR TIMESAT PHENOLOGY METRICS.

| | r | P |
|---|---|---|
| **MILROY (N=19)** | | |
| Start of Season | –0.4 | 0.07 |
| End of Season | **0.6** | <0.01 |
| Season Length | 0.1 | 0.75 |
| Peak Time | 0.4 | 0.1 |
| Peak Value | **0.8** | <0.001 |
| Amplitude | **0.7** | <0.001 |
| Rate of green-up | 0.4 | 0.09 |
| Rate of die-off | **0.6** | <0.01 |
| Small Integral | **0.6** | <0.01 |
| | | |
| **GRANDVIEW (N=15)** | | |
| Start of Season | **–0.6** | <0.05 |
| End of Season | 0.03 | 0.9 |
| Season Length | **–0.6** | <0.05 |
| Peak Time | **0.6** | <0.05 |
| Peak Value | –0.2 | 0.6 |
| Amplitude | **–0.7** | <0.01 |
| Rate of green-up | 0.2 | 0.4 |
| Rate of die-off | –0.3 | 0.2 |
| Small Integral | –0.2 | 0.4 |

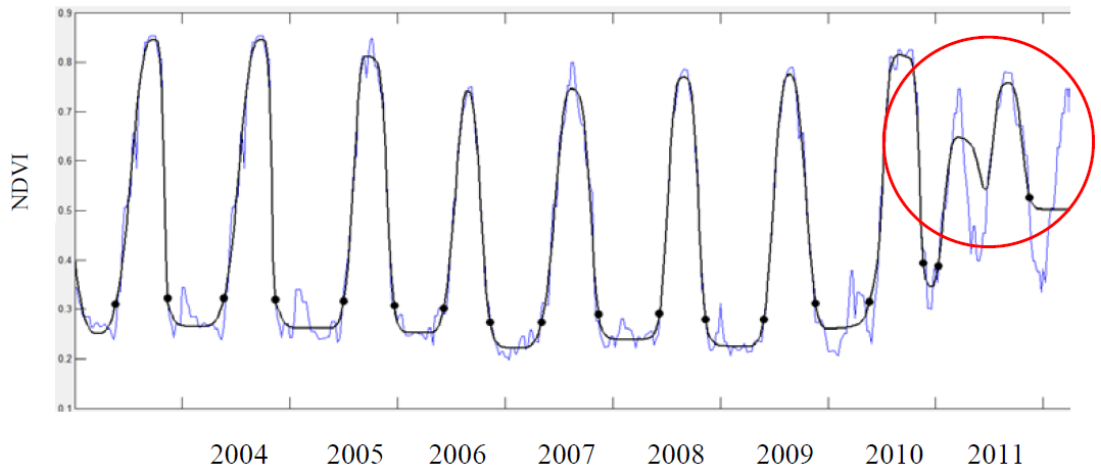


**FIGURE 4.6:** TIME-SERIES SEQUENCE FOR A MODIS PIXEL IN "GRANDVIEW" PADDOCK GV39, SHOWING THE EFFECT OF FLOODING RAINS (CIRCLE IN RED) ON CURVE FITTING FOR "GRANDVIEW" PADDOCKS IN 2011, RESULTING IN MULTIPLE FLUSHES OF PASTURE GROWTH AND ANOMALOUS METRICS FOR 2011 (ALSO REFLECTED IN FIGURE 4.5 C).

## 4.4 DISCUSSION

The research outlined in this chapter further tested Hypothesis 1, that "*spatial variation in biomass production over time is correlated between the cropping and pasture phases of mixed farming enterprises*".

At "Milroy", the start of season metric indicated that pastures emerge earlier than crops. This is to be expected, as the emergence of self-sown pastures is determined by rainfall/soil moisture, whereas crop emergence is also determined by sowing date, which commences around 25 April each year at "Milroy" (Hall, pers. comm.).

Variations in emergence times between pixels both within and between paddocks at "Milroy" are quite large and likely due to the presence of duplex soil layers and water-repellent gravels, particularly in paddocks M41 and M45. The emergence of both crop and pasture at "Grandview" is more uniform and largely reflective of the fact that both crops and pastures are sown into prepared seedbeds at "Grandview", with pastures under-sown into the final crop rotation. The crop and pasture data at "Grandview" were unfortunately limited by the fact that there were only two pasture years—2004, which was the last year of a pasture phase, and 2011, which

was the start of a new pasture phase and production in the intervening crop years was affected by the "Millennium drought" (Heberger, 2011; van Dijk et al., 2013).

In Figure 4.4, the effects of the 2006 and 2010 drought years in the south-west of WA on biomass production at "Milroy" (as measured by the small integral) are clearly visible, as are the differences in responses of individual pixels within and across years. For paddock M25, 2008 was a 'one off' self-sown pasture containing lots of stubble. The pasture did not establish well and was also grazed heavily by sheep to reduce the stubble load (Hall, pers. comm.). Additionally, pastures in M25 were spray-topped in 2004, 2006 and 2008. This may account for the anomalous behaviour observed in 2005 and 2008 in Figure 4.4. For paddock M41, a subterranean clover/serradella pasture mix was sown in 2006. The 2006 drought affected the subsequent seed-set, and the pasture did not re-establish well in 2007. A canola crop sown in 2008 did not establish well and had to be re-sown (Hall, pers. comm.).

The farm owner also reported that "Milroy" suffered ongoing frosts in 2006 and 2010 (Hall, pers. comm.). He also advised that pasture emergence and growth in 2010 was poor in M41 because of low rainfall, resulting in poor seed-set and pasture establishment for both 2010 and 2011. Additionally, this paddock was coming out of a largely continuous crop rotation from 2004 to 2009, with little residual clover seed in the soil. The 2010 pasture had no grazing capacity and the low pasture biomass and subsequent poor seed-set in that year meant that the 2011 pasture was also poor.

At "Milroy" there were some strong, positive correlations in the phenology metrics for the crop and pasture phases (Table 4.9). These correlations were for the end of season and seasonal amplitude or rate of die-off, which can be explained by the determinate nature of annual crops and pastures. There were also strong correlations between peak NDVI value and biomass production as measured by the small integral. Again, these results were expected with annual species. However, correlations at "Grandview" were either poor or confoundingly negative in many cases. This may be reflective of the fact that the two permanent pasture years

measured in the study were either side of six years of crops where production was affected by extreme weather events.

The NDVI data for "Grandview" (2004–2011) encompassed a severe drought between 2006 and 2009 during which all three paddocks were in a cropping phase, which would have impacted on the crop–pasture interactions. Additionally, between October 2010 and December 2011, "Grandview" received nearly 980 mm of rainfall, which would have disproportionately influenced NDVI for perennial pastures over crop for 2011. This can be seen in Figure 4.6, where the 'smoothed' curve for 2011 is highly irregular. The effect is also apparent in Figure 4.5 a–c, where the small integral values for all pixels are strongly divergent.

The TIMESAT software added limited interpretive value to the analysis conducted in Chapter 3. The difficulties associated with using large 6.25 ha MODIS pixels to explore sub-paddock variation in small paddocks (<100 ha) was evident from this analysis, as it was in the previous chapter. The small number of pixels available for analysis after removing 'corrupted' pixels also means that the statistical analysis is of doubtful validity. The use of MODIS NDVI is much better suited to analysis at the regional or whole-farm scale, such as that reported by Hill and Donald (2003), Bradley et al. (2007) and Smith et al. (2011).

Timesat was developed for regional scale interpretation of MODIS imagery and has been reported in land use studies, e.g. across Europe (Klisch and Atzberger, 2014), rangelands in Africa (Fensholt et al., 2013) and for assessing forests in regions of Brazil (Teles et al., 2015), rather than for identifying spatial variation in small farm paddocks. While it has been used for large area crop interpretation (Chakraborty et al., 2012; Pan et al., 2015; Xu et al., 2014), it has never been reported in the literature as being used to discriminate between crop and pasture phases within a single paddock. The software is clearly able to extract phenology metrics at the sub-paddock scale required for interpretation of mixed farm production patterns, however the size of the MODIS pixels themselves ultimately becomes the limiting factor in its usefulness as interpreting smaller areas inevitably means using fewer data samples and prevents the use of appropriate statistical analyses to support research outcomes.

## 4.5 CONCLUSION

The objective in using TIMESAT to analyse the MODIS NDVI data sets was to further refine the analysis from Chapter 3 to investigate the behaviour of crop and pasture phases at the sub-paddock scale over time.

Of interest in this research is whether crop and pasture phases demonstrate similar growth behaviour within a pixel. Although using relatively low-resolution imaging and small data sets, the calculation of phenology metrics for both cropping and pasture phases in two geographically different regions could characterise seasonal growth characteristics, including total production, season duration and spatial variability. However, for a large number of the phenology metrics, the software was not able to add substantial interpretive value to support the hypothesis being tested that, "*spatial variation in biomass production over time is correlated between the cropping and pasture phases of mixed farming enterprises*". Moderate to high correlations were observed for some metrics in the annual systems at "Milroy" which were primarily related to biomass production—the small integral, seasonal amplitude, peak value, peak time, season end and rate of brown-off—however the analysis was limited because of the low sample sizes. The results point to the need to obtain much higher resolution data on grain yield and pasture biomass production to answer the questions raised by the hypothesis that spatial variation in biomass production over time is correlated between the cropping and pasture phases of mixed farming enterprises.

In the following chapters, the acquisition and analysis of high-resolution crop, pasture and soil data gathered post-drought at "Milroy" and "Grandview" is described. High-resolution data will be the key to adding interpretive value to the relationships between crop and pasture phases in mixed farming systems and to developing management systems that allow spatial and temporal variability to be exploited to maximise economic returns.

## 4.6 REFERENCES

Beck, P. S. A., Atzberger, C., Høgda, K. A., Johansen, B., & Skidmore, A. K. (2006). Improved monitoring of vegetation dynamics at very high latitudes: a new method using MODIS NDVI. *Remote Sensing of Environment*, *100*(3), 321–334.

Bradley, B. A., Jacob, R. W., Hermance, J. F., & Mustard, J. F. (2007). A curve fitting procedure to derive inter-annual phenologies from time series of noisy satellite NDVI data. *Remote Sensing of Environment*, *106*(2), 137–145. doi: 10.1016/j.rse.2006.08.002

Chakraborty, A., Das, P. K., Sesha Sai, M. V. R., & Behera, G. (2012). Spatial pattern of temporal trend of crop phenology matrices over India using timeseries GIMMS NDVI data (1982–2006). *International Archives of the Photogrammetry, Remote Sensing and Spatial Information Sciences–ISPRS Archives*, *38*, 113–118.

Chen, J., Jönsson, P., Tamura, M., Gu, Z., Matsushita, B., & Eklundh, L. (2004). A simple method for reconstructing a high-quality NDVI time-series data set based on the Savitzky-Golay filter. *Remote Sensing of Environment*, *91*(3–4), 332–344. doi: 10.1016/j.rse.2004.03.014

Eklundh, L., & Jonsson, P. (2011). *Timesat 3.1 Software Manual*. Lund Sweden: Lund University Sweden.

Fensholt, R., Rasmussen, K., Kaspersen, P., Huber, S., Horion, S., & Swinnen, E. (2013). Assessing land degradation/recovery in the African Sahel from long-term earth observation based primary productivity and precipitation relationships. *Remote Sensing*, *5*(2), 664–686. doi: 10.3390/rs5020664

Gao, F., Morisette, J. T., Wolfe, R. E., Ederer, G., Pedelty, J., Masuoka, E., . . . Nightingale, J. (2008). An algorithm to produce temporally and spatially continuous MODIS-LAI time series. *Geoscience and Remote Sensing Letters*, IEEE, *5*(1), 60–64. doi: 10.1109/LGRS.2007.907971

Heberger, M. (2011). Australia's Millennium Drought: Impacts and Responses. In P. H. Gleick (Ed.), *The World's Water: The Biennial Report on Freshwater Resources* (pp. 97–125). Washington, DC: Island Press/Center for Resource Economics.

Henebry, G. M., & de Beurs, K. M. (2013). Remote sensing of land surface phenology: a prospectus. In M. D. Schwartz (Ed.), *Phenology: an integrative environmental science* (pp. 385–411). New York: Springer.

Hill, M. J., & Donald, G. E. (2003). Estimating spatio-temporal patterns of agricultural productivity in fragmented landscapes using AVHRR NDVI time series. *Remote Sensing of Environment*, *84*(3), 367–384. doi: 10.1016/s0034-4257(02)00128-1

Hird, J. N., & McDermid, G. J. (2009). Noise reduction of NDVI time series: an empirical comparison of selected techniques. *Remote Sensing of Environment*, *113*(1), 248–258.

Jönsson, P., & Eklundh, L. (2002). Seasonality extraction by function fitting to time-series of satellite sensor data. *IEEE Transactions on Geoscience and Remote Sensing*, *40*(8), 1824–1832.

Jönsson, P., & Eklundh, L. (2004). TIMESAT-a program for analyzing time-series of satellite sensor data. *Computers & Geosciences*, *30*(8), 833–845.

Klisch, A., & Atzberger, C. (2014). Evaluating phenological metrics derived from the MODIS time series over the European continent. *Photogrammetrie Fernerkundung Geoinformation, 5*, 409–421. doi: 10.1127/1432-8364/2014/0233

Pan, Z., Huang, J., Zhou, Q., Wang, L., Cheng, Y., Zhang, H., . . . Liu, J. (2015). Mapping crop phenology using NDVI time-series derived from HJ-1 A/B data. *International Journal of Applied Earth Observation and Geoinformation*, *34*(1), 188–197. doi: 10.1016/j.jag.2014.08.011

Reed, B. C., Schwartz, M. D., & Xiao, X. (2009). Remote sensing phenology: status and the way forward. In A. Noormets (Ed.), *Phenology of ecosystem processes* (pp. 231–246). New York: Springer.

Smith, R. C. G., Adams, M., Gittins, S., Gherardi, S., Wood, D., Maier, S., . . . Allen, A. (2011). Near real-time feed on offer (FOO) from MODIS for early season grazing management of mediterranean annual pastures. *International Journal of Remote Sensing*, *32*(16), 4445–4460.

Teles, T. S., Galvao, L. S., Breunig, F. M., Balbinot, R., & Gaida, W. (2015). Relationships between MODIS phenological metrics, topographic shade, and anomalous temperature patterns in seasonal deciduous forests of south Brazil. *International Journal of Remote Sensing*, *36*(18), 4501–4518. doi: 10.1080/01431161.2015.1084437

Tuanmu, M. N., Viña, A., Bearer, S., Xu, W., Ouyang, Z., Zhang, H., & Liu, J. (2010). Mapping understory vegetation using phenological characteristics derived from remotely sensed data. *Remote Sensing of Environment*, *114*(8), 1833–1844.

Xu, Q., Yang, G., Long, H., Wang, C., Li, X., & Huang, D. (2014). Crop information identification based on MODIS NDVI time-series data. *Nongye Gongcheng Xuebao/Transactions of the Chinese Society of Agricultural Engineering*, *30*(11), 134–144. doi: 10.3969/j.issn.1002-6819.2014.11.017

van Dijk, A. I. J. M., Beck, H. E., Crosbie, R. S., de Jeu, R. A. M., Liu, Y. Y., Podger, G. M., . . . Viney, N. R. (2013). The Millennium Drought in southeast Australia (2001–2009): Natural and human causes and implications for water resources, ecosystems, economy, and society. *Water Resources Research*, *49*(2), 1040–1057. doi:10.1002/wrcr.20123

# CHAPTER 5. PROXIMAL SOIL SENSING AND SOIL CHEMICAL ANALYSIS OF FIELD STUDY SITES TO PROVIDE HIGH-RESOLUTION DATA FOR COMPARISONS BETWEEN CROPPING AND PASTURE PHASES

## 5.1 INTRODUCTION

The previous two chapters examined the relationships between biomass production in pasture and cropping phases of two mixed farming systems, one located on the east and the other on the west coast of Australia. This was done using MODIS NDVI as a proxy for biomass. Although relatively coarse resolution data was used in that study, when the impacts of low rainfall years are taken into account, the results indicated a definite relationship over time between spatial variation in biomass production in the cropping and pasture phases at the sub-paddock scale. The relationships appeared to hold for annual pastures at “Milroy” and to a lesser extent for perennial pastures at "Grandview" where results were affected by the Millenium drought. The limitations of applying low-resolution, remotely sensed data to relatively small paddocks were discussed. The need for high-resolution data to better identify within-paddock spatial variation was identified.

This chapter describes the field acquisition and analysis of geo-referenced, high-resolution soil data, using vehicle-mounted electromagnetic induction (Doolittle and Brevik, 2014) and gamma radiometric (Wong et al., 2009) sensors. The use of both techniques has been described extensively in the literature, and the technical background is described in the literature review (Chapter 2, sections 2.5.1–2.5.3). Because of the speed and comparative ease of use, relatively low cost, and the large number of geo-referenced measurements collected, both EMI and GR sensing have significant advantages over traditional methods used to collect soil information. The proximally sensed data is then used in combination with traditional, low-density soil physical and chemical analysis obtained from field sampling and laboratory testing. Within-paddock soil variability is then mapped to determine if spatially dense datasets can be useful either alone or in combination with traditional field sampling

to characterise soil texture and chemical properties that are related to crop and pasture productivity.

The spatial variability of soil characteristics and relationships to pasture productivity have been documented in a limited number of pasture paddocks (Fu et al., 2010, 2013; McCormick et al., 2009; Serrano et al., 2010, 2011; Shi et al., 2000) but has not been widely studied in Australian grazing systems (King et al., 2006; Merry et al., 1990). Very few studies have investigated the spatial variability of soil characteristics in the context of constraints to the overall productivity of crop and pasture phases in mixed farming systems (Stefanski and Simpson, 2010). Historically, fertiliser has been applied uniformly to pastures, with little consideration of the spatial variability that might exist in nutrient levels and the potential response.

This chapter describes the collection and manipulation of soil electrical conductivity (EMI) and gamma radiometric (GR) data as well as soil chemical and physical properties for "Milroy" and "Grandview" paddocks. The data is mapped and also tested for a range of correlations. The data gathered will be used to inform the testing of Hypothesis 2 that, "*spatial variation of production in the crop and pasture phases of a mixed farming system can be identified and quantified at high resolution using PA technologies*" in Chapter 6, and Hypothesis 3 that, "*data acquired using PA technologies can be used to create a single index of paddock productivity that describes the spatial variation in, and temporal stability of, crop and pasture production over time*" in Chapter 7.

## 5.2 MATERIAL AND METHODS

### *5.2.1 STUDY SITES*

The study sites (Table 5.1) were the same as those described in Chapters 3 and 4, with the addition of two years of data (2012 and 2013) and an additional paddock (GV3) included at "Grandview".

**TABLE 5.1:** PADDOCK SIZES, ROTATIONS AND RAINFALL DATA FOR "MILROY" AND "GRANDVIEW".

| Paddock (size) | 2004 | 2005 | 2006 | 2007 | 2008 | 2009 | 2010 | 2011 | 2012 | 2013 |
|---|---|---|---|---|---|---|---|---|---|---|
| **"MILROY"** | | | | | | | | | | |
| M25 | W | P | P | B | P | W | P | P | P | P |
| M41 | L | B | P | P | C | W | P | P | P | P |
| M45 | W | L | P | C | W | P | B | P | P | C |
| GSR (mm) | 264 | 428 | 228 | 370 | 416 | 328 | 162 | 331 | 234 | 371 |
| Annual rainfall (mm) | 304 | 501 | 392 | 392 | 494 | 439 | 256 | 467 | 300 | 461 |
| **"GRANDVIEW"** | | | | | | | | | | |
| GV3 | | | | | | | | P | P | P |
| GV4 | P | W | O | C | W | C | W | P | P | P |
| GV8 | P | C | W | W | C | W | W | P | P | P |
| GV39 | P | C | W | C | W | W | B | P | P | P |
| GSR (mm) | 260 | 334 | 148 | 190 | 155 | 245 | 407 | 243 | 218 | 254 |
| Annual rainfall (mm) | 365 | 568 | 217 | 355 | 334 | 293 | 794 | 688 | 658 | 394 |

W = wheat, C = canola, L = lupin, B = barley, O = oats, P = pasture

Both sites received below average growing season rainfall (except "Milroy" 2013) during the period of research described in this chapter (2011–2013), resulting in likely soil moisture constraints on both pasture and crop production.

### *5.2.2 EMI AND GR PROXIMAL SENSING*

*"Milroy", Western Australia*

At "Milroy", proximally sensed geophysical data was acquired using a commercial contractor in October 2012. EMI measurements were taken using a Geonics DUALEM 21S sensor (Geonics Limited, Ontario, Canada). The unit was set to measure to a depth of 50 cm in horizontal dipole mode (ECah) and 100 cm in vertical mode (ECav). Potassium, thorium, uranium and total count GR emission data were gathered with a Radiation Solutions RSX1 sensor with a vehicle-mounted

4.0 L thallium-activated sodium iodide crystal (Radiation Solutions, Ontario, Canada) (Figure 5.1). The probability of gamma rays reaching the sensor depends on both the mass density and electron density of the medium they travel through. Soil water affects the results of gamma surveys because it attenuates gamma emissions, thus reducing the depth from which gamma sources are detected, which can confound the interpretation of the parent material abundance (Loijens, 1980). The IAEA (2003) recommend that to maximise resolution, gamma surveys should be conducted when soil is dry and should not be conducted within three hours of rain. The gamma survey at "Milroy" was undertaken in October 2012. Soil was reasonably dry and total rainfall for June–October was 188 mm with evaporation of 460 mm. The rainfall data would indicate that the soil moisture would be likely to be quite uniform to the depth that gamma emittance would be detected (30–40 cm). Because there was a single scan, the influence of variations in underlying geology (and soil types) in the geologically complex zones that underlie "Milroy" are likely to be more important on the gamma signal than the scale of influence of variations in soil moisture due to recent rainfall. Soil coring was also undertaken by the contractor to ground-truth the data and support the interpretation of the gamma results. The data were processed to account for Compton scattering (Cook et al., 1996). The geophysical data was gathered on 35 m transects at a sampling rate of one reading/sec and a groundspeed of between 15 and 20 km/h, resulting in a sampling density of approximately 60 readings/ha. All data (elevation, EMI and GR) was geo-referenced using a real-time kinematic (RTK) differential correction signal.

**FIGURE 5.1:** VEHICLE EQUIPPED WITH RADIATION SOLUTIONS RSX1 AND GEONICS DUALEM 21S SENSORS USED AT "MILROY".

*"Grandview", Victoria*

At "Grandview", only EMI data was collected, again using a commercial contractor. In this instance, a Geonics EM38-MK2 with 0.5 m and 1.0 m intercoil spacings was used. The instrument was housed in a sealed Pelican case on a rubber sled, towed behind a four-wheel drive vehicle. It was used in horizontal mode (ECah) for all paddocks, giving a conductivity of 0.38 m at 0.5 m coil separation and 0.75 m conductivity at 1.0 m coil separation. Transect width was 30 m. The horizontal mode was used at the recommendation of the contractor, who has many years of EMI sensing experience in the region. The instrument was calibrated on-site as per instructions outlined in the Geonics EM38-MK2 Ground Conductivity Meter Operating Manual, July 2008. Data was logged using an Allegro CX Field PC (Juniper Systems, Logan, Utah, USA) loaded with Geonics EM38-MK2 software. The data logger was set to acquire and record survey data from the EM38-MK2 system at four readings per second. Output feed and guidance was provided using a Raven 'Cruizer' GPS (Raven Industries, Sioux Falls, South Dakota, USA). Scans were taken in 2013.

### *5.2.3 EMI AND GR DATA MAPPING*

Raw data was processed using the protocol developed by Taylor et al. (2007). Data points more than 2.5 standard deviations (s.d.) above and below the paddock mean

were removed. The data was then imported into ArcGIS 10.2 (ESRI, Redlands, California), converted to Universal Transverse Mercator (UTM) projection, and mapped to a standard square 5 m x 5 m grid. Data was interpolated to the grid with Vesper 1.62 (Australian Centre for Precision Agriculture, The University of Sydney, NSW) using an exponential variogram and a block size of 10 m x 10 m. Interpolated data were then converted to raster surfaces in ArcGIS 10.2 to produce maps of the spatial variability in soil ECa and GR counts for each paddock.

### *5.2.4 SOIL SAMPLING AND TESTING*

*"Milroy"*

Ground-truthing of the proximally sensed soil data was carried out shortly after the EMI or GR surveys, using the soil ECa and gamma maps to identify soil sampling sites.

The paddocks surveyed were all in an annual pasture rotation. Sampling sites were selected according to the range of EMI or GR total count (depending on the landscape), GR potassium and GR thorium values. Soil cores were taken at a sampling density sufficient to enable accurate mapping at a scale of 1:30,000 on the recommendations of CSIRO for surveying soil and land resources (McKenzie et al., 2008).

EMI-based soil sampling was done at 0–10 cm, 10–30 cm and 30–60 cm. GR-based soil sampling was done at 0–10 cm and 10–30 cm (gamma rays having little ground penetration beyond 35 cm (IAEA, 2003)).

Samples were collected using a hydraulic soil corer of 50 mm diameter, with 0–10 cm samples bulked from seven evenly arranged points along the perimeter of a circle of 35 cm diameter to account for nutritional distributional differences.

In 2014, additional soil testing was carried out at eight sites in paddock M41 as part of a paddock liming analysis carried out by the farm owner. Samples for these tests were taken between 0 cm and 50 cm, at 10 cm intervals, using a hydraulic soil coring drill.

All soil analyses were conducted by the CSBP soil testing laboratories (Kwinana, WA). The location of "Milroy" soil testing sites is shown in Figure 5.2. Detailed soil test data for paddock M25 is in Appendix 7, M41 in Appendix 8, and M45 in Appendix 9.

*"Grandview"*

All paddocks surveyed with the EM38 were in permanent pasture. Soil core samples were taken a week after the EMI acquisition using a 50 mm hydraulic soil corer (Figure 5.3), based on sites selected after the EMI data had been interpolated in ArcGIS and analysed (Figure 5.4).

The ECa datasets were divided into 'low', 'medium' and 'high' categories, based on the ECa histogram for each paddock. The bottom 10% of values constituted the 'low' conductivity zone and the top 10% of values the 'high' conductivity zone. Soil test sites concentrated on low and medium ECa zones. Soil samples were taken at 0–10 cm and 10–50 cm. Soil analyses were conducted by CSBP soil testing laboratories (Kwinana, WA). Detailed soil test data for paddocks GV8 and GV39 are at Appendix 11.

Soil texture maps for "Milroy" paddocks M25 and M41 and "Grandview" paddocks GV8 and GV39 were also created based on each farm owner's personal knowledge and observations with these paddocks. These maps are at Figures 5.9 and 5.10 ("Milroy") and Figure 5.12 (Grandview).

The soil test results were evaluated by comparing individual site soil test values with critical values corresponding to nationally recognised, responsive values for pastures (Table 5.2). The 'critical soil test value' is the soil test value where 95% of maximum pasture production occurs. These values were established from soil test–pasture response relationships. The 95% critical soil test value is a simple, commonly used reference point to define where further applications of nutrients are unlikely to markedly increase pasture production (Gourley et al., 2007).

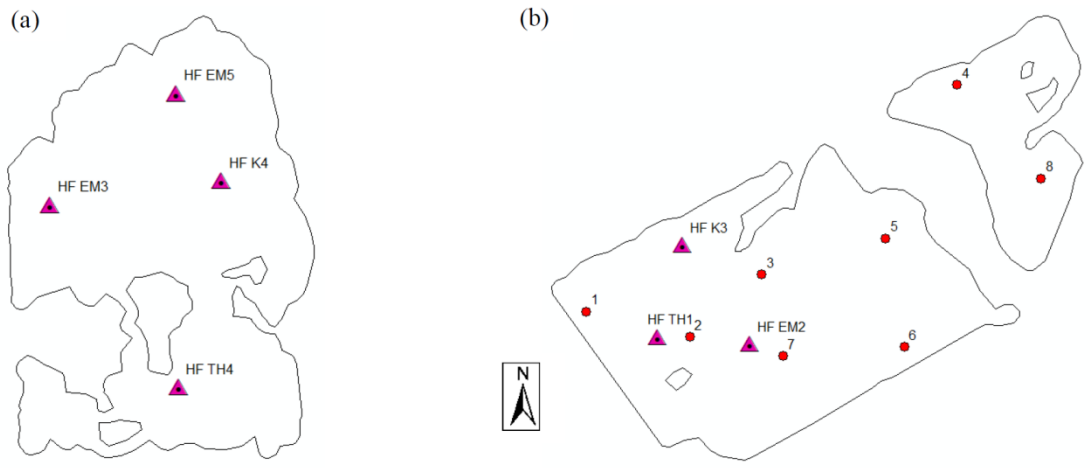


**FIGURE 5.2:** SOIL TESTING SITES FOR "MILROY" PADDOCKS M25 (A) AND M41 (B). ▲ INDICATES TEST SITES RELATED TO ELECTROMAGNETIC AND GAMMA RADIOMETRIC SENSING IN 2012 AND ● TO SOIL TESTING IN 2014.

**FIGURE 5.3:** SOIL CORE SAMPLING, "GRANDVIEW".

**TABLE 5.2:** CRITICAL VALUES FOR KEY SOIL NUTRIENTS (FROM GOURLEY ET AL., 2007).

| Parameter | Critical value |
|---|---|
| Phosphorus | 30 mg/kg |
| Potassium | 140 mg/kg |
| Sulphur | >8 mg/kg |
| Organic carbon:sand | 0.5–1.0% |
| Organic carbon:clay loam | 1.2–2.0% |
| Conductivity (ECe) | 4–8 dS/m |
| pH ($CaCl_2$) | 4.8 |
| PBI | low = <100 |

To visualise the spatial variability of soil chemistry characteristics, the soil test values were plotted as points onto individual paddock maps (Figures 5.16–5.19).

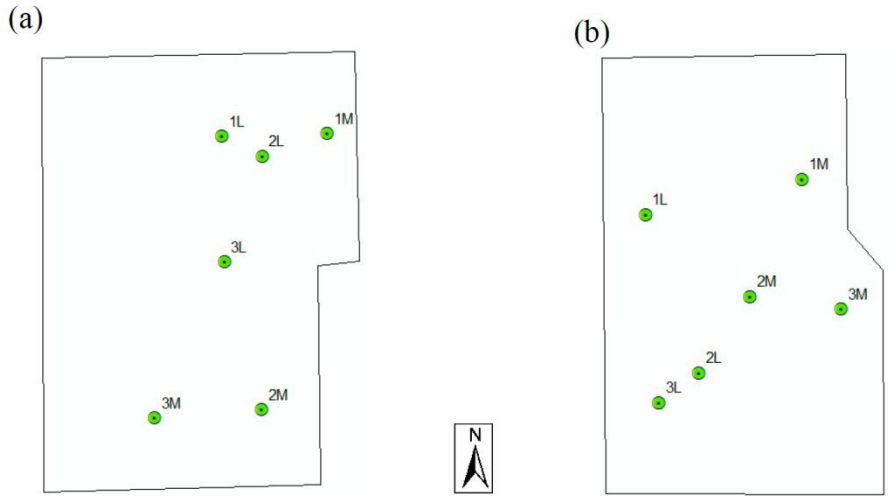


**FIGURE 5.4:** SOIL TEST LOCATIONS FOR "GRANDVIEW" PADDOCKS GV8 (A) AND GV39 (B) ARE DEPICTED BY ⊙. SITES WERE DETERMINED BY ECA VALUES FROM EM38 SENSING IN 2013. 1L = SOIL TEST SITE NUMBER 1 IN THE LOW CONDUCTIVITY ZONE, 1M = SOIL TEST SITE 1 IN THE MEDIUM CONDUCTIVITY ZONE AND SO ON.

*Soil electrical conductivity*

Soil electrical conductivity (EC) is routinely measured by soil laboratories using a 1:5 soil/water suspension (EC1:5) due to its processing speed and relatively low cost (Rayment and Lyons, 2010). The EC1:5 test provides a rapid estimate of the concentration of electrically-charged water-soluble salts that can move into and persist in the soil solution. Measuring salinity (conductivity) in a saturated extract (ECe) is a more robust measure of conductivity relative to plant growth as it takes into account soil texture. This is important because water content at saturation and the dilution of salts are directly affected by soil texture. Therefore, soil EC1:5 values were converted to saturation salinity (ECe) using a multiplication factor based on soil texture (Shaw, 1999), using the formula:

ECe (dS/m) = EC1.5 (dS/m) x conversion factor (Hazelton and Murphy, 2007).

The conversion factors are shown in Table 5.3, and ECe salinity tolerance ratings in Table 5.4.

**TABLE 5.3:** CONVERSION FACTORS FOR CONVERTING EC1:5 (DS/M) TO AN APPROXIMATE VALUE OF ECE (DS/M). SOIL TEXTURE GRADES ARE AS DESCRIBED BY MCDONALD AND ISBELL (2009).

| Soil texture grade | Conversion factor |
|---|---|
| Sand, loamy sand, clayey sand | 23 |
| Sandy loam, fine sandy loam, light sandy clay loam | 14 |
| Loam, fine sandy loam, silty loam, sandy clay loam | 9.5 |
| Clay loam, silty clay loam, fine sandy clay loam, sandy clay, silty clay, light clay | 8.6 |
| Light–medium clay | 8.6 |
| Medium clay | 7.5 |
| Heavy clay | 5.8 |

Source: Hazelton and Murphy (2007)

**TABLE 5.4:** SALINITY RATINGS FOR SOIL BASED ON ECE.

| Rating | ECe (dS/m) | Effect on plants |
|---|---|---|
| Non-saline | <2 | Mostly negligible |
| Slightly saline | 2–4 | Yields of sensitive crops affected |
| Moderately saline | 4–8 | Yields of many crops affected |
| Highly saline | 8–16 | Only tolerant crops yield satisfactorily |
| Extremely saline | >16 | Only very tolerant crops yield satisfactorily |

Source Hazelton and Murphy (2007)

### *5.2.5 ELEVATION DATA*

Geo-referenced elevation values were obtained from the EMI/GR sensing GPS data for "Milroy". For "Grandview", elevation data from the yield monitor output was used. The elevation data was imported into ArcGIS 10.2, converted to UTM projection and mapped to a standard square 5 m x 5 m grid.

Data was interpolated to the grid with Vesper 1.62 using an exponential variogram and a block size of 10 m x 10 m. Interpolated data was then converted to raster surfaces in ArcGIS 10.2 to produce elevation maps for each paddock.

## 5.3 RESULTS

The results shown here are for "Milroy" paddocks M25 and M41 and "Grandview" paddocks GV8 and GV39. These were the paddocks for which pasture data was obtained in both 2012 and 2013. The results for other paddocks are contained within Appendices 5, 6, 9 and 10, but will not be described further here.

### *5.3.1 SPATIAL VARIABILITY OF ECA AND GR DATA*

Figures 5.5 and 5.6 show the spatial distributions of the ECa and GR data for "Milroy"; Figure 5.7 shows mapped ECa data for "Grandview". Table 5.5 presents descriptive statistics for pre-processed ECa datasets collected from the EMI surveys of the "Milroy" and "Grandview" paddocks. Histograms showing the distribution of ECa data points recorded by the EMI sensor are in Figure 5.8 a–d for "Milroy" and

5.8 e–f for “Grandview”. Mean ECa values are higher for the “Grandview” sites. The differences in mean ECa reflect the contrasting soil textures between the highly weathered, sandy soils at “Milroy” and the finer-textured clays at “Grandview”. The CVs are much higher for “Milroy” compared to “Grandview”, suggesting much greater soil variability at the “Milroy” sites. There also appears to be considerable variability in the 0–38 cm region at “Grandview” GV39.

In comparing the 0–50 cm and 0–100 cm ECa maps for “Milroy” (Figure 5.5), paddock M25 showed similar patterns between the 0–50 cm and 0–100 cm ECa maps, while M41 showed some dissimilarities between the same zones.

At “Grandview”, the 0–38 cm and 0–75 cm ECa maps (Figure 5.7) showed similar patterns of spatial distribution. ECa values appear to be lowest in paddock GV39 in the north-east section of the farm. GV39 has the highest elevation in the landscape of the “Grandview” paddocks analysed. The overall paddock means for 0–50 cm ECa in the “Milroy” paddocks ranged from 7.6 to 7.9 mS/m, with overall paddock CVs ranging from 82 to 98% (Table 5.5). The mean 0–100 cm ECa ranged from 12.7 to 21 mS/m with CVs ranging from 84 to 104% (Table 5.5). The values were considerably greater for the “Grandview” paddocks, with the mean 0–38 cm ECa ranging from 16.4 to 43.8 mS/m, with CVs ranging from 20.5 to 60% (Table 5.5). The mean “Grandview” 0–75 cm ECa ranged from 79.5 to 103.8 mS/m, with CVs ranging from 9.7 to 12%.

### *5.3.2 RELATIONSHIPS BETWEEN ECA, GR DATA, SOIL PHYSICAL AND SOIL CHEMICAL PROPERTIES*

*ECa and soil texture: “Milroy"*

The results from the soil analysis indicated that the majority of soils in the “Milroy” paddocks had more than 60% sand and less than 20% clay throughout the profile (0–60 cm depth), and thus were classified as either sandy, sandy loam or duplex (sand over clay) soils (Table 5.6). The range in percentage sand 0–60 cm was 74 to 94%. These high sand percentages are typical of soils in the south-west of Western Australia. Sand content did not change with depth to 60 cm, while clay content increased marginally. In gravel soils, the gravel percentage increased markedly with

depth. Average clay content ranged from 4.4 to 21%, and a low average silt content (<7%) was observed throughout the profiles.

Analysis of the relationship between ECa and clay content measured at various depth intervals (0–10 cm, 10–30 cm and 30–60 cm) showed variable correlation (Table 5.8). There was a strong positive correlation at 10–30 cm with all five data points included (Figure 5.15 a), and a strong positive correlation at 0–10 cm and 30–60 cm when one highly sodic outlier was removed. There was also a strong positive correlation between ECa 0–50 cm and ECe 10–30 cm (Figure 5.15 b). The percentage sand was negatively correlated with ECa in the "Milroy" paddocks. ECa 0–50 cm generally showed a stronger correlation with sand content than ECa (0–100 cm).

There is also a reasonable similarity between the soil texture zones identified by the farm owner in paddock M25 (Figure 5.9) with the ECa 0–100 cm map (Figure 5.5 b) and the gamma K map (Figure 5.6 b). Similarly, the farm owners' soil texture map for paddock M41 (Figure 5.10) shows resemblances to ECa 0–100 (Figure 5.5 d) and gamma TC (Figure 5.6 e).

*ECa and soil texture: "Grandview"*

Across all paddocks at "Grandview", subsoil textures were fine clays (45–55% clay) (Table 5.7, Figures 5.12 and 5.13). In the more elevated sections of the paddocks, the "Grandview" soils (0–10 cm) had more than 20% clay and were classified as sandy loam/sandy clay loam soils. The lower-lying areas had more than 35% clay (0–10 cm). ECa values appear to be lowest in paddock GV39 (Figure 5.7), which is located in the north-west part of the farm. GV39 has the highest elevation of the "Grandview" paddocks analysed (Figure 5.14).

In terms of texture, GV39 also appeared to comprise increased sandy clay loam over clay than the other "Grandview" paddocks tested. There were significant differences in soil texture between the tops of hills, mid-slopes and points of lowest elevation in GV8 and GV39. On the tops of the hills, the topsoil tended to be stonier sandy clay loams, transforming to chromosols down the slope. The was no evidence of an A2 horizon.

There were strong positive correlations between ECa 0–38 cm values and clay content at 0–10 cm and 10–50 cm (Figure 5.15 c, Table 5.9). The soil texture properties in lower-lying areas with the highest conductivity corresponded with sodosols, with pockets of vertosols (Isbell 2016). There was a strong positive correlation between ECa 0–38 cm and ECe 10–50 cm (Figure 5.15 d).

The soils at "Grandview" have been characterised in the APSoil database (Keating et al., 2003). The relevant reference soils are Yarrawonga Nos. 210 and 629 for clay and Yarrawonga Nos. 208 and 596 for sandy clay loam over clay. Based on the APSoil database, the corresponding plant available water capacities (PAWC) from 0–180 mm were estimated as clay (high conductivity zone) at 120.5 mm; sandy clay loam over clay (medium conductivity zone) at 114 mm and sandy clay loam over clay (low conductivity zone) at 85 mm.

There is also a reasonable similarity between the soil texture zones identified by the farm owner in paddock GV8 (Figure 5.12 a) with the ECa 0–50 and 0–100 cm maps (Figure 5.7 a, b). Similarly, the soil texture map for paddock GV39 (Figure 5.12 b) shows a strong resemblance to the ECa 0–50 and 0–100 cm maps (Figure 5.7 c, d).

*Soil pH: "Milroy"*

The soil test pH (0–10 cm) across the two paddocks ranged from 4.0 to 5.6 (mean 4.6) for M25 and from 4.7 to 5.1 (mean 4.87) for M41 (Figures 5.16 a and 5.17 a). There was some evidence of a spatial trend in pH in paddock M41, increasing with elevation as soil texture changed from deep sand to sandy loam.

Seven of the nine pH sites in M25 were below the critical pH value of 4.8 (Appendix 9) whereas, in M41, only one site was below the critical value and at eight of the 11 sites, pH increased with depth. There were no significant correlations between either ECa or GR data and pH.

*Soil pH: "Grandview"*

The soil test pH (0–10 cm) across the two paddocks ranged from 4.5 to 5.2 (mean 4.95) for GV8 and from 5.2 to 6.3 (mean 5.83) for GV39 (Figures 5.18 b and 5.19 a).

One site in GV8 was below the critical value. There were no significant correlations between ECa data and pH.

*Phosphorus: "Milroy"*

The range of soil test phosphorus concentrations across each of the paddocks was similar, being 23 to 51 mg/kg for M25 and 25 to 55 mg/kg for M41 (Figures 5.16 b and 5.17 b). The lowest P-value in M41 was in the lowest part of the paddock, in deep sand.

There appeared to be little association between soil phosphorus levels and elevation in either paddock or with animal camping behaviour. The mean soil P-value for each paddock (32.8 mg/kg for M25 and 45.2 mg/kg for M41) was above the critical value of 30 mg/kg. However, several sites in each paddock had Colwell P values well above or below the critical value. This reflects the variability in soils in "Milroy" paddocks, from deep sands to sandy loams/gravels. The correlations between ECa and GR data and Colwell P were weak and negative (not shown).

Surface (0–10 cm) phosphorus buffering index (PBI) varied between 30 and 69 in M25 (Figure 5.16 e) and 11 and 124 in M41 (Figure 5.17 f). There were strong positive correlations between both ECa 0–10 cm and gamma thorium 0–10 cm with PBI in the 0–10 cm zone (Table 5.8). High thorium readings are indicative of soils with gravel content. Iron falls within the decay chain of thorium, so soils with higher iron oxide levels tend to have high PBI values. These areas generally correspond to lateritic soils.

*Phosphorus: "Grandview"*

The range of Colwell P concentrations across each of the paddocks was similar, being 30 to 74 mg/kg for GV8 and 29 to 72 mg/kg for GV39 (Figures 5.18 a and 5.19 b). These values are much higher than the coarser-textured soils at "Milroy". Lower phosphorus levels in GV39 were associated with elevation (Figures 5.14 d and 5.19 b).

There appeared to be little association between soil phosphorus, as measured by Colwell P, and elevation in paddock GV8. The mean soil P-value for each paddock (51.5 mg/kg for GV8 and 45 mg/kg for GV39) was well above the critical P-value (30

mg/kg). Like “Milroy”, the correlations between ECa and Colwell P were weak and negative (Table 5.9).

*Potassium: “Milroy”*

Soil test potassium values ranged from 29 to 320 mg/kg for M25 and 47 to 277 mg/kg for M41 (Figures 5.16 d and 5.17 d). The areas of high potassium concentration tended to be associated with sandy loam textured soils. Five of the eight sites in M25 were well below the critical value for K (140 mg/kg) as were five of the ten sites in M41. There were no significant correlations between ECa, Colwell K and gamma K or other radiometric data (Table 5.8).

*Potassium: “Grandview”*

The soil test potassium values ranged from 213 to 506 mg/kg for GV8 and 420 to 631 mg/kg for GV39 (Figures 5.18 d and 5.19 d). All values were well above the critical value (140 mg/kg) and significantly higher than the values recorded at “Milroy”. There was no relationship between ECa values and Colwell K at “Grandview”.

*Sulphur: “Grandview” only*

Sulphur levels ranged from 6.4 to 9.8 mg/kg in GV8 and 4 to 28.1 mg/kg in GV39 (Figures 5.18 e and 5.19 h). Spatial trends between S and elevation were not observed in GV8, although high levels of S appeared to be associated with the lowest elevations in GV39 (Figures 5.14 d and 5.19 h). Although the mean sulphur concentrations for both paddocks (8.45 mg/kg for GV8 and 12.0 mg/kg for GV39) were above the critical value (8 mg/kg), variability in GV39 at the sub-paddock scale was considerable.

*Aluminium: “Milroy”*

Values were obtained for both exchangeable aluminium and Al ($CaCl_2$). There were no significant correlations between ECa and either Al ($CaCl_2$) or exchangeable Al. There were significant correlations between gamma thorium and exchangeable Al at 0–10 cm and 10–30 cm (Table 5.8).

Sites with lower gamma thorium and low ECa values tended to have higher soil test aluminium values. “Milroy” soils are highly weathered and have lower levels of exchangeable cations and are therefore prone to acidification, as evidenced by the soil pH results described above, allowing aluminium to become available.

*Aluminium: “Grandview”*

There was no correlation evident between ECa and exchangeable Al.

*Chloride: “Milroy” only*

There were strong correlations between ECa 10–30 cm and 30–60 cm and chloride (Table 5.6). These correlations reflect the typically strong electrolytic effect of chloride on EMI readings. The ECa 0–100 cm data had an anomalous negative point corresponding to a thorium value of 54 ppm. It is suspected that the high gravel content lateritic soil at this sample point interfered with the magnetics on the deep EM38 channel. This can be caused by lateritic bauxite deposits which are common throughout remnant areas of the Darling Scarp where “Milroy” is located. The soil core image for this point (Figure 5.11 c) shows high gravel content 30–60 cm. Removal of this outlier gave a significant correlation. There were no correlations between GR data and chloride.

*Cations: “Milroy”*

Cation exchange capacity (CEC) at “Milroy” showed strong correlations with ECa 0–10, 10–30 and 30–60 cm (Table 5.8). There were strong significant correlations of CEC with gamma total count and gamma U (Table 5.8).

There were also strong correlations between exchangeable sodium percentage (ESP) and ECa 10–30 and 30–60 cm (Table 5.8). Site EM5 (paddock M25) recorded an ESP of 12%.

*Cations: “Grandview”*

Clay content in these soils increased to more than 50% over the 10–50 cm depth range. Most subsoil profiles were sodic with ESP greater than 6% at six of the 11 sites (Figures 15.6 g and 15.7 f). There were no strong correlations between ECa and CEC or ESP (Table 5.9).

*Organic carbon: "Milroy"*

Organic carbon (OC) levels ranged from 1.22 to 2.96% in M25 and 0.06 to 0.59% in M41 (Figures 5.16 f and 5.17 g). These values reflected soil texture classes in M25 but in M41 were generally below the threshold values.

There were significant correlations between ECa 0–50 cm and organic carbon at 0–10 and 10–30 cm and OC at 0–10 cm with gamma thorium, gamma uranium and total count (Table 5.8).

*Organic carbon: "Grandview"*

Organic carbon levels ranged from 1.9 to 3.98% in GV8 and 2.37 to 4.06% in GV39 (Figures 5.18 f and 5.19 g) which were above the threshold values. These values are greater than at "Milroy" and reflect the finer-textured soils at "Grandview".

There were strong negative correlations between ECa 0–38 cm and OC 0–50 cm and ECa 0–75 cm and OC 10–50 cm (Table 5.7).

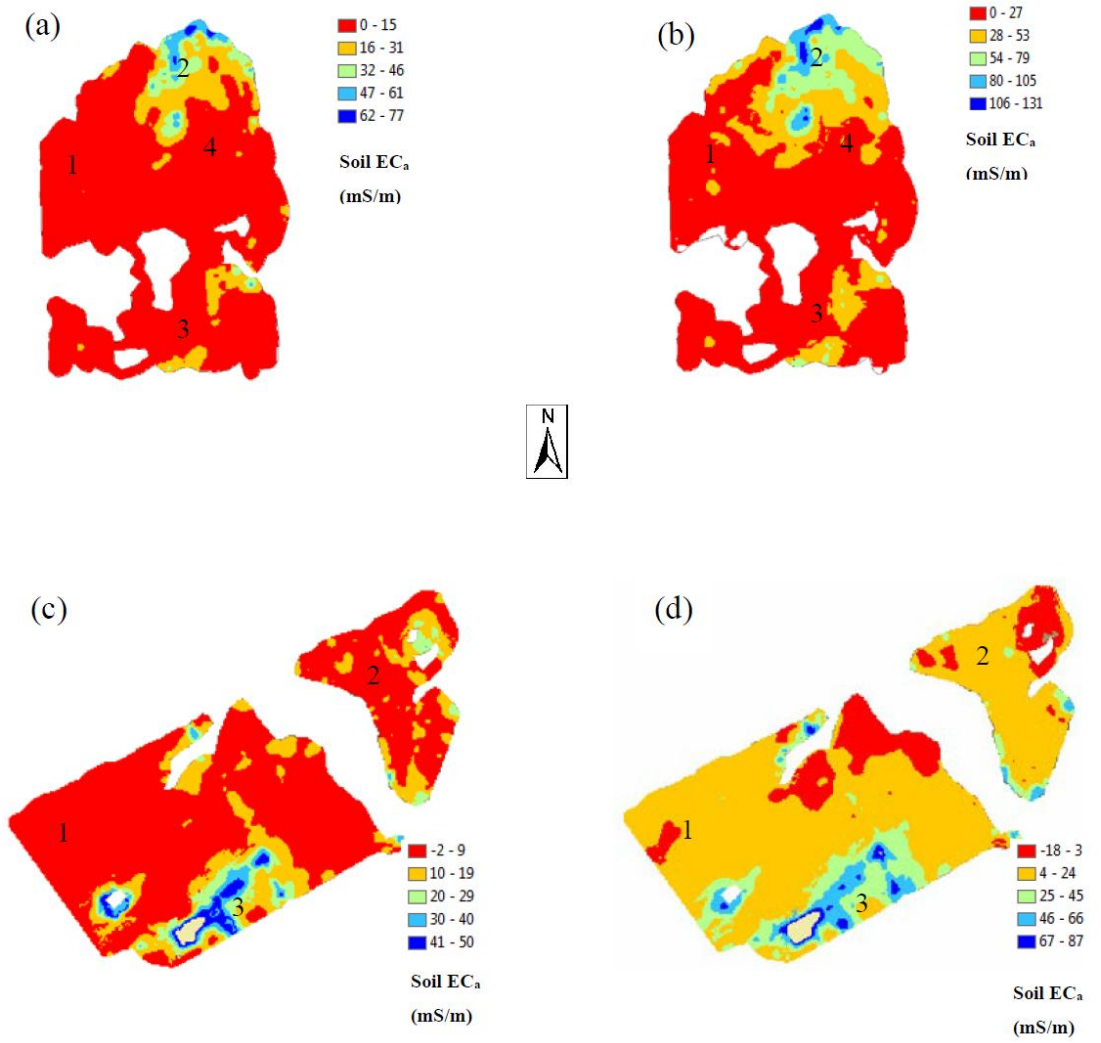


**FIGURE 5.5:** MAPS OF SOIL ECA FROM EMI SCANS OF "MILROY" PADDOCKS M25 AND M41 CONDUCTED IN OCTOBER 2012. (A) M25 0–50 CM SOIL DEPTH, (B) M25 0–100 CM, (C) M41 0–50 CM AND (D) M41 0–100 CM. NUMBERS WITHIN MAPS RELATE TO ECA/GAMMA INTERPRETATION SITES.

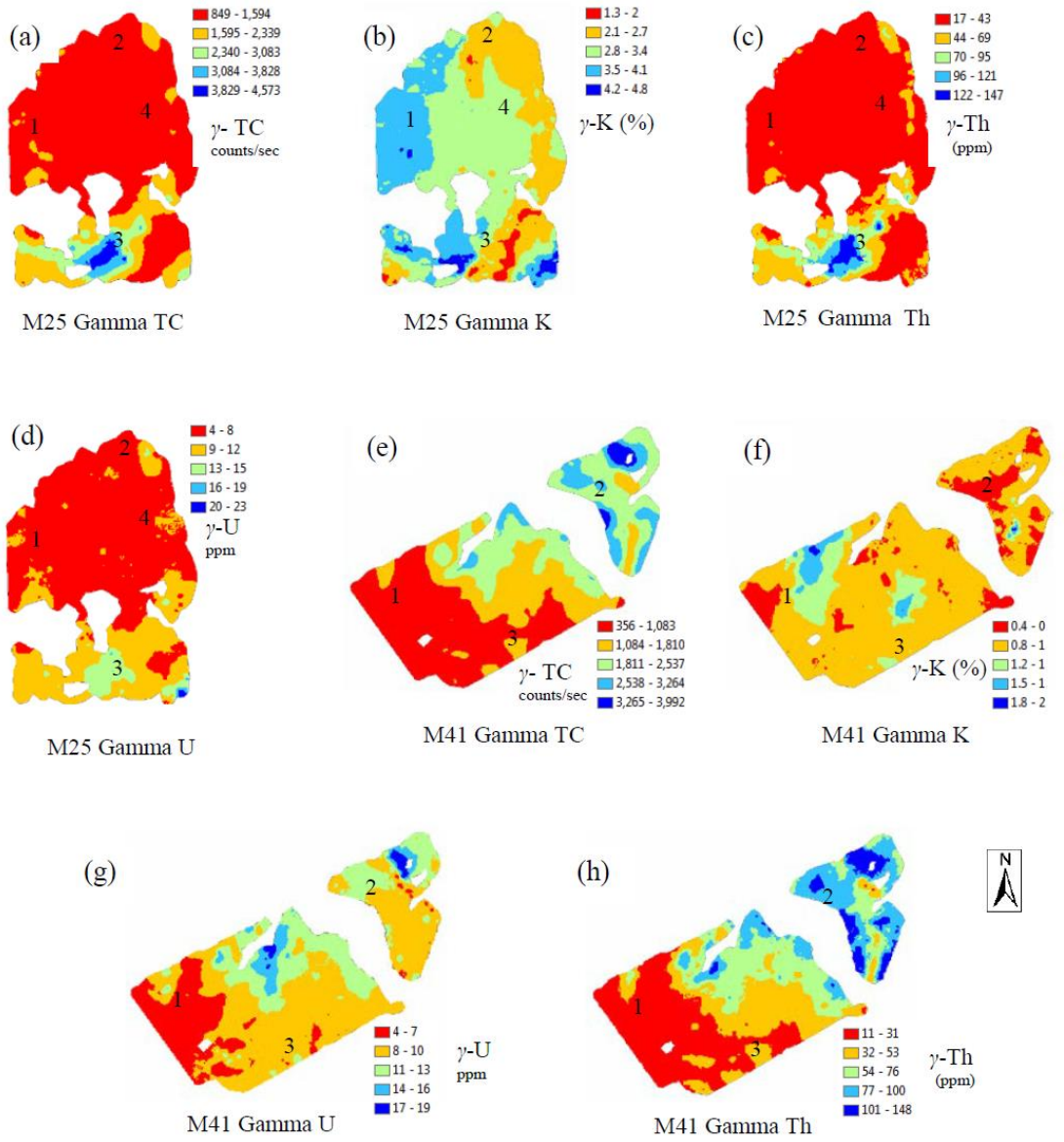


**FIGURE 5.6:** SPATIAL ESTIMATES OF γ-RAY EMISSION FROM TOTAL EMISSION (TC), POTASSIUM (K), THORIUM (TH) AND URANIUM (U) FOR "MILROY" PADDOCK M25 AND M41. (A) M25 γ TOTAL COUNT, (B) M25 γK, (C) M25 γTH, (D) M25 γU, (E) M41 γ TOTAL COUNT, (F) M41 γK, (G) M41 γU, (H) M41 γTH. NUMBERS WITHIN MAPS RELATE TO ECA/GAMMA INTERPRETATION SITES.

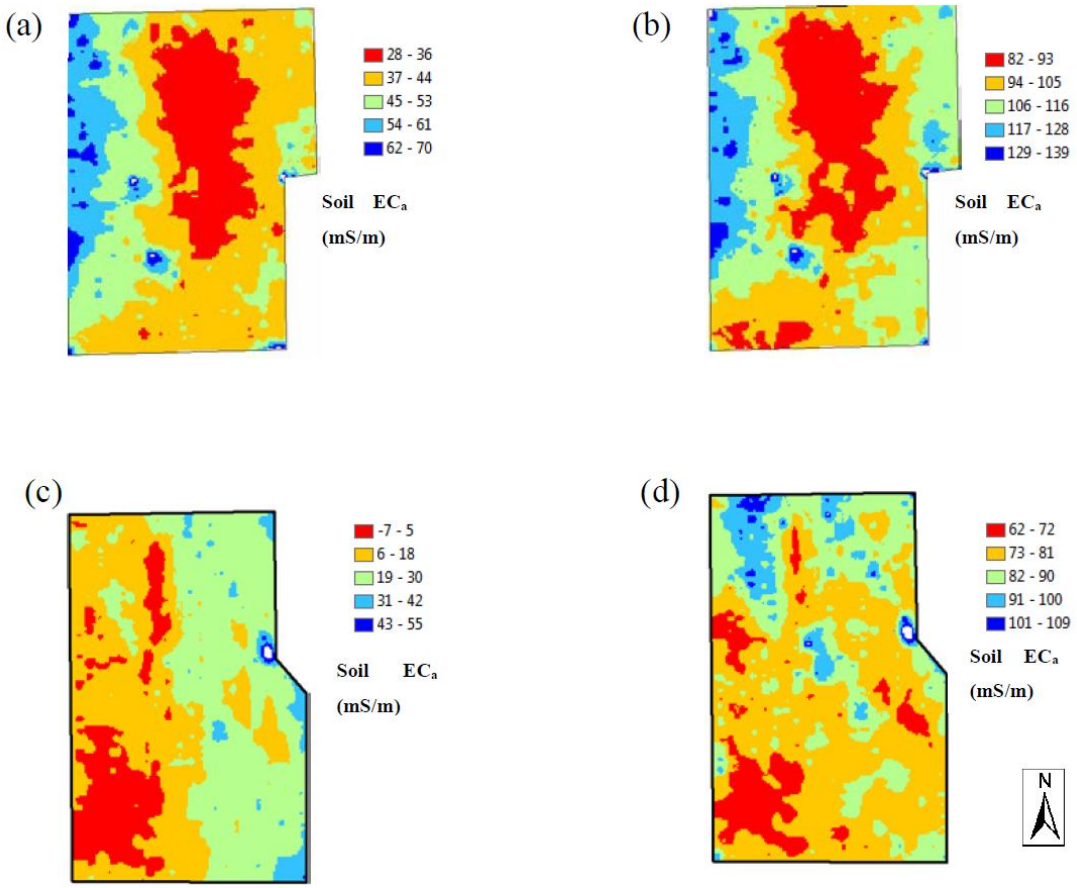


**FIGURE 5.7:** MAPS OF SOIL ECA FROM EM38 SCANS OF "GRANDVIEW" PADDOCKS GV8 AND GV39 CONDUCTED IN OCTOBER 2013. (A) GV8 0–38 CM, (B) GV8 0–75 CM, (C) GV39 0–38 CM AND (D) GV39 0–75 CM. SCANS WERE CONDUCTED WITH THE EM38 IN HORIZONTAL MODE (ECA*H*).

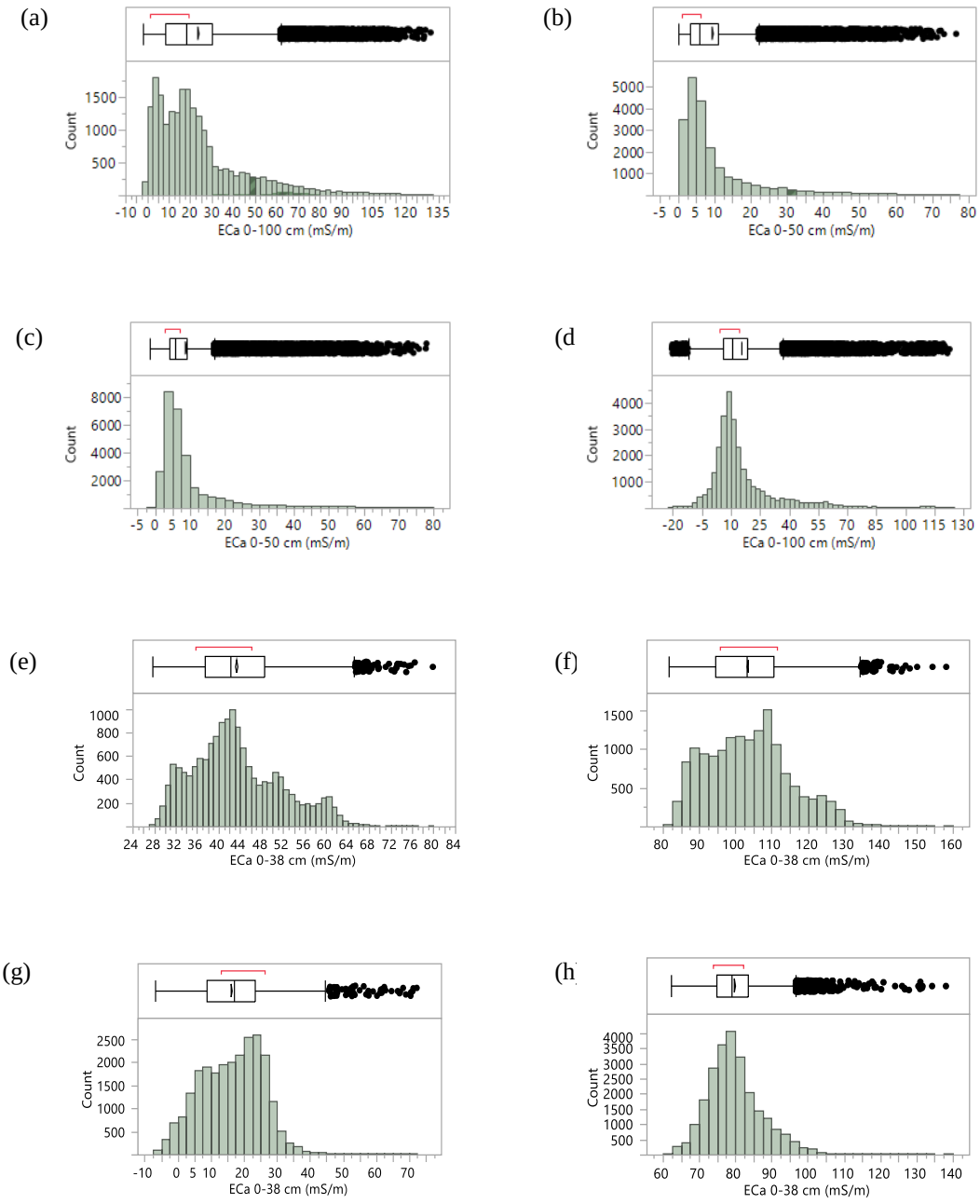


**FIGURE 5.8:** DISTRIBUTION OF ECA DATA POINTS FOR "MILROY" M25 (A) 0–50 CM, (B) 0–100 CM, M41 (C) 0–50 CM, (D) 0–100 CM AND "GRANDVIEW" GV8 (E) 0–38 CM, (F) GV8 0–75 CM, GV39 (G) 0–38 CM AND (H) 0–75 CM. THE RED BRACKET OUTSIDE OF THE BOX IDENTIFIES THE SHORTEST HALF, WHICH IS THE MOST DENSE 50% OF THE OBSERVATIONS (ROUSSEUW AND LEROY 1988).

**TABLE 5.5:** DESCRIPTIVE STATISTICS FOR ECA DATASETS COLLECTED FROM EMI SURVEYS OF "MILROY" AND "GRANDVIEW" PADDOCKS. N= THE NUMBER OF SENSOR DATA POINTS COLLECTED.

| Paddock | EM38 depth (cm) | N | Mean (mS/m) | Standard deviation | Median (mS/m) | CV (%) |
|---|---|---|---|---|---|---|
| **"Milroy"** | | | | | | |
| M25 | 50 | 2911 | 7.94 | 7.8 | 5.2 | 98.0 |
| | 100 | 2936 | 21.0 | 17.6 | 16.8 | 84.0 |
| M41 | 50 | 3654 | 7.6 | 6.2 | 5.6 | 82.0 |
| | 100 | 3652 | 12.7 | 13.2 | 9.4 | 104.0 |
| **"Grandview"** | | | | | | |
| GV8 | 38 | 6239 | 43.78 | 8.99 | 42.58 | 20.5 |
| | 75 | 6228 | 103.8 | 12.50 | 103.13 | 12.0 |
| GV39 | 38 | 7762 | 16.39 | 9.81 | 17.58 | 60.0 |
| | 75 | 7687 | 79.45 | 7.77 | 78.63 | 9.7 |

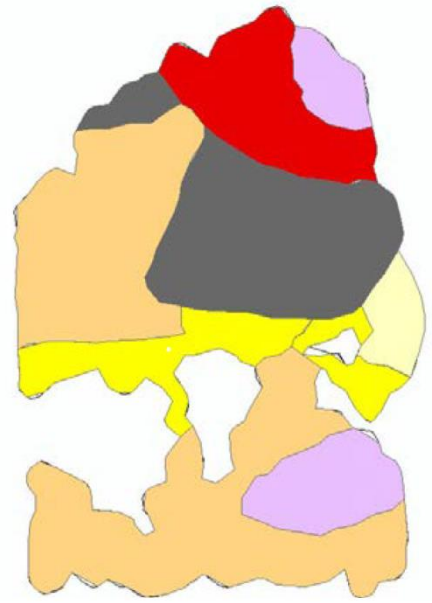

**FIGURE 5.9:** SOIL TEXTURE MAP FOR MILROY PADDOCK M25. THE MAP WAS CREATED FROM FARMER KNOWLEDGE (MURRAY HALL, PERS. COMM.). SANDY LOAM, WHITE CLAY, SHALLOW SANDY DUPLEX, SAND ON CLAY LOAM, DEEP SAND, DEEP SANDY DUPLEX.

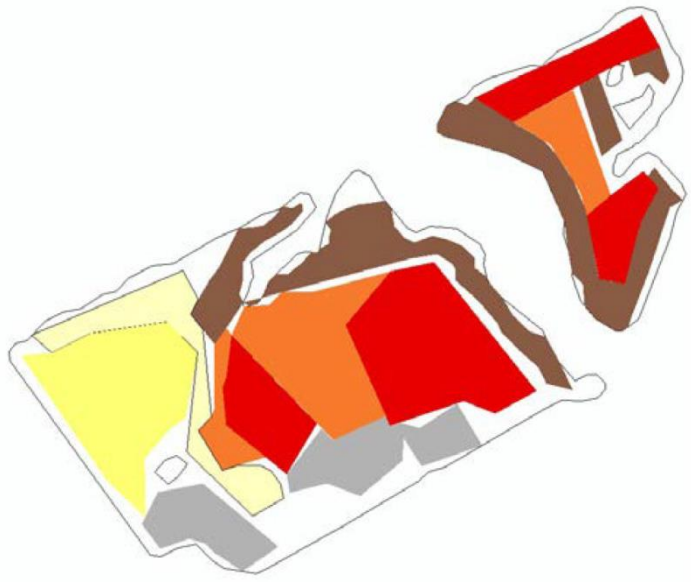

**FIGURE 5.10:** SOIL TEXTURE MAP FOR "MILROY" PADDOCK M41. THE MAP WAS CREATED FROM FARMER KNOWLEDGE (MURRAY HALL, PERS. COMM.). SANDY LOAM, FRIABLE SAND, GRAVELS, SANDY DUPLEX (SODIC), SAND ON CLAY LOAM, DEEP SAND.

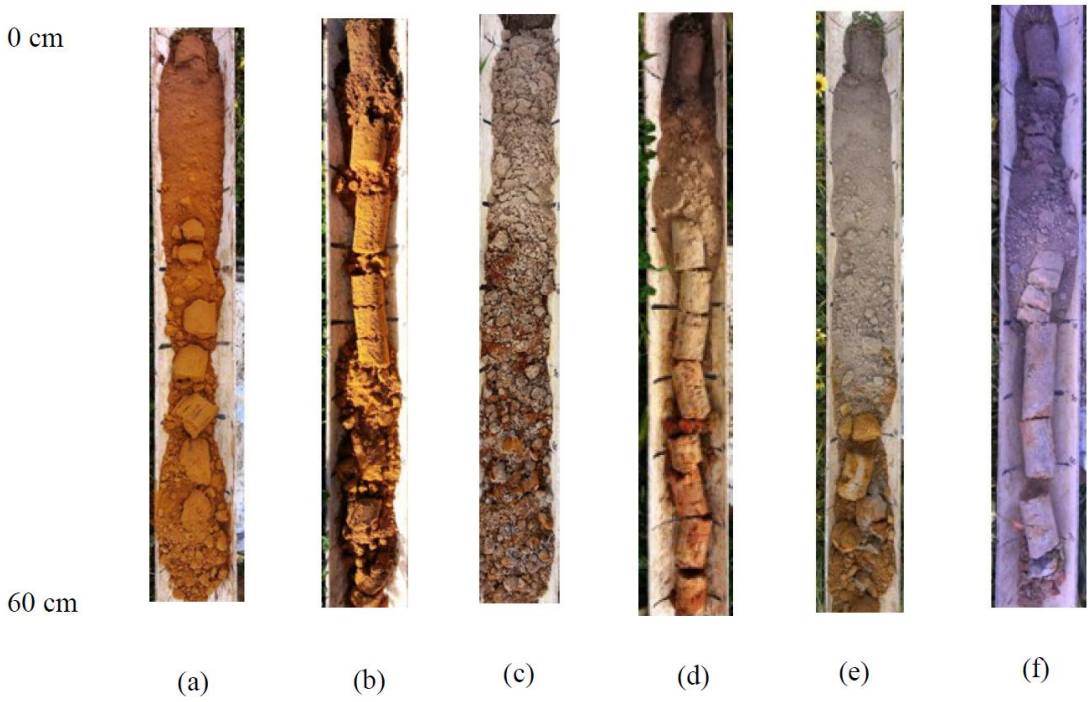


**FIGURE 5.11:** TYPICAL SOILS ON "MILROY": (A) SANDY LOAM, (B) FRIABLE SAND, (C) SANDY DUPLEX, (D) SAND OVER CLAY LOAM, (E) DEEP SAND AND (F) SALINE WHITE CLAY.

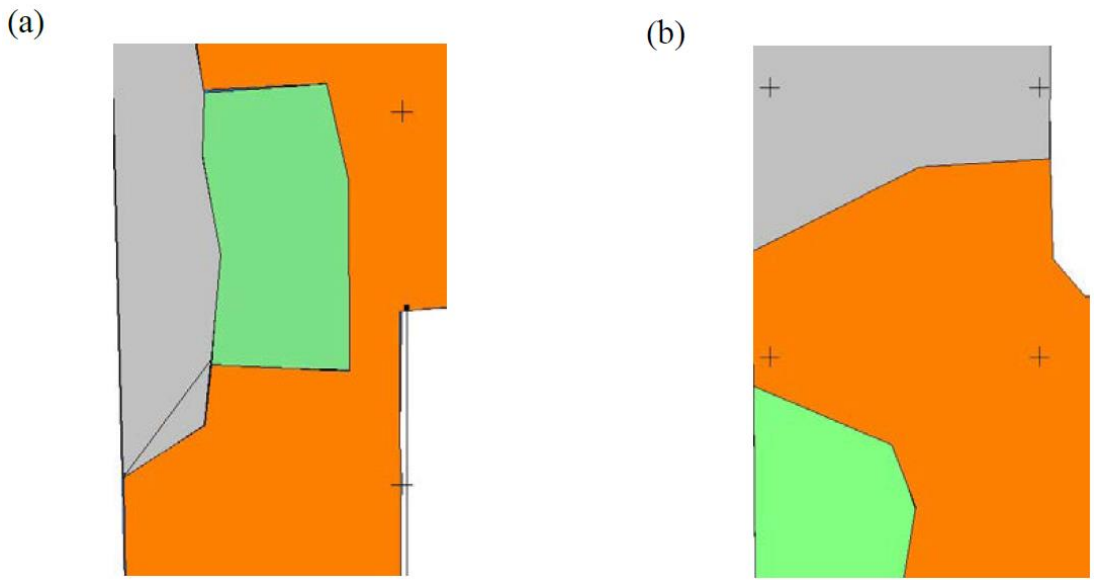


**FIGURE 5.12:** BROAD SOIL TEXTURE MAP FOR "GRANDVIEW" PADDOCK (A) GV8 AND (B) GV39. THE MAPS WERE CREATED FROM FARMER KNOWLEDGE (ADAM INCHBOLD, PERS. COMM.). SANDY CLAY LOAM OVER MEDIUM CLAY, SANDY CLAY LOAM OVER SODIC FINE CLAY, CLAY LOAM OVER FINE CLAY.

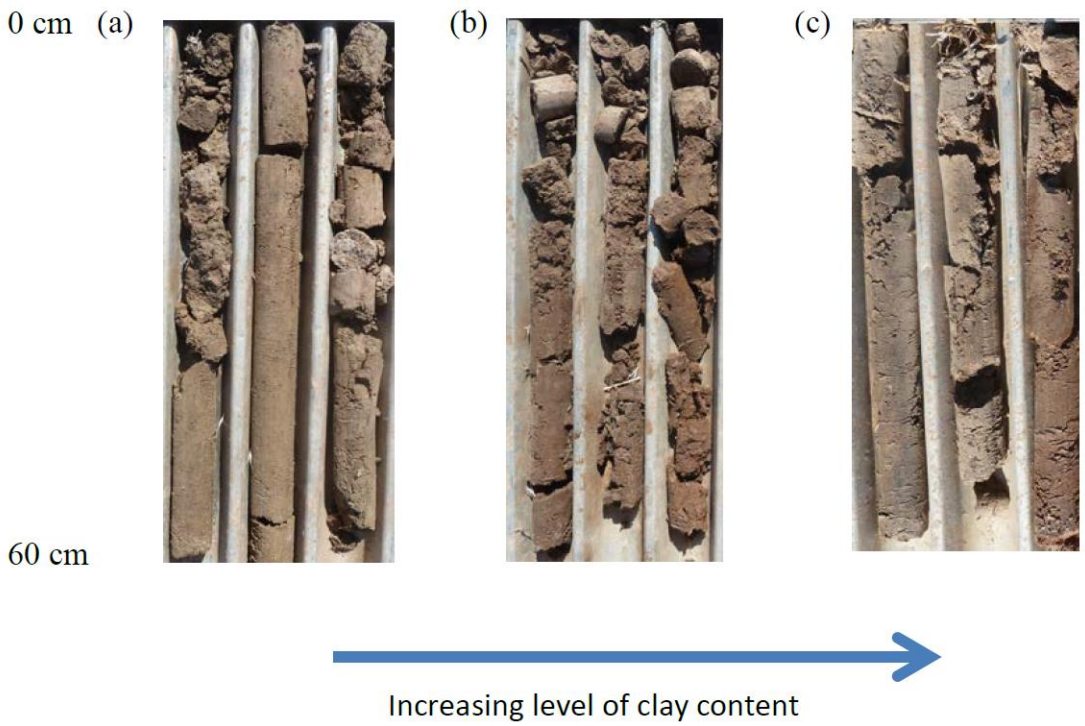


**FIGURE 5.13:** TYPICAL "GRANDVIEW" SOILS, TAKEN FROM (A) A LOW ECA ZONE, (B) A MEDIUM ECA ZONE AND (C) A HIGH ECA ZONE.

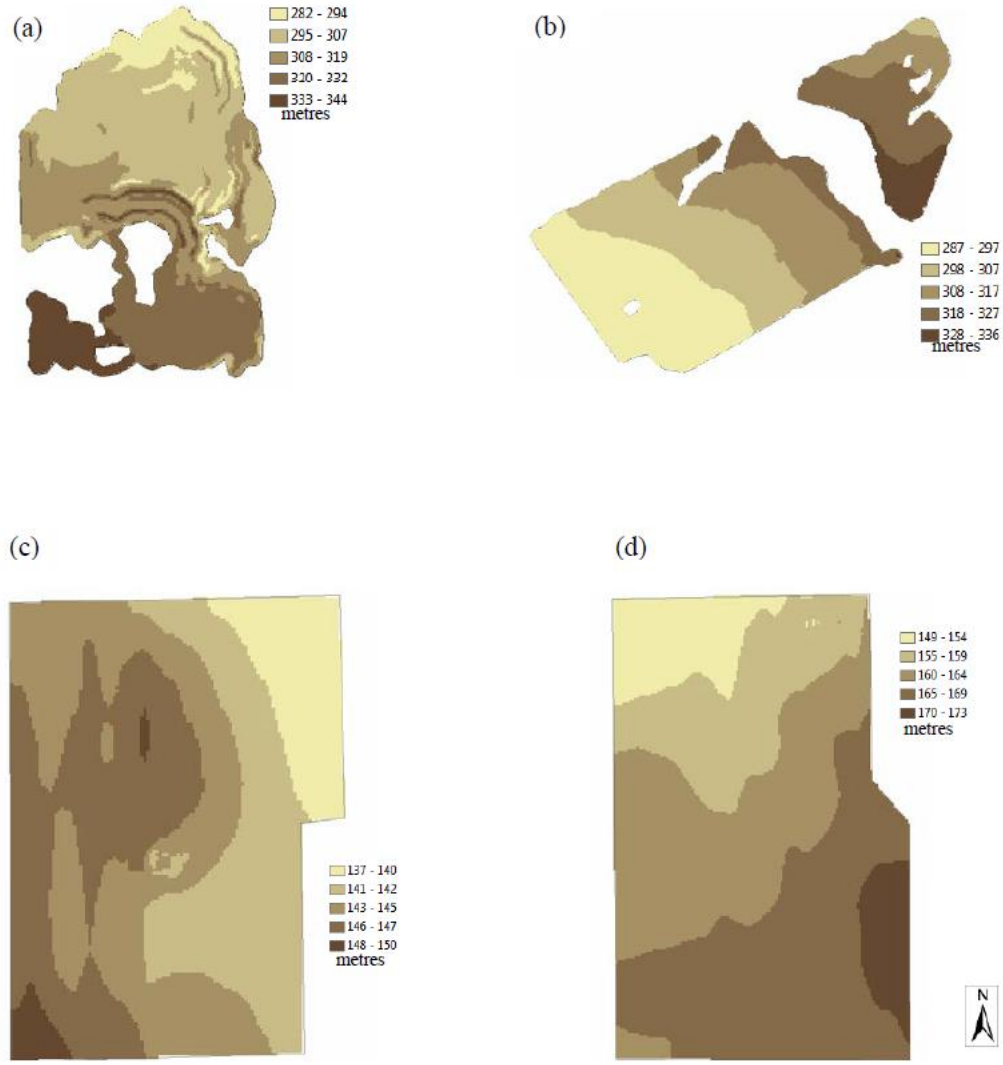


**FIGURE 5.14:** "MILROY" PADDOCK ELEVATION SURFACES M25 (A), M41 (B), DERIVED FROM REAL-TIME KINEMATIC (RTK) GPS HEIGHTS FROM GAMMA RADIOMETRIC SENSING AND "GRANDVIEW" PADDOCK ELEVATION SURFACES GV8 (C), GV39 (D), DERIVED FROM YIELD MONITOR GPS HEIGHTS.

**TABLE 5.6**: SOIL COLOURS AND TEXTURES FOR "MILROY" PADDOCKS M25 AND M41. THE CSBP SOIL DESCRIPTION CHART IS IN APPENDIX 24.

| Paddock | Site | Depth (cm) | Colour | Sand (%) | Silt (%) | Clay (%) | Gravel (%) |
|---|---|---|---|---|---|---|---|
| M25 | EM3 | 0–10 | BRGR | 87.8 | 6.2 | 6.0 | 0 |
| | | 10–30 | BRGR | 90 | 5.9 | 4.1 | 27.5 |
| | | 30–60 | GRWH | 85.9 | 6.6 | 7.5 | 37.5 |
| | EM5 | 0–10 | BR | 76.1 | 8.4 | 15.4 | 5 |
| | | 10–30 | BR | 63.7 | 8.2 | 28.1 | 5 |
| | | 30–60 | BR | 80.7 | 1.5 | 17.8 | 0 |
| | Th4 | 0–10 | DKGR | | | | 0 |
| | | 10–30 | BRRD | | | | 0 |
| | K4 | 0–10 | GRBR | | | | 5 |
| | | 10–30 | BRYW | | | | 5 |
| M41 | EM2 | 0–10 | LTBR | 75.5 | 6.8 | 17.7 | 0 |
| | | 10–30 | OR | 80.9 | 6.7 | 12.5 | 0 |
| | | 30–60 | OR | 73.4 | 6.7 | 19.9 | 0 |
| | Th1 | 0–10 | GR | | | | 0 |
| | | 10–30 | LTGR | | | | 0 |
| | K3 | 0–10 | GRBR | | | | 5 |
| | | 10–30 | BRWH | | | | 5 |

**TABLE 5.7**: SOIL COLOURS AND TEXTURES FOR "GRANDVIEW" PADDOCKS GV8 AND GV39. THE CSBP SOIL DESCRIPTION CHART IS IN APPENDIX 24.

| Paddock | Site | Colour | Clay (%) 0–10 cm | Clay (%) 10–50 cm |
|---|---|---|---|---|
| GV8 | L1 | DKGR | 30 | 45 |
| | L2 | GR | 25 | 45 |
| | L3 | GR | 30 | 45 |
| | M1 | LTBR | 35 | 45 |
| | M2 | BRGR | 40 | 50 |
| | M3 | BR | 35 | 45 |
| GV39 | L1 | GR | 35 | 50 |
| | L2 | BR | 35 | 45 |
| | L3 | GR | 35 | 50 |
| | H1 | LTBR | 35 | 55 |
| | H2 | GR | 40 | 50 |
| | H3 | BRGR | 40 | 50 |

**TABLE 5.8:** PEARSON CORRELATION COEFFICIENTS (R) AND REGRESSION COEFFICIENTS ($R^2$) FOR RELATIONSHIPS BETWEEN ECA AND GAMMA RADIOMETRIC DATA WITH SOIL PARAMETERS AT "MILROY". SIGNIFICANT RESULTS ARE SHOWN IN BOLD.

| **MILROY** | **r** | ***p*** | **N** | **$R^2$** |
|---|---|---|---|---|
| **ECa (mS/m) 0–50 cm and:** | | | | |
| % clay 0–10 cm | 0.44 | 0.45 | 5 | 0.20 |
| % clay 0–10 cm | **0.96** | <0.05 | 4 | **0.92** |
| % clay 10–30 cm | **0.91** | <0.05 | 5 | **0.84** |
| % clay 30–60 cm | 0.43 | 0.50 | 5 | 0.19 |
| Colwell K (mg/kg) 0–10 cm | **0.77** | <0.001 | 22 | 0.60 |
| Colwell K (mg/kg) 30–60 cm | **0.94** | <0.001 | 26 | 0.62 |
| OC (%) 0–10 cm | **0.85** | <0.001 | 18 | **0.73** |
| OC (%) 10–30 cm | **0.80** | <0.001 | 15 | **0.70** |
| ECe (mS/m) 0–10 cm | 0.50 | <0.01 | 30 | 0.25 |
| ECe (mS/m) 10–30 cm | **0.91** | <0.001 | 29 | **0.83** |
| pH 10–30 cm | 0.60 | <0.001 | 29 | 0.36 |
| PBI 0–10 cm | **0.83** | <0.001 | 28 | **0.70** |
| PBI 30–50 cm | **0.89** | <0.01 | 14 | 0.50 |
| Exch. Al (%) 0–30 cm | –0.80 | 0.10 | 5 | 0.64 |
| Exch. Al (%) 0–60 cm | –0.76 | 0.14 | 5 | 0.57 |
| Chloride (mg/kg) 10–30 cm | **0.98** | <0.05 | 5 | **0.96** |
| Chloride (mg/kg) 30–60 cm | **0.98** | <0.01 | 5 | **0.96** |
| CEC (cmol/kg) 0–10 cm | **0.90** | <0.05 | 5 | **0.80** |
| CEC (cmol/kg) 10–30 cm | **0.98** | <0.01 | 5 | **0.96** |
| CEC (cmol/kg) 30–60 cm | **0.97** | <0.01 | 5 | **0.95** |
| ESP (%) 0–10 cm | 0.74 | 0.15 | 5 | 0.55 |
| ESP (%) 10–30 cm | **0.99** | <0.001 | 5 | **0.97** |
| ESP (%) 30–60 cm | **0.96** | <0.01 | 5 | **0.92** |
| **Gamma K (%) and:** | | | | |
| CEC 0–10 cm | 0.67 | 0.2 | 5 | 0.64 |
| **Gamma Th (ppm) and:** | | | | |
| ECa (mS/m) | **0.90** | <0.001 | 13 | **0.81** |
| OC (%) 0–10 cm | **0.90** | <0.05 | 5 | **0.80** |
| PBI 0–10 cm | **0.91** | <0.001 | 13 | **0.83** |
| pH 0–30 cm | **0.88** | <0.001 | 12 | **0.78** |
| Exch. Al (cmol/kg) 0–10 cm | **0.90** | <0.05 | 5 | **0.81** |
| Exch. Al (cmol/kg) 10–30 cm | **0.91** | <0.05 | 5 | **0.82** |
| ESP (%) 0–10 cm | 0.80 | 0.1 | 5 | 0.64 |
| **Gamma TC (counts/sec) and:** | | | | |
| ECa (mS/m) | **0.76** | <0.01 | 13 | 0.58 |
| OC (%) 0–10 cm | **0.90** | <0.05 | 5 | **0.87** |
| ESP (%) 0–10 cm | **0.87** | 0.05 | 5 | **0.75** |
| **Gamma U (ppm) and:** | | | | |
| OC (%) 0–10 cm | **0.85** | 0.05 | 5 | **0.78** |
| ESP (%) 0–10 cm | **0.90** | 0.05 | 5 | **0.82** |

Note: where Pearson's r was below 0.25 data is not shown.

**TABLE 5.9:** PEARSON CORRELATION COEFFICIENTS (R) AND REGRESSION COEFFICIENTS ($R^2$) FOR RELATIONSHIPS BETWEEN ECA DATA WITH SOIL PARAMETERS AT "GRANDVIEW". SIGNIFICANT RESULTS ARE SHOWN IN BOLD.

| **GRANDVIEW** | **r** | ***p*** | **N** | **$R^2$** |
|---|---|---|---|---|
| **ECa 0–38 cm and:** | | | | |
| % clay 0–10 cm | **0.86** | <0.001 | 24 | **0.74** |
| % clay 10–50 cm | **0.87** | <0.001 | 24 | **0.77** |
| pH 0–10 cm | 0.34 | 0.1 | 24 | 0.12 |
| pH 10–50 cm | **0.77** | <0.001 | 20 | 0.59 |
| Col P 0–10 cm | –0.27 | <0.05 | 24 | 0.07 |
| Col P 10–50 cm | –0.53 | <0.05 | 15 | 0.30 |
| Col K 0–10 cm | **–0.72** | <0.001 | 24 | 0.51 |
| Col K 10–50 cm | –0.66 | <0.05 | 20 | 0.44 |
| OC 0–50 cm | **–0.84** | <0.001 | 20 | **0.71** |
| CEC 0–10 cm | –0.44 | <0.05 | 24 | 0.19 |
| CEC 10–50 cm | **0.72** | <0.001 | 20 | 0.51 |
| ESP 0–10 cm | 0.59 | <0.05 | 24 | 0.34 |
| ESP 10–50 cm | **0.77** | <0.001 | 20 | 0.60 |
| **ECa 0–75 cm and:** | | | | |
| % clay 0–10 cm | **0.78** | <0.001 | 24 | 0.61 |
| % clay 10–50 cm | **0.85** | <0.001 | 20 | **0.75** |
| pH 10–50 cm | **0.80** | <0.001 | 20 | **0.70** |
| ESP 10–50 cm | **0.78** | <0.001 | 20 | 0.61 |
| OC 10–50 cm | **–0.83** | <0.001 | 20 | **0.70** |
| CEC 10–50 cm | **0.79** | <0.001 | 20 | 0.61 |

Note: where Pearson's r was below 0.25 data is not shown.

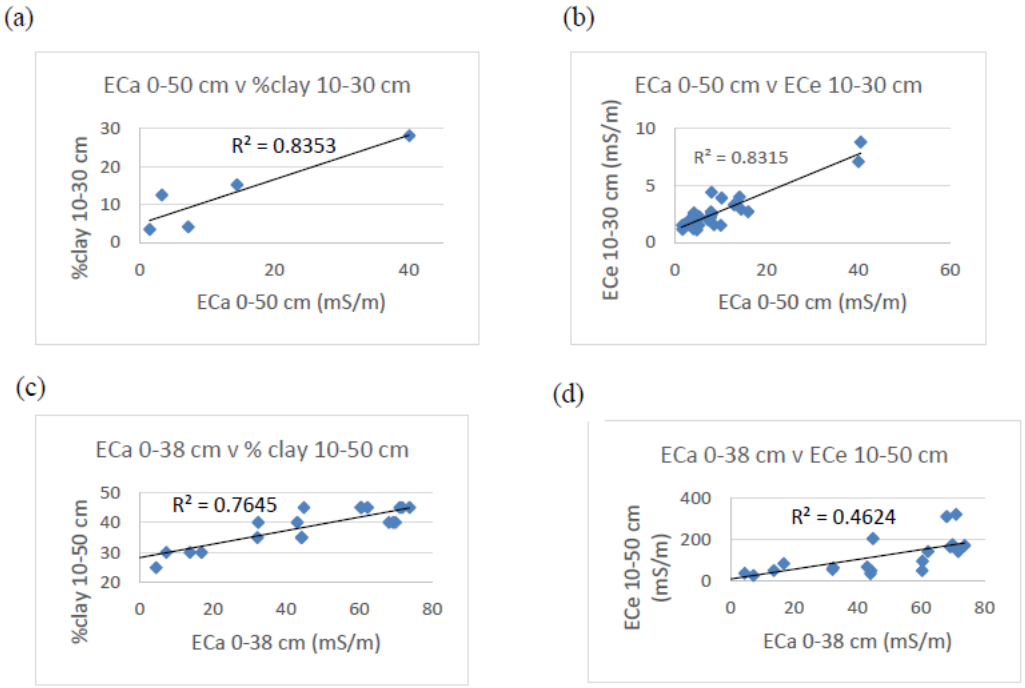


**FIGURE 5.15:** DISTRIBUTION OF ECA VALUES FOR REGRESSION AGAINST % CLAY AND ECE FOR "MILROY" PADDOCKS (A) AND (B) AND "GRANDVIEW" PADDOCKS (C) AND (D).

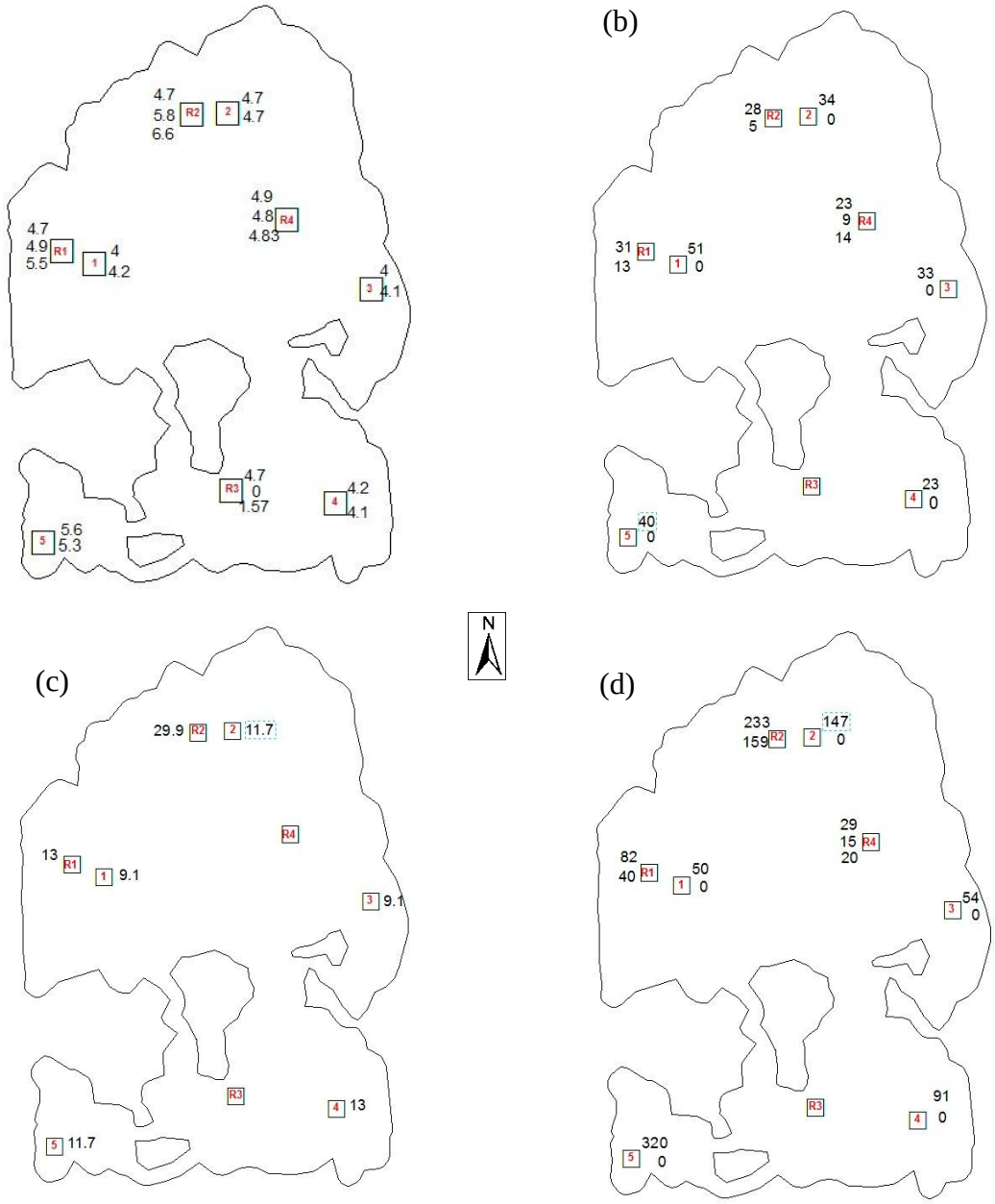


**FIGURE 5.16:** SOIL TEST RESULTS FOR MILROY PADDOCK M25. (A) PH ($CaCl_2$), (B) COLWELL P (MG/KG), (C) KG N/HA 0–50 CM AND (D) COLWELL K (MG/KG). WHERE A SINGLE RESULT IS SHOWN AT A POINT, THE DEPTH IS 0–10 CM, WHERE MULTIPLE RESULTS ARE SHOWN, THE DEPTHS ARE 0–10 CM, 10–30 CM AND 30–60 CM.

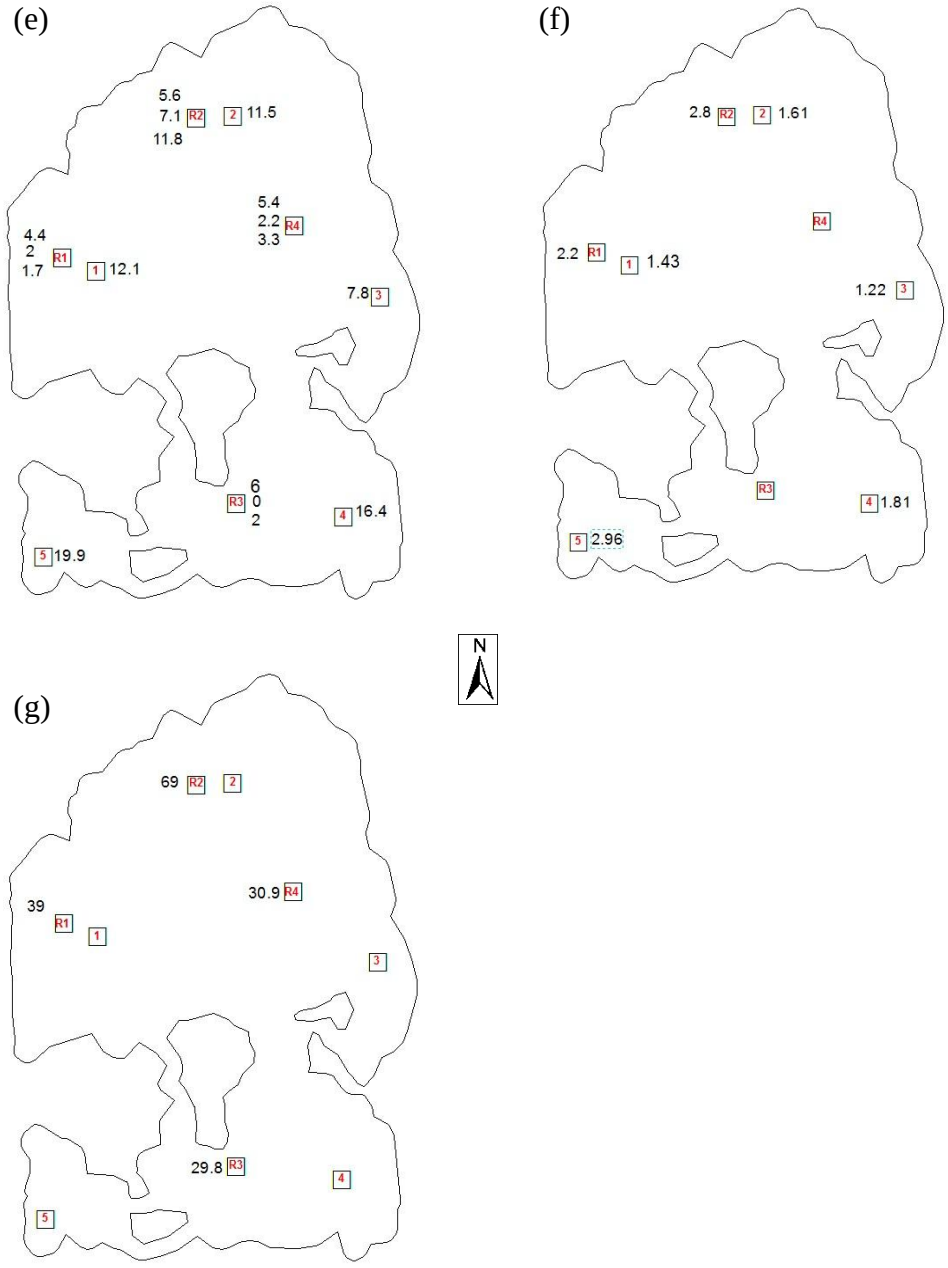


**FIGURE 5.16 (CONT.):** SOIL TEST RESULTS FOR MILROY PADDOCK M25. (E) ECE (DS/M), (F) OC (%) AND (G) PBI. WHERE A SINGLE RESULT IS SHOWN AT A POINT, THE DEPTH IS 0–10 CM, WHERE MULTIPLE RESULTS ARE SHOWN, THE DEPTHS ARE 0–10 CM, 10–30 CM AND 30–60 CM.

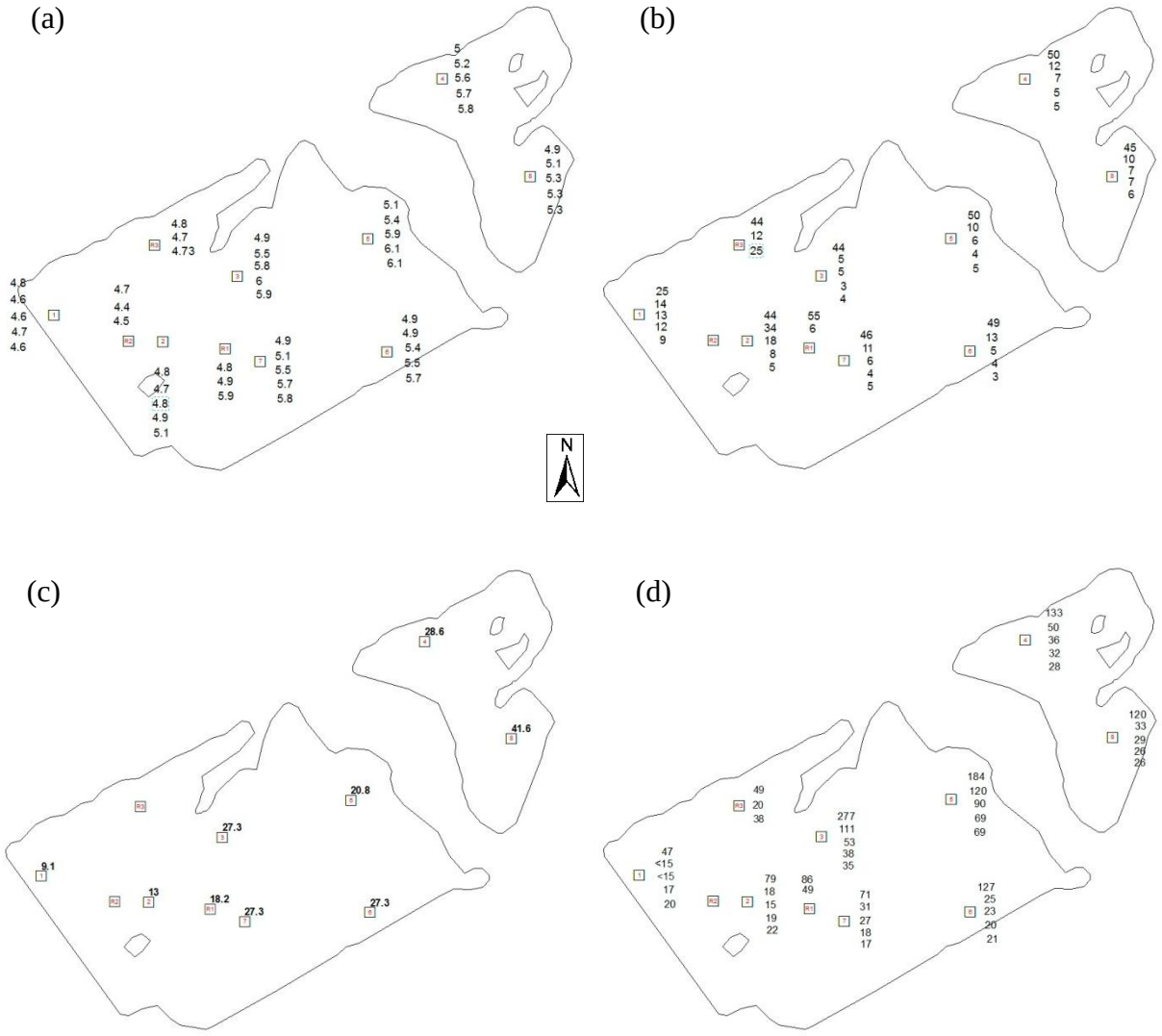


**FIGURE 5.17:** SOIL TEST RESULTS FOR MILROY PADDOCK M41. (A) PH ($CaCl_2$), (B) COLWELL P (MG/KG), (C) KG N/HA 0–50 CM AND (D) COLWELL K (MG/KG). WHERE A SINGLE RESULT IS SHOWN AT A POINT, THE DEPTH IS 0–10 CM, WHERE THREE VALUES ARE SHOWN, THE DEPTHS ARE 0–10 CM, 10–30 CM AND 30–60 CM. WHERE FIVE VALUES ARE SHOWN, DEPTHS ARE AT 10 CM INTERVALS, FROM 0–10 CM.

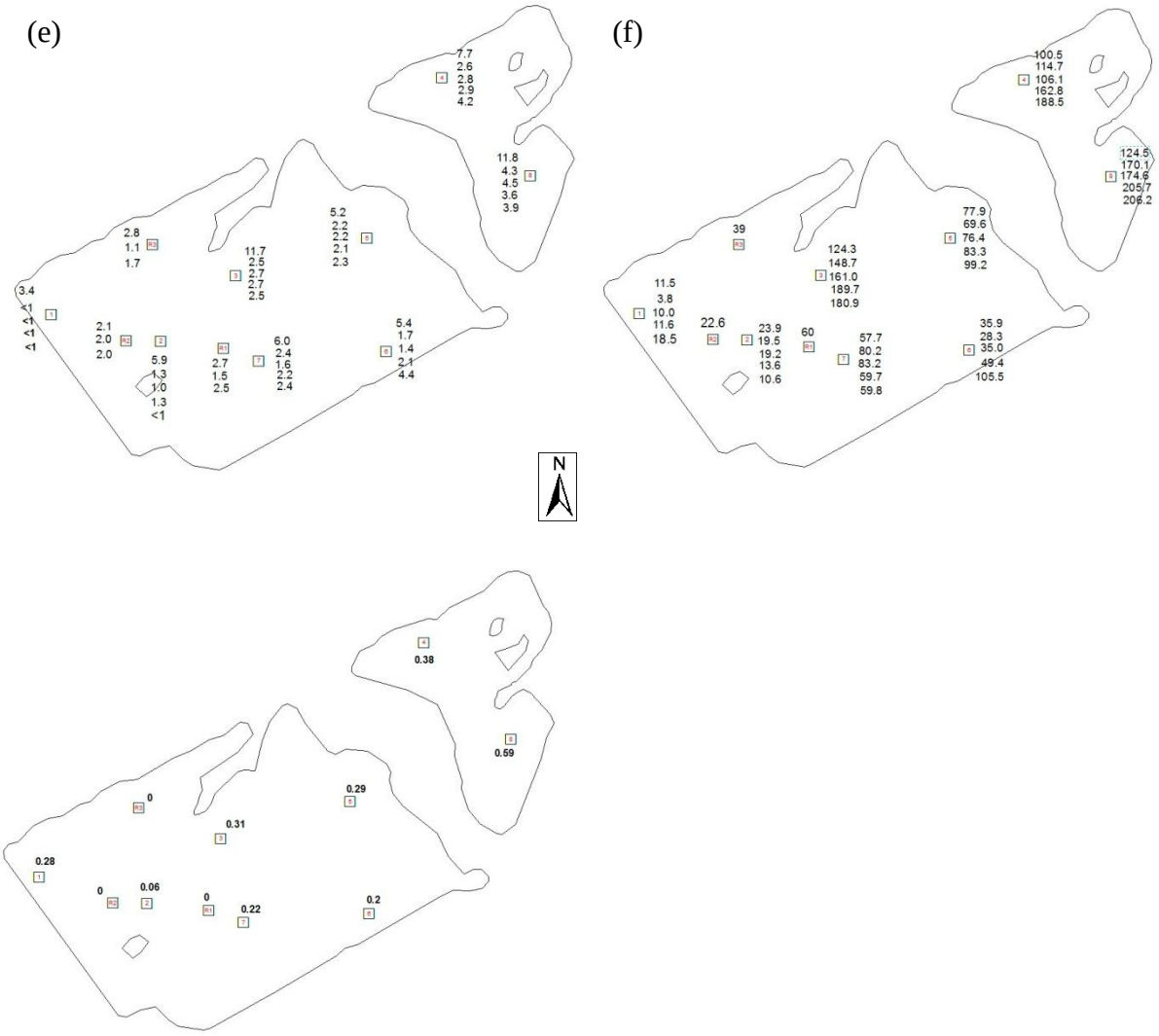


**FIGURE 5.17 (CONT.):** SOIL TEST RESULTS FOR MILROY PADDOCK M41. (E) ECE (DS/M), (F) PBI AND (G) OC (%). WHERE A SINGLE RESULT IS SHOWN AT A POINT, THE DEPTH IS 0–10 CM, WHERE THREE VALUES ARE SHOWN, THE DEPTHS ARE 0–10 CM, 10–30 CM AND 30–60 CM. WHERE FIVE VALUES ARE SHOWN, DEPTHS ARE AT 10 CM INTERVALS, FROM 0–10 CM.

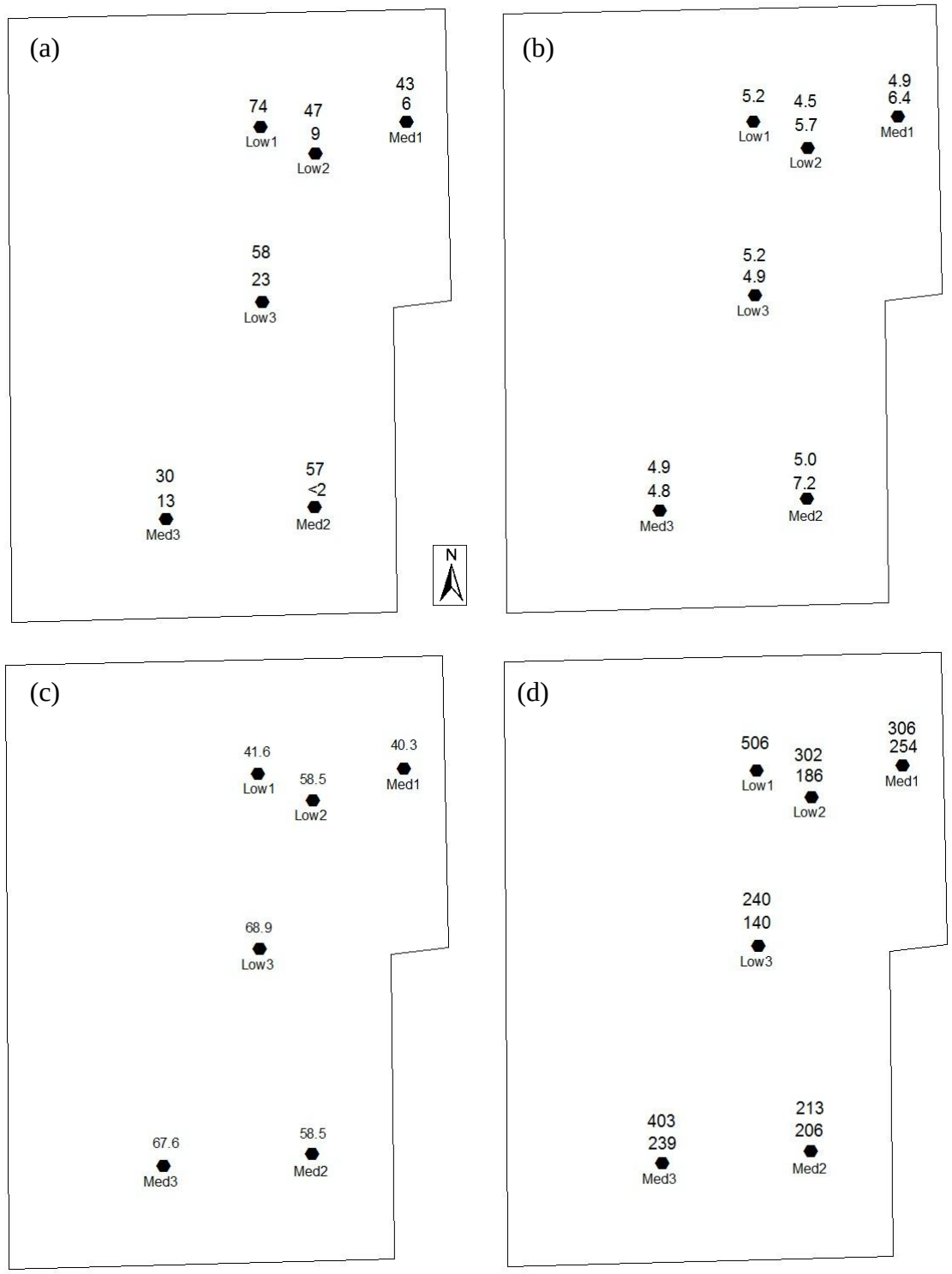


**FIGURE 5.18:** SOIL TEST RESULTS FOR GRANDVIEW PADDOCK GV8. (A) COLWELL P (MG/KG), (B) PH ($CaCl_2$), (C) KG N/HA 0–50 CM AND (D) COLWELL K (MG/KG). WHERE A SINGLE RESULT IS SHOWN AT A POINT, DEPTH IS 0–10 CM. MULTIPLE VALUES AT A SITE ARE 0–10 CM AND 10–50 CM.

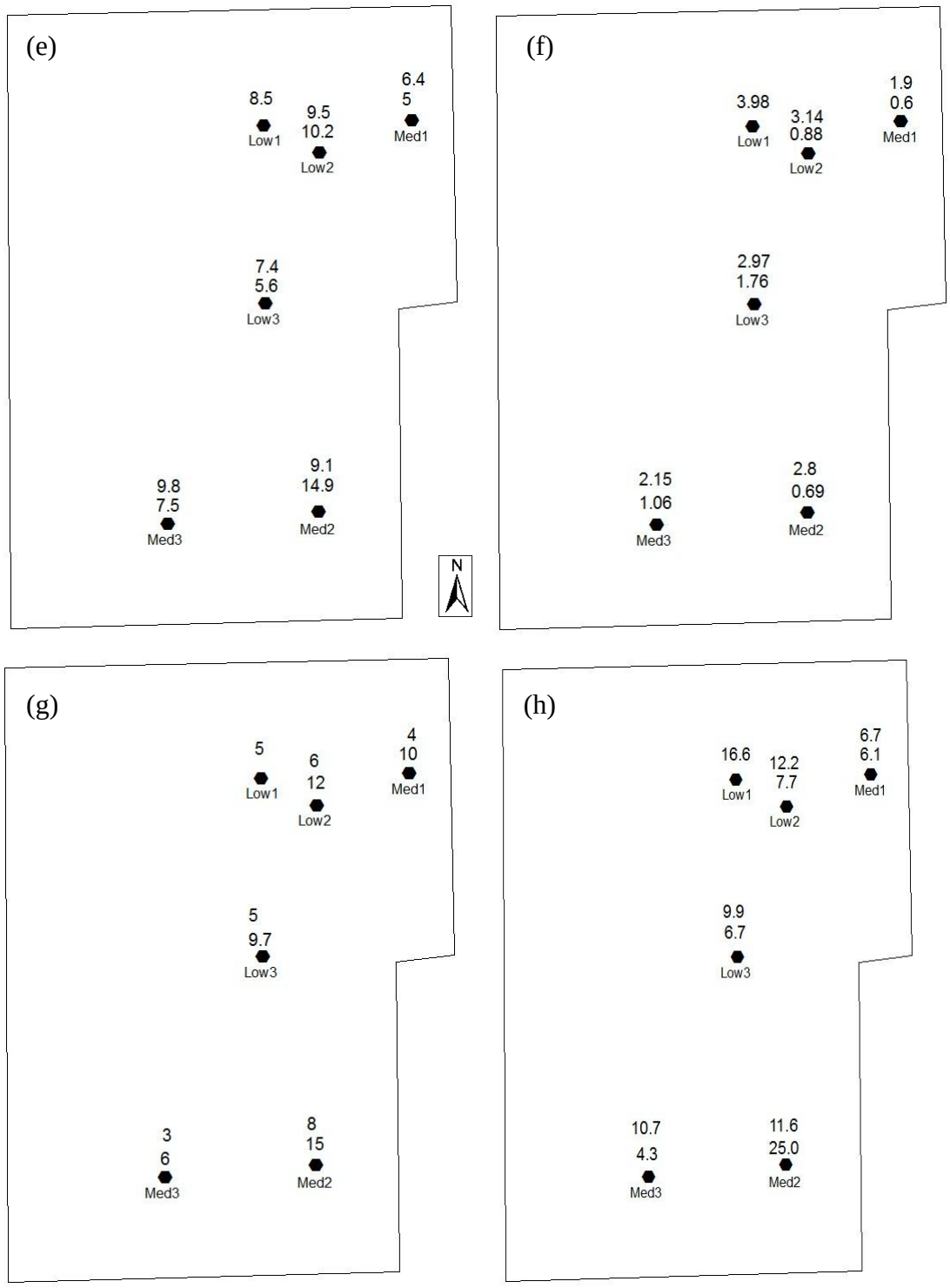


**FIGURE 5.18 (CONT.):** SOIL TEST RESULTS FOR GRANDVIEW PADDOCK GV8. (E) S (MG/KG), (F) OC (%), (G) ESP (%) AND (H) ECE (DS/M). WHERE A SINGLE RESULT IS SHOWN AT A POINT, DEPTH IS 0–10 CM. MULTIPLE VALUES AT A SITE ARE 0–10 CM AND 10–50 CM.

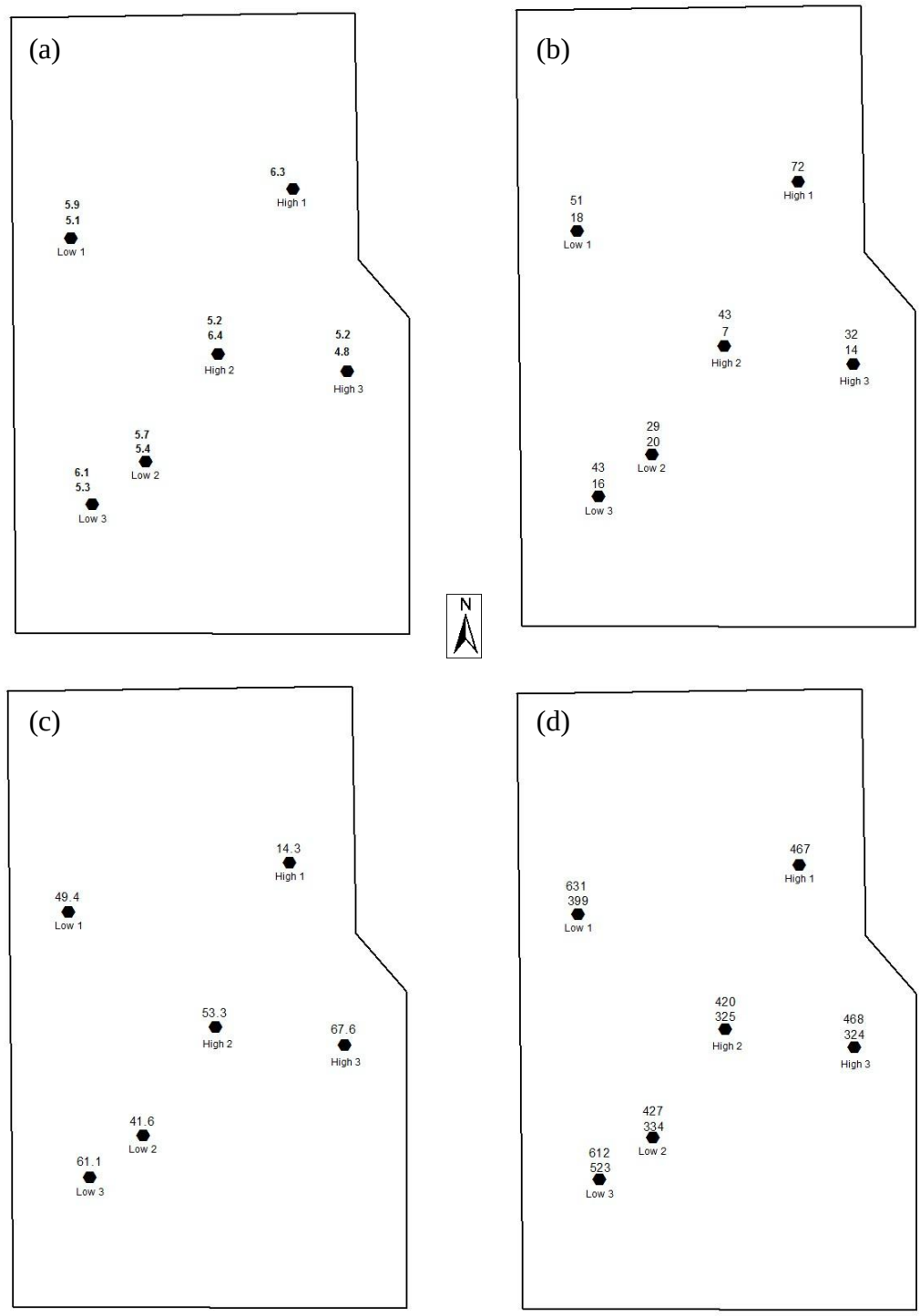


**FIGURE 5.19:** SOIL TEST RESULTS FOR GRANDVIEW PADDOCK GV39. (A) PH ($CaCl_2$), (B) COLWELL P (MG/KG), (C) KG N/HA 0–50 CM AND (D) COLWELL K (MG/KG). WHERE A SINGLE RESULT IS SHOWN AT A POINT, DEPTH IS 0–10 CM. MULTIPLE VALUES AT A SITE ARE 0–10 CM AND 10–50 CM.

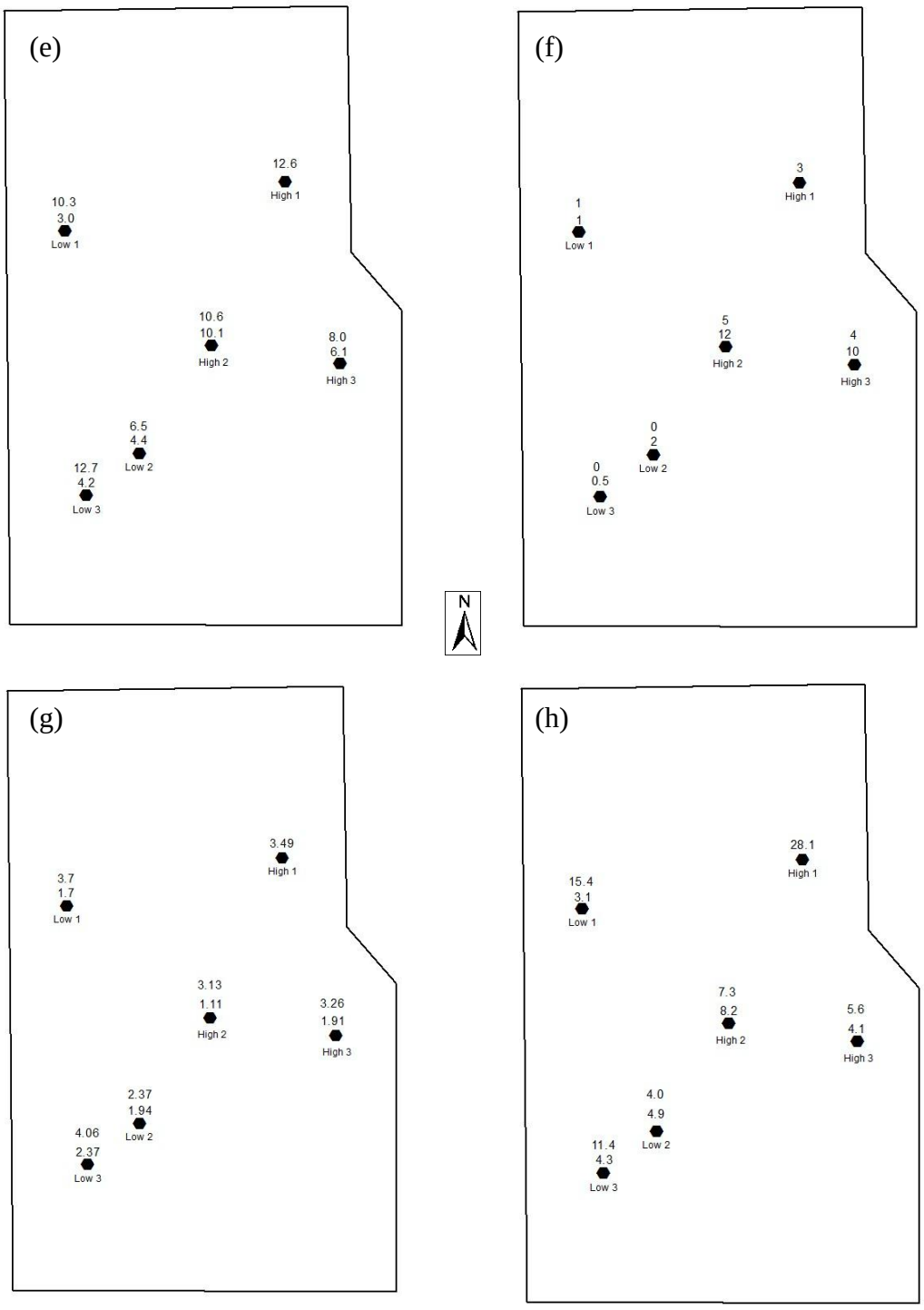


**FIGURE 5.19 (CONT.):** SOIL TEST RESULTS FOR GRANDVIEW PADDOCK GV39. (E) ECE (DS/M), (F) ESP (%), (G) OC (%) AND (H) S (MG/KG). WHERE A SINGLE RESULT IS SHOWN AT A POINT, DEPTH IS 0–10 CM. MULTIPLE VALUES AT A SITE ARE 0–10 CM AND 10–50 CM.

## 5.4 DISCUSSION

This chapter has described the acquisition and analysis of baseline data that is required for the hypotheses that will be tested in Chapters 6 and 7, that:

1. *Spatial variation of production in the crop and pasture phases of a mixed farming system can be identified and quantified at high resolution using PA technologies*, and
2. *Data acquired using PA technologies can be used to create a single index of paddock productivity that describes the spatial variation in, and temporal stability of, crop and pasture production over time*.

The objectives of this chapter were to i) investigate the use of EMI and GR sensing to map soil variability at a sub-paddock scale, and (ii) to relate the EMI and GR observations to measured soil physical and chemical properties related to crop and pasture productivity.

The results show that the use of EMI alone or EMI and GR sensing in combination can provide relatively low-cost, high-resolution, spatially-dense data sets to help quantify the extent and nature of spatial variability in soil properties across a paddock. The results generally support findings reported in the literature regarding the use of EMI and/or GR sensing in predicting properties such as soil textural changes, clay content and soil moisture (Corwin and Lesch, 2005; Doolittle and Brevik, 2014; Rodrigues Jr et al., 2015; Sudduth et al., 2013; Wong et al., 2009, 2010).

### *5.4.1 RELATIONSHIPS BETWEEN PROXIMALLY SENSED DATA AND SOIL TEXTURE*

In general, the mapped soil ECa and GR patterns (Figures 5.5–5.7) reflected local topography (Figure 5.14). That is, higher soil ECa values (reflecting higher soil moisture content and/or finer soil textures) generally occurred in lower-lying parts of the paddocks. The relatively low ECa values at “Milroy” also reflected the coarser-textured, highly weathered lateritic soils of the Darling escarpment where “Milroy” is located (Anand and Butt, 2003). Gamma radiometric patterns for potassium and thorium concentrations appeared to be related to the occurrence of geological features which influenced both soil texture and the presence of lateritic

gravels. The highest concentrations of gamma thorium and gamma potassium appeared to be distributed across the property where heavier-textured soils occur, apart from where sandy gravels occur, which are high in thorium and generally have low ECa levels.

In “Milroy” paddock M25, there are areas where both the ECa and gamma emissions are low (site 1 in Figure 5.5 a and b and Figure 5.6 a–d). This would indicate the presence of a uniform sand. However at M25 site 3, ECa is low, but gamma emissions are high. The difference in the gamma emissions between sites 1 and 3 is due to the presence of gravel at site 3. The gravel is as poorly conductive as sand, giving a low ECa value, but high gamma emission. This would indicate an area of shallow sand over gravel. The area of high ECa at M25 site 2 in Figures 5.5 a and b is not picked up in the gamma survey. The higher ECa values are usually due to an increase in soil moisture content and potentially an associated rise in salinity.

At M25 site 4, ECa and gamma thorium are both as low as at site 1, which would indicate a deep sand. However, gamma K here is elevated, indicating an underlying finer-textured soil, such as a sand over clay duplex soil, which was confirmed by soil coring (Figure 5.11 d). In paddock M41, site 1 (Figure 5.5 c and d and Figure 5.6 e–h) has low ECa and low gamma emissions, indicating a uniform deep sand. Site 2 has low ECa and high gamma, indicating shallow soil over gravel. Site 3 is situated on a saline drainage line and therefore has high ECa values, but is not picked up in the gamma survey.

The more uniform clay soils at “Grandview” exhibited higher mean electrical conductivities than “Milroy” (Table 5.5). This is related to closer contact between soil particles in the fine clays of “Grandview” and the resulting capacity to better retain soil moisture (Corwin and Lesch, 2003; Heil and Schmidhalter, 2012). The “Grandview” soils also have higher levels of sodium in the 10–50 cm layer than the sandier soils of “Milroy”.

Although there are only a small number of data points from “Milroy” for ECa vs. clay, the data points are well-distributed along the regression line from low ECa values to high (Figure 5.15 a). There was one very high ECa value (~40 mS/m). Removal of this point did not affect the slope of the regression line, i.e. this point

was not affecting the correlation relationship. At “Grandview”, there was also a strong correlation between ECa and clay content (Figure 5.15 c, Table 5.9).

Overall, the general trend of the relationship between ECa and clay content showed that ECa increased linearly with increasing clay content across all paddocks over two different geographic regions of Australia. Percentage clay was positively correlated with ECa in all the study paddocks. The positive relationship of ECa with percentage clay is consistent with findings in several previous studies (Castrignanò et al., 2012; Doolittle and Brevik, 2014; Kitchen et al., 2005; Kweon et al., 2013; Triantafilis and Lesch, 2005).

The combined use of EMI and GR sensing in the highly weathered landscapes where “Milroy” is located shows clear advantages over EMI alone. The approach proved valuable because areas of non-wetting gravels which could not be differentiated from deep sands using EMI sensing alone were identified with gamma sensing. Similarly, GR data helped with the interpretation in areas of the paddocks where high ECa values could be attributed to either clay or salinity in otherwise coarse-textured soils.

These interpretations also correspond reasonably well with the soil maps for “Milroy” M25 and M41 in Figures 5.9 and 5.10 and “Grandview” paddocks GV8 and GV39 in Figure 5.12, which were derived from the knowledge and experience of the farm owners (pers. comm.).

### *5.4.2 RELATIONSHIPS BETWEEN ECA AND SOIL CHEMISTRY*

There were strong correlations between ECa and salinity (conductivity as measured by ECe) at 10–30 cm at “Milroy”, except for one very high ECa value (~40 mS/m). However, as with ECa vs. clay content, removal of this point did not affect the slope of the regression line, i.e. the value was not driving the correlation relationship. At “Grandview”, the regression for ECa vs. conductivity (ECe) at 10–30 cm could only explain 46% of the variation in ECe.

The histograms of ECa data point distribution (Figure 5.8 a–d) illustrate the generally low ECa values in the two “Milroy” paddocks. The occurrence of very high ECa values in these paddocks was atypical and would indicate that salinity is not a

major plant growth restrictor at “Milroy” except for relatively small lenses of salinity, as seen in Figure 5.5.

In contrast, high ECa values occurred more frequently in the distributions for “Grandview” (Figure 5.8 e–f). These are indicative of both the higher levels of clay and also higher electrical conductivities influenced by high ESP values in the subsoil (Figures 5.18 g and 5.19 f).

The descriptive statistics of ECa data (Table 5.5) revealed that coefficients of variation (CV) for the “Milroy” sites were significantly higher than at “Grandview”, (with the exception of GV39, 0–38 cm), reflecting a substantially greater level of spatial variability in “Milroy” soils than those at “Grandview”. The high degree of within-paddock variation in soil ECa at “Milroy”, as defined by CV, may indicate that whole-paddock uniform management currently being practised might not be the most effective strategy.

At “Milroy”, some reliable relationships (Table 5.8) between the EMI and GR survey data and important soil properties were identified, many of which have been previously reported in the literature. The most robust relationships with agronomic significance were between ECa (0–50 cm) and soil texture (clay content), PBI, ESP, chloride, CEC and OC. This suggests that ECa data could be a useful tool in identifying different nutrient management zones for site-specific management strategies. The strong associations between ECa, ESP and chloride at “Milroy” (Table 5.8) can be used to identify areas of problem soils within this landscape. CEC is a measure of a soil’s capacity to adsorb and hold cations and provides an indication of the amount of nutrients available in the soil. The low CEC, sandy (low ECa) soils at “Milroy” would retain smaller quantities of cations, and a program of multiple, smaller applications of highly mobile nutrients such as K and S may be warranted in those areas, and of P where PBI is low. In areas identified as having higher ECa (higher clay content, CEC and OC), less frequent and larger applications may be appropriate (Hazelton and Murphy, 2007; Price, 2006).

The relationships with GR data were less consistent, with gamma thorium correlating with PBI 0–10 cm, exchangeable Al and OC 0–10 cm. CEC and OC increased with increasing ECa as would be expected. Interestingly, there were no

consistent relationships between GR potassium and Colwell K at “Milroy”, which was unexpected. Gamma ray spectrometry measures radiation from all forms of potassium contained within the soil, some of which is readily available while some is contained in mineral structures and poorly available. Wong and Harper (1999) reported strong correlations between gamma emission from K and Colwell K soils in the Western Australian cropping zone. However, the authors also pointed out that this relationship may not hold in all situations because of the impacts of local geology and pedologic history on soil formation processes. The owner of “Milroy” has been applying high levels of fertiliser K to both paddocks, which may have confounded the relationship between Colwell K and total K as measured by the gamma survey. The soils at “Milroy” are generally highly leached and coarse textured and therefore have a lower capacity to retain potassium ions, possibly leading to lower Colwell K values. Plant responses to potassium fertilisers have been reported in soils with exchangeable potassium values below 0.2 meq/100 g (Abbott and Vimpany, 1989). Three of the five sites tested were at, or below, this level. The other aspect to consider is management, in terms of import and export of K.

At “Grandview”, the results were less consistent. The combined data for both paddocks demonstrated robust relationships between ECa 0–38 cm and soil texture (clay content) and organic carbon and ECa 0–75 cm with clay, pH and OC (Table 5.9). In some instances, the relationships between ECa and agronomic factors of importance were negative or showed no relationship. Individual paddock data was also generally inconclusive.

This accords with reported work on “Grandview” (Inchbold et al., 2009) where the medium ECa zone (comprising 80% of ECa values) was highly unstable and thus unpredictable when adding farm inputs such as nitrogen and phosphorus. In contrast, responses to these inputs on the high and low ECa zones were highly predictable (Inchbold et al., 2009; P. Baines pers. comm.).

The farm owner at “Grandview” has been employing variable rate phosphorus applications during cropping phases (replacement P based on previous year’s yield map) for many years. The soil phosphorus results would appear to reflect this management practice, showing relatively uniform soil P across the paddocks. During

pasture phases (2004 and 2011), the farm owner aimed to apply approximately 8 kg/ha of P as 100 kg/ha of single superphosphate. The highest P-value in GV39 was associated with a cattle camp and feed trough, indicating that there may have been some nutrient transfer occurring. The highest P-value in GV8 was also associated with a cattle camping area. Surprisingly, there was no relationship between ECa and CEC. Changes in CEC are usually associated with changes in clay content. Because "Grandview" soils have a clay loam/clay texture, a positive correlation of ECa with clay content and CEC would have been expected in these paddocks over depth.

Mean sulphur concentrations for both paddocks (8.45 mg/kg for GV8 and 12.0 mg/kg for GV39) were above the critical value (8 mg/kg), variability in GV39 at the sub-paddock scale was considerable, suggesting potential value from variable rate application of sulphur.

The results described here have demonstrated the capacity and efficiency of EMI and GR sensing to improve the accuracy and reliability of sub-paddock soil maps and provide more detailed information on variations in soil textures and soil properties within a paddock. In highly weathered areas such as "Milroy", which contain sandy, clayey, gravelly and salt-affected soils, the integration of multi-sensor data improved the characterisation of sub-paddock soil properties compared to using an EMI sensor alone.

Overall, the results emphasised that each property differed and that the relationships between the sensor data and soil properties measured are complex and cannot be generalised. The results also showed that the relationships of ECa with soil texture were generally more consistent than those with chemical properties. Laboratory soil test results from paddock sampling did not always correlate positively with the proximally sensed estimates of those properties, sometimes creating ambiguous and inconsistent relationships. Interpretation of the results can sometimes be confounded by the complex interactions among different soil properties. This accords with similar findings that differences in soil physical properties can have a greater influence over variation in ECa than differences in soil chemical properties (Castrignanò et al., 2012; Doolittle and Brevik, 2014; Jung et al., 2005). For these reasons, it is clear that any proximal sensing approach has to be

supported by ground-truthing and calibration in the form of field sampling and soil testing if proximally sensed data is to be interpreted beyond a basic observation of the extent to which a particular paddock is variable. It is physically difficult and expensive to accurately map the extent of within-paddock soil variability at the spatial resolution required by precision agriculture methodologies using conventional laboratory-based soil testing techniques alone. This reinforces the point that proximal soil sensing technologies alone cannot replace the detail provided by manual soil sampling in the paddock. Instead, traditional soil sampling and proximal sensing techniques should be used together to provide even more information about the soils at a given site than is possible using either approach alone.

Indeed, the research described in this chapter would have benefitted from more extensive soil testing, but was restricted by budgetary constraints. Nonetheless, across two contrasting sites on either side of the continent, maps of soil characteristics predicted from the proximally sensed data will be helpful in understanding within-paddock variation.

## 5.5 CONCLUSION

Although a considerable body of research has described measuring and understanding the spatial variability of soil characteristics in cropping systems, there is little information available in the literature describing the same characteristics in mixed farming systems. The work described in this chapter sought to evaluate the potential use of relatively low-cost EMI and GR sensor data in mixed farming production systems for testing the hypotheses in Chapters 6 and 7. Overall, some strong positive correlations were evident between remotely sensed data and soil textural properties. Correlations between ECa values and soil chemical properties were less consistent, and the relationships were specific to the paddocks they were taken in.

In the following chapters, the acquisition of further high-resolution datasets and maps will be explored and used in conjunction with the proximally sensed soil data obtained here. This high-resolution data will be used to explore sub-paddock

variations in and productive stability of mixed farming systems in both space and time.

## 5.6 REFERENCES

Abbott, T. S., & Vimpany, I. A. (1989). *BCRI soil testing: methods and interpretation*: Biological and Chemical Research Institute, NSW Department of Agriculture & Fisheries.

Anand, R. R., & Butt, C. R. M. (2003). Distribution and evolution of 'laterites' and lateritic weathering profiles, Darling Range, Western Australia. *Australian Geomechanics, 38*, 41–58.

Castrignanò, A., Wong, M. T. F., Stelluti, M., De Benedetto, D., & Sollitto, D. (2012). Use of EMI, gamma-ray emission and GPS height as multi-sensor data for soil characterisation. *Geoderma, 175–176*, 78–89. doi: 10.1016/j.geoderma.2012.01.013

Cook, S., Corner, R., Groves, P., & Grealish, G. (1996). Use of airborne gamma radiometric data for soil mapping. *Soil Research, 34*(1), 183–194. doi: http://dx.doi.org/10.1071/SR9960183

Corwin, D. L., & Lesch, S. M. (2003). Application of soil electrical conductivity to precision agriculture: theory, principles, and guidelines. *Agronomy Journal, 95*(3), 455.

Corwin, D. L., & Lesch, S. M. (2005). Apparent soil electrical conductivity measurements in agriculture. *Computers and Electronics in Agriculture, 46*(1–3), 11–43.

Doolittle, J. A., & Brevik, E. C. (2014). The use of Electromagnetic Induction techniques in soils studies. *Geoderma, 223*, 33–45.

Fu, W., Tunney, H., & Zhang, C. (2010). Spatial variation of soil test phosphorus in a long-term grazed experimental grassland field. *Journal of Plant Nutrition and Soil Science, 173*(3), 323–331.

Fu, W., Zhao, K., Jiang, P., Ye, Z., Tunney, H., & Zhang, C. (2013). Field-scale variability of soil test phosphorus and other nutrients in grasslands under long-term agricultural managements. *Soil Research, 51*(6), 503–512.

Gourley, C. J. P., Peverill, K. I., & Dougherty, W. J. (2007). *Making better fertiliser decisions for grazed pastures in Australia, accounting for nutrients and fertcare*. Paper presented at the Australian Fertilizer Industry Conference.

Hazelton, P. A., & Murphy, B. W. (2007). *Interpreting soil test results: what do all the numbers mean?* Collingwood, Victoria, Australia: CSIRO Publishing.

Heil, K., & Schmidhalter, U. (2012). Characterisation of soil texture variability using the apparent soil electrical conductivity at a highly variable site. *Computers & Geosciences, 39*, 98–110. doi: http://dx.doi.org/10.1016/j.cageo.2011.06.017

IAEA. (2003). *Guidelines for radioelement mapping using gamma ray spectrometry data*: International Atomic Energy Agency, Nuclear Fuel Cycle Materials Section. Retrieved from: http://www-pub.iaea.org/mtcd/publications/pdf/te_1363_web.pdf

Inchbold, A., Whelan, B., & Baines, P. (2009). Making money out of precision agriculture. *Improving winter cropping systems in the Riverine Plains*. Yarrawonga, Victoria: Riverine Plains Inc.

Isbell, R. (2016). *The Australian soil classification*: CSIRO Publishing.

Jung, W. K., Kitchen, N. R., Sudduth, K. A., Kremer, R. J., & Motavalli, P. P. (2005). Relationship of apparent soil electrical conductivity to claypan soil properties. *Soil Science Society of America Journal, 69*(3), 883–892. doi: 10.2136/sssaj2004.0202

Keating, B. A., Carberry, P. S., Hammer, G. L., Probert, M. E., Robertson, M. J., Holzworth, D., . . . Smith, C. J. (2003). An overview of APSIM, a model designed for farming systems simulation. *European Journal of Agronomy, 18*(3–4), 267–288.

King, W. M., Dowling, P., Michalk, D., Kemp, D., Millar, G., Packer, I., . . . Tarleton, J. (2006). Sustainable grazing systems for the Central Tablelands of New South Wales. 1. Agronomic implications of vegetation–environment associations within a naturalised temperate perennial grassland. *Animal Production Science, 46*(4), 439–456.

Kitchen, N. R., Sudduth, K. A., Myers, D. B., Drummond, S. T., & Hong, S. Y. (2005). Delineating productivity zones on claypan soil fields using apparent soil electrical conductivity. *Computers and Electronics in Agriculture, 46*(1–3), 285–308.

Kweon, G., Lund, E., & Maxton, C. (2013). Soil organic matter and cation-exchange capacity sensing with on-the-go electrical conductivity and optical sensors. *Geoderma, 199* (May), 80–89. doi: http://dx.doi.org/10.1016/j.geoderma.2012.11.001

Loijens, H. S. (1980). Determination of soil water content from terrestrial gamma radiation measurements. *Water Resources Research*, 16(3), 565–573.

McCormick, S., Jordan, C., & Bailey, J. (2009). Within and between-field spatial variation in soil phosphorus in permanent grassland. *Precision Agriculture, 10*(3), 262–276.

McDonald, R. C., & Isbell, R. F. (2009). Soil Profile *Australian Soil and Land Survey Field Handbook* (3rd ed.). Collingwood: CSIRO Publishing.

McKenzie, N. J., Grundy, M., Webster, R., & Ringrose-Voase, A. (2008). *Guidelines for surveying soil and land resources*: CSIRO Publishing.

Merry, R., Tiller, K., & Richards, A. (1990). Variability in characteristics of some acidic pasture soils in South Australia and implications for lime application. *Soil Research, 28*(1), 27–38.

Price, G. (2006). *Australian Soil Fertility Manual* (3rd ed.). Collingwood Victoria: CSIRO Publishing.

Rayment, G. E., & Lyons, D. J. (2010). *Soil Chemical Methods–Australasia* Collingwood: CSIRO Publishing.

Rodrigues Jr, F. A., Bramley, R. G. V., & Gobbett, D. L. (2015). Proximal soil sensing for Precision Agriculture: simultaneous use of electromagnetic induction and gamma radiometrics in contrasting soils. *Geoderma, 243–244*, 183–195. doi: http://dx.doi.org/10.1016/j.geoderma.2015.01.004

Rousseuw, P. J., & Leroy, A. M. (1988). A robust scale estimator based on the shortest half. *Statistica Neerlandic*a, *42*, 103–116. doi:10.1111/j.1467-9574.1988.tb01224.x

Serrano, J. M., Peça, J. O., Marques da Silva, J. R., & Shahidian, S. (2011). Spatial and temporal stability of soil phosphate concentration and pasture dry matter yield. *Precision Agriculture, 12*(2), 214–232.

Serrano, J. M., Peça, J. O., Marques da Silva, J. R., & Shaidian, S. (2010). Mapping soil and pasture variability with an electromagnetic induction sensor. *Computers and Electronics in Agriculture, 73*(1), 7–16.

Shaw, R. J. (1999). Soil Salinity–Electrical conductivity and Chloride. In K. Peverill, L. Sparrow, & D. Reuter (Eds.), *Soil Analysis: An Interpretation Manual*. Collingwood: CSIRO Publishing.

Shi, Z., Wang, K., Bailey, J., Jordan, C., & Higgins, A. (2000). Sampling strategies for mapping soil phosphorus and soil potassium distributions in cool temperate grassland. *Precision Agriculture, 2*(4), 347–357.

Stefanski, A., & Simpson, R. J. (2010). *Uneven nutrient distributions in hillside paddocks indicate potential need for variable rate fertiliser applications to pastures*. Paper presented at the 15th Agronomy Conference "Food Security from Sustainable Agriculture", Lincoln, New Zealand.

Sudduth, K. A., Myers, D. B., Kitchen, N. R., & Drummond, S. T. (2013). Modeling soil electrical conductivity–depth relationships with data from proximal and penetrating ECa sensors. *Geoderma, 199*, 12–21. doi: http://dx.doi.org /10.1016/j.geoderma.2012.10.006

Taylor, J. A., McBratney, A. B., & Whelan, B. M. (2007). Establishing management classes for broadacre agricultural production. *Agronomy Journal, 99*(5), 1366–1376. doi: 10.2134/agronj2007.0070

Triantafilis, J., & Lesch, S. M. (2005). Mapping clay content variation using electromagnetic induction techniques. *Computers and Electronics in Agriculture, 46*(1–3), 203–237.

Wong, M. T. F., Oliver, Y. M., & Robertson, M. J. (2009). Gamma-radiometric assessment of soil depth across a landscape not measurable using electromagnetic surveys. *Soil Science Society of America Journal, 73*(4), 1261–1267.

Wong, M. T. F., Wittwer, K., Oliver, Y. M., & Robertson, M. J. (2010). Use of EM38 and gamma ray spectrometry as complementary sensors for high-resolution soil property mapping. In R. Viscarra-Rossel (Ed.), *Proximal Soil Sensing* (pp. 343–349): Springer Science.

# CHAPTER 6. HIGH-RESOLUTION ACTIVE OPTICAL SENSING FOR MIXED FARMING SYSTEMS

## 6.1 INTRODUCTION

In Chapters 3 and 4, MODIS NDVI was used as a proxy for measuring crop and pasture biomass to confirm the hypothesis that, "*spatial variation in biomass production over time is correlated between the cropping and pasture phases of mixed farming enterprises"*. It was also noted that the MODIS pixel size of 250 m (6.25 ha) limited the opportunity to identify within-paddock spatial variability at a sufficiently fine scale. Much higher resolution data was needed to enable identification of sub-paddock variation in biomass and soil physical and chemical properties and their correlation to production in cropping and pasture phases. Chapter 5 then described preliminary work using 'on-the-go' proximal soil sensors as a means of rapidly obtaining high-resolution information about variations in soil texture (and associated soil PAWC) and chemistry using soil conductivity (ECa) and radioactivity (gamma). Paddock maps identifying spatial variability in soil conductivity and gamma emissions at a spatial resolution of 10 m were created. These maps showed strong correlations with actual soil texture variations across each paddock (Chapter 5, Figure 5.15). There were also good correlations with some soil chemical properties (Chapter 5, Tables 5.8–5.9).

This chapter describes the acquisition and analysis of high-resolution crop and pasture yield data. This data, in combination with the soil physical and chemical information from Chapter 5, will be used to test Hypothesis 2 (Chapter 2, p. 36) that "*spatial variation of production in the crop and pasture phases of a mixed farming system can be identified and quantified at high resolution using PA technologies*".

At present, managers of mixed farming systems have no practical way of quantifying dry matter pasture production and the associated sub-paddock variability at high resolution during pasture phases. This is a significant problem when the spatial heterogeneity commonly associated with pastures is taken into

consideration (Laca, 2009). In contrast, most modern crop harvesters are equipped with yield monitors which allow crop producers to compile a high-resolution (10 m) database of spatial variation in crop yields (yield maps) over time. This data, combined with other information relating to crop performance (including paddock histories, soil chemical and physical properties, growing season rainfall, disease loads, frost events and satellite NDVI data) can be used to make decisions about site-specific management of crops, including variable rate management (Cook and Bramley, 1998; Whelan and Taylor, 2013). In this chapter, pasture yield data is determined by using a Crop Circle™ active optical sensor to measure the level of pasture production in selected paddocks during pasture–livestock rotations on "Milroy" and "Grandview". Compared to spatial variation in crop yields, relatively little is known about the degree of within-paddock spatial variation during the pasture–livestock phase in mixed farming systems. Most of the reported research in this regard has been undertaken on international grassland farming systems (Edirisinghe et al., 2012; Lee et al., 2011; Marques Da Silva et al., 2008; Serrano et al., 2010, 2011; Suzuki et al., 2012; Zhao et al., 2007), with a much smaller body of relevant work on Australian dryland pasture systems (Trotter, 2010; Trotter et al., 2008, 2010; Virgona and Hackney, 2008). None of this research has been conducted on mixed farming systems. Knowledge of the spatial variation in pasture biomass, its underlying causes, and how it compares to grain harvest yield variation during the cropping phase could significantly enhance the capacity for a manager to implement highly effective site-specific management strategies in a continuous sequence of pasture and cropping phases.

The combined soil ECa paddock elevation data is therefore used in combination with crop yield data and the pasture dry matter data derived from Crop Circle™ sensing to delineate potential management classes suitable for differential management. Here, the protocol described by Taylor et al. (2007) for use in cropping systems is extended to incorporate both pasture dry matter yields and crop yields. The advantage of this methodology is that it can capture high spatial density data from every year in a rotation, not just the cropping years. For example, at "Grandview", which has five-year pasture phases, the only precision data being

collected at present is crop yield, which only occurs five years in ten. Even at "Milroy", which has shorter pasture phases ranging from one to three years, precision yield data is only captured somewhere between three years in four to three years in six.

## 6.2 MATERIALS AND METHODS

### *6.2.1 STUDY SITES*

The study sites were the same as those described previously (Chapter 3, pp. 58–61). Crop harvest yield data was available at both sites for all paddocks between 2004 and 2014. However, not all yield data could be used due to in-paddock problems with yield sensors, calibration and/or operator error. Both sites received below mean annual and mean growing season rainfall over most seasons and years of the conducted research, resulting in likely soil moisture constraints on both pasture and crop production. Table 6.1 summarises crop and pasture rotations for both properties as well as available yield data. Rainfall data is shown in Table 6.2.

**TABLE 6.1:** PADDOCK ROTATIONS FOR "MILROY" AND "GRANDVIEW" AND CROP HARVESTER YIELD MONITOR DATA THAT WAS AVAILABLE FOR ANALYSIS, 2004–2014.

| Paddock | 2004 | 2005 | 2006 | 2007 | 2008 | 2009 | 2010 | 2011 | 2012 | 2013 | 2014 |
|---|---|---|---|---|---|---|---|---|---|---|---|
| **"MILROY"** | | | | | | | | | | | |
| M25 | W[A] | P | P | B[C] | P | W[A] | P | P | P | W | W |
| M41 | L[A] | B[C] | P | P | C[C] | W[A] | P | P | P | P | W |
| **"GRANDVIEW"** | | | | | | | | | | | |
| GV8 | P | C[A] | W[C] | W[A] | C[C] | W[A] | W[C] | W | P | P | P |
| GV39 | P | C[C] | W[C] | C[A] | W[A] | W[A] | B[C] | P | P | P | P |

B = barley, C = canola, L = lupin, W = wheat, P = pasture

[A] = Yield data available for this year; [C] = yield data was corrupted and unusable in this year

**TABLE 6.2:** ANNUAL RAINFALL (AR) AND GROWING SEASON RAINFALL (GSR) FROM 2004 TO 2014 FOR "MILROY" AND "GRANDVIEW". THE GROWING SEASON IS DEFINED AS THE PERIOD BETWEEN 1 APRIL AND 31 OCTOBER. MEAN RAINFALL VALUES ARE FROM THE AUSTRALIAN BUREAU OF METEOROLOGY BROOKTON AND YARRAWONGA PATCHED-POINT DATA 1970–2000.

| YEAR | mean | 2004 | 2005 | 2006 | 2007 | 2008 | 2009 | 2010 | 2011 | 2012 | 2013 | 2014 |
|---|---|---|---|---|---|---|---|---|---|---|---|---|
| **"MILROY"** | | | | | | | | | | | | |
| AR (mm) | 437 | 304 | 501 | 392 | 392 | 494 | 439 | 256 | 467 | 300 | 461 | 371 |
| GSR (mm) | 357 | 264 | 428 | 228 | 370 | 416 | 328 | 162 | 331 | 234 | 371 | 348 |
| **"GRANDVIEW"** | | | | | | | | | | | | |
| AR (mm) | 539 | 365 | 568 | 217 | 355 | 334 | 293 | 794 | 688 | 658 | 394 | 531 |
| GSR (mm) | 359 | 260 | 334 | 148 | 190 | 155 | 245 | 407 | 243 | 218 | 254 | 327 |

### *6.2.2 CROP HARVEST YIELD DATA AND YIELD MAPPING*

At "Milroy", grain yield data was acquired on a Case 2388 harvester (2004–2008) and Case 2388 and 8010 harvesters (2009–2014) connected to a differentially corrected real-time kinematic (RTK) GPS system. At "Grandview", grain yield data was acquired with a New Holland CR960 harvester coupled to a differentially corrected RTK GPS system.

Raw yield data was processed using the protocol developed by Taylor et al. (2007). Data was inspected and trimmed to more realistic values by removing obvious outliers by constraining to a lower threshold of 0 t/ha and an upper threshold of 5.5 t/ha at "Milroy" and a lower threshold of 0 t/ha and an upper threshold of 7.5 t/ha at "Grandview". Extremely high yield registrations can result from the harvester suddenly slowing and low registrations can result from driving with the comb down but not harvesting or taking a full swath. After trimming, data points more than 2.5 standard deviations (s.d.) above the paddock mean and 1.5 s.d. below the paddock mean were removed, after first plotting and inspecting the data in PAM Precision Data Processor (v.3.3.7) (Fairport Farm Software, Perth, WA) to confirm that the cleaned data 'made sense'.

Figure 6.1 a–c shows the change in the histogram as a yield data layer, in this case, when "Milroy" paddock M25 in 2009 (wheat) was cleaned. The diagrams show (a) the histogram of the raw data and the presence of extreme values, (b) the same data after values are manually constrained to sensible limits, and (c) the cleaned data after final trimming using 2.5 s.d. above the paddock mean and 1.5 s.d. below the paddock mean as thresholds (Taylor et al., 2007).

Yield data was then imported into ArcGIS 10.2 (ESRI, Redlands, California), converted to UTM projection, and mapped to a standard square 5 m x 5 m grid. Data was interpolated to the grid with Vesper 1.62 (Australian Centre for Precision Agriculture, The University of Sydney, NSW) using an exponential variogram and a block size of 10 m x 10 m. Interpolated data was then converted to raster surfaces in ArcGIS 10.2 to produce harvest yield maps for each paddock.

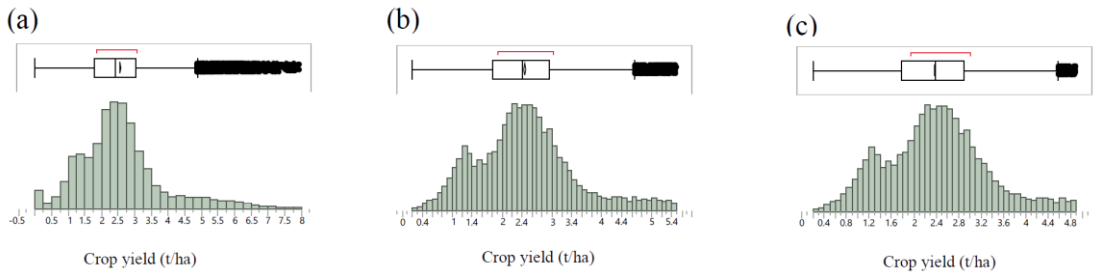


**FIGURE 6.1:** EFFECT OF TRIMMING YIELD DATA: HISTOGRAMS SHOW (A) RAW YIELD DATA FROM "MILROY" PADDOCK M25 IN 2009, (B) SAME DATA CONSTRAINED TO SENSIBLE THRESHOLDS BY REMOVING OBVIOUS NONSENSICAL VALUES, AND (C) DATA TRIMMED USING 2.5 S.D. ABOVE THE PADDOCK MEAN AND 1.5 S.D. BELOW THE PADDOCK MEAN AS THRESHOLDS.

### *6.2.3 MAPPING PASTURE GREEN HERBAGE MASS IN PASTURES*

Red and near-infrared (NIR) reflectance values for the calculation of vegetation indices were acquired using a Crop Circle™ ACS-210 active sensor (Holland Scientific Inc., Lincoln, NE, USA). The Crop Circle™ was chosen over the GreenSeeker® because the Crop Circle™ records individual signal values for red and NIR to a data logger, enabling the calculation of a range of vegetation indices based on red and NIR values. The GreenSeeker® provides values for NDVI only.

For mapping of pasture biomass, the Crop Circle™ sensor head was linked to a Trimble EZ-Guide 250 GPS Lightbar guidance system (Trimble, Sunnyvale, CA, USA) and a Holland Scientific GeoSCOUT 400 series data logger set to record geo-referenced red and NIR outputs at 1 Hz. The Crop Circle™ sensor head, data logger and Trimble lightbar were mounted on a Honda four-wheel motorbike at "Milroy" and on the front of a Toyota Hilux at "Grandview" (Figure 6.2). On both vehicles, the ACS-210 sensor was mounted so that its height was approximately 90 cm above the ground. At this height, the angular field of view of the device ($32^{o}$ x $6^{o}$) produced a beam footprint of ~56 cm long x 12 cm wide. All Crop Circle™ data was collected along transects spaced 40 m apart (Figure 6.3). The initial transect path for each paddock was recorded in the Trimble EZ-Guide 250 memory so that, when returning to a paddock, the transect paths could be repeated. Speed across the paddocks was approximately 10–15 km/hr. NDVI values from the transects were trimmed to remove NDVI values <0.1 and >0.9. Remaining points were then imported into ArcGIS 10.2 converted to UTM projection and mapped to a standard square 5 m x 5 m grid. The standard grid is required to enable data from different years and different sources to be analysed simultaneously. The grid was established in ArcGIS 10.2 using the Geospatial Modelling Environment platform (Spatial Ecology, http://www.spatialecology.com) and kept constant throughout the analysis. Data was interpolated to the grid using Vesper 1.62 software (Australian Centre for Precision Agriculture, The University of Sydney, NSW) (Whelan et al., 2001). Block kriging was used with an exponential variogram and a block size of 10 m x 10 m. General settings were as described in the Vesper 1.62 User Manual (Australian Centre for Precision Agriculture, The University of Sydney, NSW) (Whelan et al., 2001). The data were then mapped in ArcGIS 10.2 to produce raster surfaces of NDVI for each paddock (Figure 6.4). At "Milroy", Crop Circle™ scans of paddocks M25 and M41 were taken in July, August and September 2012 and in August/September 2013. At "Grandview", paddocks GV8 and GV39 were scanned in August and September 2012 and September 2013.

(a) (b)

**FIGURE 6.2:** CROP CIRCLE™ ACS-210 MOUNTED ON A QUAD BIKE AT "MILROY" (A) AND A TOYOTA HILUX AT "GRANDVIEW" (B) CONNECTED TO A GEOSCOUT 400 DATA LOGGER AND TRIMBLE EZ-GUIDE 250 LIGHTBAR GPS. THE SENSOR WAS MOUNTED SO THAT ITS HEIGHT WAS APPROXIMATELY 90 CM ABOVE THE GROUND.

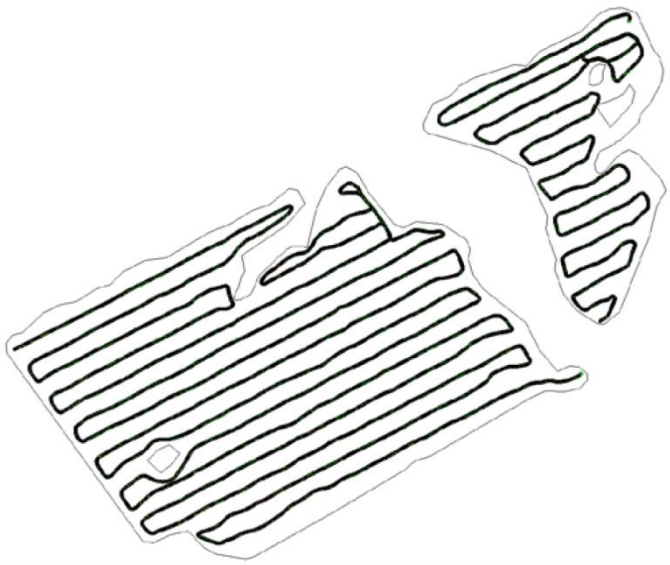

**FIGURE 6.3:** EXAMPLE OF 40 M TRANSECT PATHS FOR CROP CIRCLE™ SCANS IN PADDOCK M41 AT "MILROY".

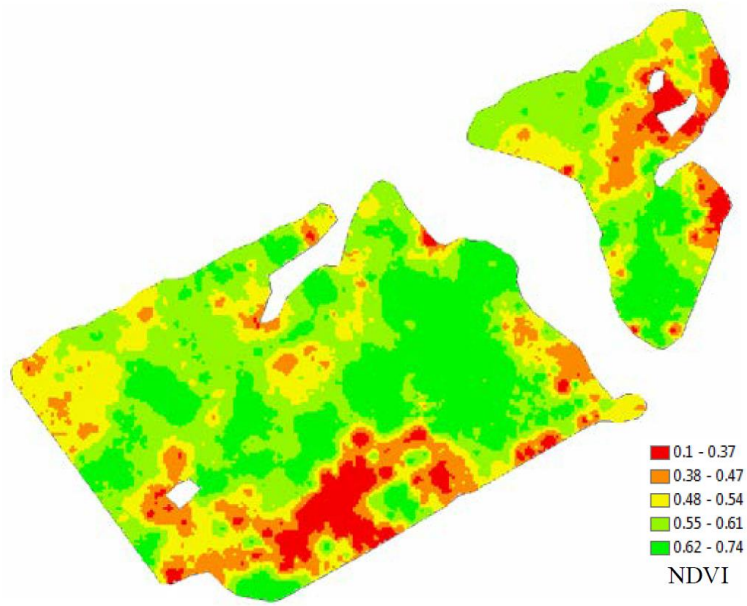


**FIGURE 6.4:** AN EXAMPLE OF AN INTERPOLATED NDVI SURFACE FOR "MILROY" PASTURE PADDOCK M41.

### *6.2.4 COLLECTION OF PASTURE SAMPLES FOR CALIBRATION OF VEGETATION INDEX*

To calibrate the NDVI scans to actual pasture biomass present in the paddock, pasture samples were taken across each paddock. For pasture recording and harvesting at calibration sites, a quadrat 56 cm long x 12 cm wide was constructed from 1 cm diameter metal rod to emulate the Crop Circle™'s footprint 90 cm above ground. The quadrat was painted flat black to minimise reflection.

Twenty-five random pasture samples were taken from each study paddock on both properties in 2012 and 2013. At "Milroy", paddocks M25 and M41 were scanned and sampled in early September 2012. In 2013, paddock M41 was scanned with the Crop Circle™ sensor and pasture samples taken in both August and September. M41 was grazed heavily before the August 2013 scan and calibration cuts. It was then left unstocked for five weeks to allow it to recover and then re-scanned, and further calibration cuts taken. The reason for doing this was to try to characterise pasture growth rate in that paddock without animal impact. Paddock M25 was in wheat in 2013 and was scanned and sampled in August 2013 before the crop became too advanced for travel across the paddock. At "Grandview", paddocks GV8 and GV39

were scanned with the Crop Circle™ sensor and pasture samples taken in early September 2012 and again in October 2013.

*Pasture calibration cuts*

Multivariate *k*-means clustering based on the Crop Circle™ NDVI values was used in JMP® 12.2 (SAS Institute Inc., Cary, NC), to randomly select 25 pasture sampling sites in each paddock. The NDVI point values from the pasture scans were divided into five clusters, and five points selected randomly from within each cluster, to give 25 sampling points for each paddock. These sites were then imported into ArcGIS 10.2 and mapped as geo-referenced points in the paddock (Figure 6.5).

To locate each sampling point for the calibration cuts, the selected pasture sites were imported into 'gpMapper' mapping software (Fairport Farm Software, Perth WA), loaded on a laptop computer and linked to the Trimble EZ-guide 250 GPS. At each sample point, Crop Circle™ was used in 'hand-held' configuration, with the sensor head at 90 cm above the ground surface and the 56 cm x 12 cm quadrat positioned so that it was within the Crop Circle™ footprint. The GeoScout 400 data logger was set to 'plot' mode. A minimum of 100 NDVI plot values were taken for each site, and the readings later averaged to arrive at a representative NDVI value. Each site was photographed, a dry-weight-rank (DWR) assessment (Jones and Hargreaves 1979) of pasture composition made and leaf area index assessed. Pasture within the quadrat was then harvested to ground level using battery powered Ryobi grass shears (Techtronic Industries Coy Ltd, Hong Kong, PRC). The cut pasture samples were placed in ziplock bags on-site and immediately refrigerated to minimise respiration losses. Samples were subsequently sorted into green and dead herbage mass fractions and legume/grass/herb to provide estimates of percentage green herbage mass. The pasture samples were oven-dried in paper bags at 80$^{o}$C for 48 hours and then weighed. Dry weights were converted from 'grams per quadrat' to 'kilograms per hectare' to provide total herbage mass in kilograms of green dry matter (TGDM) per hectare for each sample site.

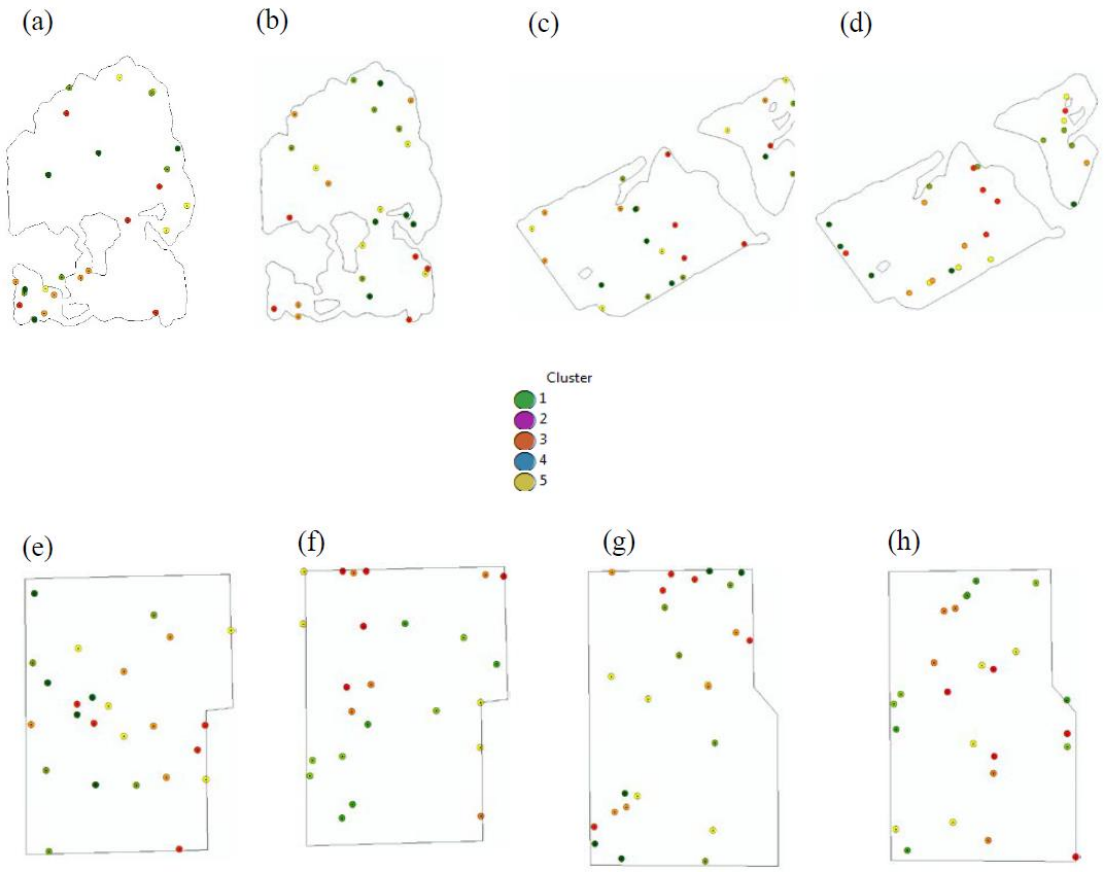


**FIGURE 6.5:** CROP CIRCLE™ PASTURE CALIBRATION SITE LOCATIONS AT "MILROY" AND "GRANDVIEW" IN 2012 AND 2013. (A) M25 2012, (B) M25 2013, (C) M41 2012, (D) M41 2013, (E) GV8 SEPTEMBER 2012, (F) GV8 OCTOBER 2013, (G) GV39 SEPTEMBER 2012 AND (H) GV39 OCTOBER 2013.

### *6.2.5 TESTING OF NDVI AGAINST SOME ALTERNATIVE VEGETATION INDICES*

To test the validity of using NDVI rather than an alternative vegetation index, the averaged red and NIR reflectance values acquired from Crop Circle™ for each pasture sample site were used to create four different spectral indices; (i) NDVI, (ii) the Soil-Adjusted Vegetation Index (SAVI), (iii) the Non-Linear Vegetation Index (NLI) and (iv) the Modified Non-Linear Vegetation Index (MNLI). The formula for each of these indices is in Table 6.3. Because of the small sample sizes involved (n=25), the datasets were validated using Leave One Out Cross Validation (LOOCV) in the R statistical package (v. 2.14.1–The R Foundation for Statistical Computing, Vienna, Austria). The script used to analyse the datasets is given in Appendix 15. The LOOCV

analysis provided root mean square error (RMSE) values for each of the indices tested. The index with the lowest RMSE for every set of calibration samples was the NDVI (Tables 6.4 and 6.5). NDVI was therefore used as the vegetation index to develop the pasture calibration equations for total green dry matter (TGDM).

### *6.2.6 CALCULATION OF TGDM CALIBRATION EQUATIONS*

The NDVI value taken at each pasture sampling cut site was regressed against the corresponding TGDM site value from the pasture sample cuts to produce a calibration equation for each paddock in each year of scanning. The calibration equations were then used to convert the geo-referenced NDVI values acquired from the Crop Circle™ pasture scans to geo-referenced TGDM values.

The TGDM values were then imported into ArcGIS 10.2 and interpolated to a 5 m x 5 m grid using Vesper 1.62 software (Australian Centre for Precision Agriculture, The University of Sydney, NSW) (Whelan et al., 2001). Raster surfaces of TGDM for each paddock were then produced in ArcGIS 10.2.

**TABLE 6.3:** VEGETATION INDICES TESTED FOR USE IN THE CROP CIRCLE™ PASTURE CALIBRATION ANALYSIS. RATHER THAN JUST USING THE NDVI, FOUR DIFFERENT VEGETATION INDICES WERE TESTED TO DETERMINE WHICH INDEX GAVE THE LOWEST ERROR OF PREDICTION.

| Index | Abbreviation | Formula | Reference |
|---|---|---|---|
| Normalised Difference Vegetation Index | NDVI | (NIR–Red)/(NIR+Red) | Rouse et al. (1973) |
| Soil-Adjusted Vegetation Index | SAVI | [(NIR–Red)/(NIR+Red+L)]x(1+L) | Huete (1988) |
| Non-Linear Vegetation Index | NLI | $(NIR^2–Red)/(NIR^2+Red)$ | Goel and Qin (1994) |
| Modified Non-Linear Vegetation Index | MNLI | $[(NIR^2–Red)x1.5]/[(NIR^2+Red)+1.5]$ | Gong et al. (2003) |

### *6.2.7 PASTURE SPECIES COMPOSITION ASSESSMENTS*

The TGDM maps derived from the NDVI scans show total biomass in a paddock. This is because NDVI simply shows greenness and cannot differentiate between a high-quality pasture and an actively photosynthesising patch of weeds—it will show both as green biomass and, therefore, both as equally 'edible' to livestock. It cannot be assumed that everything in a pasture is edible, so it is very important to ground-truth the NDVI-derived TGDM maps to identify just what is growing in the paddock. This was done using the DWR technique (Jones and Hargreaves, (1979).

Geo-referenced DWR sampling points were established across each paddock on 80 m transects using the Trimble EZ-Guide 250 Lightbar GPS mounted as previously described, with sample points between 100 m and 150 m apart (Figure 6.6). At each sample point, a minimum of ten DWR estimates was conducted, using a 0.1 $m^2$ quadrat thrown randomly around a 5 m radius such that ~500 quadrats were assessed across each paddock at each sampling time. Individual pasture species were grouped into either legume, grass or broadleaf classes.

The DWR procedure records the species that rank first, second and third in each quadrat according to their estimated contribution to pasture dry matter. The data were entered in a Microsoft Excel spreadsheet for analysis. Firstly, the rankings (first, second or third for each species) were multiplied by the constants 70.2, 21.1 and 8.7, respectively. These multipliers were derived by Jones and Hargreaves (1979) from a least-squares analysis of many sets of hand-sorted samples, using the constraint that the sum of the multipliers equals 100. The resulting figures were then added to give the percentage of each species expressed in terms of dry weight. Where required, tied ranks (e.g. where more than one species is ranked first) were used (Cayley and Bird 1996). The array and frequency functions of Excel were used to condense the data into a summary table of geo-referenced rankings.

The geo-referenced DWR data points were imported into ArcGIS 10.2 and interpolated to the 5 m x 5 m grid using Vesper 1.62 software (Australian Centre for Precision Agriculture, The University of Sydney, NSW). Raster surfaces of the three

main pasture components of each paddock (grass, legume, herb) were then produced in ArcGIS 10.2.

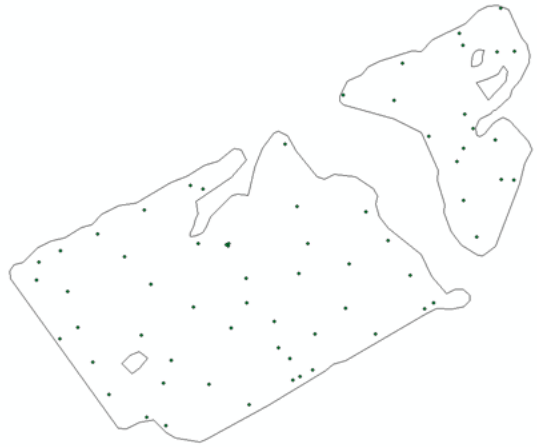

**FIGURE 6.6:** DRY-WEIGHT-RANK (DWR) SAMPLING LOCATIONS FOR "MILROY" PADDOCK M41 IN SEPTEMBER 2012. AT EACH POINT, A MINIMUM OF TEN ESTIMATES OF PASTURE COMPOSITION WAS MADE USING THE DWR TECHNIQUE, AS MODIFIED BY JONES AND HARGREAVES (1979), USING A 0.1 $M^2$ QUADRAT. THE DWR ESTIMATES CONDUCTED AT THE 25 PASTURE CALIBRATION SITES (FIGURE 6.5) WERE ALSO INCLUDED.

### *6.2.8 ESTABLISHING SUB-PADDOCK MANAGEMENT CLASSES*

A multivariate *k*-means clustering analysis was carried out using JMP® 12.2 on selected data layers (crop yield, pasture dry matter yield, elevation and ECa) to assess and partition the within-paddock variability in both crop yield and pasture dry matter production. Although the use of *k*-means clustering is a common methodology for identifying potential yield zones in cropping situations (Cupitt and Whelan, 2001; Florin et al., 2009; Taylor et al., 2007; Whelan and McBratney, 2003), there is no reference in the literature to using this approach to analyse and identify potential management classes for site-specific management across the combined cropping and pasture phases of mixed farming systems.

The datasets used had previously been mapped onto a common 5 m grid via block kriging with local variograms using VESPER 1.62 (Australian Centre for Precision Agriculture, The University of Sydney, NSW) (Whelan et al., 2001). The *k*-means

analysis was configured to produce solutions for two, three and four clusters. This number of clusters was considered to encompass a range of management classes that would be acceptable to farm managers in terms of practical differential zonal management.

To verify whether differences between potential management classes derived from the *k*-means clustering were genuine and significant, a confidence interval (CI) approach was used, as described by Cupitt and Whelan (2001) and modified by Taylor et al. (2007).

For two management classes to statistically differ,

$$|\bar{Y}_{classA} - \bar{Y}_{classB}| \geq \left(\tilde{\sigma}_{krig} \times 1.96\right) \text{ x } 2 \qquad \text{(Taylor et al., 2007)}$$

where $\bar{Y}_{\text{ClassA}}$ is the mean of Class A, $\bar{Y}_{\text{ClassB}}$ is the mean of Class B, and $\tilde{\sigma}^2_{krig}$ is the median kriging variance.

The point of this statistic is to establish whether the difference in mean crop and pasture yield values from the *k*-means clustering process is significantly greater than the error associated with the spatial prediction of the yield data. If this is the case, then there is a reasonable degree of confidence that the class means from the clustering process are not equal.

*"Milroy" paddocks M25 and M41*

The data layers used were the crop yield monitor data for 2004 and 2009 for M25 (both wheat) and 2009 and 2014 for M41 (both wheat) growing seasons together with TGDM for September 2012 and August 2013 and the soil electrical conductivity and elevation data described in Chapter 5.

*"Grandview" paddocks GV8 and GV39*

The same process was carried out on the "Grandview" data. For paddock GV8, crop yield data was available for 2005 (wheat), 2007 (canola) and 2009 (wheat). For paddock GV39, crop yield data was available for 2007 (canola), 2008 (wheat) and 2009 (wheat). Total green pasture dry matter was available for 2012 and 2013 with the soil electrical conductivity and elevation data described in Chapter 5.

To identify any influence on zone partitioning from including TGDM variation, clustering was firstly carried out in JMP using the crop yield data only with ECa and elevation and then repeated using both crop yield data and the pasture TGDM with ECa and elevation.

## 6.3 RESULTS

The results shown here are for "Milroy" paddocks M25 and M41 and "Grandview" paddocks GV8 and GV39. These were the paddocks for which pasture green dry matter data was available in both 2012 and 2013. The results for the other paddocks are contained within Appendices 12–14, 17 and 18 but will not be described further in the results.

### *6.3.1 CROP YIELD MAPS*

*"Milroy"*

The yield maps for paddock M25 (Figure 6.7 a and b) show similar spatial variation in yield, despite being five years apart and having different growing season rainfall (GSR), 264 mm (2004) and 328 mm (2009) (Table 6.2). The patterns of spatial variation in paddock M41 (Figure 6.7 c and d) for 2009 and 2014 are also similar.

*"Grandview"*

Figure 6.8 a–c shows crop harvest yield maps for paddock GV8 in 2005 (canola), 2007 (wheat) and 2009 (wheat). In 2005, the GSR of 334 mm was close to the mean, but 2007 (190 mm) and 2009 (245 mm) were well below. The 2005 map for GV8 shows less variation across the paddock, suggesting that there was sufficient rainfall for all parts of the paddock to perform well.

From 2006 to 2008, annual rainfall was in the lowest 10–20% of years recorded at "Grandview" and GSR was well below average. The 2006 year only had 217 mm total annual rainfall, so little residual moisture was available for the 2007 season. For paddock GV39, the yield maps for 2007–2009 are shown in Figure 6.8 d–f. The effect of the drought on crop yields can be clearly seen in Figure 6.8 d and e. A higher proportion of the paddock yielded poorly, although some areas still recorded reasonable yields of around 4 t/ha.

As was the case in paddock GV8, the more elevated part of GV39 (south-east corner) (Chapter 5, Figure 5.14 d) yielded better in the very dry years. Nonetheless, yield variation within paddocks is apparent, even during the drought years. When GSR was closer to the mean (2009), the lower parts of the paddock also yielded well (Figure 6.8 f).

### *6.3.2 CROP CIRCLE™ NDVI SCANS*

Figures 6.9 and 6.10 show the maps of spatial variation in NDVI reflectance from Crop Circle™ scans of pasture for "Milroy" paddocks M25 and M41 and "Grandview" paddocks GV8 and GV39, respectively.

*"Milroy"*

Figure 6.9 a–c shows the NDVI maps for paddock M25 for August 2012, September 2012 and August 2013. This is late winter–early spring and pasture is limited and growth rates slow. Sites 2, 3 and 4 have the highest NDVI values across all scans. The NDVI maps for "Milroy" paddock M41 are in Figure 6.9 d–g. The impact of grazing on pasture growth (and therefore NDVI) can be seen between maps (f) and (g), reflecting the heavy grazing just prior to the August 2013 scan. Map (g) shows the response of pasture growth in the paddock to rainfall, aspect and soil types, without the added factor of animal impact. The "Milroy" paddock M25 image from Pasture Watch™ for September 2012 (Figure 6.11) demonstrates the relative lack of detail provided by the large MODIS pixels in comparison to the high resolution of the Crop Circle™ scans.

*"Grandview"*

For "Grandview", GSR was below the long-term mean of 359 mm in both years, with 218 mm received in 2012 and 254 mm in 2013. The scans in 2013 were conducted in October in a season with a particularly low annual rainfall of 394 mm, with annual pastures beginning to senesce, compared to the 2012 scans which occurred in the cooler months of August and September in a year of above average annual rainfall (658 mm).

The productivity of the more elevated parts of paddock GV8 is evident again in Figure 6.10 a and b. The NDVI scans for GV39 in 2012 (Figure 6.10 d and e) showed

higher reflectance values in the more elevated parts of the paddock. The area of medium NDVI reflectance increased between August and September 2012.

### *6.3.3 PREDICTION OF PASTURE DRY MATTER FROM NDVI SCANS*

*Comparison of the performance of TGDM prediction by selected vegetation indices using LOOCV*

Tables 6.4 and 6.5 show the performance of selected vegetation indices in predicting TGDM on the pasture calibration datasets for "Milroy" paddocks M25 and M41 and "Grandview" paddocks GV8 and GV39, respectively.

For all paddocks, NDVI had the lowest RMSE of prediction (kg TGDM/ha) and was therefore chosen as the most appropriate to use for the NDVI to TGDM calibration process.

*Correlation between Crop Circle™ NDVI and pasture biomass (TGDM)*

Figures 6.12 ("Milroy") and 6.13 ("Grandview") show the regression of the Crop Circle™ NDVI scan values at each of the 25 pasture harvesting sites in each paddock against the actual TGDM harvested at each site for 2012 and 2013.

In all cases, a non-linear relationship best represented the capacity of NDVI to predict TGDM, with $R^2$ values ranging from 0.66 to 0.88 at "Milroy" and 0.76 to 0.84 at "Grandview". The regression curves for Milroy M45 and Grandview GV3 and 4 are at Appendix 16.

### *6.3.4 PASTURE BIOMASS 'YIELD' MAPS*

Figures 6.14 and 6.15 show the predicted pasture TGDM 'yield' maps for "Milroy" paddocks M25 and M41 and "Grandview" paddocks GV8 and GV39, respectively. These maps were created by applying the prediction equations from Figures 6.12 and 6.13 to the Crop Circle™ NDVI scan values at each sampling time for each paddock.

Variability of TGDM in each paddock was also characterised with histograms showing the distribution of TGDM and related descriptive statistics in each year. The histograms for "Milroy" and "Grandview" are in Figures 6.16 and 6.17, respectively.

*"Milroy"*

Paddock M25 had low levels of TGDM when scanned, except the northern area around site 2 (Figure 6.14 a and b) which showed the highest amount of TGDM in the paddock. Site 2 comprised mostly subterranean clover (*Trifolium subterraneum* L.) with some barley grass (*Hordeum glaucum* L.) (Figure 6.19).

Site 1 was an area of very low TGDM. Site 4 had some areas of low–moderate TGDM (Figure 6.14 a and b). A significant part of M25 was covered in capeweed (*Arctotheca calendula* L.) and storksbill (*Erodium* spp.) in September 2012 (Figure 6.18). Both plants have a prostrate growing habit, producing a relatively high NDVI value when green and actively growing but, like succulents, produce little dry matter.

An NDVI scan of the paddock can, therefore, show relatively high NDVI values where capeweed or storksbill are present, but a TGDM map of the same area shows low levels of dry matter, which is reflected in the TGDM map for September 2012. The histogram of TGDM distribution for this paddock in September 2012 (Figure 6.16 a) shows a mean TGDM of 1116 kg/ha, which is very close the recommended minimum residual pasture mass of 1000–1200 dry matter kg/ha in spring for lactating ewes (http://www.lifetimewool.com.au/Sheep%20Zones/zonecerealsheepwa.aspx). The distribution is positively skewed, showing that the paddock has little available feed, with 75% of TGDM present below 1286 kg/ha (and 90% below 1600 kg/ha). Figure 6.14 a shows available feed mostly in the area around site 2.

Paddock M41 in September 2012 (Figure 6.14 c) and September 2013 (Figure 6.14 e) had a similar pattern in the spatial variation of TGDM distribution across both years. The south-eastern area of the paddock, including around site 1 (Figure 6.14 c–e) shows low TGDM. The pasture here was dominated by capeweed, with small amounts of subterranean clover (Figure 6.20 b). The area around site 3 had very low TGDM, with only sparse vegetation (Figure 6.22). The remainder of the paddock, including around sites 2 and 4, was dominated by subterranean clover, with some annual ryegrass (*Lolium rigidum* L.) and capeweed (Figure 6.21 a and b).

The TDGM histogram for September 2012 (Figure 6.16 b) shows a mean TGDM of 819 kg/ha, which is close to the recommended spring minimum residual pasture green dry matter for sheep grazing pastures (1000–1200 kg DM/ha; Lifetime Wool, 2006). With 100% of TGDM below 1072 kg/ha, animals would have been using all available feed in the paddock. This is reflected in the map of spatial variation in TGDM at Figure 6.14 c.

The histogram for September 2013 (Figure 6.16 c) is negatively skewed, but around a mean of 1667 kg/ha TGDM, which indicates that the paddock has been lightly stocked. The paddock had been spelled for six weeks after intense grazing in August, with 75% of pasture green dry matter above 1400 kg/ha and with a maximum of 2260 kg/ha. There is also a much higher frequency of low-yielding areas in 2013 compared to 2012 as indicated by the thicker tail to the left of the distribution curve. The absence of any stock has led to a significant increase in pasture green dry matter, and the spatial pattern of growth (Figure 6.14 e) is similar to that in September 2012. In the absence of any grazing by livestock, pasture growth is largely dictated by moisture and spatial variation in soil texture and chemistry.

*"Grandview"*

Maps showing the spatial variation in TGDM for paddocks GV8 and GV39 are in Figure 6.15. The generally better TGDM yields occurred in areas of higher elevation (Chapter 5, Figure 5.14 c and d) in both paddocks in 2012. Flooding rainfall preceded the 2012 growing season, with nearly 350 mm recorded from late February to early March. However, "Grandview" then received only 218 mm GSR, which was below average. GSR in 2013 was a little closer to the long-term mean at 254 mm, but the June–September cumulative rainfall was also higher in 2013 (184 mm) than 2012 (122 mm).

For "Grandview" paddock GV8, the histogram for September 2012 (Figure 6.17 a) shows a mean TGDM of 953 kg/ha, with 90% of TGDM below 1242 kg/ha, which is close the recommended minimum residual pasture green dry matter for cattle grazing pasture (1500 kg green DM/ha; http://mbfp.mla.com.au/pasture-

utilisation). The distribution is close to a normal curve, with higher kurtosis. The map of TGDM in Figure 6.15 a shows most of the paddock in the 557–1194 kg/ha TGDM range. In October 2013, the mean TGDM for paddock GV8 was 1900 kg/ha, with 90% above 1600 kg/ha. The map for October 2013 (Figure 6.15 b) has a much higher proportion of the paddock classified as high TGDM, in the 1841–2557 kg/ha range. The differences in TGDM present between the 2012 and 2013 seasons at pasture sampling sites 1 to 4 for paddock GV8 is reflected in the photographs in Figure 6.23 a–g.

The histogram for "Grandview" paddock GV39 in September 2012 (Figure 6.17 c) shows TGDM to be fairly normally distributed around a mean of 1113 kg/ha with 75% of TGDM below 1300 kg/ha. The spatial distribution map in Figure 6.14 c shows most biomass in the 685–1399 kg/ha range. The histogram of TGDM for October 2013 shows a higher mean TGDM of 1574 kg/ha, with 75% above 1362 kg/ha. The histogram has a slight negative skew. The differences in TGDM present between the 2012 and 2013 seasons at pasture sampling sites 1 and 2 for paddock GV39 is reflected in the photographs in Figure 6.24 a–d.

### *6.3.5 DRY-WEIGHT-RANK (DWR) PASTURE SPECIES ASSESSMENTS*

Figures 6.25 and 6.26 show the DWR of pasture composition for "Milroy" paddocks M25 and M41, respectively. The assessments show pasture composition categorised into legume, grass and broadleaf species by percentage. Assessments were conducted in M25 for 2012 only and in paddock M41 in 2012 and 2013. Figure 6.25 b shows that paddock M25 was heavily dominated by broadleaf weeds (*Arctotheca calendula* L. and *Erodium* spp.) and, according to the farm owner, was the principal reason for the paddock being returned to crop in 2013. The only significant area of better quality pasture (subterranean clover/ryegrass) was around site 2.

Grasses were mainly confined to the gravel-dominated margins of the paddock. Figures 6.18 and 6.19 are photographs of the areas around sites 4 and 2, respectively, illustrating the differences in pasture composition. Figures 6.20–6.22 are photographs in paddock M41 of the areas around sites 1, sites 2 and 4, and site 3, respectively, illustrating the differences in pasture composition. The paddock

maintained a high legume content in both years, particularly around sites 2 and 4 (Figure 6.21 a and b).

The lowest elevation portion of the paddock (south-west boundary including site 1) was dominated by broadleaf weeds (*Arctotheca calendula* L. and *Erodium* spp.) in both years (Figure 6.20 c and d). The area around site 3 predominantly hosted weeds, with some legume present along the drainage line and rise to the east (Figure 6.22 a and b).

At "Grandview", legume pastures (particularly lucerne) dominated in the more elevated, coarser-textured soils in both paddocks (sites 2 and 3 in GV8 and site 1 in GV39). Barley grass tended to dominate in areas that were more heavily wooded (site 4 in GV8 and site 2 in GV39 and sites marked 'T' in both paddocks).

### *6.3.6 ESTABLISHING SUB-PADDOCK MANAGEMENT CLASSES USING K-MEANS CLUSTERING*

*"Milroy"*

Potential management zones are depicted in Figures 6.28 (paddock M25) and 6.29 (paddock M41). For both paddocks, maps a, c and e, show zones derived with crop yield data only and maps b, d and f show zones with both crop yield and pasture TGDM included.

The clustering maps clearly show that there is little difference in the resulting spatial patterns when the pasture data is included in the analysis. Tables 6.6 (crop data only) and 6.7 (crop and pasture data) show the cluster means, the median $\sigma_{krig}$ and the CI statistic (Equation 1, p. 175) for each variable for paddock M25. Tables 6.8 and 6.9 show this same data for paddock M41.

The management class (zone) maps at Figures 6.28 and 6.29 and information contained in Tables 6.6–6.9 were used to determine the optimum number of management classes in the paddock. In the case of M25, the two-management class output produced a significant result for both years. The three-management-class output produced significant results for two of the three classes for both years. So a two- or three-class solution is possible, largely depending on the preference of the farm owner. For M41, the analysis also showed a significant difference between the

class means for two classes. When three or four zones were considered, there were some non-significant differences between class means. That is, the possibility that the variability in the mapping and zoning procedures could incorrectly describe the spatial patterns cannot be discounted. Therefore, for M41, the analysis showed that a two-class solution may be optimal.

For both "Milroy" paddocks, the two-class solution split the ECa values into a high conductivity zone and a low conductivity zone (Tables 6.7 and 6.9). The three-class solutions for both paddocks created a third class by splitting the low conductivity zone in two, with the lowest conductivity zone having higher mean yields for crop and TGDM than the higher of the low conductivity zones. The two-class solution for "Milroy" M25 partitioned the capeweed and clover/barley grass into separate management classes.

The three-class solution for "Milroy" M41 again split the low conductivity values into two zones that partition the less fertile, deep sands and gravel soils into one class (zone of lowest conductivity), the sandy loam areas (marginally higher conductivity) into a second class and the saline area into a third, high conductivity zone. It also largely partitioned the legume/broadleaf/grass distribution in accordance with the results of the DWR surveys.

*"Grandview"*

Potential management classes produced by the *k*-means clustering are depicted in Figures 6.30 (paddock GV8) and 6.31 (paddock GV39). As with the "Milroy" analysis, the *k*-means clustering Figures 6.30 and 6.31 a, c and e show the results from using crop yield data alone and Figures 6.30 and 6.31 b, d and f show the results for both crop yield and pasture TGDM included. For paddock GV8, a two-class solution is optimal based on the confidence interval analysis (Tables 6.10 and 6.11). Class 'A' comprised the higher yielding areas, Class 'B' the lower. For GV39, a two-class solution is the only outcome which had significantly different means across all crop and TGDM values. The three-class solutions for both paddocks GV8 and GV39 split the ECa values into three distinct zones—low conductivity, medium conductivity and high conductivity (Tables 6.12 and 6.13).

The standard deviations for the clusters for "Milroy" and "Grandview" (Tables 6.14 and 6.15, respectively) also show the effects of partitioning into classes, with a reduction in the variability of crop yields within classes compared to whole-paddock management (single class). This is generally the case with TGDM, except for "Milroy" M25 where both two- and three-class solutions showed increased variability on the more productive soil in the northern tip of the paddock, which was a mix of subterranean clover and barley grass. On both properties, the clustering process also split the classes on ECa values.

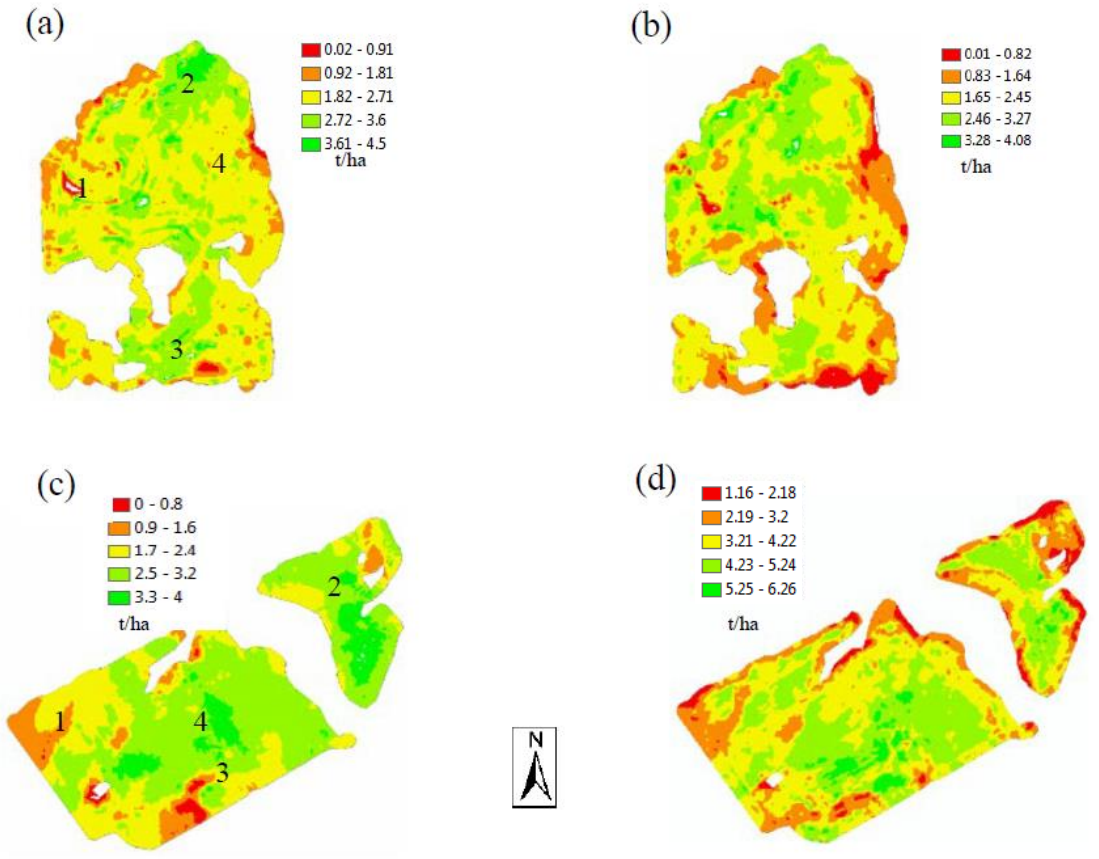


**FIGURE 6.7:** GRAIN YIELD MAPS DERIVED FROM YIELD MONITOR DATA FOR "MILROY" PADDOCK M25 IN (A) 2004 (WHEAT) AND (B) 2009 (WHEAT), AND PADDOCK M41 IN (C) 2009 (WHEAT) AND (D) 2014 (WHEAT). YIELDS SHOWN ARE IN T/HA.

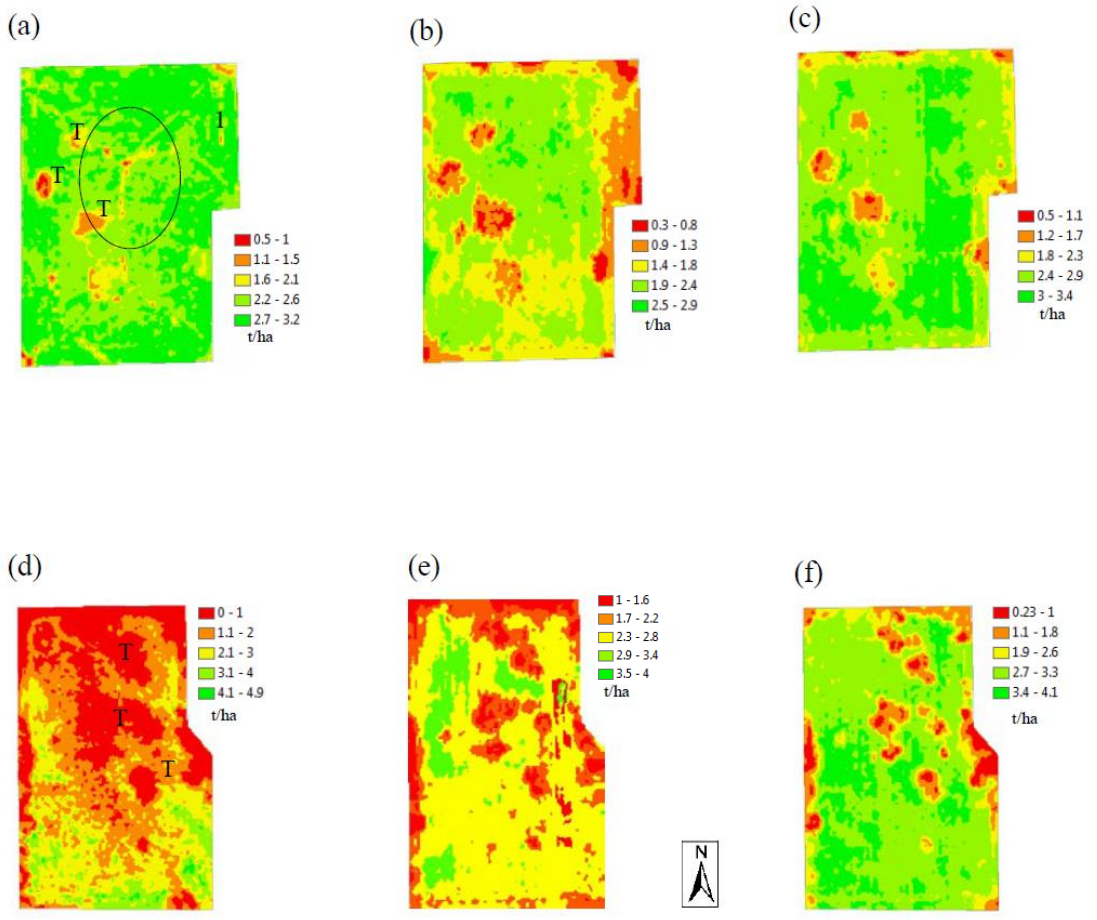


**FIGURE 6.8:** GRAIN YIELD MAPS DERIVED FROM YIELD MONITOR DATA FOR "GRANDVIEW" PADDOCKS GV8 IN (A) 2005 (CANOLA), (B) 2007 (WHEAT) AND (C) 2009 (WHEAT), AND GV39 IN (D) 2007 (CANOLA), (E) 2008 (WHEAT) AND (F) 2009 (WHEAT). YIELDS SHOWN ARE IN T/HA. THE SITES MARKED 'T' ON MAPS (A) AND (D) CONTAIN MANY TREES AND ARE THE CAUSE OF LOW YIELDS IN THESE AREAS. THE AREA CIRCLED IN (A) IS AN AREA OF HIGHER ELEVATION WITH COARSER-TEXTURED STONY SOILS.

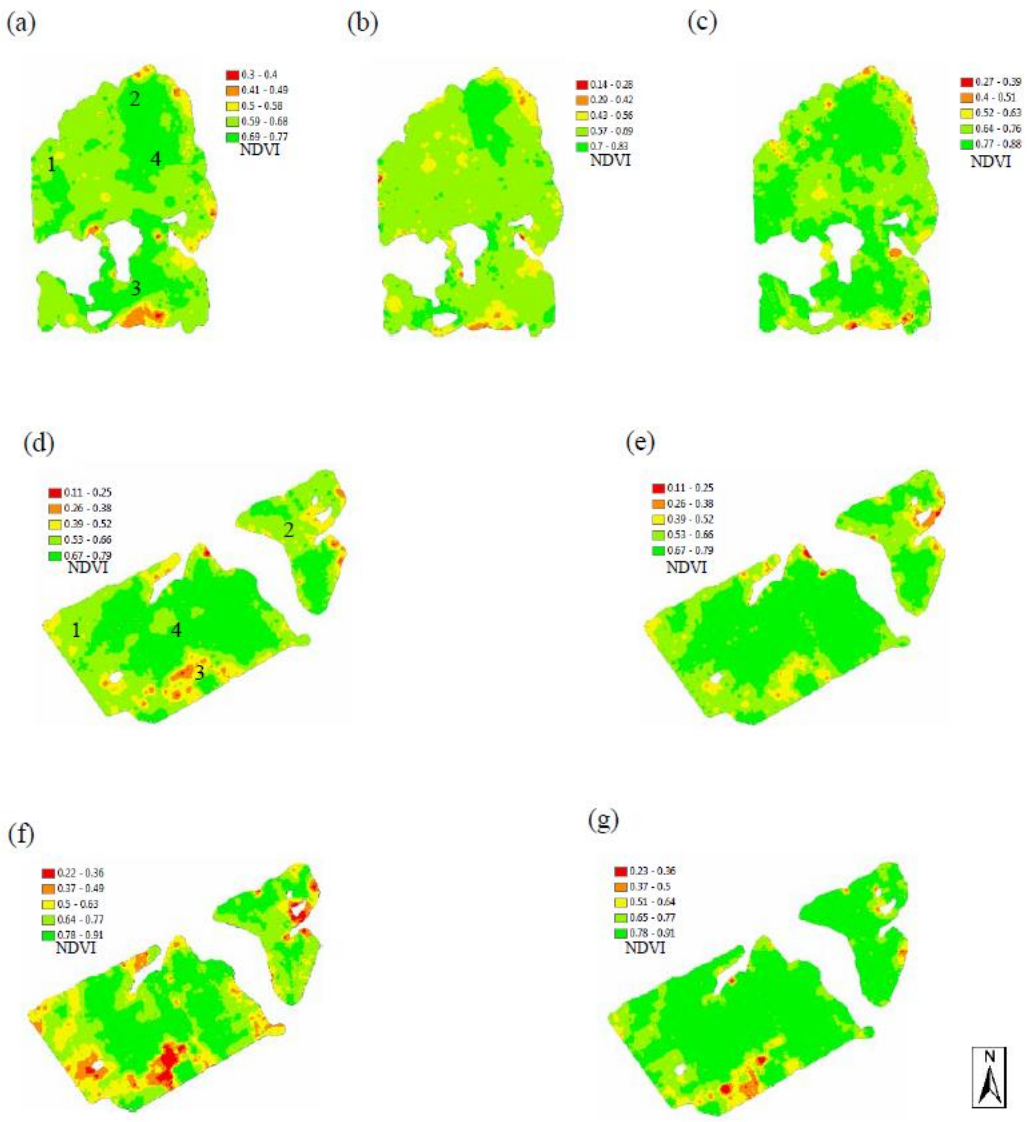


**FIGURE 6.9:** MAPS OF CROP CIRCLE™ NDVI SCANS FOR "MILROY" PADDOCKS M25 AND M41 CONDUCTED IN 2012 AND 2013. (A) M25 AUGUST 2012, (B) M25 SEPTEMBER 2012, (C) M25 AUGUST 2013, (D) M41 AUGUST 2012, (E) M41 SEPTEMBER 2012, (F) M41 AUGUST 2013 AND (G) SEPTEMBER 2013. PADDOCK M41 WAS GRAZED HEAVILY BEFORE THE AUGUST 2013 SCAN AND LEFT UNSTOCKED UNTIL AFTER THE SEPTEMBER 2013 SCAN. BOTH PADDOCKS WERE IN ANNUAL PASTURE, EXCEPT M25 WHICH WAS IN WHEAT IN 2013.

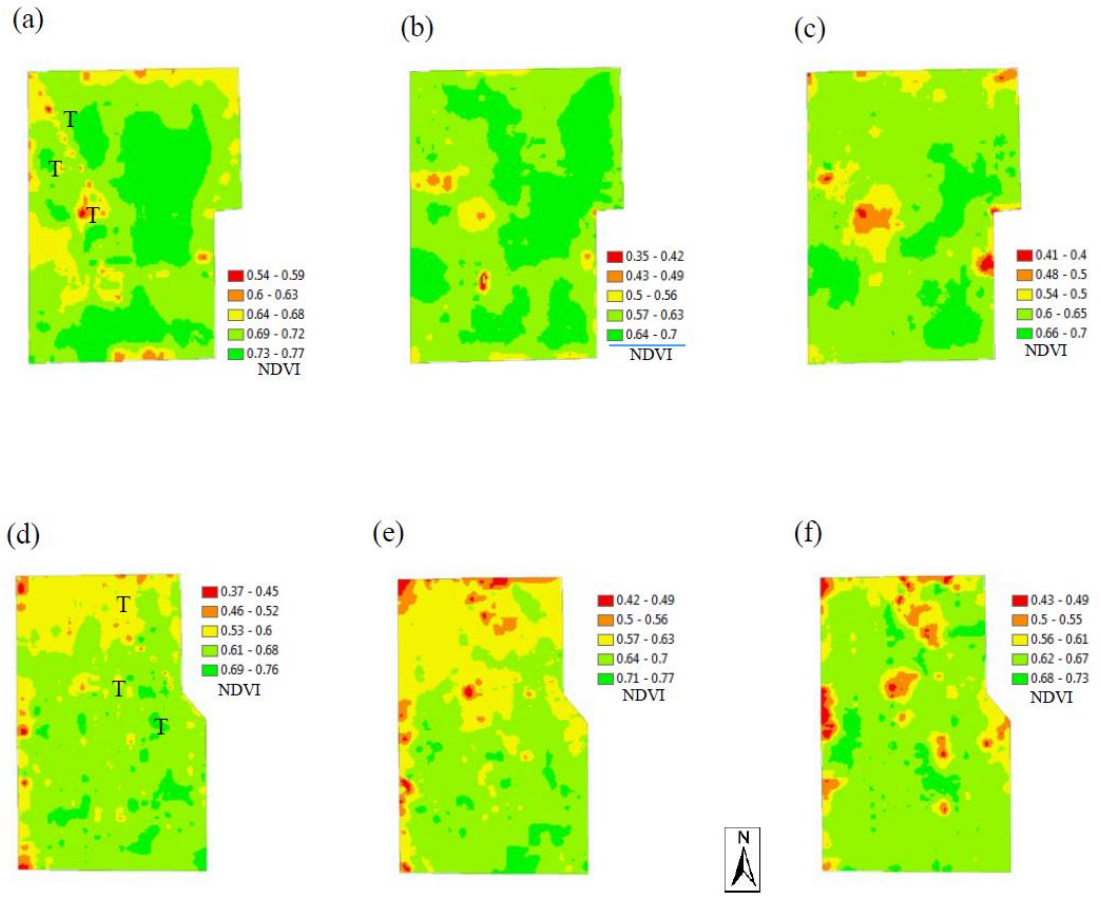


**FIGURE 6.10:** MAPS OF CROP CIRCLE™ NDVI SCANS FOR "GRANDVIEW" PADDOCKS GV8 AND GV39 CONDUCTED IN 2012 AND 2013. (A) GV8 AUGUST 2012, (B) GV8 SEPTEMBER 2012, (C) GV8 OCTOBER 2013, (D) GV39 AUGUST 2012, (E) GV39 SEPTEMBER 2012, (F) GV39 OCTOBER 2013. BOTH PADDOCKS WERE IN PERENNIAL PASTURE. THE SITES MARKED 'T' ON MAPS (A) AND (D) CONTAIN WOODED AREAS.

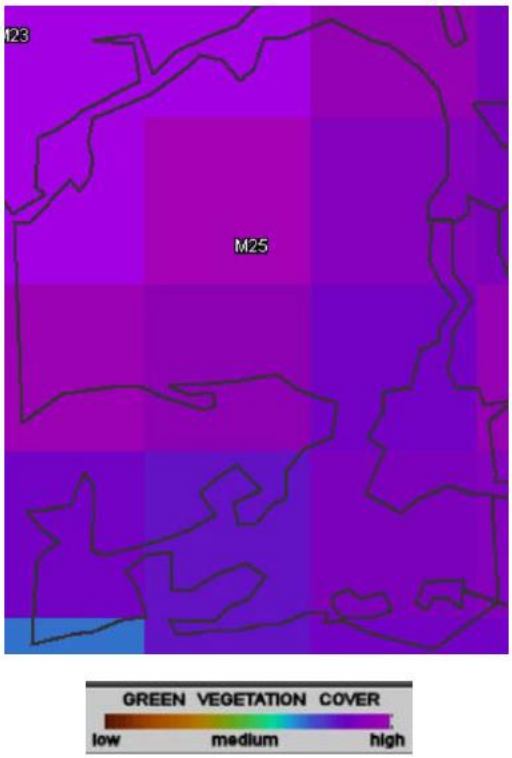


**FIGURE 6.11:** IMAGE OF "MILROY" PADDOCK M25 FROM PASTURE WATCH™ FOR SEPTEMBER 2012. PASTURE WATCH™ USES MODIS NDVI.

**TABLE 6.4:** PERFORMANCE OF SELECTED VEGETATION INDICES TO PREDICT TOTAL GREEN DRY MATTER ON THE CALIBRATION DATASETS FOR "MILROY" PADDOCKS M25 AND M41 USING LEAVE ONE OUT CROSS VALIDATION WITH A VALIDATION SET OF 25. ROOT MEAN SQUARE ERROR (RMSE) OF PREDICTION (KG TGDM/HA) IS SHOWN FOR EACH INDEX. ON THE BASIS OF THESE RESULTS, NDVI WAS CHOSEN AS THE MOST APPROPRIATE INDEX AS IT CONSISTENTLY GAVE THE LOWEST RMSE.

| | September 2012 | | | | August 2013 | | | | September 2013 | | | |
|---|---|---|---|---|---|---|---|---|---|---|---|---|
| **Paddock** | **NDVI** | **SAVI** | **NLI** | **MNLI** | **NDVI** | **SAVI** | **NLI** | **MNLI** | **NDVI** | **SAVI** | **NLI** | **MNLI** |
| M25 | 338.75 | 337.66 | 360.92 | 390.68 | 1158.51 | 1157.69 | 1280.44 | 1184.14 | | | | |
| M41 | 197.31 | 209.25 | 199.35 | 203.08 | 157.65 | 173.47 | 196.57 | 186.39 | 420.58 | 443.80 | 441.47 | 452.62 |

Note: Paddock M25 was sown to wheat in 2013 and therefore not used for calibration in that year. The scans were taken while the wheat crop was in early growth stage. In 2013, paddock M41 was grazed heavily until August, then destocked, scanned, and allowed to recover for five weeks before re-scanning. NDVI = normalised difference vegetation index, SAVI = soil-adjusted vegetation index, NLI = non-linear vegetation index, MNLI = modified non-linear vegetation index.

**TABLE 6.5:** PERFORMANCE OF SELECTED VEGETATION INDICES TO PREDICT TOTAL GREEN DRY MATTER ON THE CALIBRATION DATASETS FOR "GRANDVIEW" PADDOCKS GV8 AND GV39 USING LEAVE ONE OUT CROSS VALIDATION WITH A VALIDATION SET OF 25. ROOT MEAN SQUARE ERROR (RMSE) OF PREDICTION (KG TGDM/HA) IS SHOWN FOR EACH INDEX. ON THE BASIS OF THESE RESULTS, NDVI WAS CHOSEN AS THE MOST APPROPRIATE INDEX AS IT CONSISTENTLY GAVE THE LOWEST RMSE.

| | September 2012 | | | | October 2013 | | | |
|---|---|---|---|---|---|---|---|---|
| **Paddock** | **NDVI** | **SAVI** | **NLI** | **MNLI** | **NDVI** | **SAVI** | **NLI** | **MNLI** |
| GV8 | 217.60 | 222.65 | 223.87 | 239.20 | 490.21 | 492.29 | 536.84 | 604.16 |
| GV39 | 449.64 | 691.20 | 625.84 | 698.85 | 533.51 | 813.67 | 614.16 | 774.81 |

NDVI = normalised difference vegetation index, SAVI = soil-adjusted vegetation index, NLI = non-linear vegetation index, MNLI = modified non-linear vegetation index.

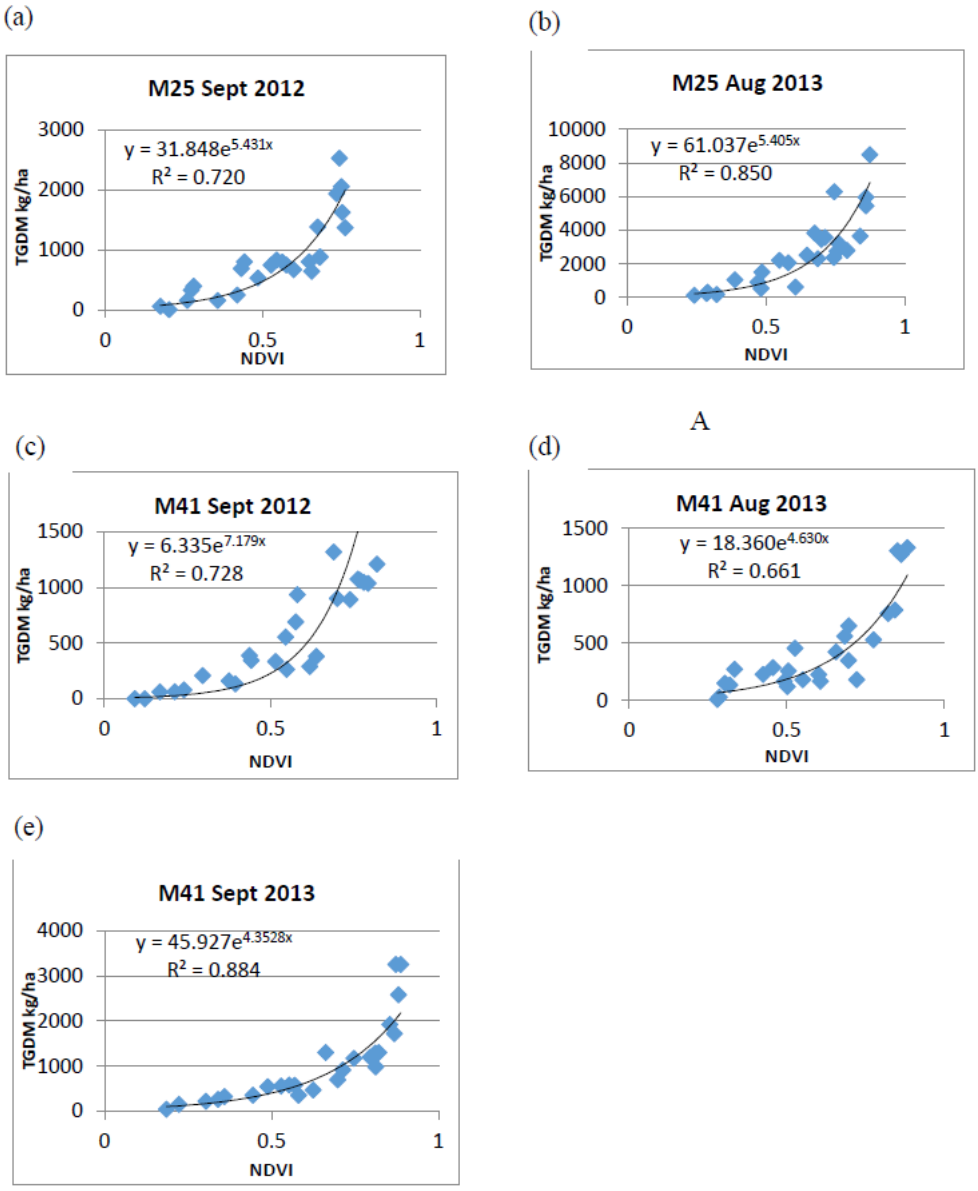


**FIGURE 6.12:** REGRESSION OF CROP CIRCLE NORMALISED DIFFERENCE VEGETATION INDEX (NDVI) VALUES AGAINST TOTAL GREEN DRY MATTER (TGDM) DETERMINED BY DIRECT HARVESTING FOR "MILROY" FIELDS M25 IN SEPTEMBER 2012 AND AUGUST 2013, AND M41 IN SEPTEMBER 2012, AUGUST 2013 AND SEPTEMBER 2013. IN 2013, FIELD M41 WAS GRAZED HEAVILY UNTIL AUGUST, THEN DESTOCKED, SCANNED, AND ALLOWED TO RECOVER FOR FIVE WEEKS BEFORE RE-SCANNING IN SEPTEMBER 2013. THE $R^2$ VALUES FOR EACH CURVE INDICATE A STRONG RELATIONSHIP BETWEEN NDVI AND TGDM, PARTICULARLY FOR NDVI VALUES BETWEEN 0.3 AND 0.7.

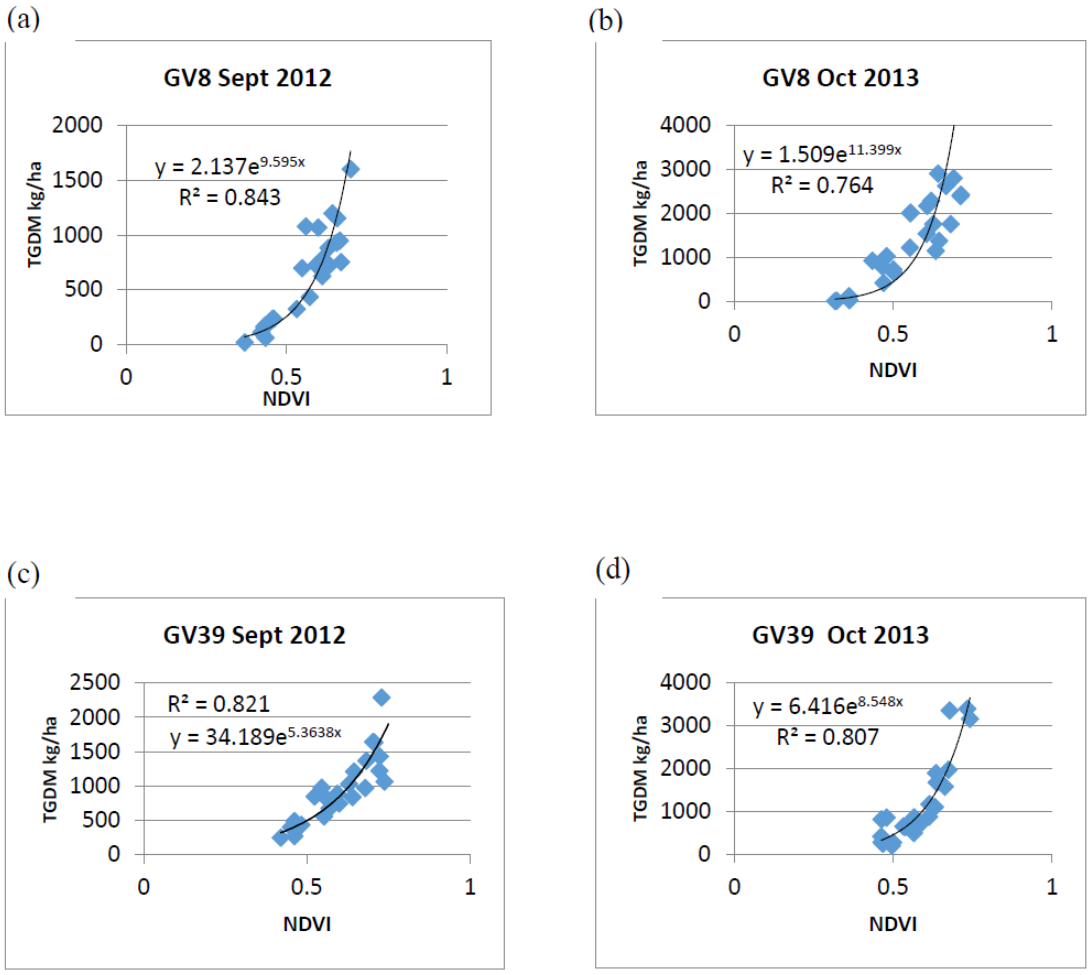


**FIGURE 6.13:** REGRESSION OF CROP CIRCLE NORMALISED DIFFERENCE VEGETATION INDEX (NDVI) VALUES AGAINST TOTAL GREEN DRY MATTER (TGDM) DETERMINED BY DIRECT HARVESTING IN "GRANDVIEW" FIELDS GV8 (A, C) AND GV39 (B, D) IN SEPTEMBER 2012 AND OCTOBER 2013, RESPECTIVELY. THE $R^2$ VALUES FOR EACH CURVE INDICATE A STRONG RELATIONSHIP BETWEEN NDVI AND TGDM, PARTICULARLY FOR NDVI VALUES BETWEEN 0.4 AND 0.7.

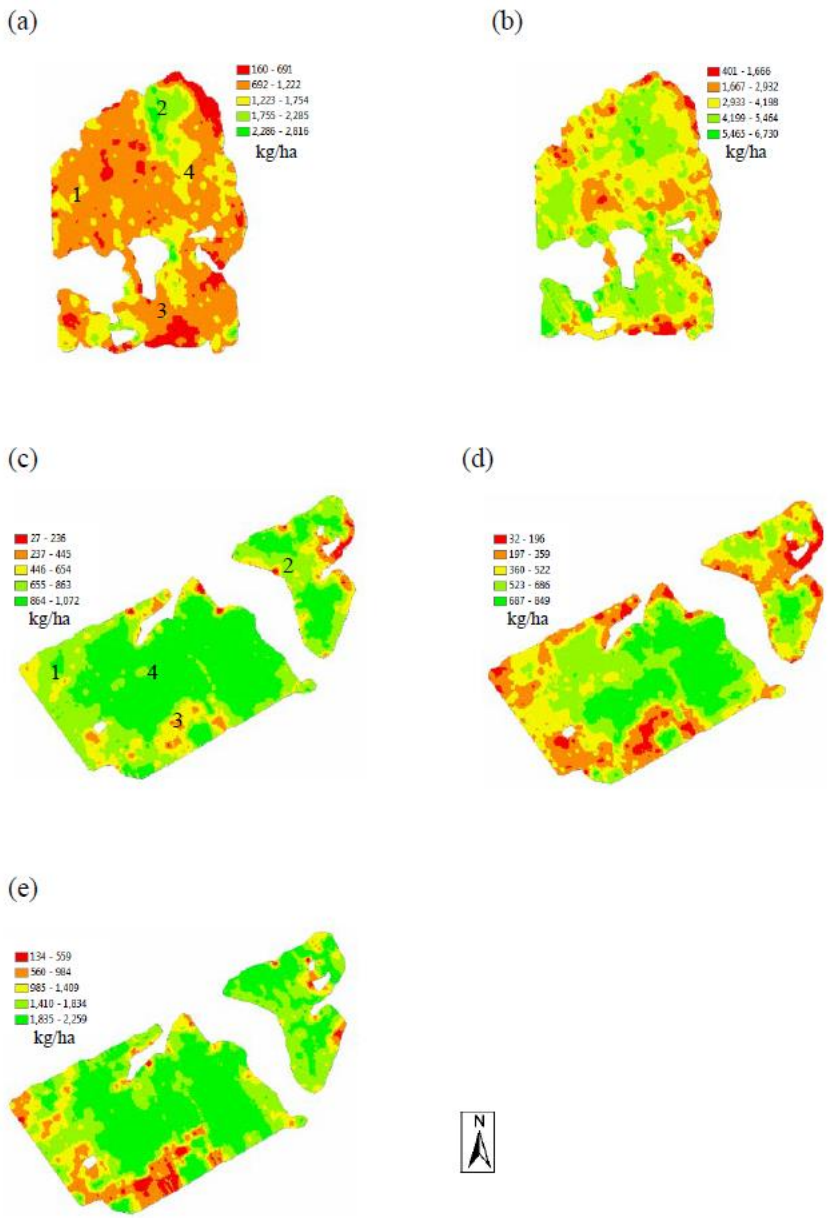


**FIGURE 6.14:** MAPS OF TOTAL GREEN DRY MATTER (TGDM) IN KG/HA, DERIVED FROM THE CALIBRATION OF CROP CIRCLE™ NDVI SCANS FOR "MILROY" PADDOCKS M25 IN (A) SEPTEMBER 2012 AND (B) AUGUST 2013, AND M41 IN (C) SEPTEMBER 2012, (D) AUGUST 2013 AND (E) SEPTEMBER 2013.

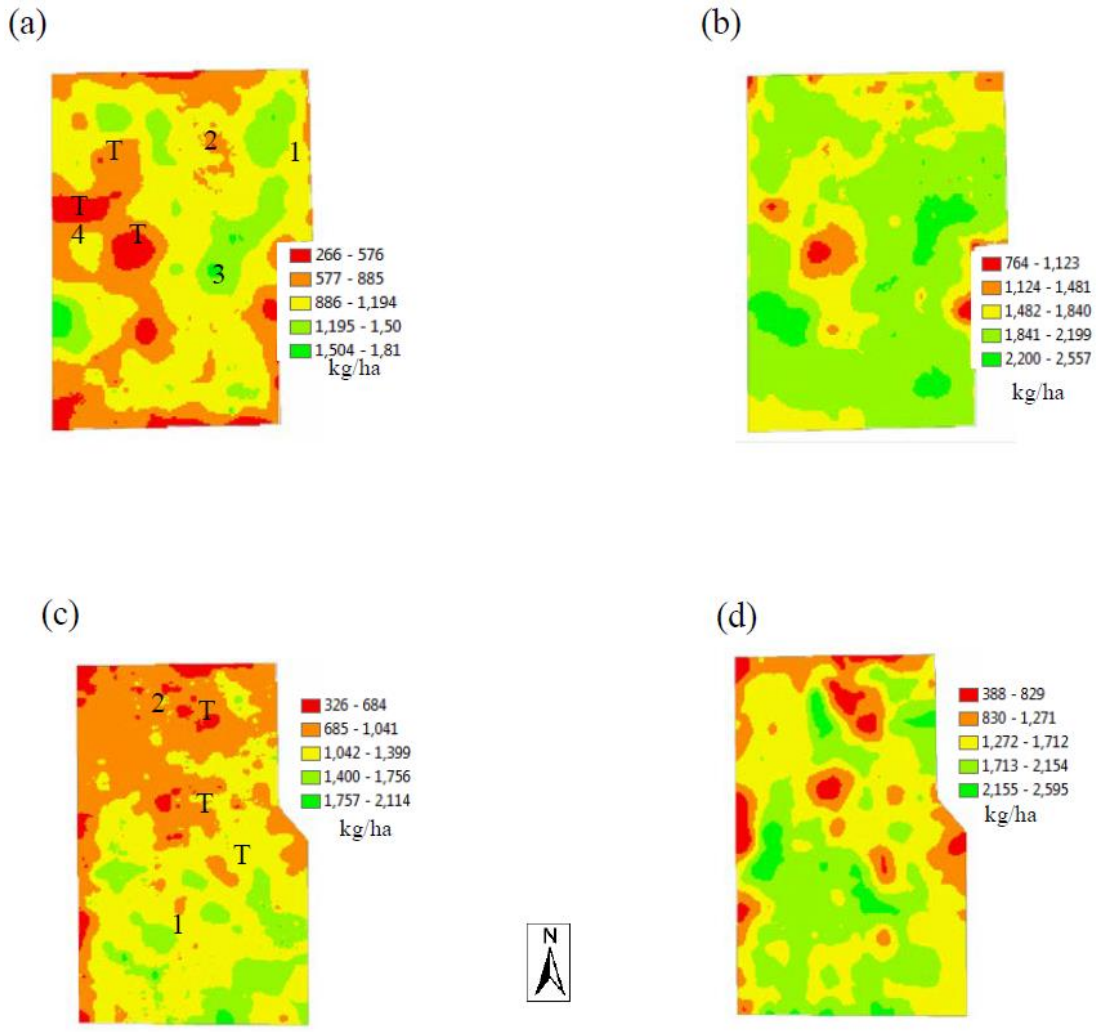


**FIGURE 6.15:** INTERPOLATED MAPS OF TOTAL GREEN DRY MATTER (TGDM) IN KG/HA, DERIVED FROM THE CALIBRATION OF CROP CIRCLE™ NDVI SCANS FOR "GRANDVIEW" PADDOCKS GV8 IN (A) SEPTEMBER 2012 AND (B) OCTOBER 2013, AND GV39 IN (C) SEPTEMBER 2012 AND (D) OCTOBER 2013. THE SITES MARKED 'T' ON MAPS (A) AND (C) CONTAIN WOODED AREAS.

(a)

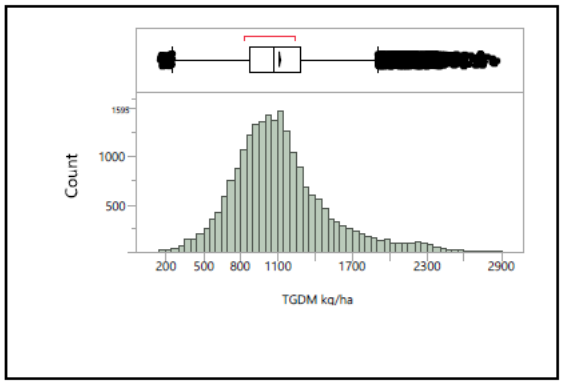


| | |
|---|---|
| Mean | 1116.3673 |
| Std Dev | 380.32691 |
| N | 21085 |
| Skewness | 0.9290296 |
| Kurtosis | 1.4200218 |
| Median | 1068.3571 |

(b)

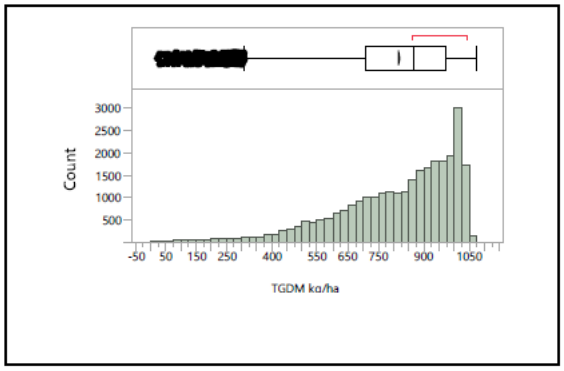


| | |
|---|---|
| Mean | 819.34857 |
| Std Dev | 185.66206 |
| N | 27850 |
| Skewness | -1.032683 |
| Kurtosis | 0.7779587 |
| Median | 866.65683 |

(c)

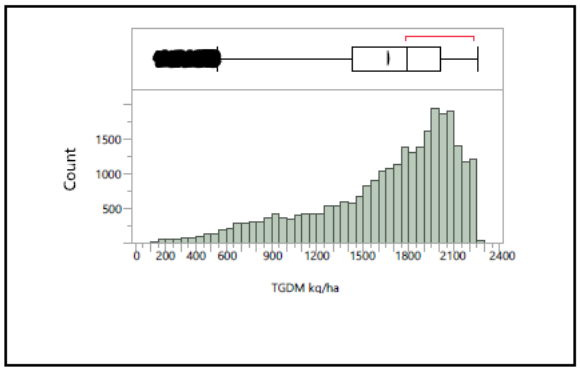


| | |
|---|---|
| Mean | 1667.3446 |
| Std Dev | 448.9779 |
| N | 27850 |
| Skewness | -0.99652 |
| Kurtosis | 0.2477732 |
| Median | 1790.5218 |

**FIGURE 6.16:** TGDM DISTRIBUTION HISTOGRAMS FOR "MILROY" PADDOCKS M25 IN SEPTEMBER 2012 (A), AND M41 IN AUGUST (B) AND SEPTEMBER (C) 2013.

(a)

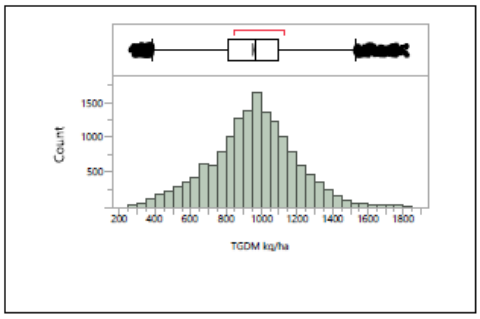


| | |
|---|---|
| Mean | 953.31174 |
| Std Dev | 233.55379 |
| N | 15076 |
| Skewness | -0.05307 |
| Kurtosis | 0.2599604 |
| Median | 963.25541 |

(b)

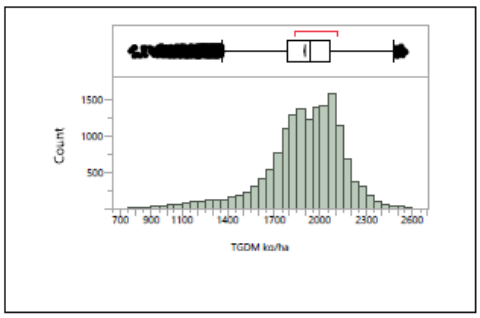


| | |
|---|---|
| Mean | 1900.2428 |
| Std Dev | 238.88684 |
| N | 15076 |
| Skewness | -0.979831 |
| Kurtosis | 1.761113 |
| Median | 1928.7723 |

(c)

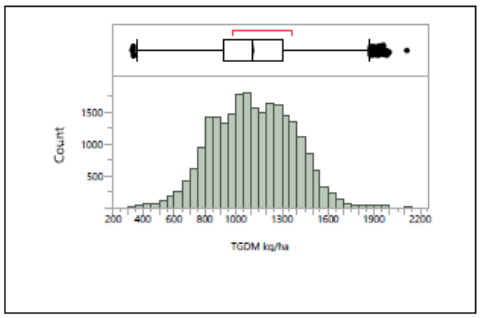


| | |
|---|---|
| Mean | 1113.0706 |
| Std Dev | 253.6188 |
| N | 23927 |
| Skewness | -0.000814 |
| Kurtosis | -0.354588 |
| Median | 1108.8095 |

(d)

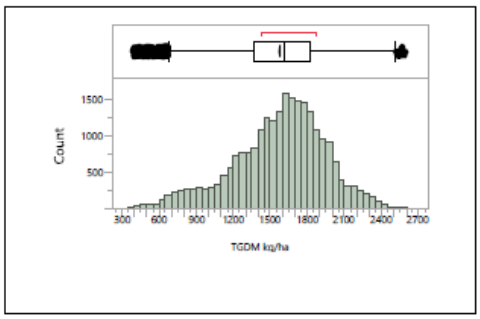


| | |
|---|---|
| Mean | 1574.2231 |
| Std Dev | 367.78178 |
| N | 23927 |
| Skewness | -0.49025 |
| Kurtosis | 0.1781962 |
| Median | 1618.0353 |

**FIGURE 6.17**: TGDM DISTRIBUTION HISTOGRAMS FOR "GRANDVIEW" PADDOCKS GV8 IN SEPTEMBER 2012 (A) AND OCTOBER 2013 (B), AND GV39 IN SEPTEMBER 2012 (C) AND OCTOBER 2013 (D).

**FIGURE 6.18:** "MILROY" PADDOCK M25 WAS HEAVILY COVERED IN CAPEWEED (*ARCTOTHECA CALENDULA* L.) AND STORKSBILL (*ERODIUM* SPP.) IN SEPTEMBER 2012. THE PHOTO WAS TAKEN LOOKING SOUTH-WEST FROM SITE 4. SITE 1 IS TO THE RIGHT.

**FIGURE 6.19:** "MILROY" PADDOCK M25 SHOWING HIGH SUBTERRANEAN CLOVER CONTENT AROUND SITE 2, HIGH ECA SOIL MOISTURE ZONE.

(a) (b)

**FIGURE 6.20:** "MILROY" PADDOCK M41 (A) LOOKING SOUTH-EAST FROM SITE 1 (DEEP SAND). THIS AREA IS THE LOWEST PART OF THE PADDOCK, LOW IN POTASSIUM AND COPPER AND DOMINATED BY CAPEWEED (B).

(a) (b)

**FIGURE 6.21:** (A) SITE 2 IN "MILROY" PADDOCK M41, HIGH SUBTERRANEAN CLOVER CONTENT, LOOKING NORTH-EAST AND (B) HIGH SUBTERRANEAN CLOVER CONTENT NEAR SITE 4.

(a)

(b)

**FIGURE 6.22:** SITE 3 IN "MILROY" PADDOCK M41, SHOWING THE IMPACT OF SALINE/SODIC SOIL ON PASTURE GROWTH LOOKING (A) NORTH-WEST AND (B) SOUTH-EAST FROM SITE 3 TOWARDS THE DRAINAGE LINE.

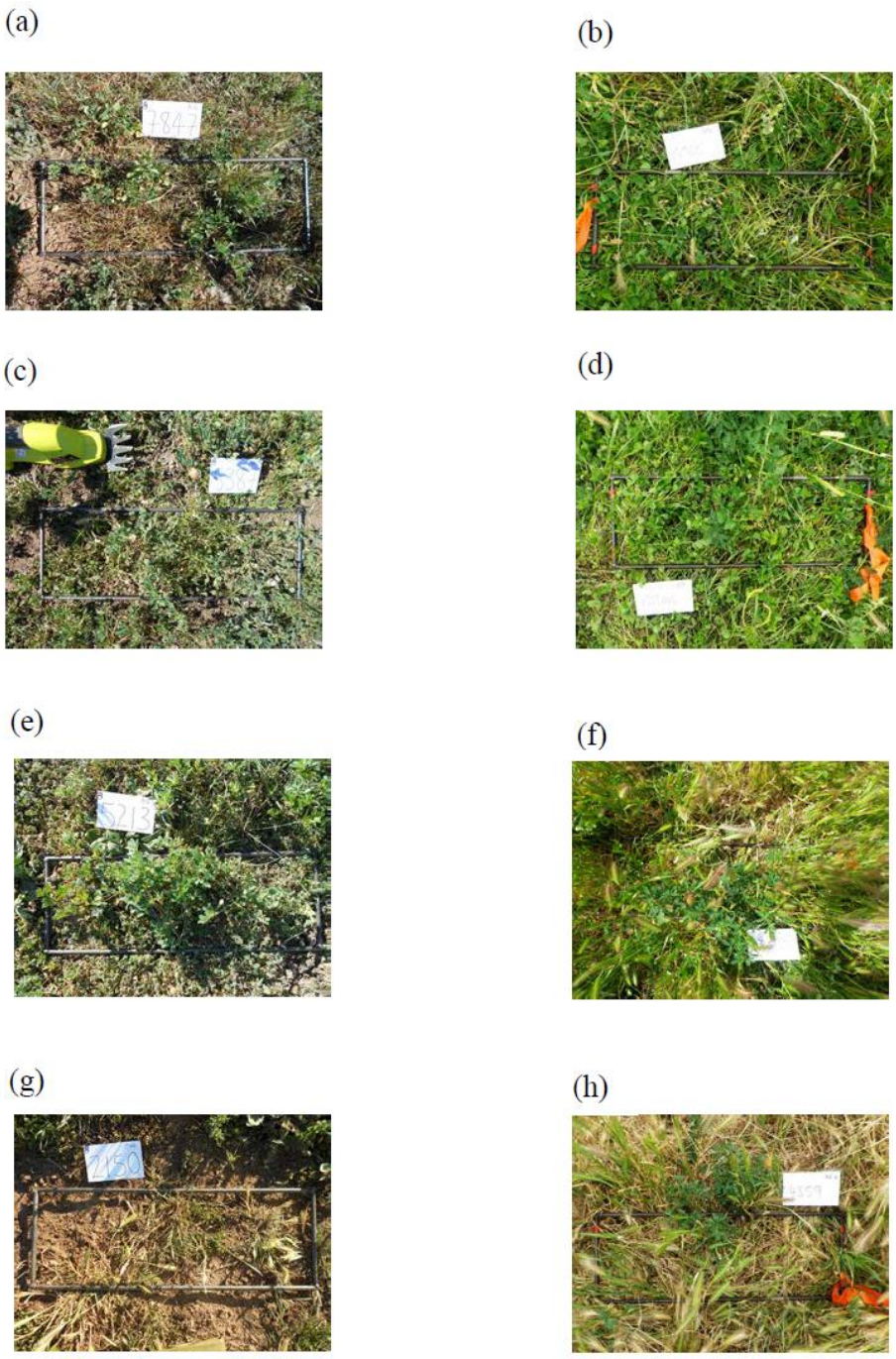


**FIGURE 6.23:** PHOTOGRAPHS OF PASTURE IN THE VICINITY OF GRANDVIEW SITES 1–4 IN PADDOCK GV8. SITE 1 IN (A) 2012 AND (B) 2013; SITE 2 IN (C) 2012 AND (D) 2013; SITE 3 IN (E) 2012 AND (F) 2013 AND SITE 4 IN (G) 2012 AND (H) 2013. THE TOTAL AMOUNT OF TGDM PRESENT WAS GREATER IN 2013 THAN 2012. GROWING SEASON RAINFALL WAS 218 MM IN 2012 AND 254 MM IN 2013. ADDITIONALLY, 62 MM MORE RAIN WAS RECEIVED BETWEEN JUNE AND SEPTEMBER 2013 THAN 2012 AND THE EFFECT ON PASTURE GROWTH AND COVERAGE IS EVIDENT FROM THE IMAGES.

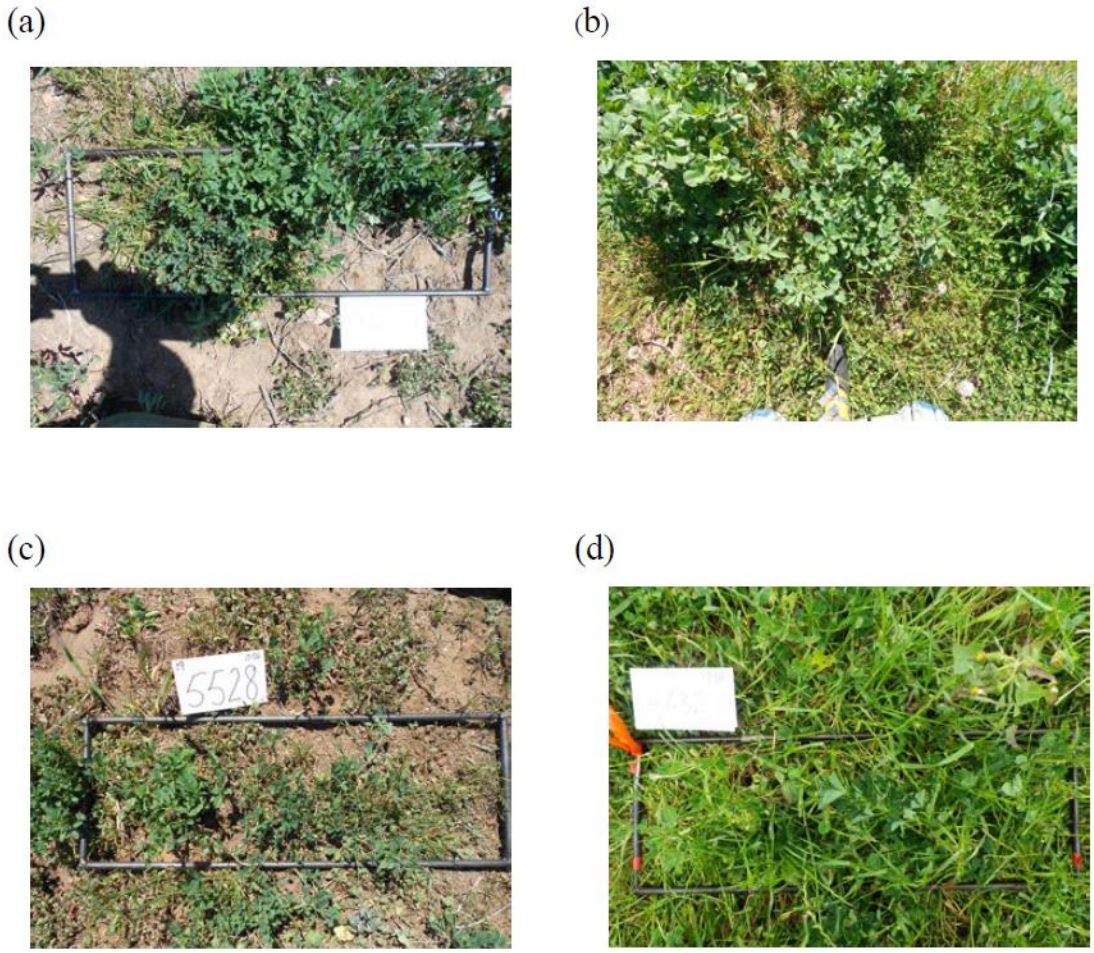


**FIGURE 6.24:** PHOTOGRAPHS OF PASTURE IN THE VICINITY OF GRANDVIEW SITES 1 AND 2 IN PADDOCK GV39. SITE 1 IN (A) 2012 AND (B) IN 2013 AND SITE 2 IN (C) 2012 AND (D) 2013. THE TOTAL AMOUNT OF TGDM PRESENT WAS GREATER IN 2013 THAN 2012. GROWING SEASON RAINFALL WAS 218 MM IN 2012 AND 254 MM IN 2013. ADDITIONALLY, 62 MM MORE RAIN WAS RECEIVED BETWEEN JUNE AND SEPTEMBER 2013 THAN 2012 AND THE EFFECT ON PASTURE GROWTH AND COVERAGE IS EVIDENT FROM THE IMAGES.

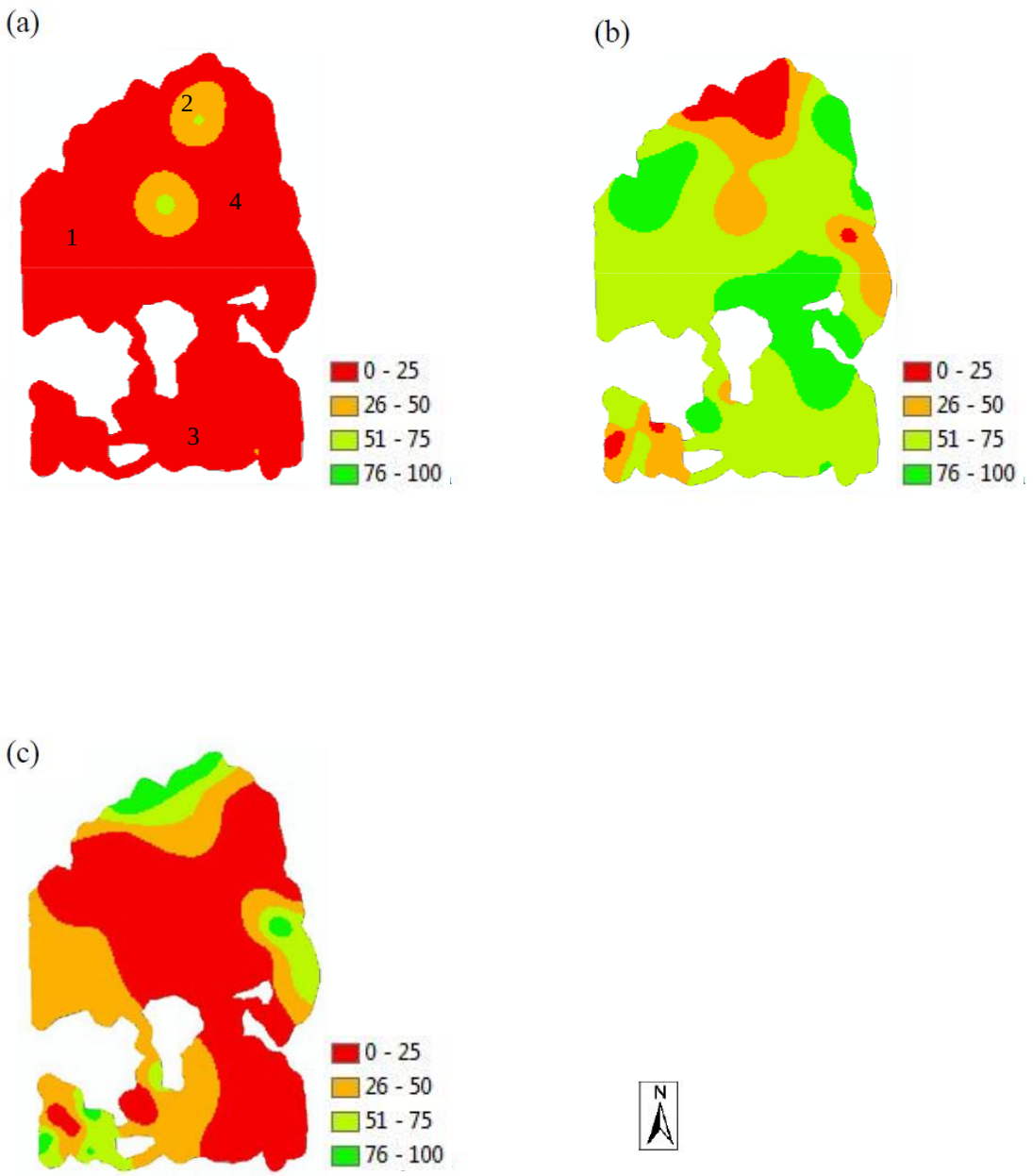


**FIGURE 6.25:** DRY-WEIGHT-RANK PASTURE COMPOSITION, BY PERCENTAGE, FOR "MILROY" PADDOCK M25 IN 2012. (A) LEGUME, (B) BROADLEAF AND (C) GRASS. RANGE CATEGORIES ARE PERCENT COMPOSITION.

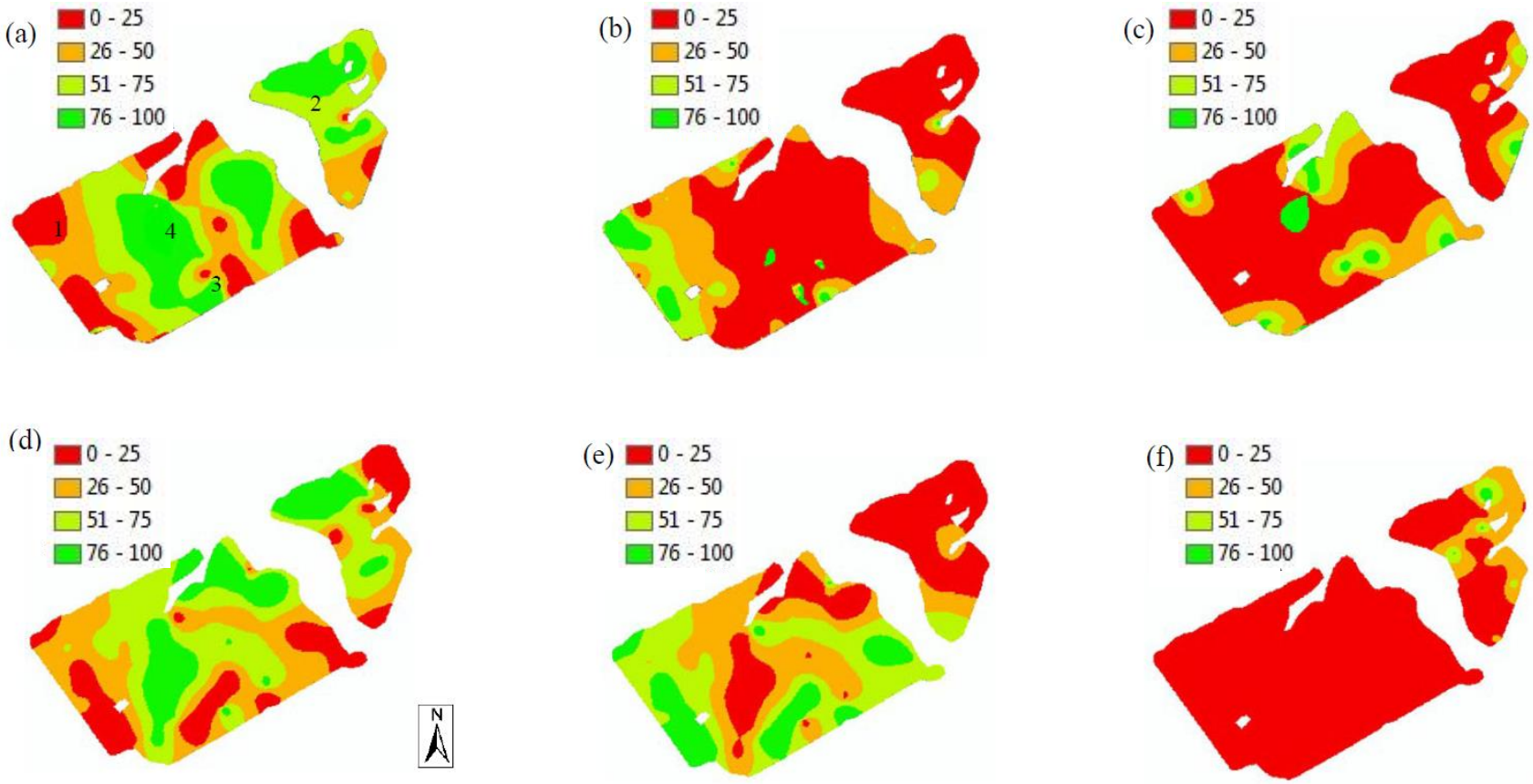


**FIGURE 6.26:** DRY-WEIGHT-RANK PASTURE COMPOSITION, BY PERCENTAGE, FOR "MILROY" PADDOCK M41 IN 2012 (A) LEGUME, (B) BROADLEAF AND (C) GRASS, AND IN 2013 (D) LEGUME, (E) BROADLEAF AND (F) GRASS. RANGE CATEGORIES ARE PERCENT COMPOSITION.

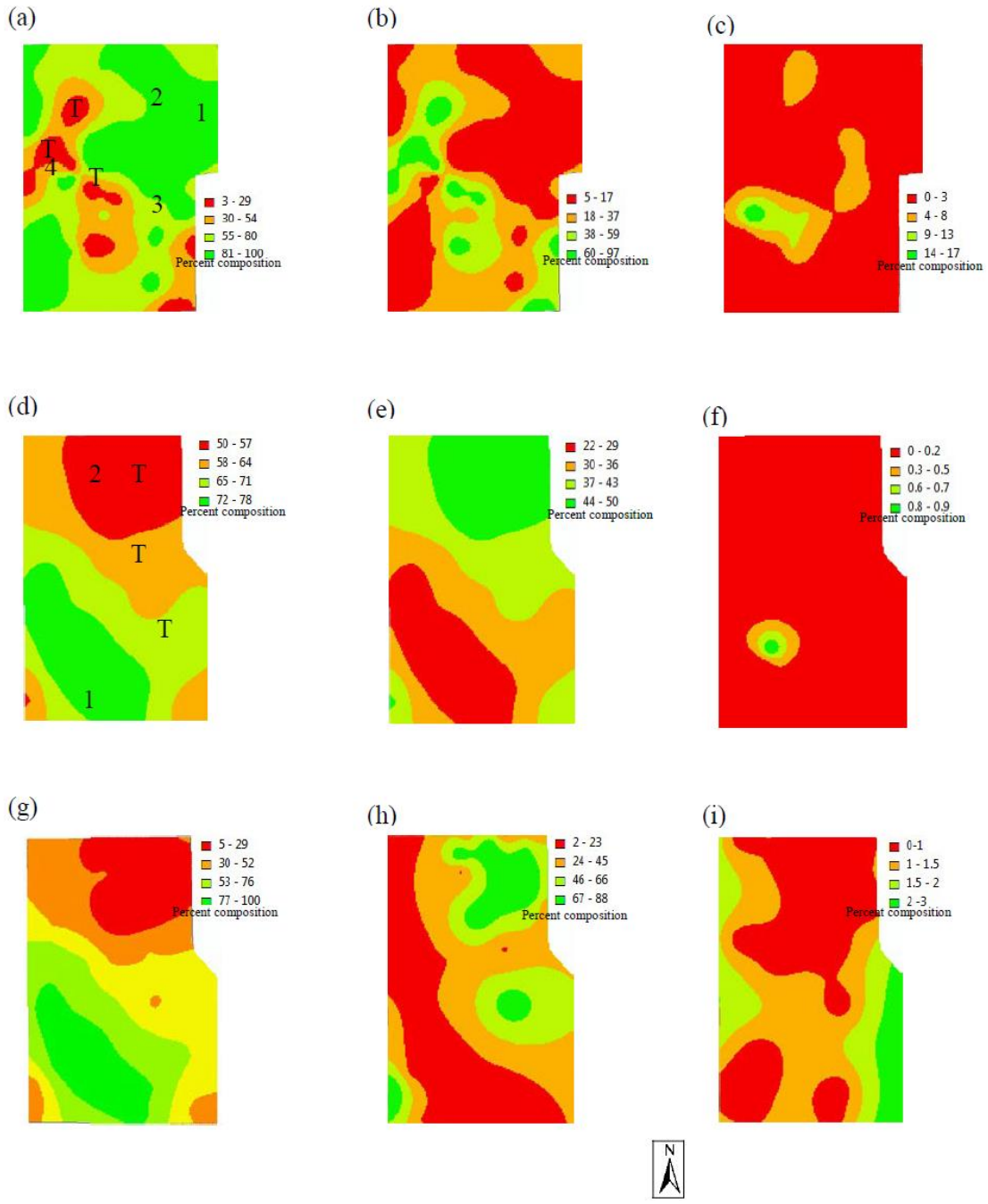


**FIGURE 6.27** DRY-WEIGHT-RANK PASTURE COMPOSITION, BY PERCENTAGE, FOR "GRANDVIEW" PADDOCK GV8 (A) LEGUME, (B) GRASS AND (C) BROADLEAF, AND FOR PADDOCK GV39 IN 2012 (D) LEGUME, (E) GRASS AND (F) BROADLEAF AND 2013 (G) LEGUME, (H) GRASS AND (I) BROADLEAF. RANGE CATEGORIES ARE PERCENT COMPOSITION. THE SITES MARKED 'T' ON MAPS (A) AND (D) CONTAIN WOODED AREAS.

**TABLE 6.6:** "MILROY" PADDOCK M25, MEAN VALUES FOR EACH MANAGEMENT CLASS COMBINATION FROM *K*-MEANS CLUSTERING OUTPUT (ON CROP YIELD VALUES ONLY) AND THE MEDIAN KRIGING VARIANCE AND 95% CONFIDENCE INTERVALS.

| Classes | Wheat 2004 (t/ha) | Wheat 2009 (t/ha) | ECa 0–100 cm (mS/m) | ECa 0–50 cm (mS/m) | Elev (m) |
|---|---|---|---|---|---|
| Two | | | | | |
| 2a | 2.83a† | 2.43a | 64.68 | 30.27 | 296.09 |
| 2b | 2.29b | 1.97b | 16.79 | 6.10 | 313.46 |
| Three | | | | | |
| 3a | 2.86a | 2.45a | 67.25 | 31.91 | 295.49 |
| 3b | 1.96b | 1.49b | 15.72 | 6.19 | 319.36 |
| 3c | 2.52a | 2.31a | 18.32 | 6.39 | 309.20 |
| Four | | | | | |
| 4a | 2.42a | 2.35a,c | 20.78 | 6.70 | 302.62 |
| 4b | 2.89b | 2.48a | 68.33 | 32.66 | 295.38 |
| 4c | 1.81c | 1.33b | 19.82 | 7.76 | 313.47 |
| 4d | 2.52a,b | 2.01c | 11.59 | 5.01 | 326.53 |
| Median $\sigma_{krig}$ | 0.099 | 0.096 | | | |
| 95% CI‡ | 0.388 | 0.376 | | | |

† Mean values with different letters indicate that the yield between management classes is significantly different. ‡CI, confidence interval

**TABLE 6.7:** "MILROY" PADDOCK M25, MEAN VALUES FOR EACH MANAGEMENT CLASS COMBINATION FROM *K*-MEANS CLUSTERING OUTPUT (ON CROP YIELD AND PASTURE TGDM VALUES) AND THE MEDIAN KRIGING VARIANCE AND 95% CONFIDENCE INTERVALS.

| Classes | Wheat 2004 (t/ha) | Wheat 2009 (t/ha) | TGDM Sep 2012 (kg/ha) | TGDM Aug 2013 (kg/ha) | ECa 0–100 cm (mS/m) | ECa 0–50 cm (mS/m) | Elev (m) |
|---|---|---|---|---|---|---|---|
| Two | | | | | | | |
| 2a | 2.87a† | 2.48a | 1423.83 | 4150.85 | 66.29 | 31.16 | 295.41 |
| 2b | 2.29b | 1.97b | 1070.79 | 3734.49 | 17.27 | 6.34 | 313.30 |
| Three | | | | | | | |
| 3a | 1.87a | 1.44a | 984.32 | 3130.61 | 20.35 | 8.06 | 313.47 |
| 3b | 2.51b | 2.24b | 1107.79 | 4019.72 | 16.70 | 5.96 | 312.87 |
| 3c | 2.93c | 2.56b | 1499.58 | 4256.31 | 68.17 | 32.13 | 294.77 |
| Four | | | | | | | |
| 4a | 3.05a | 2.77a | 1834.07 | 4602.89 | 71.44 | 33.95 | 294.37 |
| 4b | 2.51b | 1.98b | 817.24 | 3456.15 | 52.25 | 23.49 | 301.02 |
| 4c | 2.53b | 2.26b | 1128.28 | 4019.84 | 15.36 | 5.45 | 313.30 |
| 4d | 1.86c | 1.48c | 1025.07 | 3277.35 | 16.76 | 6.07 | 314.39 |
| Median $\sigma_{krig}$ | 0.099 | 0.096 | | | | | |
| 95% CI‡ | 0.388 | 0.376 | | | | | |

† Mean values with different letters indicate that the yield between management classes is significantly different. ‡CI, confidence interval

**TABLE 6.8:** "MILROY" PADDOCK M41, MEAN VALUES FOR EACH MANAGEMENT CLASS COMBINATION FROM *K*-MEANS CLUSTERING OUTPUT (ON CROP YIELD VALUES ONLY) AND THE MEDIAN KRIGING VARIANCE AND 95% CONFIDENCE INTERVALS.

| Classes | Wheat 2009 (t/ha) | Wheat 2014 (t/ha) | ECa 0–100 cm (mS/m) | ECa 0–50 cm (mS/m) | Elev (m) |
|---|---|---|---|---|---|
| Two | | | | | |
| 2a | 2.32a† | 3.88a | 11.15 | 6.55 | 307.57 |
| 2b | 1.67b | 3.57a | 57.24 | 32.85 | 297.98 |
| Three | | | | | |
| 3a | 2.51a | 4.36a | 13.03 | 6.72 | 307.22 |
| 3b | 1.94b | 2.93b | 8.17 | 6.57 | 308.16 |
| 3c | 1.62b | 3.52c | 58.89 | 34.05 | 297.53 |
| Four | | | | | |
| 4a | 2.53a | 4.30a | 8.51 | 7.37 | 308.6 |
| 4b | 2.18a,c | 3.55a,c | 13.67 | 6.34 | 298.15 |
| 4c | 1.26b | 3.01b | 59.66 | 35.10 | 295.64 |
| 4d | 1.92c | 4.41c | 13.33 | 6.24 | 308.82 |
| Median $\sigma_{krig}$ | 0.136 | 0.134 | | | |
| 95% CI‡ | 0.534 | 0.523 | | | |

† Yield values with different letters indicate that the mean between management classes is significantly different. ‡CI, confidence interval

**TABLE 6.9:** "MILROY" PADDOCK M41, MEAN VALUES FOR EACH MANAGEMENT CLASS COMBINATION FROM *K*-MEANS CLUSTERING OUTPUT (ON CROP YIELD AND PASTURE TGDM VALUES) AND THE MEDIAN KRIGING VARIANCE AND 95% CONFIDENCE INTERVALS.

| Classes | Wheat 2009 (t/ha) | Wheat 2014 (t/ha) | TGDM Sep 2012 (kg/ha) | TGDM Aug 2013 (kg/ha) | ECa 0–100 cm (mS/m) | ECa 0–50 cm (mS/m) | Elev (m) |
|---|---|---|---|---|---|---|---|
| Two | | | | | | | |
| 2a | 2.43a† | 4.11a | 894.16 | 1858.94 | 10.98 | 6.36 | 308.58 |
| 2b | 1.75b | 3.10b | 596.73 | 1097.21 | 28.28 | 16.58 | 301.73 |
| Three | | | | | | | |
| 3a | 2.50a | 4.31a | 923.99 | 1906.64 | 11.94 | 6.48 | 307.59 |
| 3b | 1.95b | 3.00b | 671.05 | 1406.77 | 10.34 | 6.99 | 307.61 |
| 3c | 1.64b | 3.58c | 583.58 | 847.55 | 57.98 | 33.79 | 296.93 |
| Four | | | | | | | |
| 4a | 1.91a,b | 3.51a,b | 745.36 | 1336.40 | 14.97 | 5.37 | 293.95 |
| 4b | 1.58a | 3.55a | 569.36 | 808.76 | 60.93 | 36.08 | 296.51 |
| 4c | 2.21bc | 3.01b | 678.33 | 1570.47 | 8.84 | 8.67 | 319.26 |
| 4d | 2.52c | 4.41c | 946.74 | 1965.79 | 11.80 | 6.59 | 307.78 |
| Median $\sigma_{krig}$ | 0.136 | 0.134 | | | | | |
| 95% CI‡ | 0.534 | 0.523 | | | | | |

† Yield values with different letters indicate that the mean between management classes is significantly different. ‡CI, confidence interval

**TABLE 6.10:** "GRANDVIEW" PADDOCK GV8, MEAN VALUES FOR EACH MANAGEMENT CLASS COMBINATION FROM *K*-MEANS CLUSTERING OUTPUT (ON CROP YIELD VALUES ONLY) AND THE MEDIAN KRIGING VARIANCE AND 95% CONFIDENCE INTERVALS.

| Classes | Wheat 2005 (t/ha) | Canola 2007 (t/ha) | Wheat 2009 (t/ha) | ECa 0–38 cm (mS/m) | ECa 0–75 cm (mS/m) | Elev (m) |
|---|---|---|---|---|---|---|
| Two | | | | | | |
| 2a | 2.49a† | 1.46a | 2.34a | 50.26 | 113.83 | 142.74 |
| 2b | 2.61b | 1.96b | 2.77b | 39.46 | 97.74 | 143.16 |
| Three | | | | | | |
| 3a | 2.60a | 1.94a | 2.72a | 53.16 | 114.69 | 144.78 |
| 3b | 2.44b | 1.20b | 2.15b | 46.70 | 110.25 | 141.36 |
| 3c | 2.61a,c | 1.95a,c | 2.76a,c | 37.77 | 95.99 | 142.94 |
| Four | | | | | | |
| 4a | 2.72a | 1.47a | 2.45a | 42.40 | 106.81 | 140.04 |
| 4b | 2.15b | 1.12b | 1.96b | 50.38 | 111.90 | 143.55 |
| 4c | 2.58c | 2.00c | 2.79c | 37.08 | 94.20 | 143.40 |
| 4d | 2.60c | 1.94c | 2.73c | 52.97 | 114.49 | 144.75 |
| Median $\sigma_{krig}$ | 0.020 | 0.032 | 0.027 | | | |
| 95% CI‡ | 0.078 | 0.125 | 0.106 | | | |

† Yield values with different letters indicate that the mean between management classes is significantly different. ‡CI, confidence interval

**TABLE 6.11:** "GRANDVIEW" PADDOCK GV8, MEAN VALUES FOR EACH MANAGEMENT CLASS COMBINATION FROM *K*-MEANS CLUSTERING OUTPUT (ON CROP YIELD AND PASTURE TGDM VALUES) AND THE MEDIAN KRIGING VARIANCE AND 95% CONFIDENCE INTERVALS.

| Classes | Wheat 2005 (t/ha) | Canola 2007 (t/ha) | Wheat 2009 (t/ha) | TGDM Sep 2012 (kg/ha) | TGDM Oct 2013 (kg/ha) | ECa 0–38 cm (mS/m) | ECa 0–75 cm (mS/m) | Elev (m) |
|---|---|---|---|---|---|---|---|---|
| Two | | | | | | | | |
| 2a | 2.62a† | 1.93a | 2.76a | 1026.86 | 1983.43 | 41.24 | 100.67 | 143.07 |
| 2b | 2.43b | 1.35b | 2.20b | 740.80 | 1659.86 | 49.17 | 111.39 | 142.85 |
| Three | | | | | | | | |
| 3a | 2.61a | 1.95a | 2.74a | 956.11 | 1967.44 | 52.66 | 113.92 | 144.74 |
| 3b | 2.62a | 1.87a | 2.72a | 1024.21 | 1964.67 | 38.21 | 97.53 | 142.37 |
| 3c | 2.30b | 1.20b | 2.06b | 679.91 | 1556.55 | 48.69 | 110.37 | 142.91 |
| Four | | | | | | | | |
| 4a | 2.58a | 2.01a | 2.80a | 1029.32 | 1972.36 | 36.91 | 94.17 | 143.32 |
| 4b | 2.72b | 1.48b | 2.46b | 970.63 | 1905.76 | 42.29 | 106.64 | 140.07 |
| 4c | 2.61a | 1.95a | 2.74a | 961.70 | 1968.02 | 52.72 | 114.08 | 144.76 |
| 4d | 2.20c | 1.18c | 2.02c | 634.06 | 1503.09 | 50.03 | 111.12 | 143.69 |
| Median $\sigma_{krig}$ | 0.020 | 0.032 | 0.027 | | | | | |
| 95% CI‡ | 0.078 | 0.125 | 0.106 | | | | | |

† Yield values with different letters indicate that the mean between management classes is significantly different. ‡CI, confidence interval

**TABLE 6.12:** "GRANDVIEW" PADDOCK GV39, MEAN VALUES FOR EACH MANAGEMENT CLASS COMBINATION FROM *K*-MEANS CLUSTERING OUTPUT (ON CROP YIELD VALUES ONLY) AND THE MEDIAN KRIGING VARIANCE AND 95% CONFIDENCE INTERVALS.

| Classes | Canola 2007 (t/ha) | Wheat 2008 (t/ha) | Wheat 2009 (t/ha) | ECa 0–38 cm (mS/m) | ECa 0–75 cm (mS/m) | Elev (m) |
|---|---|---|---|---|---|---|
| Two | | | | | | |
| 2a | 0.56a† | 1.77a | 2.16a | 19.78 | 85.66 | 159.76 |
| 2b | 1.12b | 2.67b | 3.15b | 13.87 | 75.98 | 165.63 |
| Three | | | | | | |
| 3a | 0.51a | 1.22a | 1.53a | 21.88 | 84.79 | 161.92 |
| 3b | 0.68b | 2.48b | 2.97b | 16.43 | 83.79 | 158.83 |
| 3c | 1.20c | 2.67c | 3.14b,c | 13.68 | 75.18 | 166.73 |
| Four | | | | | | |
| 4a | 0.57a,c | 1.37a | 1.71a | 11.96 | 77.82 | 163.36 |
| 4b | 0.70a | 2.53b | 3.00b | 16.56 | 83.79 | 158.95 |
| 4c | 1.21b | 2.68b | 3.16b | 13.76 | 75.15 | 166.77 |
| 4d | 0.49c | 1.22a | 1.56a | 26.50 | 88.33 | 160.86 |
| Median $\sigma_{krig}$ | 0.048 | 0.095 | 0.083 | | | |
| 95% CI‡ | 0.188 | 0.372 | 0.325 | | | |

† Yield values with different letters indicate that the mean between management classes is significantly different. ‡CI, confidence interval

**TABLE 6.13:** "GRANDVIEW" PADDOCK GV39, MEAN VALUES FOR EACH MANAGEMENT CLASS COMBINATION FROM *K*-MEANS CLUSTERING OUTPUT (ON CROP YIELD AND PASTURE TGDM VALUES) AND THE MEDIAN KRIGING VARIANCE AND 95% CONFIDENCE INTERVALS.

| Classes | Canola 2007 (t/ha) | Wheat 2008 (t/ha) | Wheat 2009 (t/ha) | TGDM Sep 2012 (kg/ha) | TGDM Oct2013 (kg/ha) | ECa 0–38 cm (mS/m) | ECa 0–75 cm (mS/m) | Elev (m) |
|---|---|---|---|---|---|---|---|---|
| Two | | | | | | | | |
| 2a | 0.56a† | 1.75a | 2.12a | 878.34 | 1241.79 | 19.56 | 85.88 | 159.84 |
| 2b | 1.10b | 2.65b | 3.14b | 1249.94 | 1768.07 | 14.17 | 76.14 | 165.42 |
| Three | | | | | | | | |
| 3a | 1.20a | 2.65a | 3.15a | 1306.90 | 1765.63 | 13.72 | 75.18 | 166.74 |
| 3b | 0.71b | 2.55a,b | 2.96a,b | 982.33 | 1612.89 | 16.63 | 83.20 | 159.38 |
| 3c | 0.50c | 1.23c | 1.60c | 855.14 | 1078.14 | 21.08 | 85.18 | 161.31 |
| Four | | | | | | | | |
| 4a | 0.72a | 2.61a | 3.00a | 982.48 | 1634.37 | 16.29 | 83.11 | 159.26 |
| 4b | 0.56a,b | 1.51b | 1.61b | 1050.24 | 1259.65 | 27.13 | 85.33 | 165.04 |
| 4c | 0.49b | 1.16b | 1.75b | 739.71 | 997.65 | 16.32 | 84.55 | 158.63 |
| 4d | 1.21c | 2.66a | 3.17a | 1309.00 | 1768.42 | 13.59 | 75.11 | 166.77 |
| Median $\sigma_{krig}$ | 0.048 | 0.095 | 0.083 | | | | | |
| 95% CI‡ | 0.188 | 0.372 | 0.325 | | | | | |

† Yield values with different letters indicate that the mean between management classes is significantly different. ‡CI, confidence interval

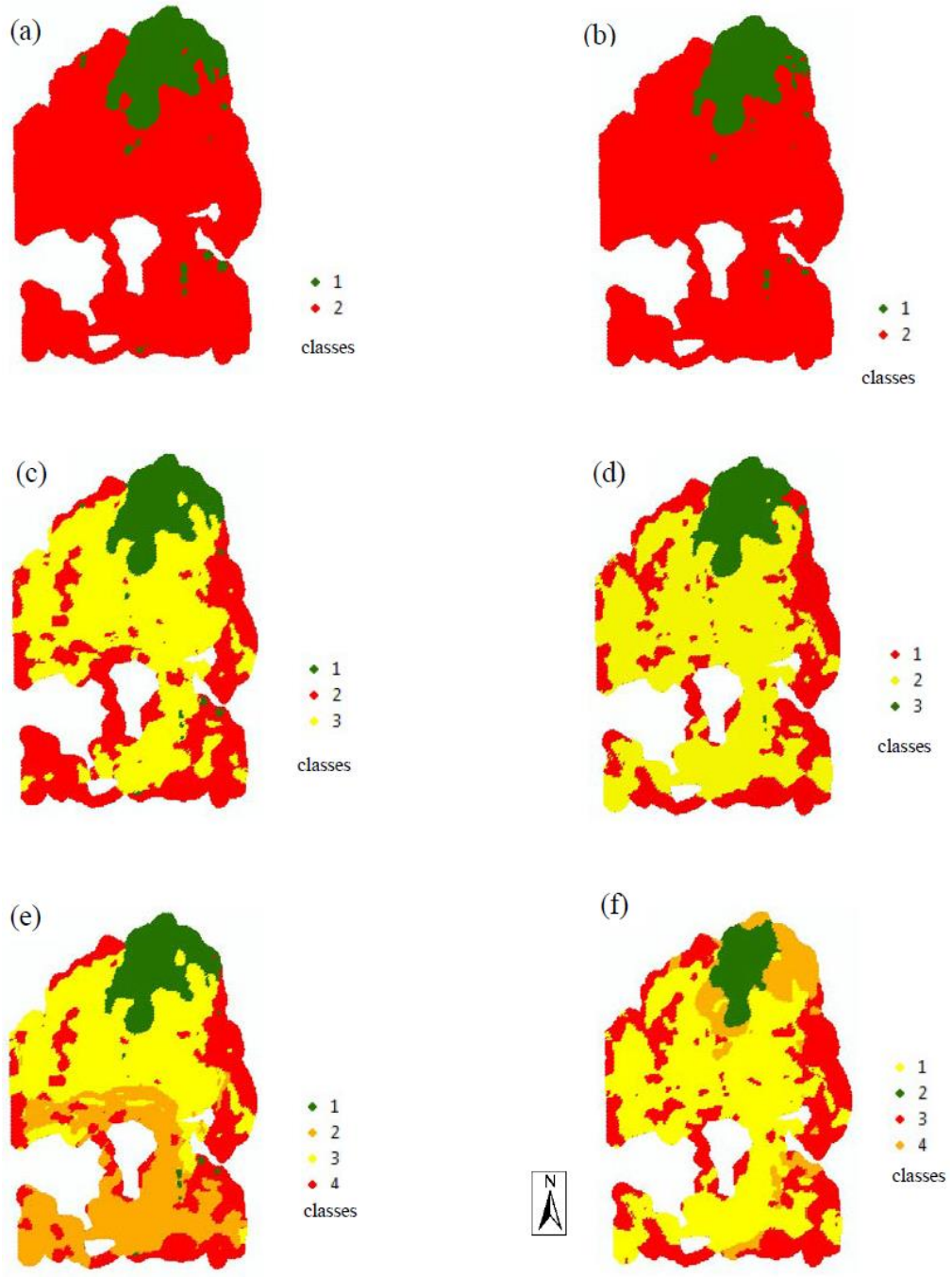


**FIGURE 6.28:** POTENTIAL MANAGEMENT CLASSES FOR "MILROY" PADDOCK M25 DERIVED FROM *K*-MEANS CLUSTERING USING CROP YIELD, PASTURE TGDM, ECA AND PADDOCK ELEVATION DATA AS INPUTS. MAPS ON THE LEFT-HAND SIDE (A, C AND E) SHOW TWO-, THREE- AND FOUR-CLASS OUTCOMES, RESPECTIVELY, DERIVED USING CROP YIELD DATA ONLY. MAPS ON THE RIGHT (B, D AND F) SHOW TWO, THREE AND FOUR CLASSES, RESPECTIVELY, INCORPORATING BOTH CROP YIELD AND PASTURE TGDM DATA IN THE *K*-MEANS CLUSTERING.

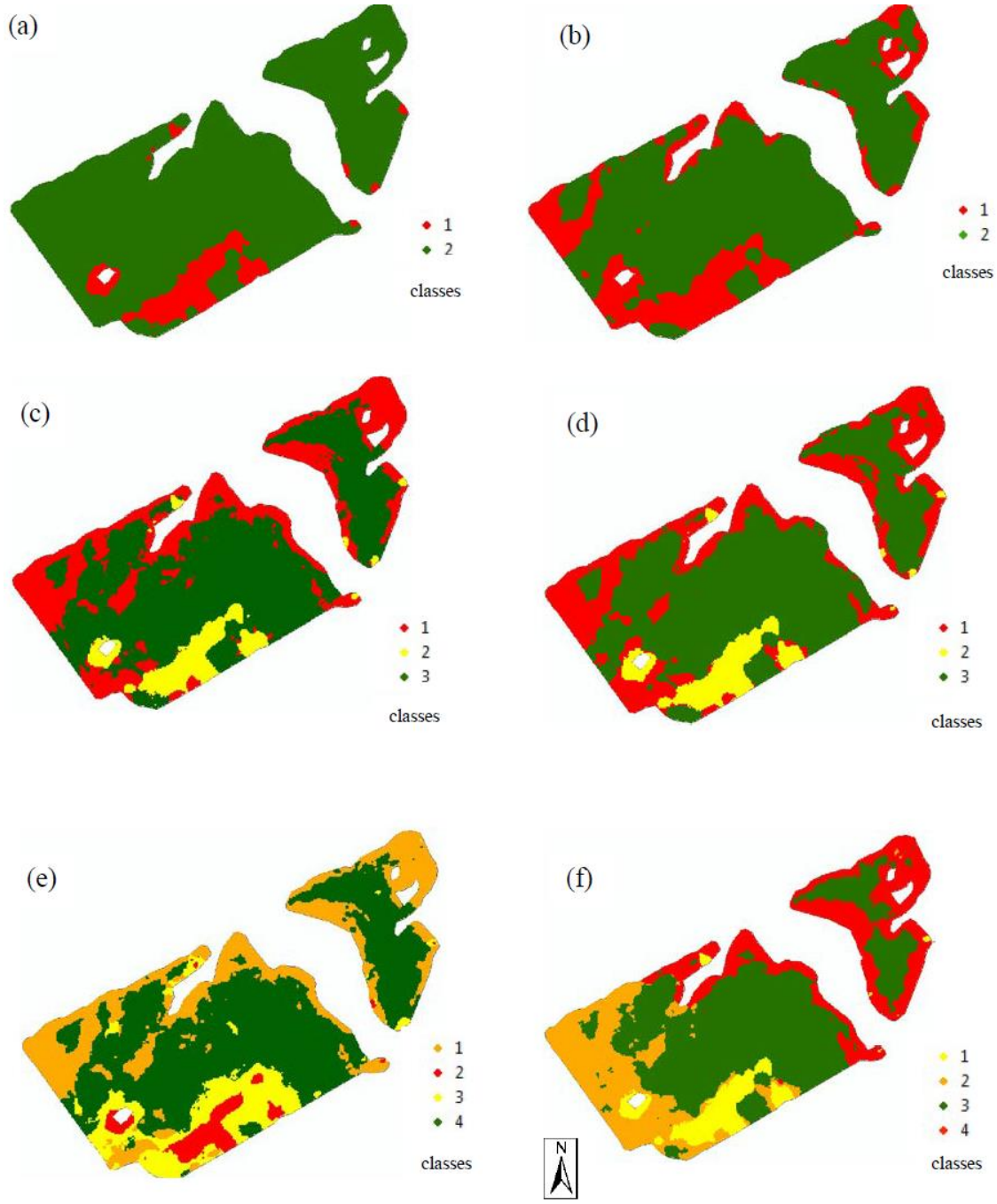


**FIGURE 6.29:** POTENTIAL MANAGEMENT CLASSES FOR "MILROY" PADDOCK M41 DERIVED FROM *K*-MEANS CLUSTERING USING CROP YIELD, PASTURE TGDM, ECA AND PADDOCK ELEVATION DATA AS INPUTS. MAPS ON THE LEFT-HAND SIDE (A, C AND E) SHOW TWO-, THREE- AND FOUR-CLASS OUTCOMES, RESPECTIVELY, USING CROP YIELD DATA ONLY. MAPS ON THE RIGHT (B, D AND F) SHOW TWO, THREE AND FOUR CLASSES, RESPECTIVELY, INCORPORATING BOTH CROP YIELD AND PASTURE TGDM DATA IN THE *K*-MEANS CLUSTERING.

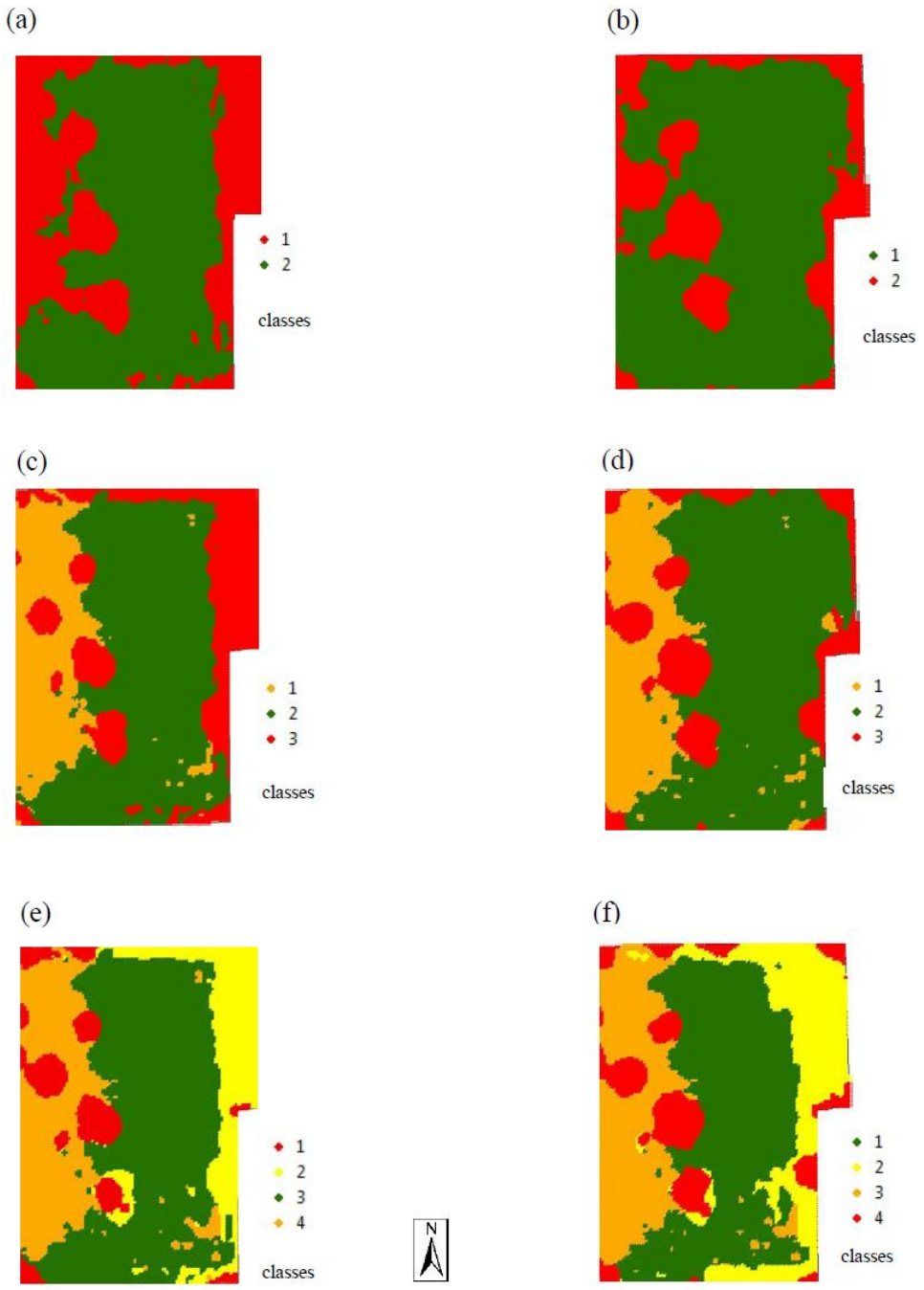


**FIGURE 6.30:** POTENTIAL MANAGEMENT CLASSES FOR "GRANDVIEW" PADDOCK GV8 DERIVED FROM *K*-MEANS CLUSTERING USING CROP YIELD, PASTURE TGDM, ECA AND PADDOCK ELEVATION DATA AS INPUTS. MAPS ON THE LEFT-HAND SIDE (A, C AND E) SHOW TWO-, THREE- AND FOUR-CLASS OUTCOMES, RESPECTIVELY, USING CROP YIELD DATA ONLY. MAPS ON THE RIGHT (B, D AND F) SHOW TWO, THREE AND FOUR CLASSES, RESPECTIVELY, INCORPORATING BOTH CROP YIELD AND PASTURE TGDM DATA IN THE *K*-MEANS CLUSTERING.

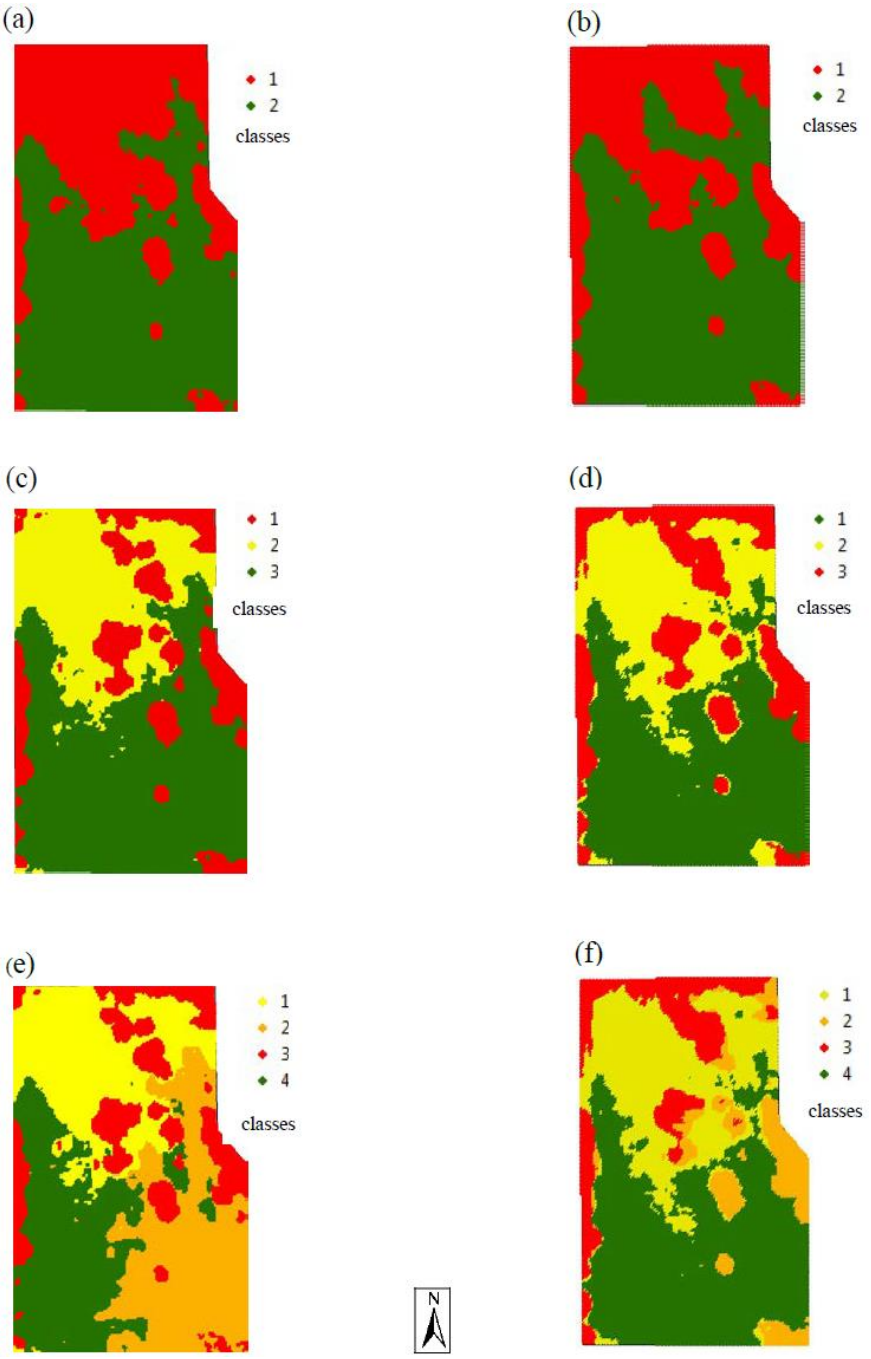


**FIGURE 6.31:** POTENTIAL MANAGEMENT CLASSES FOR "GRANDVIEW" PADDOCK GV39 DERIVED FROM *K*-MEANS CLUSTERING USING CROP YIELD, PASTURE TGDM, ECA AND PADDOCK ELEVATION DATA AS INPUTS. MAPS ON THE LEFT-HAND SIDE (A, C AND E) SHOW TWO-, THREE- AND FOUR-CLASS OUTCOMES, RESPECTIVELY, USING CROP YIELD DATA ONLY. MAPS ON THE RIGHT (B, D AND F) SHOW TWO, THREE AND FOUR CLASSES, RESPECTIVELY, INCORPORATING BOTH CROP YIELD AND PASTURE TGDM DATA IN THE *K*-MEANS CLUSTERING.

**TABLE 6.14:** THE EFFECT OF CREATING WITHIN-PADDOCK MANAGEMENT CLASSES ON THE STANDARD DEVIATIONS (S.D.) OF CROP YIELDS AND PASTURE TGDM IN "MILROY" PADDOCKS M25 AND M41. 'ONE CLASS' IS EQUIVALENT TREATING THE WHOLE PADDOCK AS ONE MANAGEMENT UNIT (I.E. UNIFORM MANAGEMENT).

| **"MILROY"** | **2004 yield s.d. (t/ha)** | **2009 yield s.d. (t/ha)** | **TGDM Sep 2012 s.d. (kg/ha)** | **TGDM Aug 2013 s.d. (kg/ha)** |
|---|---|---|---|---|
| M25 | | | | |
| one class | 0.50 | 0.60 | 380 | 1018 |
| two classes | 0.46 | 0.54 | 608 | 1112 |
| | 0.46 | 0.58 | 309 | 993 |
| three classes | 0.38 | 0.49 | 321 | 953 |
| | 0.33 | 0.42 | 300 | 889 |
| | 0.43 | 0.47 | 589 | 1029 |
| four classes | 0.41 | 0.39 | 409 | 743 |
| | 0.43 | 0.52 | 302 | 1116 |
| | 0.32 | 0.42 | 300 | 913 |
| | 0.36 | 0.50 | 303 | 946 |
| | **2009 yield s.d. (t/ha)** | **2014 yield s.d. (t/ha)** | **TGDM Sep 2012 s.d. (kg/ha)** | **TGDM Aug 2013 s.d. (kg/ha)** |
| M41 | | | | |
| one class | 0.32 | 0.49 | 186 | 449 |
| two classes | 0.35 | 0.70 | 164 | 394 |
| | 0.50 | 0.87 | 133 | 288 |
| three classes | 0.32 | 0.55 | 160 | 376 |
| | 0.42 | 0.65 | 147 | 338 |
| | 0.61 | 0.97 | 83 | 228 |
| four classes | 0.43 | 0.68 | 146 | 344 |
| | 0.62 | 0.98 | 198 | 323 |
| | 0.38 | 0.71 | 75 | 192 |
| | 0.31 | 0.51 | 111 | 363 |

**TABLE 6.15:** THE EFFECT OF CREATING WITHIN-PADDOCK MANAGEMENT CLASSES ON THE STANDARD DEVIATIONS (S.D.) OF CROP YIELDS AND PASTURE TGDM IN "GRANDVIEW" PADDOCKS GV8 AND GV39. 'ONE CLASS' IS TREATING THE WHOLE PADDOCK AS ONE MANAGEMENT UNIT (I.E. UNIFORM MANAGEMENT).

| **"GRANDVIEW"** | **2005 yield s.d. (t/ha)** | **2007 yield s.d. (t/ha)** | **2009 yield s.d. (t/ha)** | **TGDM Sep 2012 s.d. (kg/ha)** | **TGDM Oct 2013 s.d. (kg/ha)** |
|---|---|---|---|---|---|
| GV8 | | | | | |
| one class | 0.32 | 0.40 | 0.34 | 234 | 239 |
| two classes | 0.17 | 0.28 | 0.20 | 194 | 165 |
| | 0.31 | 0.36 | 0.30 | 207 | 256 |
| three classes | 0.16 | 0.25 | 0.22 | 231 | 192 |
| | 0.17 | 0.32 | 0.23 | 187 | 162 |
| | 0.30 | 0.28 | 0.27 | 193 | 251 |
| four classes | 0.17 | 0.23 | 0.19 | 171 | 164 |
| | 0.13 | 0.29 | 0.24 | 232 | 176 |
| | 0.16 | 0.23 | 0.22 | 225 | 197 |
| | 0.27 | 0.28 | 0.29 | 176 | 245 |
| | **2007 yield s.d. (t/ha)** | **2008 yield s.d. (t/ha)** | **2009 yield s.d. (t/ha)** | **TGDM Sep 2012 s.d. (kg/ha)** | **TGDM Oct 2013 s.d. (kg/ha)** |
| GV39 | | | | | |
| one class | 0.38 | 0.77 | 0.74 | 254 | 368 |
| two classes | 0.17 | 0.78 | 0.77 | 164 | 309 |
| | 0.32 | 0.54 | 0.35 | 188 | 238 |
| three classes | 0.29 | 0.54 | 0.36 | 168 | 236 |
| | 0.18 | 0.54 | 0.34 | 135 | 267 |
| | 0.15 | 0.48 | 0.58 | 189 | 278 |
| four classes | 0.18 | 0.53 | 0.31 | 131 | 265 |
| | 0.22 | 0.50 | 0.62 | 128 | 242 |
| | 0.12 | 0.48 | 0.61 | 127 | 267 |
| | 0.28 | 0.53 | 0.33 | 168 | 234 |

## 6.4 DISCUSSION

This chapter tested Hypothesis 2 (Chapter 2, p. 36) that, *"spatial variation of production in the crop and pasture phases of a mixed farming system can be identified and quantified at high resolution using PA technologies".*

There were three main outcomes from the research described in this chapter:

1. Within-paddock variations in pasture biomass production were identified, quantified and mapped at a high resolution using relatively low cost 'on-the-go' sensing technologies commonly used in precision agriculture.
2. The variations in crop yield and pasture green dry matter production within a paddock were generally related to the underlying variability in soil properties and soil chemistry.
3. Crop yield and pasture green dry matter production were used in combination with EMI and elevation data to delineate potential management classes for whole-farm differential management of paddocks in mixed farming systems.

On the basis of the results described in this chapter, there are sufficient grounds to accept Hypothesis 2. The study is unique in that it used high-resolution NDVI pasture scans to estimate pasture TGDM in mixed farming systems involving both volunteer annual pastures in south-west WA and sown perennial pastures in north-east Victoria. NDVI-based pasture measurement studies reported in the literature have mostly been in paddocks that were highly managed monocultures where pasture species distribution was not an issue, e.g. perennial ryegrass (*Lolium perenne* L.) alone or with white clover (*Trifolium repens* L.) in Europe (Schut et al., 2006; Suzuki et al., 2012), fescue (*Festuca arundinacea*) in the USA (Flynn et al., 2008), and fescue or perennial ryegrass/white clover in Australia and New Zealand (Cosby et al., 2016; Edirisinghe et al., 2012; Pullanagari et al., 2011; Trotter et al., 2010).

On both properties, the spatial variation in both crop and pasture yields corresponded strongly with the spatial variation in ECa (and GR sensing in the case of "Milroy") and hence to soil texture changes (Chapter 5, Tables 5.8 and 5.9). Numerous studies have shown that soil texture and soil moisture are primary

drivers of ECa variation in non-saline soils (Brevik et al., 2006; Corwin and Lesch, 2005; Dang et al., 2011; Doolittle and Brevik, 2014; Rodrigues Jr et al., 2015; Sudduth et al., 2005, 2013) and this was reflected in the results from Chapter 5. Crop and pasture production are often strongly reliant on soil type and the ability of the soil to hold water and subsequently release it to the plant. Where rainfall is limited, soil water supply to plants is closely related to plant available water capacity (PAWC) which, in turn, is associated with soil textural changes (Oliver et al., 2006, 2009; Wong and Asseng, 2006). For example, the sites labelled '1' in the "Milroy" M25 and M41 yield maps (Figure 6.7) are both areas of low grain yield and correspond to the ECa and GR interpretation of these areas as deep sand. "Milroy" M25 site 2 and M41 site 4 (Figure 6.7) are high-yielding areas and correspond with the ECa/GR interpretation as sandy clay loam textures.

At "Grandview", crops were under soil moisture stress in most years of this study due to the severe drought occurring across south-eastern Australia. Variability in crop growth from variable soil textures and chemistry is a common feature of the Riverine Plains landscape where "Grandview" is situated (Inchbold et al., 2009). In both GV8 and GV39 in low rainfall years (2007 and 2009), the yields in areas of higher elevation in each paddock, where coarser-textured stony soils occurred (low ECa, e.g. the region of GV8 circled in Figure 6.8 a), were higher than the lower-lying areas of finer-textured clay soils (higher ECa) (Chapter 5, Figure 5.7 and this chapter, Figure 6.8). The area along the eastern side of GV8, marked '1' in Figure 6.8 a, is the lowest part of the paddock and, in the poor rainfall years of 2007 and 2009, had the lowest yields. In a higher rainfall year (2005), this difference in yield was not evident. For paddock GV39, the effect of the drought on crop yields in 2007 and 2008 can be clearly seen in Figure 6.8 d and e. The deep (0–75 cm) ECa map shows an area of high soil moisture in the northern part of the paddock (lowest elevation), which is not picked up by the 0–38 cm EMI scan, but appears to yield well when rainfall is less limiting (2009) and plant roots can access moisture at depth.

Previous research at "Grandview" (Inchbold et al., 2009) reported that, although higher elevated areas of paddocks had low conductivity (low ECa) values and 20% less total water than the areas of high conductivity, the low ECa zones showed

water movement to the greatest depth, indicating an ability of the coarser-textured soils to 'wet up' more quickly. Despite the research being conducted during very dry years, the authors reported that soils showing medium conductivity (mid-range ECa values) always had surplus soil water, leading to the conclusion that rooting depth in these soils was limited by factors other than moisture (e.g. salinity or elevated ESP in subsoils). The farm owner reported little water extraction below 60 cm on the medium ECa soils (Adam Inchbold, pers. comm.). The high conductivity zone had the least water at depth, therefore requiring more moisture to 'wet up'. The authors concluded that, at "Grandview", although the low conductivity areas of a paddock held less water, the water that *was* held was used more effectively by plants through unimpeded root exploration and water extraction to greater depths. This accords with the results being reported in this study, where the coarser soils of the low conductivity areas, which were generally situated in the more elevated parts of the paddock, were the most productive, particularly in the drier years. The farm owner also reported that the elevated areas, although of lower inherent fertility, would yield well with sufficient fertiliser application (Adam Inchbold, pers. comm.).

The spatial variation of the Crop Circle™ pasture NDVI scans in both "Milroy" and "Grandview" paddocks was similar to the spatial variation of crop yield. This was also consistent with the results from the MODIS NDVI study reported in Chapters 3 and 4. That is, areas of the paddocks that had higher relative crop yield were also areas of higher NDVI under pasture in 2012 and 2013 and vice versa. The interpretive value of the much higher resolution scans of pasture obtained with Crop Circle™ is clearly illustrated in the differences between a Pasture Watch™ (MODIS NDVI) map of "Milroy" paddock M25 from September 2012 (Figure 6.11), and the corresponding Crop Circle™ derived NDVI map (Figure 6.9 b). This reinforces the comments made in Chapters 3 and 4 regarding the limitations of MODIS NDVI to provide sufficient detail for comparisons with crop yield monitor data in small paddocks.

At "Grandview", the pattern of variation in NDVI in 2013 was almost identical to crop yield in 2009 (Figure 6.8 f). Predicting TGDM from the Crop Circle™ NDVI scans

revealed strong correlations between NDVI and the harvested pasture biomass, with $R^2$ values between 0.72 and 0.85 across both properties, except "Milroy" M41 in August 2013 ($R^2$ = 0.66) (Tables 6.4 and 6.5). This would indicate that the methodology used here provides a suitable estimate and is (i) fast in comparison to 'traditional' methods for estimating pasture biomass and (ii) robust, whether used on an annual pasture system on the sandy soils of south-west WA, or a perennial pasture system on the clay-based soils of north-east Victoria. Depending on the paddock, prediction errors (RMSE) ranged from 157–533 kg/ha which compared favourably to the more time-consuming traditional methods using devices such as rising plate meters, capacitance meters or pasture rulers. Reported errors for these instruments range from 200–500 kg/ha (Sanderson et al., 2001; Serrano et al., 2011). Hyperspectral sensing on pure ryegrass pastures reported estimation errors between 167 and 477 kg/ha (Schut et al., 2006) and an RMSE of 388 kg/ha (Kunnemeyer et al., 2001).

The high-resolution maps of predicted TGDM derived from Crop Circle™ scans (Figures 6.14 and 6.15) are essentially 'yield maps' of pasture biomass, which can be compared to crop yield maps. The TGDM map for "Milroy" paddock M25 in August 2013 displayed a spatial variation in biomass consistent with the soil texture zones identified by the ECa and GR scanning (Figure 6.14 b and Chapter 5, Figures 5.5 a and b, 5.6 a–d). The spatial variation in TGDM was also consistent with that shown by the crop yield maps for this paddock in 2009 (Figure 6.7 b). A similar situation occurred with "Milroy" M41.

At "Grandview", the general pattern of pasture TGDM variation in both GV8 and GV39 for 2013 (Figure 6.15 b and d) reflects that of crop yield in 2009 (Figure 6.8 c and f). GSR in those years was similar at 245 mm and 254 mm, respectively. In relatively dry years, the areas of low ECa performed well, presumably through deeper root exploration and therefore a longer extraction period leading to better use of the little water that fell. Higher TGDM yields tended to occur on the coarser-textured soils of higher elevation in both paddocks, echoing the situation which occurred in the cropping phase.

The distribution of species within pastures from the DWR analysis highlights the different management requirements of annual and perennial pastures grazed by sheep and cattle, respectively (Figures 6.25–6.27). The typical south-west WA annual pasture composition, dominated by subterranean clover and capeweed, is evident at "Milroy". The species distribution patterns also reflected broad soil texture variations. At "Milroy", capeweed dominated in the less fertile, deep sands, with grasses generally restricted to gravelly margins. The sandy loam soils were dominated by subterranean clover, with some capeweed. Grass species formed a negligible component of the pasture mix at "Milroy" and their presence is actively managed by the farm owner. The presence of grasses in annual pastures and the associated herbicide resistance are an ongoing threat to cereal production. The perennial legume/grass system at "Grandview" has five-year pasture phases. The less-intensive grazing pressure of cattle compared to sheep is reflected in the much higher grass component in the pasture composition maps. The owners of both properties confirmed that the DWR maps reflected their understanding of species distribution across the paddocks. The greater presence of legume pastures in the higher elevation parts of both paddocks is also evident and reflects the variation observed in the cropping phase. The deep rooting capacity of lucerne would appear to enable it to explore for deep moisture in the lighter-textured soil in the higher parts of both GV8 and GV39 at "Grandview".

The inclusion of pasture TGDM, as well as crop yields, into the *k*-means clustering analysis did not significantly change the shape or extent of the management class solutions at either "Milroy" or "Grandview" (Figures 6.28–6.31). The management classes produced conformed with both farm owners' general perceptions regarding the productivity of their paddocks. Incorporating the spatial variability of pasture productivity into the analysis has not materially affected the number, shape or size of management classes for differentially managing variability across both pasture and crop rotations. This provides further evidence in support of Hypothesis 1 that, "*spatial variation in biomass production over time is correlated between the cropping and pasture phases of mixed farming enterprises*".

The results from the *k*-means clustering showed that on both properties there were important differences between management classes, irrespective of whether the paddock was in crop or pasture.

Firstly, there are genuine soil type differences within the same paddock. It is, therefore, reasonable to assume that clustering of crop and pasture TGDM yields with ECa and paddock elevation (which affects water movement) divided the paddocks into zones of similar soil texture and soil moisture condition.

Secondly, these differences influence crop and pasture growth sufficiently to be statistically separated by differences in mean production levels. The *k*-means analysis identified a two-class solution as the only management class outcome having statistically different class means based on crop yield (Tables 6.7–6.14) on all paddocks.

Thirdly, even where there may not be a statistically significant difference for all class means, the clustering process can reveal subtle differences based on ECa/soil texture relationships. So, from a practical farm management perspective, there was evidence to suggest that a uniform management approach across both crop and pasture rotations will not necessarily achieve optimal production and that, at a minimum, two-zone differential management is likely to be highly effective, even on the broken landscapes of “Milroy”. For example, the two-class solution for “Milroy” M25 partitioned the capeweed and clover/barley grass into separate management classes.

It is also noteworthy that the three-class solutions for both “Milroy” paddocks create a third management class by partitioning the low conductivity zone into two classes, with the zone of lowest ECa values having higher mean yields for crop and TGDM than the zone with higher ECa values. Similarly, the three-class solution for “Milroy” M41 split the low conductivity values into two zones that partitioned the less fertile deep sands and gravel soils into one class (areas of lowest ECa), the sandy loam areas (marginally higher ECa values) into a second class, and the saline area into a third, high ECa zone. It also largely partitioned the legume/broadleaf/grass distribution in accordance with the results of the DWR surveys. This is potentially a valuable management tool for decision making around

differential paddock management in the sandy "Milroy" soils. While a two-management zone solution may be statistically optimal for "Milroy", the three-zone solution provides the farm owner with the knowledge to identify and decide whether to separately manage 'problem' soils. This opportunity is not provided by the two-zone solution.

At "Grandview", previous research had identified that the optimal way to differentially manage cropping soils in the Riverine Plains was to 'zone up' based on areas of low, medium and high soil conductivity (P. Baines, pers. comm.). Analysis of the results of the *k*-means clustering for "Grandview" described here, provide evidence for arrival at the same conclusion, but from a different perspective.

## 6.5 CONCLUSION

In this chapter, the use of high-resolution proximally sensed data for both crop grain yield and pasture biomass was used to estimate the within-paddock spatial distribution of production in mixed farming systems, in order to test Hypothesis 2 that, ***"****spatial variation of production in the crop and pasture phases of a mixed farming system can be identified and quantified at high resolution using PA technologies****".*** The evidence from the results in this chapter provides sufficient grounds to accept this hypothesis.

The use of an active optical NDVI sensor such as Crop Circle™ proved effective in calibrating pasture NDVI to pasture TGDM in paddocks, irrespective of whether they were in annual or perennial pasture, with consistently high $R^2$ values. It is important to note that the sensing and measurement of both crops and pastures used equipment and software that already exists on many farms that are using PA technologies. The issue of animal grazing impact on the spatial distribution of TGDM in a paddock was unable to be accounted for. This is less than ideal but was unavoidable given the limited resources and time available.

At both properties, under two entirely different management systems and distinct climatic zones, the *k*-means clustering algorithm identified potential management classes that conformed to general topographical changes and changes in soil type across both landscapes. The management class statistics helped identify and

understand the potential underlying causes of yield variation in both pastures and crops.

The inclusion of some of the environmental data from Chapter 5 (ECa and elevation) in the *k*-means analysis provided stability to the clustering algorithm inputs and gave an indication of potential yields, where rainfall is not limiting. Now, instead of having yield maps based solely on the cropping phase of a rotation, a producer can have a continuous sequence of high-resolution yield data across both crop and pasture phases to allow management decisions to be made with more confidence from a whole-farm perspective. In the following chapter, this data will be used to develop a single paddock index for the identification and management of spatial and temporal stability of both crop and pasture phases in mixed farming systems.

## 6.6 REFERENCES

Brevik, E., Fenton, T., & Lazari, A. (2006). Soil electrical conductivity as a function of soil water content and implications for soil mapping. *Precision Agriculture, 7*(6), 393–404. doi: 10.1007/s11119-006-9021-x

Cayley, J. W. D., & Bird, P. R. (1996). Techniques for measuring pastures: Pastoral and Veterinary Institute Hamilton, Victoria, Australia.

Cook, S. E., & Bramley, R. G. V. (1998). Precision agriculture–opportunities, benefits and pitfalls of site-specific crop management in Australia. *Australian Journal of Experimental Agriculture, 38*(7), 753–763. doi:10.1071/EA97156

Corwin, D. L., & Lesch, S. M. (2005). Characterizing soil spatial variability with apparent soil electrical conductivity: II. Case study. *Computers and Electronics in Agriculture, 46*(1–3), 135–152.

Cosby, A. M., Falzon, G. A., Trotter, M. G., Stanley, J. N., Powell, K. S., & Lamb, D. W. (2016). Risk mapping of redheaded cockchafer (*Adoryphorus couloni*) (Burmeister) infestations using a combination of novel *k*-means clustering and on-the-go plant and soil sensing technologies. *Precision Agriculture, 17*(1), 1–17. doi: 10.1007/s11119-015-9403-z

Cupitt, J., & Whelan, B. (2001). *Determining potential within-field crop management zones.* Paper presented at the 3rd European Conference on Precision Agriculture, Montpellier, France.

Dang, Y. P., Pringle, M. J., Schmidt, M., Dalal, R. C., & Apan, A. (2011). Identifying the spatial variability of soil constraints using multi-year remote sensing. *Field Crops Research, 123*(3), 248–258. doi: 10.1016/j.fcr.2011.05.021

Doolittle, J. A., & Brevik, E. C. (2014). The use of Electromagnetic Induction techniques in soils studies. *Geoderma, 223*, 33–45.

Edirisinghe, A., Clark, D., & Waugh, D. (2012). Spatio-temporal modelling of biomass of intensively grazed perennial dairy pastures using multispectral remote sensing. *International Journal of Applied Earth Observation and Geoinformation, 16*, 5–16.

Florin, M. J., McBratney, A. B., & Whelan, B. M. (2009). Quantification and comparison of wheat yield variation across space and time. *European Journal of Agronomy, 30*(3), 212–219. doi: 10.1016/j.eja.2008.10.003

Flynn, E. S., Dougherty, C. T., & Wendroth, O. (2008). Assessment of pasture biomass with the normalized difference vegetation index from active ground-based sensors. *Agronomy Journal, 100*(1), 114.

Goel, N. S. & Qin, W. (1994). Influences of canopy architecture on relationships between various vegetation indices and LAI and FPAR: a computer simulation. *Remote Sensing Reviews*, *10*(4), 309–347.

Gong, P., Pu, R., Biging, G. S., & Larrieu, M. R. (2003). Estimation of forest leaf area index using vegetation indices derived from Hyperion hyperspectral data. *IEEE Transactions on Geoscience and Remote Sensing, 41*(6), 1355–1362. doi: 10.1109/TGRS.2003.812910

Huete, A. R. (1988). A soil-adjusted vegetation index (SAVI). *Remote Sensing of Environment, 25*(3), 295–309.

Inchbold, A., Whelan, B., & Baines, P. (2009). Making money out of precision agriculture. *Improving winter cropping systems in the Riverine Plains*. Yarrawonga, Victoria: Riverine Plains Inc.

Jones, R. M., & Hargreaves, J. N. G. (1979). Improvements to the dry-weight-rank method for measuring botanical composition. *Grass and Forage Science, 34*(3), 181–189. doi: 10.1111/j.1365-2494.1979.tb01465.x

Künnemeyer, R., Schaare, P. N., & Hanna, M. M. (2001). A simple reflectometer for on-farm pasture assessment. *Computers and Electronics in Agriculture, 31*(2), 125–136. doi: http://dx.doi.org/10.1016/S0168-1699(00)00168-X

Laca, E. A. (2009). New approaches and tools for grazing management. *Rangeland Ecology & Management, 62*(5), 407–417. doi: 10.2111/08-104.1

Lee, H. J., Kawamura, K., Watanabe, N., Sakanoue, S., Sakuno, Y., Itano, S., & Nakagoshi, N. (2011). Estimating the spatial distribution of green herbage biomass and quality by geostatistical analysis with field hyperspectral measurements. *Grassland Science, 57*(3), 142–149.

Lifetime Wool. (2006). *Optimum Ewe Condition Score Profile — Cereal Sheep Zone Western Australia*. Retrieved from http://www.lifetimewool.com.au /Sheep%20Zones/zonecerealsheepwa.aspx

Marques Da Silva, J. R., Peça, J. O., Serrano, J. M., De Carvalho, M. J., & Palma, P. M. (2008). Evaluation of spatial and temporal variability of pasture based on topography and the quality of the rainy season. *Precision Agriculture, 9*(4), 209–229.

Oliver, Y., Wong, M., Robertson, M. J., & Wittwer, K. (2006). *PAWC determines spatial variability in grain yield and nitrogen requirement by interacting with rainfall on northern WA sandplain*. Paper presented at the 13th Australian Agronomy Conference, "Groundbreaking Stuff", Perth, WA.

Oliver, Y. M., Robertson, M. J., Stone, P. J., & Whitbread, A. (2009). Improving estimates of water-limited yield of wheat by accounting for soil type and within-season rainfall. *Crop and Pasture Science, 60*(12), 1137–1146. doi:10.1071/CP09122

Pullanagari, R. R., Yule, I., King, W., Dalley, D., & Dynes, R. (2011). The use of optical sensors to estimate pasture quality. *International Journal on Smart Sensing and Intelligent Systems, 4*(1), 125–137.

Rodrigues Jr, F. A., Bramley, R. G. V., & Gobbett, D. L. (2015). Proximal soil sensing for Precision Agriculture: simultaneous use of electromagnetic induction and gamma radiometrics in contrasting soils. *Geoderma, 243–244*, 183–195. doi: http://dx.doi.org/10.1016/j.geoderma.2015.01.004

Rouse, J. W., Haas, R. H., Schell, J. A., & Deering, D. W. (1973). *Monitoring vegetation systems in the Great Plains with ERTS.* Paper presented at the Third Earth Resources Technology Satellite–1 Symposium, Washington, DC.

Sanderson, M. A., Rotz, C. A., Fultz, S. W., & Rayburn, E. B. (2001). Estimating forage mass with a commercial capacitance meter, rising plate meter, and pasture ruler. *Agronomy Journal, 93*(6), 1281–1286. doi: 10.2134/agronj2001.1281

Schut, A. G. T., van der Heijden, G. W. A. M., Hoving, I., Stienezen, M. W. J., van Evert, F. K., & Meuleman, J. (2006). Imaging spectroscopy for on-farm measurement of grassland yield and quality. *Agronomy Journal, 98*(5), 1318–1325. doi: 10.2134/agronj2005.0225

Serrano, J. M., Peça, J. O., Marques da Silva, J., & Shahidian, S. (2011). Calibration of a capacitance probe for measurement and mapping of dry matter yield in mediterranean pastures. *Precision Agriculture, 12*(6), 860–875.

Serrano, J. M., Peça, J. O., Marques da Silva, J. R., & Shaidian, S. (2010). Mapping soil and pasture variability with an electromagnetic induction sensor. *Computers and Electronics in Agriculture, 73*(1), 7–16.

Sudduth, K. A., Kitchen, N. R., Wiebold, W. J., Batchelor, W. D., Bollero, G. A., Bullock, D. G., . . . Thelen, K. D. (2005). Relating apparent electrical conductivity to soil properties across the north-central USA. *Computers and Electronics in Agriculture, 46*(1–3), 263–283.

Sudduth, K. A., Myers, D. B., Kitchen, N. R., & Drummond, S. T. (2013). Modeling soil electrical conductivity–depth relationships with data from proximal and penetrating ECa sensors. *Geoderma, 199*, 12–21. doi: http://dx.doi.org/10.1016/j.geoderma.2012.10.006

Suzuki, Y., Okamoto, H., Takahashi, M., Kataoka, T., & Shibata, Y. (2012). Mapping the spatial distribution of botanical composition and herbage mass in pastures using hyperspectral imaging. *Grassland Science, 58*, 1–7.

Taylor, J. A., McBratney, A. B., & Whelan, B. M. (2007). Establishing management classes for broadacre agricultural production. *Agronomy Journal, 99*(5), 1366–1376. doi: 10.2134/agronj2007.0070

Trotter, M. G. (2010). *Precision agriculture for pasture, rangeland and livestock systems*. Paper presented at the 15th Australian agronomy conference "Food Security from Sustainable Agriculture" Lincoln, New Zealand.

Trotter, M. G., Lamb, D. W., Donald, G. E., & Schneider, D. A. (2010). Evaluating an active optical sensor for quantifying and mapping green herbage mass and growth in a perennial grass pasture. *Crop and Pasture Science, 61*(5), 389–398.

Trotter, T. F., Frazier, P., Trotter, M. G., & Lamb, D. W. (2008). *Objective biomass assessment using an active plant sensor (Crop Circle), preliminary experiences on a variety of agricultural landscapes*. Paper presented at the 9th International Conference on Precision Agriculture, Denver Colorado.

Virgona, J., & Hackney, B. (2008). *Within-paddock variation in pasture growth: landscape and soil factors.* Paper presented at the 14th Australian Agronomy Conference, "Global Issues, Paddock Action", Adelaide, South Australia.

Whelan, B., & Taylor, J. (2013). *Precision Agriculture for Grain Production Systems*: CSIRO Publishing.

Whelan, B. M., & McBratney, A. B. (2003). *Definition and interpretation of potential management zones in Australia*. Paper presented at the 11th Australian Agronomy Conference: "Solutions for a better environment", Geelong, Victoria.

Whelan, B. M., McBratney, A. B., & Minasny, B. (2001). *Vesper 1.5–spatial prediction software for precision agriculture.* Paper presented at the 3rd European Conference on Precision Agriculture, Montpellier, France.

Wong, M. T. F., & Asseng, S. (2006). Determining the causes of spatial and temporal variability of wheat yields at sub-field scale using a new method of upscaling a crop model. *Plant and Soil, 283*(1–2), 203–215.

Zhao, D., Starks, P. J., Brown, M. A., Phillips, W. A., & Coleman, S. W. (2007). Assessment of forage biomass and quality parameters of bermudagrass using proximal sensing of pasture canopy reflectance. *Grassland Science, 53*(1), 39–49.

# CHAPTER 7. DEVELOPMENT OF A SINGLE PADDOCK INDEX TO DEFINE CROP AND PASTURE VARIABILITY OVER TIME

## 7.1 INTRODUCTION

The underlying objective of this body of research was to use precision agriculture (PA) technologies to identify and measure spatial variation in the pasture phases of two mixed farming systems and then integrate this knowledge with existing crop yield data to facilitate whole-of-farm management at the sub-paddock scale.

Chapters 5 and 6 described the acquisition and analysis of high-resolution paddock data to help identify and investigate the factors contributing to spatial variability in both crop and pasture yields. Chapter 6 described a methodology for measuring pasture biomass production at a fine scale so that it could be compared to crop yield at the same point. Chapter 6 also extended the traditional analysis of crop management zones by incorporating pasture yield as well as crop yield data to create common management classes across both crop and pasture phases. The identification and use of management zones is a popular PA strategy for managing spatial variability in a system of 'site-specific management' (SSM) (Plant, 2001; Taylor et al., 2007). However, experience has indicated that spatial variation in yield is not always consistent, but influenced by seasonal variations and often temporally unstable (McBratney et al., 1997; Wong and Asseng, 2006). Nuttall and Armstrong (2006) found that grain and grain legume crops in the Mallee (north-western Victoria) on clay loam soils 'flip-flopped' between high, medium or low yielding in different years, thus opening 'a Pandora's box of uncertainty' for the agronomic interpretation of yield maps (Cook and Bramley, 2001).

These anomalous interactions were put down to interactions between rainfall, soil microrelief and crop type. While Chapter 6 focused on the spatial variation of crop and pasture production within a paddock, this chapter explores the temporal variation of pasture and crop production by calculating productive stability in two paddocks at "Milroy" and two at "Grandview". In doing so, it will test Hypothesis 3

(Chapter 2, p. 36) that, *"data acquired using PA technologies can be used to create a single index of paddock productivity that describes the spatial variation in, and temporal stability of, crop and pasture production over time".*

The assessment of temporal stability is important because it affects the reliability of management zones as a strategy for differential management in crop and pasture phases. At present, no research is reported in the literature about the similarities of spatial and temporal variation between cropping and pasture phases within the same paddock and whether or not it would be feasible to manage such variability in combination with crops in a site-specific way. To determine the temporal stability of yield patterns, a methodology is required to enable comparisons between different years.

Several approaches have been used to identify regions of temporal stability in crops (Blackmore, 2000; Blackmore et al., 2003; Dobermann et al., 2003; Marques da Silva, 2006) and in pastures (Marques da Silva et al., 2008; Serrano et al., 2011; Xu et al., 2006). These approaches used an averaged standardised yield combined with an arbitrarily defined threshold value of the coefficient of variation, standard deviation, or variance. Lawes et al. (2009) used regression against both yield means and growing season rainfall to characterise spatio-temporal variation in crops alone.

In the work described here, inter-annual spatial variability maps of both crop and pasture production were obtained following the methodology of Blackmore (2000) by calculating the standardised temporal arithmetic mean of crop or pasture yield using the data from Chapter 6. While Blackmore's analysis was concerned with either mixed crops (2000) or cereal crops only (2003), the analysis presented here is unique in that it includes both crop and pasture yield data. By combining both crop and pasture data, significant knowledge gaps are filled for the farm manager, who currently only has crop yield data to make decisions about paddock management.

## 7.2 MATERIALS AND METHODS

### *7.2.1 STUDY SITES*

The study sites were the same as those described previously (Chapter 3, pp. 58–61 and Chapter 6, pp. 167–168).

### *7.2.2 CALCULATING THE SPATIAL TREND OF YIELD*

Crop rotations at "Milroy" and "Grandview" included cereals (wheat) and oilseed (canola) crops as well as annual ("Milroy") and perennial ("Grandview") pastures (Table 7.1). The crop yield and pasture TGDM data had already been kriged to a regular grid (Chapter 6, pp. 168–170). The spatial trend of yield for crops and pastures was determined by averaging the yield at each grid point over a sequence of yield maps. Since different crops were involved in some rotations at "Grandview", and because of the large absolute difference in yield potential between cereals and oilseeds, a simple averaging technique (i.e. summing the yield values at a point over *x* years and dividing by *x*) could not be used to calculate the yield trends for crops and pastures. Therefore, the yield data was standardised to remove the yield units, replacing them with a relative percentage yield that allowed comparison between crops and pastures. The standardised yield was calculated as per Blackmore (2000) as follows:

$$s_i = \left(\frac{y_i}{\bar{y}}\right) \times 100 \qquad (1)$$

where $s_i$ is the standardised crop or pasture yield (%) at point *i*; $y_i$ is the interpolated yield at point *i*; and $\bar{y}$ is the mean yield for that year.

The point mean was then calculated over the years of interest, enabling different crops or pasture to be included and compared:

$$\bar{s}_i = \left(\sum_{t=1}^{n} s_{i,t}\right)/n \qquad (2)$$

where $\bar{s}_i$ is the average of $s_i$ , the standardised yield at point *i*, over *n* years.

This standardised yield shows, at any point, in any one year, how the yield differs from the paddock mean (100%). The standardised data were then classified into four yield zones in relation to the relative percentage difference from the paddock mean (100%); the areas for which this value was greater than the paddock mean

were classified as 'above average' (AA) and 'relatively high yielding' (RHY), while the areas for which this value was less than 100% were defined as 'below average' (BA) and 'relatively low yielding' (RLY). The yield data distribution quartiles were used to define the yield categories. The standardised yield data was then imported into ArcGIS 10.2 (Environmental Systems Research Institute, Redlands, California) and mapped to a standard square 5 m x 5 m grid. The data was interpolated to the grid with Vesper 1.62 using an exponential variogram and a block size of 10 m x 10 m. Interpolated data was then converted to raster surfaces in ArcGIS 10.2 to produce yield maps of standardised data for each year of crop grain yield and each year of pasture DM yield.

Spatial trend yield maps were then created by averaging the standardised yield at each grid cell over the years being considered (effectively 'combining' yield maps) and processed in ArcGIS 10.2. These spatial trend maps show the spatial yield pattern in a paddock over time for both crops and pastures.

### *7.2.3 TEMPORAL STABILITY*

The temporal stability of crop or pasture production comprises two elements. The first is the variation that occurs between the paddock mean yield from year to year. Blackmore (2000) referred to this as the 'inter-year offset' and defined it as the difference between the mean yield value between two years in the same paddock. The largest driver of this variation in temperate-climate cropping zones is variability in annual rainfall (Turner and Asseng, 2005).

The second temporal effect involves situations in which a particular part of a paddock produces above average yield in one year and below average yield in another year, irrespective of rainfall. This alternating pattern of relative grain yield has been referred to as the 'flip-flop effect' (Nuttall and Armstrong, 2006). Blackmore et al. (2003) termed this variation the 'temporal variance at a single point'.

### *7.2.4 CALCULATING TEMPORAL STABILITY*

To estimate how stable in time the crop and pasture yields were at "Milroy" and "Grandview", the coefficient of variation (CV) in yield was calculated at each point

in the paddock for which there was a yield value for either grain yield or pasture TGDM, following the procedure developed by Blackmore (2000). In his later work, Blackmore (2003) used standard deviation rather than CV. However, in that study, Blackmore was dealing with paddocks of a single crop (wheat). In the research reported here, multiple crops were sometimes involved (wheat and canola) as well as pasture. The advantage of using CV is that it is unit-less. This allows the CVs of multiple crops and pastures to be compared with each other, which is not the case for standard deviation or root mean squared residuals.

For multiple crops, the CV was calculated from the standardised yield values calculated previously, using the equation from Blackmore (2000):

$$\mathrm{CV}s_i = \frac{\left(\frac{n\sum_{t=1}^{n} s_{i_t}^2 - \left(\sum_{t=1}^{n} s_{i_t}\right)^2}{n(n-1)}\right)^{0.5}}{\bar{s}_i} \times 100 \qquad (3)$$

where CV$s_i$ is the coefficient of variation of the standardised data at point *i*, over *n* years.

Using this equation, the CVs of crop grain yield and pasture TGDM yield were calculated for "Milroy" paddocks M25 and M41 and "Grandview" paddocks GV8 and GV39, for both cropping and pasture phases for the years with sufficient data (Table 7.1).

**TABLE 7.1:** CROP YIELD AND PASTURE TGDM DATA USED FOR CALCULATING THE PADDOCK STABILITY INDICES FOR "MILROY" AND "GRANDVIEW".

| Paddock | 2004 | 2005 | 2007 | 2008 | 2009 | 2012 | 2013 | 2014 |
|---|---|---|---|---|---|---|---|---|
| **"MILROY"** | | | | | | | | |
| M25 | wheat | | | | wheat | pasture | pasture | |
| M41 | | | | wheat | | pasture | pasture | wheat |
| **"GRANDVIEW"** | | | | | | | | |
| GV8 | | canola | wheat | | wheat | pasture | pasture | |
| GV39 | | | canola | wheat | wheat | pasture | pasture | |

The CV data for crop yields and pasture DM yields were imported into ArcGIS 10.2 (ESRI, Redlands, California) and mapped to a standard square 5 m x 5 m grid and interpolated using Vesper 1.62 as previously described. The interpolated data was then converted to raster surfaces in ArcGIS 10.2 to produce maps showing the range of CV values (%) across each paddock for crop grain yield and pasture TGDM yield. The CV shows a low value if a particular area of the paddock has a yield value that is always close to the mean. These areas can be considered areas of stable yield (less dispersed) in temporal terms. If the yield in other areas of the paddock sometimes approaches the mean and sometimes deviates from it, then these can be regarded as areas of temporally unstable yield. The temporal stability maps can then be classified into stable yield zones and unstable yield zones when a given temporal CV value (threshold) is adopted to subdivide the two zones.

A threshold value for the temporal CV of 30% was used by Blackmore (2000) for cereal crops, and two threshold values (15 and 25%) were used by Xu et al. (2006) and Serrano et al. (2011), respectively, for grassland. Blackmore (2000) concluded that his use of a CV of 30% to define these two zones was too high, as it resulted in no zones being regarded as unstable for all fields and years of his study.

For this current work, rather than selecting an arbitrary value, the mean CV value for crop yield and pasture TGDM distributions for each paddock were calculated in JMP 12.2 and used as threshold values.

### *7.2.5 CREATING A SPATIAL AND TEMPORAL TREND MAP*

By combining the data behind the spatial trend maps and the temporal stability, a single representation of each paddock over time and across rotations (i.e. both crop and pasture–livestock phases) can be arrived at by classifying the paddock into four categories based on yield (high or low) and stability (stable or unstable) at a point in time. The four classes are described in Table 7.2. Because yield and stability are not mutually exclusive variables, there are four possible combinations for these two variables: high and stable (HS); high and unstable (HUS); low and stable (LS), and low and unstable (LUS).

Crop grain and pasture TGDM yields were considered high if a particular point value was above the mean (>100%) and vice versa. The stability of yield at that point was compared to a threshold value—in this case, the mean of the distribution of yield CV values for the paddock—to determine if the yield at that point was stable (<mean CV) or unstable (>mean CV) (Table 7.2).

The spatial trend and temporal stability categories for the crop and pasture rotations were then concatenated to create an overall stability index for each paddock. Mapping this index shows areas of the paddock that are high and stable in both crop and pasture yield, areas that are high and unstable, etc. Because the crop and pasture maps will never correlate perfectly, there are areas that are neither HS, HUS, LS nor LUS in the overall stability map, leaving areas that are uncategorised. These areas were filled in by adding, firstly, areas that were high and stable in crop and low and stable in pasture and vice versa (HLS) and, secondly, areas that were high and unstable in crop and low and unstable in pasture and vice versa (HLUS).

### *7.2.6 CORRELATION BETWEEN PADDOCK STABILITY ZONES AND SOIL CHEMICAL AND TEXTURAL PROPERTIES*

The results of geo-located soil tests which were mapped in Chapter 5 (Figures 5.16–5.19) were overlain on the stability index maps to see if there were any correlations between particular paddock stability zones and soil test values which might indicate if soil constraints may be influencing zone partitioning.

Because there were relatively few soil test sites per paddock, the EMI data (Chapter 5, p. 115) was also tested. EMI is an indicator of soil textural change and was measured at the same scale and same paddock points as both pasture and crop yields.

**TABLE 7.2:** STABILITY INDEX (SI) CLASS CODES AND THE CONDITIONS FOR MEETING A CLASS (FROM BLACKMORE, 2000).

| Management class (code) | Condition 1 | Condition 2 |
|---|---|---|
| High and stable (HS) | $\bar{s}_i$ >100 | $\mathrm{CV}s_i$ < mean CV |
| High and unstable (HUS) | $\bar{s}_i$ >100 | $\mathrm{CV}s_i$ > mean CV |
| Low and stable (LS) | $\bar{s}_i$ <100 | $\mathrm{CV}s_i$ < mean CV |
| Low and unstable (LUS) | $\bar{s}_i$ <100 | $\mathrm{CV}s_i$ > mean CV |

### *7.2.7 STATISTICAL ANALYSIS*

Because of the large number of data points in each paddock (>15,000), a representative sample of points was used for the statistical analyses. Randomised points were generated in ArcGIS across all four stability zones in each paddock using the standardised crop yield data. The number of points generated was proportional to the area of each zone, with the smallest zone within a paddock always having a minimum of 30 points. Crop and pasture TGDM and CV values for these points were extracted in ArcGIS. The pasture TGDM and CV values were then tested against the crop yield and CV point values at each random point.

For each paddock, analyses were conducted on that paddock's random dataset to compare the relationships across all four zones (HS, HUS, LS and LUS). Since the stability indices are categorical data, a Chi-squared analysis was used. Not all of the datasets were from normal distributions, so non-parametric analysis was used—in this case Spearman's rho—to test correlation of the whole dataset, using JMP 12.2. The Kruskal–Wallis one-way ANOVA test (Kruskal and Wallis, 1952) was used to test for differences between stability zones using the R statistical package (v3.2.4). The script used in "R" is in Appendix 19.

The Kruskal–Wallis test computes a test statistic and P-value (assuming a Chi-square distribution) as well as pairwise comparisons at a specified alpha level (0.05 in this case). For the Kruskal–Wallis tests, the null hypothesis was that the medians of all zones were equal, and the alternative hypothesis was that the population median of

at least one zone was different from the population median of at least one other zone.

The following combinations were tested for each paddock: crop yield, pasture yield, crop yield CV, pasture yield CV, crop yield minus pasture yield, and crop CV minus pasture CV, with the stability zones as the categorical variable in each case. The expectation was that: (i) the medians of the standardised values for the high-yielding zones (HS and HUS) would be similar as would yields in the two low-yielding zones (LS and LUS) but that the yield medians between both groups (HS, HUS) and (LS, LUS) would differ. For the stability measure (coefficient of variation), the expectation was that the medians of CV for the stable zones (HS and LS) would be similar as would the unstable zones (HUS and LUS) and that the CV medians between both groups (HS, LS) and (HUS, LUS) would differ.

The EMI data was tested by using the same randomised points as those for crop and pasture yields described above, but substituting the corresponding ECa value and testing that with Kruskal–Wallis for comparisons between stability zones (HS, HUS, LS and LUS) and ECa values to see if the EMI results could explain any differences between the zones.

### *7.2.8 CORRELATION ANALYSIS OF POINT VALUES FOR CROP GRAIN YIELD AND PASTURE DRY MATTER PRODUCTION*

To see if there was any relationship between crop and pasture yields at a point, a correlation analysis was conducted using JMP 12.2 on between-year crop yields and pasture TGDM yields for each paddock.

## 7.3 RESULTS

### *7.3.1 INTER-ANNUAL SPATIAL VARIABILITY MAPS*

The maps of spatial variability of standardised yield over time for both crop and pasture are presented in Figure 7.1 for each “Milroy” paddock and Figure 7.2 for each “Grandview” paddock. Yields were categorised by quartiles of yield data distribution and coded as relatively low yielding (1$^{st}$ quartile), below average (2$^{nd}$ quartile), above average (3$^{rd}$ quartile) and relatively high yielding (4$^{th}$ quartile).

### *7.3.2 TEMPORAL VARIABILITY MAPS*

The maps of temporal variability of standardised yield over time for both crop and pasture are presented in Figure 7.3 for each “Milroy” paddock and Figure 7.4 for each “Grandview” paddock.

### *7.3.3 STABILITY INDEX MAPS (SPATIAL AND TEMPORAL TREND MAPS)*

The stability index maps for both crop and pasture phases are shown at Figure 7.5 for “Milroy” paddocks M25 and M41 and Figure 7.6 for Grandview paddocks GV8 and GV39. In these maps, the data from the spatial trend and temporal stability maps have been combined into four classes—high or low yielding depending on whether the data value was above or below the spatial mean, and stable or unstable depending on whether the data value was above or below the stability threshold. The stability thresholds used in each paddock are shown in Table 7.3. Figure 7.7 illustrates the process used to create these maps.

Figures 7.8–7.11 show the overall paddock stability maps which combine the crop and pasture spatial trend and temporal stability data into one map. In each figure, map (a) shows areas of the paddock where the yields for both crop and pasture, over time, responded in a similar fashion—either high yield and stable (HS), high yield and unstable (HUS), low yield and stable (LS) or low yield and unstable (LUS). The areas of the map that remain uncoloured represent other combinations of yield and stability other than HS, HUS, LS or LUS zones. Map (b) shows the stability zones from map (a) (HS, HUS, LS or LUS) plus those areas of the paddock that were always temporally stable (where CV < mean), but flip-flopped in terms of yield for crop and pasture (e.g. HS for crop and LS for pasture, or vice versa). These areas are designated HLS on the maps, i.e. areas that are high or low yielding, but stable. Map (c) is map (b) with the added inclusion of all zones that are temporally unstable (where CV > mean), i.e. either HUS in crop and LUS in pasture, or vice versa. So zones with green tones are showing stable areas of the paddock whereas red/yellow tones are showing unstable areas.

### *7.3.4 CORRELATION BETWEEN PADDOCK STABILITY ZONES AND SOIL CHEMICAL AND TEXTURAL PROPERTIES*

Examples of the soil test maps overlain on stability index are in Figure 7.12. The remaining overlain maps are in Appendices 20–23. There were no clear correlations between stability zones and soil test results. Unfortunately, the soil tests were conducted 12–18 months prior to the stability zones being delineated so soil tests did not target particular stability zones.

### *7.3.5 STATISTICAL ANALYSIS*

*"Milroy" (Table 7.4)*

The Spearman's rho correlation revealed a moderately strong, statistically significant relationship in paddock M41 between the standardised values for crop yield and pasture TGDM for the randomised points ($\rho$=0.66, P<0.0001, N=262) (Figure 7.13), but the relationship in paddock M25 was poor ($\rho$=0.25, P<0.0004, N=199).

The Kruskal–Wallis one-way ANOVA showed that the stability index categories (HS, HUS, LS, LUS) for paddock M41 had significantly different medians for most of the differences between high and low yield zones and stable and unstable zones (Table 7.4). This was also the case when yield differences (crop yield minus pasture yield) were tested. The exception was M41 pasture median TGDM stability (CV). In M25, crop yield medians differed significantly between high- and low-yielding areas, but pasture TGDM median differences did not differ between HS, HUS, LS and LUS. The same situation occurred with M25 pasture TGDM stability (Table 7.4). However, even where the Kruskal–Wallis test did not identify one median as being significantly different, median values were still generally grouped along yield or stability categories. For example, the pasture yield medians for M25, although not significantly different, were (103.4 and 102.3) for high yielding and (97.4 and 96.7) for low yielding. The stability difference between crop and pasture in M41 (crop CV minus pasture CV) were stable (3.2 and 6.6) and unstable (11.4 and 14.8) even though these median values in each case did not statistically differ (Table 7.4).

*"Grandview" (Table 7.5)*

The Spearman's rho correlation revealed a statistically significant relationship between the standardised values for crop yield and pasture TGDM for the randomised points for both paddock GV8 ($\rho$=0.57, P<0.0001, N=253) and GV39 ($\rho$=0.66, P<0.0001, N=192).

The Kruskal–Wallis one-way ANOVA showed that paddock GV8 had significantly different medians for both crop yield and pasture TGDM between high- and low-yielding areas. Crop yield medians differed, but were grouped into stable (6.7 and 9.7) and unstable (15.0 and 20.6) values (Table 7.5). The same result occurred with yield differences, with high yielding (8.5 and 7.2) and low yielding (10.8 and 12.9) (Table 7.5). This grouping was not apparent with pasture CV or crop–pasture CV differences.

The results for paddock GV39 showed a similar outcome, with crop yield and pasture TGDM yield partitioned to discrete high- and low-yielding areas. Crop and pasture stability medians did not always show significant differences between stable and unstable areas, but both were grouped correctly (Table 7.5). For example, crop CV values for stable (12.0 and 16.7) and unstable (29.4 and 30.5). The same occurred with crop–pasture differences, with yields falling into high (10.1 and 13.8) and low (14.9 and 17.3) and stable (6.3 and 12.3) and unstable (19.1 and 17.2).

*EMI data (Table 7.6): "Milroy"*

The Kruskal–Wallis test showed that no ECa median values differed from any of the others across the four stability zone categories for paddock M25. In paddock M41, the Kruskal–Wallis test on ECa shallow (0–50 cm) showed significant differences between the medians of (HS and HUS), (HS and LUS), (HUS and LS) and (LS and LUS). In the 0–100 cm range, there were significant differences between the medians of (HS and LS), (HUS and LS) and (LS and LUS).

*EMI data (Table 7.6): "Grandview"*

In paddock GV8, the Kruskal–Wallis test for ECa at 0–38 cm depth showed significant differences in the medians for (HS and LS), (HUS and LS) and (HUS and

LUS). At 0–75 cm, there were significant differences in the medians for (HS and HUS), (HS and LS), (HUS and LS) and (HUS and LUS). For paddock GV39, ECa 0–38 cm showed significant differences between the medians for (HS and LS) and (HS and LUS). At 0–75 cm, there were significant differences between the medians for (HS and LS), (HS and LUS), (HUS and LS) and (HUS and LUS).

**TABLE 7.3:** STABILITY THRESHOLDS USED IN THE CALCULATION OF STABILITY INDICES FOR "MILROY" AND "GRANDVIEW" PADDOCKS. IN EACH CASE, THE MEAN VALUE OF THE DISTRIBUTION OF CV VALUES FOR CROP OR PASTURE WERE USED.

| Property | Paddock | Stability threshold | |
|---|---|---|---|
| | | Crop | Pasture |
| "MILROY" | M25 | 18% | 21% |
| | M41 | 13% | 13% |
| "GRANDVIEW" | GV8 | 13% | 12% |
| | GV39 | 22% | 12% |

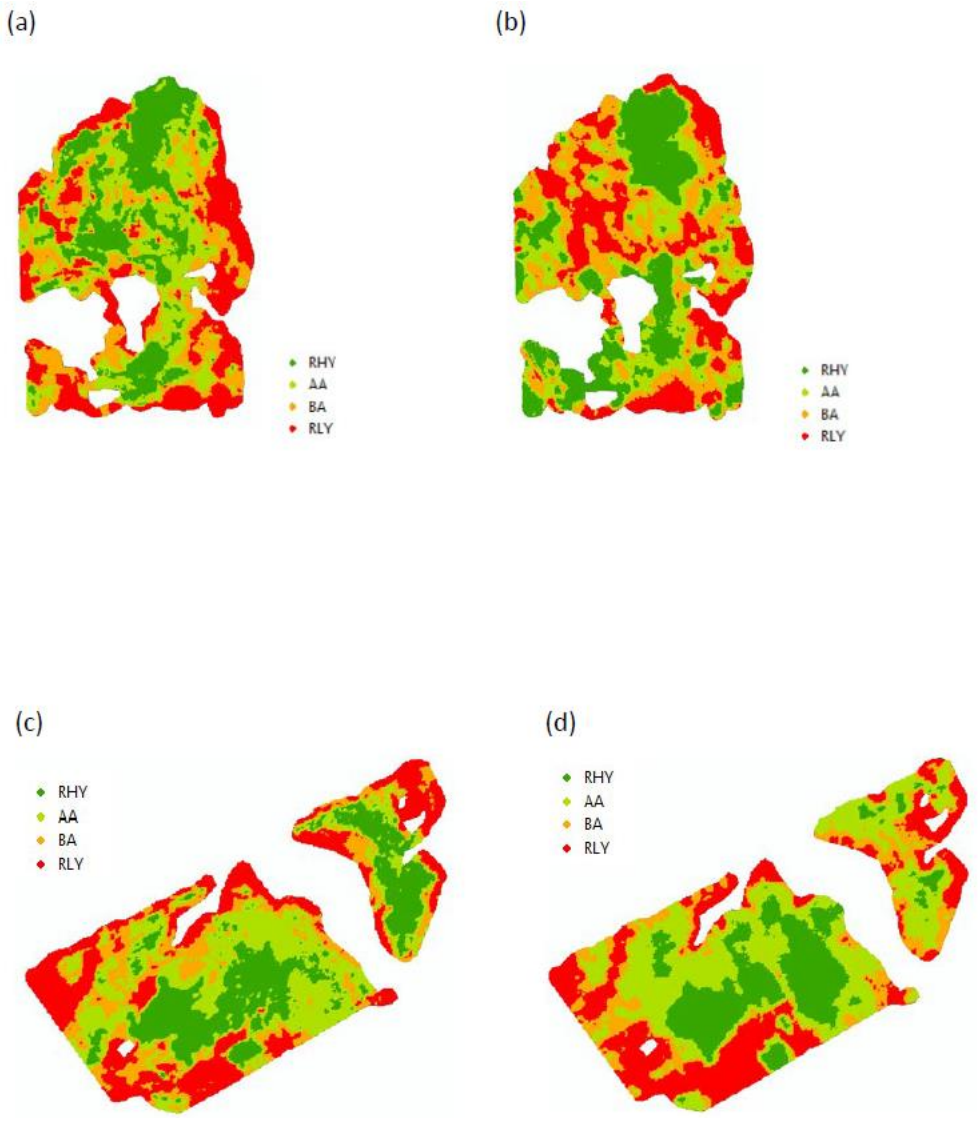


**FIGURE 7.1:** MAPS OF MEAN STANDARDISED YIELD DATA FOR "MILROY" PADDOCKS M25 (A) CROP YIELD AND (B) PASTURE TGDM, AND M41 (C) CROP YIELD AND (D) PASTURE TGDM. RHY = RELATIVELY HIGH YIELDING, AA = ABOVE AVERAGE YIELD, BA = BELOW AVERAGE YIELD AND RLY = RELATIVELY LOW YIELDING. CATEGORIES ARE BASED ON QUARTILES.

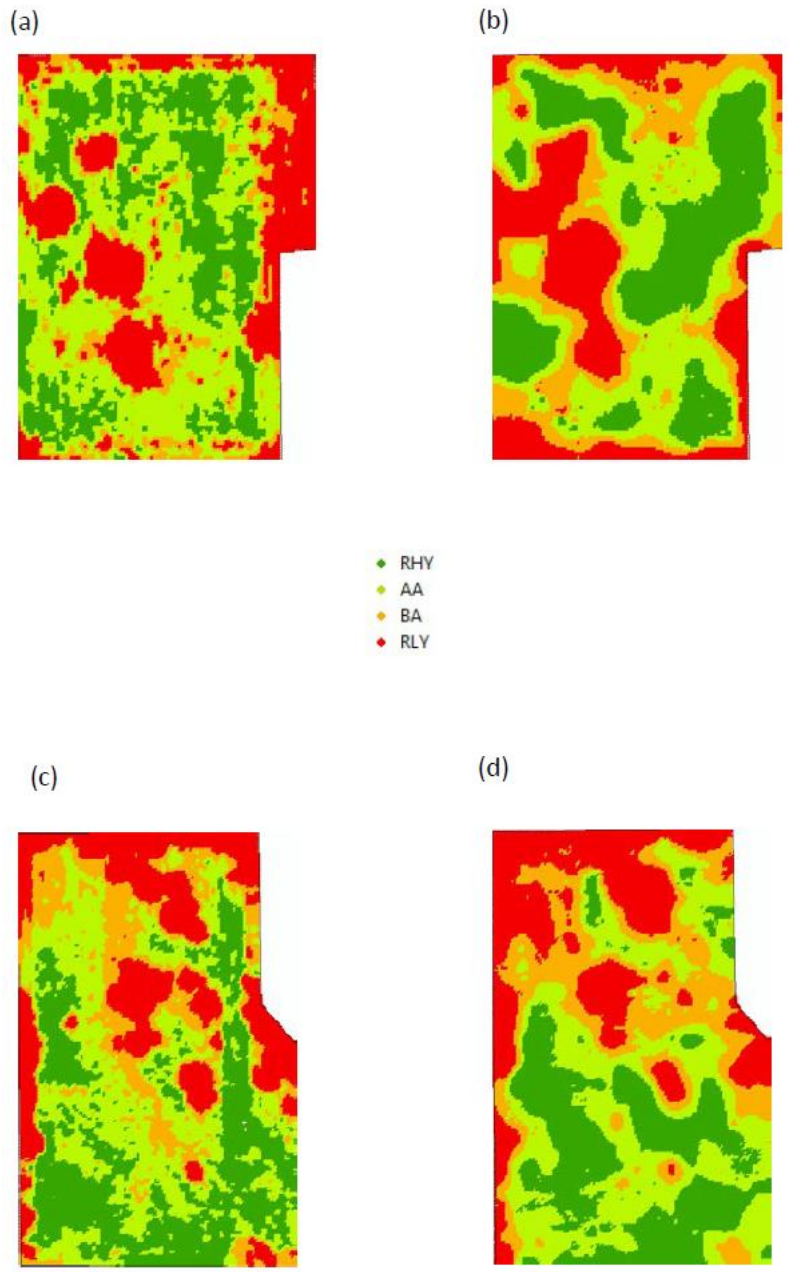


**FIGURE 7.2:** MAPS OF MEAN STANDARDISED YIELD DATA FOR "GRANDVIEW" PADDOCKS GV8 (A) CROP YIELD AND (B) PASTURE TGDM, AND GV39 (C) CROP YIELD AND (D) PASTURE TGDM. RHY = RELATIVELY HIGH YIELDING, AA = ABOVE AVERAGE YIELD, BA = BELOW AVERAGE YIELD AND RLY = RELATIVELY LOW YIELDING. CATEGORIES ARE BASED ON QUARTILES.

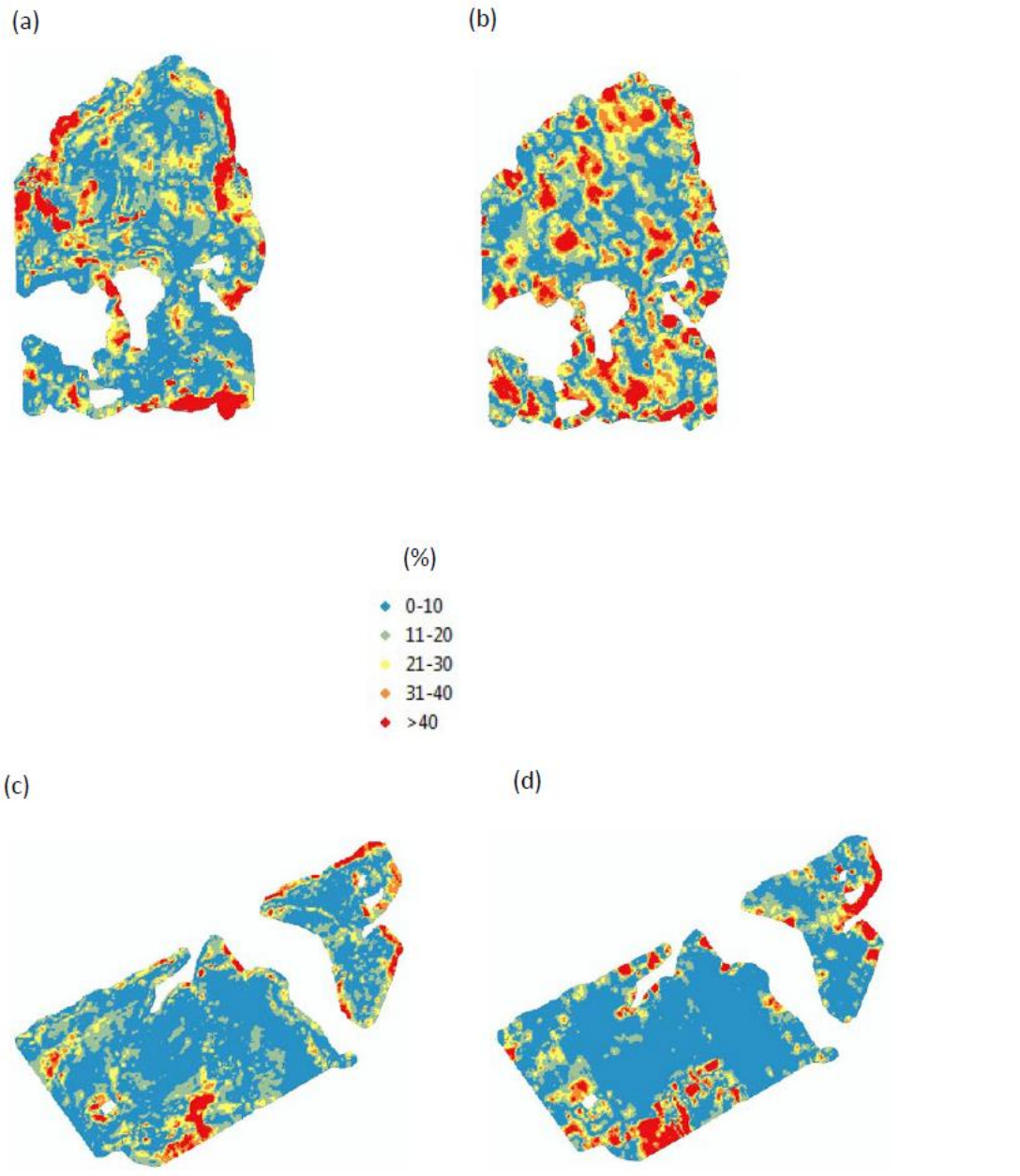


**FIGURE 7.3:** MAPS SHOWING THE DISTRIBUTION OF CVS OF STANDARDISED YIELD OVER TIME (TEMPORAL VARIABILITY) FOR "MILROY" PADDOCKS M25 (A) CROP YIELD AND (B) PASTURE TGDM AND M41 (C) CROP YIELD AND (D) PASTURE TGDM. THE BLUE AREAS INDICATE THE MOST STABLE YIELDS AND THE RED AREAS INDICATE THE LEAST STABLE YIELDS.

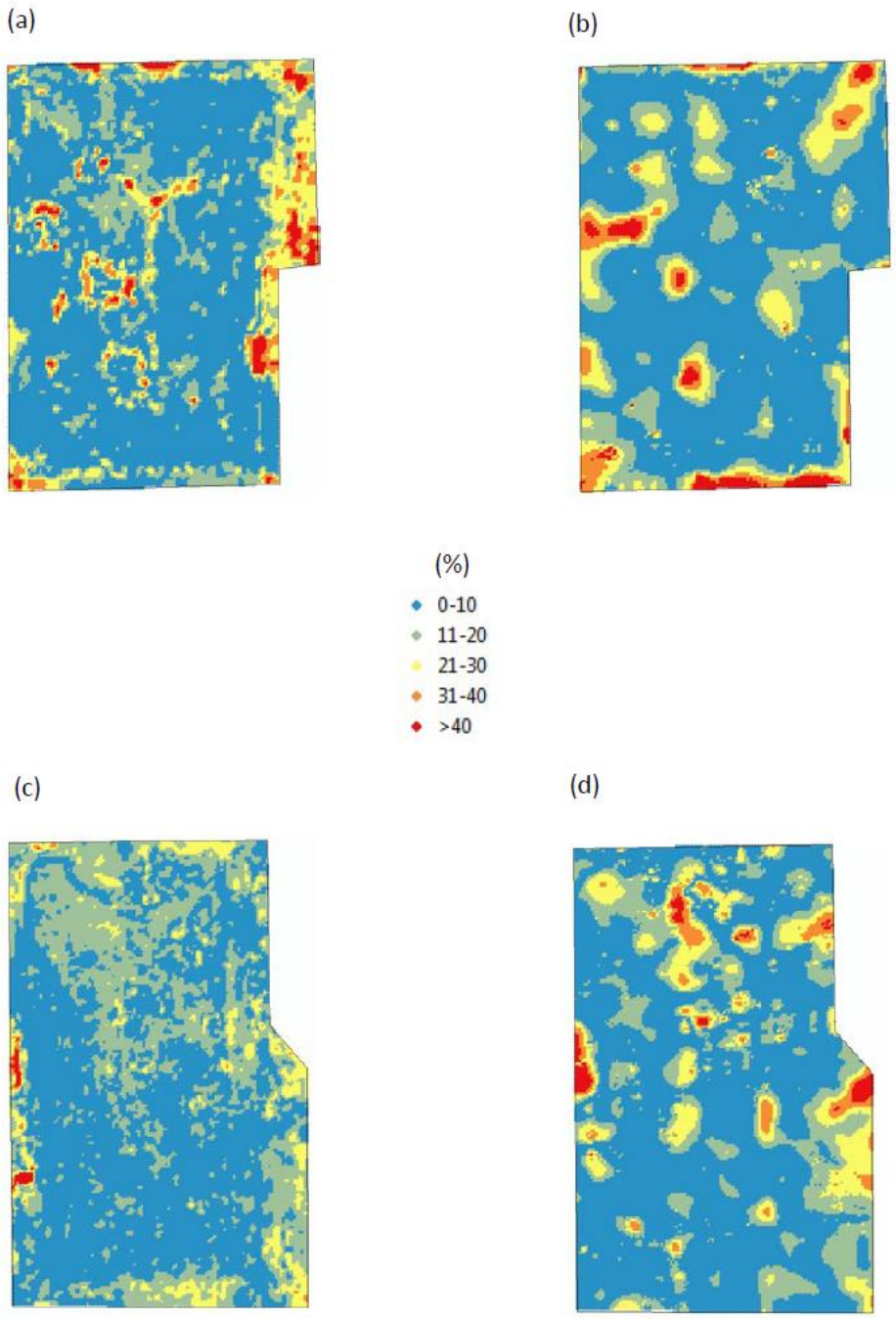


**FIGURE 7.4:** MAPS SHOWING THE DISTRIBUTION OF CVS OF STANDARDISED YIELD OVER TIME (TEMPORAL VARIABILITY) FOR "GRANDVIEW" PADDOCKS GV8 (A) CROP YIELD AND (B) PASTURE TGDM AND GV39 (C) CROP YIELD AND (D) PASTURE TGDM. THE BLUE AREAS INDICATE THE MOST STABLE YIELDS AND THE RED AREAS INDICATE THE LEAST STABLE YIELDS.

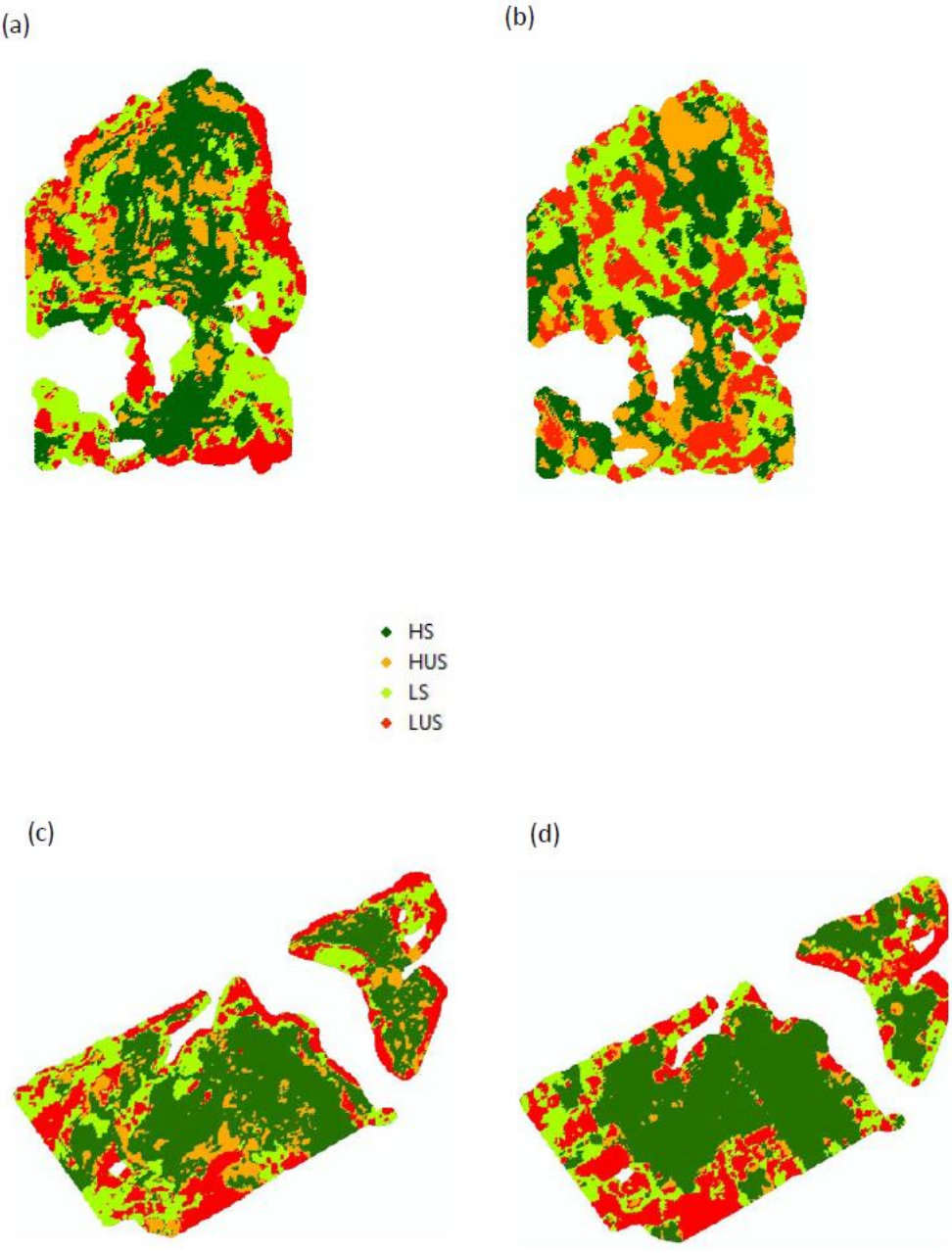


**FIGURE 7.5:** STABILITY INDEX MAPS FOR "MILROY" PADDOCKS M25 (A) STANDARDISED CROP YIELD AND (B) STANDARDISED PASTURE TGDM, AND M41 (C) STANDARDISED CROP YIELD AND (D) STANDARDISED PASTURE TGDM. HS = HIGH AND STABLE YIELDING ZONES, HUS = HIGH AND UNSTABLE, LS = LOW AND STABLE AND LUS = LOW AND UNSTABLE.

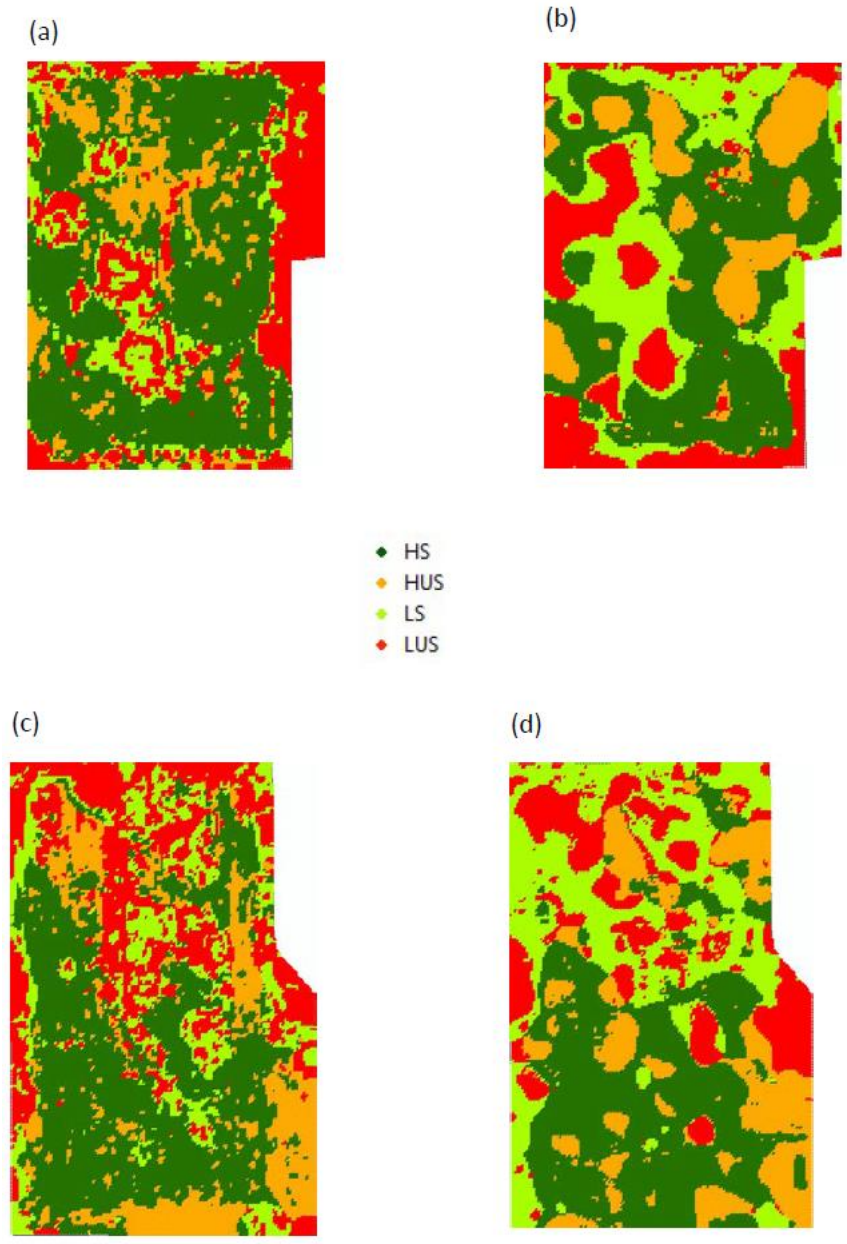


**FIGURE 7.6:** STABILITY INDEX MAPS FOR "GRANDVIEW" PADDOCKS GV8 (A) STANDARDISED CROP YIELD AND (B) STANDARDISED PASTURE TGDM, AND GV39 (C) STANDARDISED CROP YIELD AND (D) STANDARDISED PASTURE TGDM. HS = HIGH AND STABLE YIELDING ZONES, HUS = HIGH AND UNSTABLE, LS = LOW AND STABLE AND LUS = LOW AND UNSTABLE.

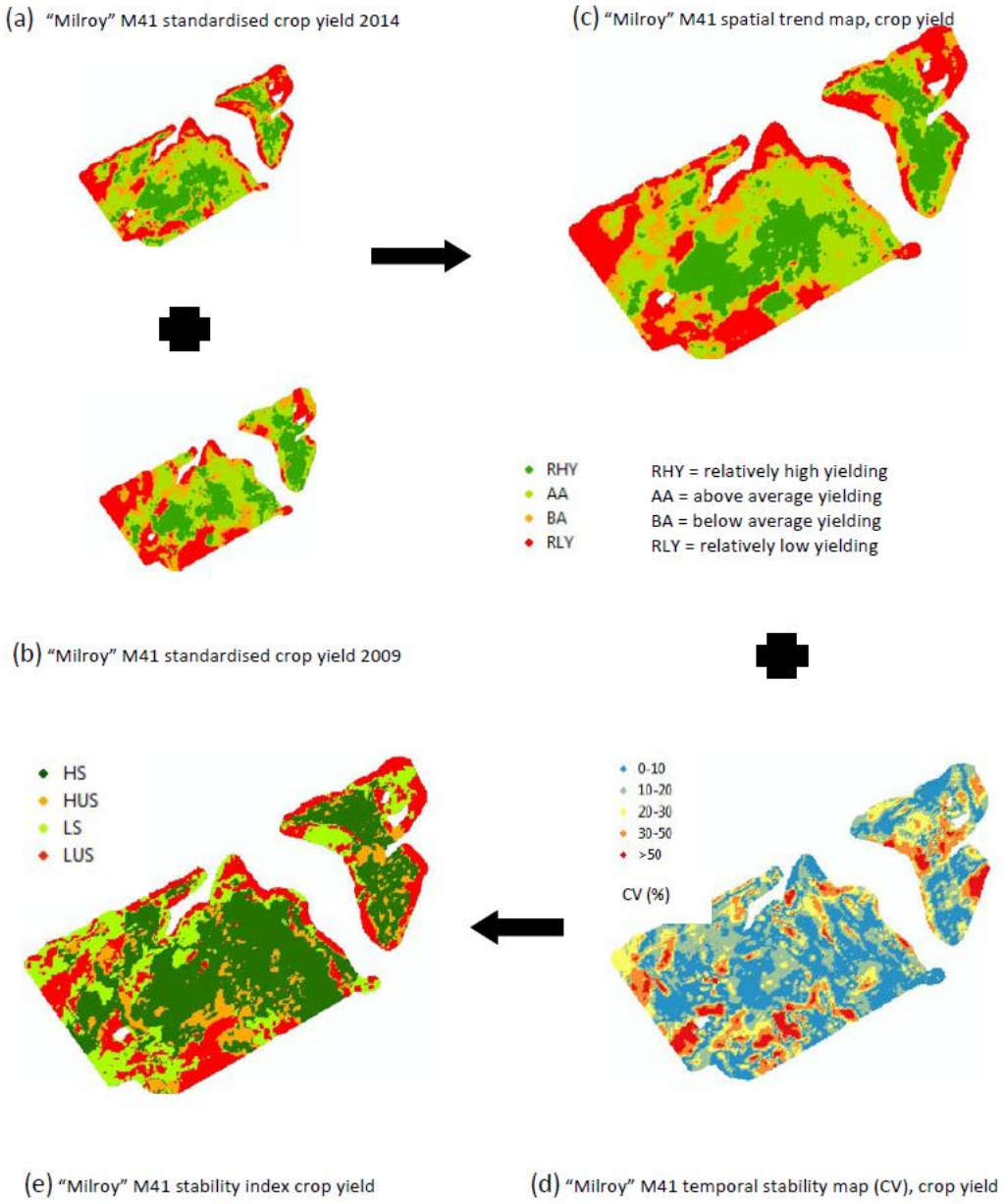


**FIGURE 7.7:** THE STABILITY INDEX MAP (E) ABOVE FOR CROP YIELD IN "MILROY" PADDOCK M41 IS A COMBINATION OF THE FEATURES FOUND IN THE SPATIAL TREND AND TEMPORAL STABILITY MAPS. STANDARDISED YIELD MAPS (A) AND (B) ARE COMBINED TO CREATE A SPATIAL TREND MAP (C) WHICH SHOWS THE MEAN STANDARDISED YIELD (SPATIAL VARIATION) OVER THE PERIOD IN QUESTION. THE TEMPORAL STABILITY MAP (D) SHOWS THE STABILITY OF YIELD (AS CV) ACROSS THE PADDOCK OVER THE SAME PERIOD. COMBINING THE SPATIAL TREND MAP (C) AND TEMPORAL STABILITY MAP (D) PROVIDES THE STABILITY INDEX MAP (E) WITH FOUR ZONES: HIGH YIELDING AND STABLE (HS), HIGH YIELDING AND UNSTABLE (HUS), LOW YIELDING AND STABLE (LS) AND LOW YIELDING AND UNSTABLE (LUS).

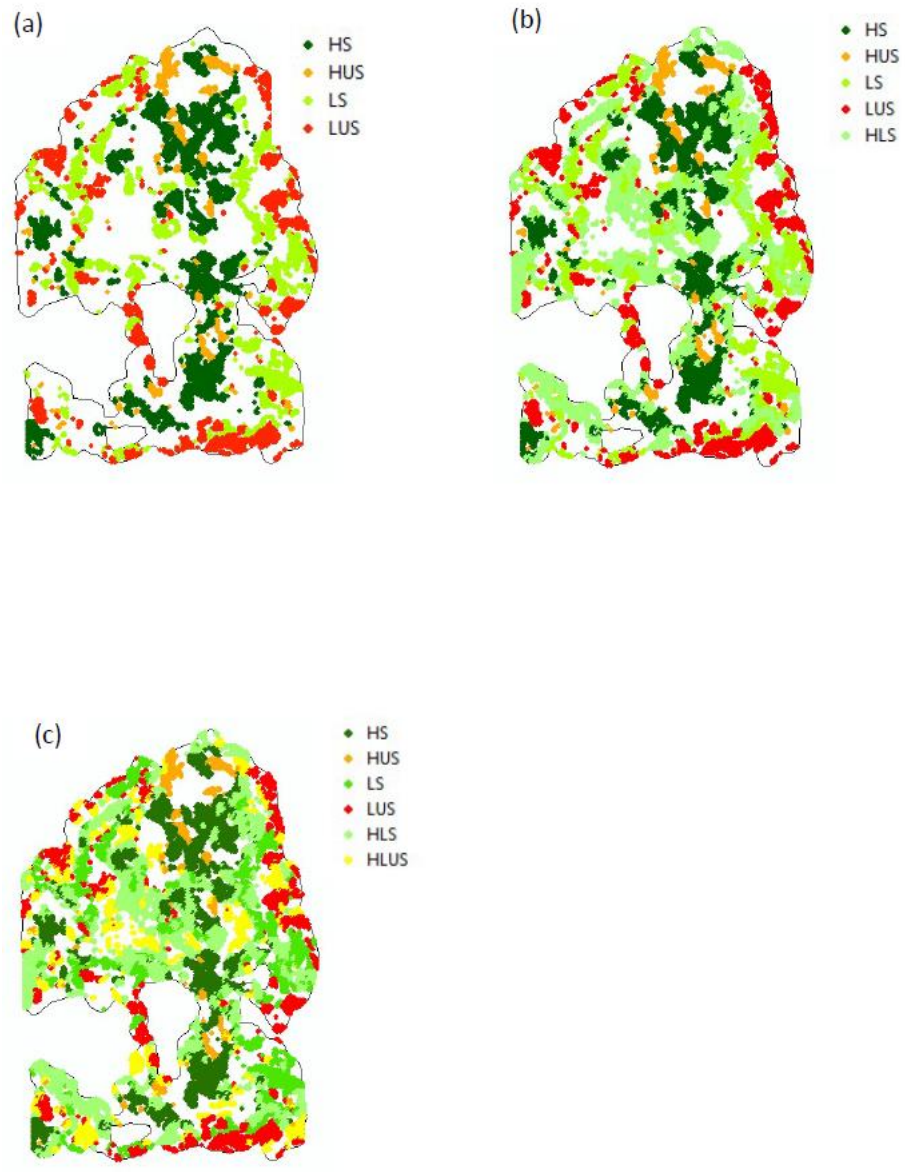


**FIGURE 7.8:** COMBINED CROP AND PASTURE STABILITY MAPS FOR "MILROY" PADDOCK M25 (A) SHOWS ALL DATA POINTS THAT ARE EITHER HS, HUS, LS AND LUS FOR BOTH CROP AND PASTURE, (B) IS MAP (A) INCLUDING POINTS WHERE YIELDS ARE TEMPORALLY STABLE, BUT EXHIBIT CONTRARY YIELD BEHAVIOUR (I.E. POINTS ARE HS IN CROP BUT LS IN PASTURE, OR VICE VERSA), (C) IS MAP (B) BUT NOW INCLUDES ALL POINTS THAT ARE TEMPORALLY UNSTABLE AND EXHIBITING CONTRARY YIELD BEHAVIOUR (I.E. POINTS ARE HUS IN CROP BUT LUS IN PASTURE, OR VICE VERSA).

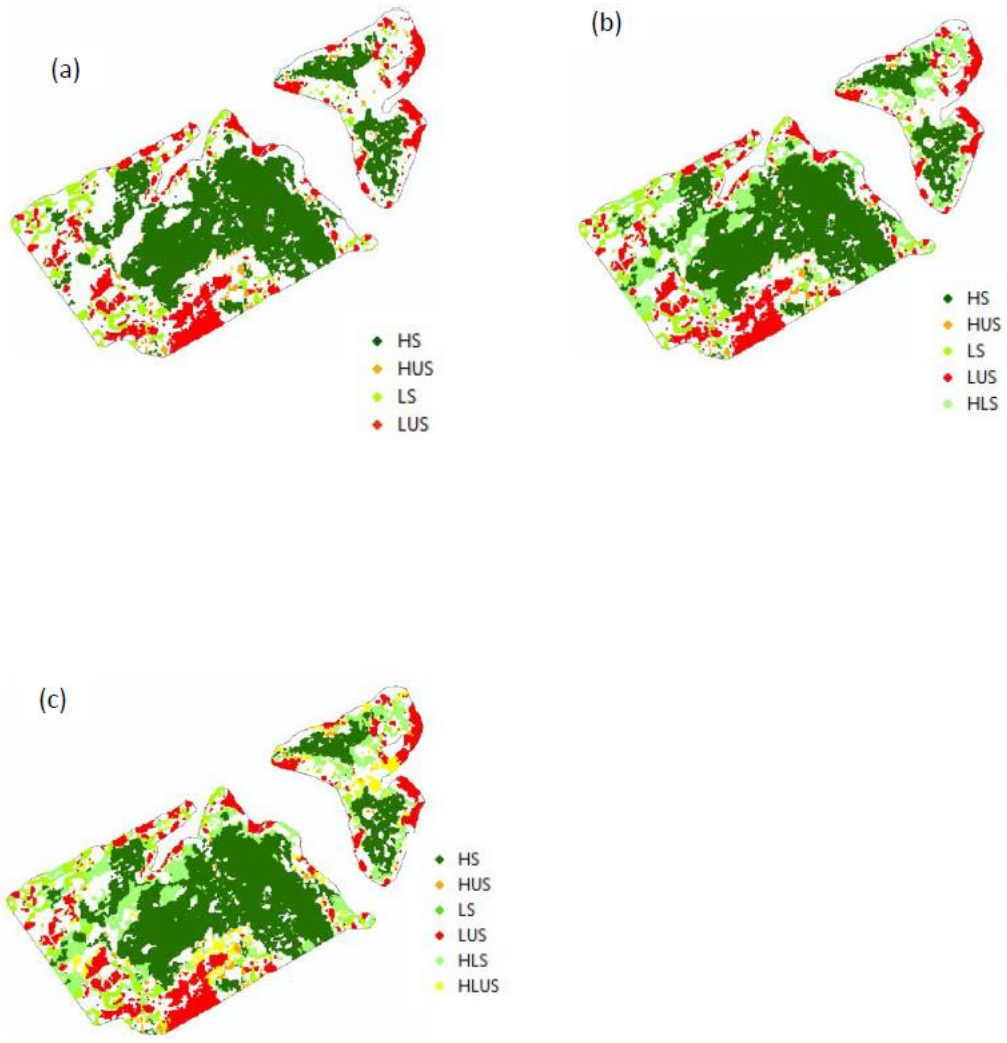


**FIGURE 7.9:** COMBINED CROP AND PASTURE STABILITY MAPS FOR "MILROY" PADDOCK M41 (A) SHOWS ALL DATA POINTS THAT ARE EITHER HS, HUS, LS AND LUS FOR BOTH CROP AND PASTURE, (B) IS MAP (A) INCLUDING POINTS WHERE YIELDS ARE TEMPORALLY STABLE, BUT EXHIBIT CONTRARY YIELD BEHAVIOUR (I.E. POINTS ARE HS IN CROP BUT LS IN PASTURE, OR VICE VERSA), (C) IS MAP (B) BUT NOW INCLUDES ALL POINTS THAT ARE TEMPORALLY UNSTABLE AND EXHIBITING CONTRARY YIELD BEHAVIOUR (I.E. POINTS ARE HUS IN CROP BUT LUS IN PASTURE, OR VICE VERSA).

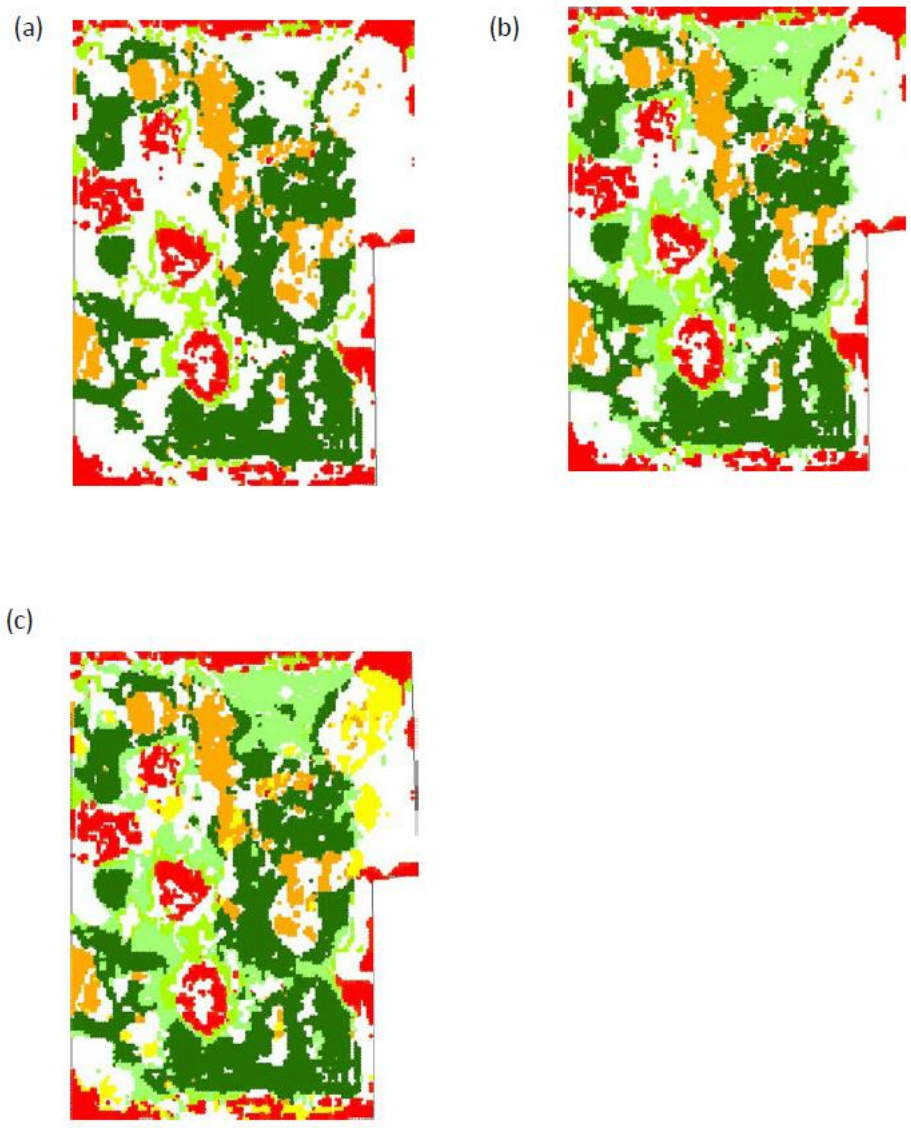


**FIGURE 7.10:** COMBINED CROP AND PASTURE STABILITY MAPS FOR "GRANDVIEW" PADDOCK GV8 (A) SHOWS ALL DATA POINTS THAT ARE EITHER HS, HUS, LS AND LUS FOR BOTH CROP AND PASTURE, (B) IS MAP (A) INCLUDING POINTS WHERE YIELDS ARE TEMPORALLY STABLE, BUT EXHIBIT CONTRARY YIELD BEHAVIOUR (I.E. POINTS ARE HS IN CROP BUT LS IN PASTURE, OR VICE VERSA), (C) IS MAP (B) BUT NOW INCLUDES ALL POINTS THAT ARE TEMPORALLY UNSTABLE AND EXHIBITING CONTRARY YIELD BEHAVIOUR (I.E. POINTS ARE HUS IN CROP BUT LUS IN PASTURE, OR VICE VERSA).

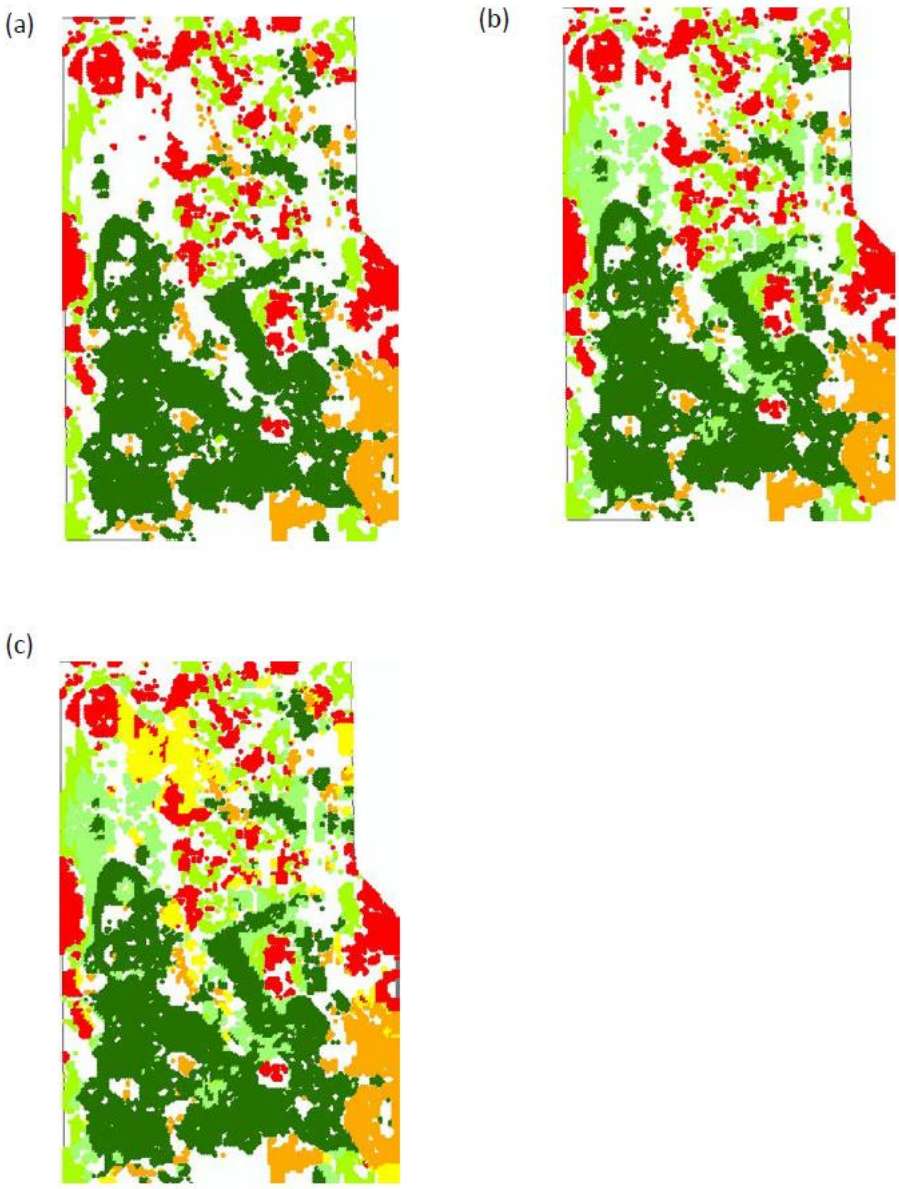


**FIGURE 7.11:** COMBINED CROP AND PASTURE STABILITY MAPS FOR "GRANDVIEW" PADDOCK GV39 (A) SHOWS ALL DATA POINTS THAT ARE EITHER HS, HUS, LS AND LUS FOR BOTH CROP AND PASTURE, (B) IS MAP (A) INCLUDING POINTS WHERE YIELDS ARE TEMPORALLY STABLE, BUT EXHIBIT CONTRARY YIELD BEHAVIOUR (I.E. POINTS ARE HS IN CROP BUT LS IN PASTURE, OR VICE VERSA), (C) IS MAP (B) BUT NOW INCLUDES ALL POINTS THAT ARE TEMPORALLY UNSTABLE AND EXHIBITING CONTRARY YIELD BEHAVIOUR (I.E. POINTS ARE HUS IN CROP BUT LUS IN PASTURE, OR VICE VERSA).

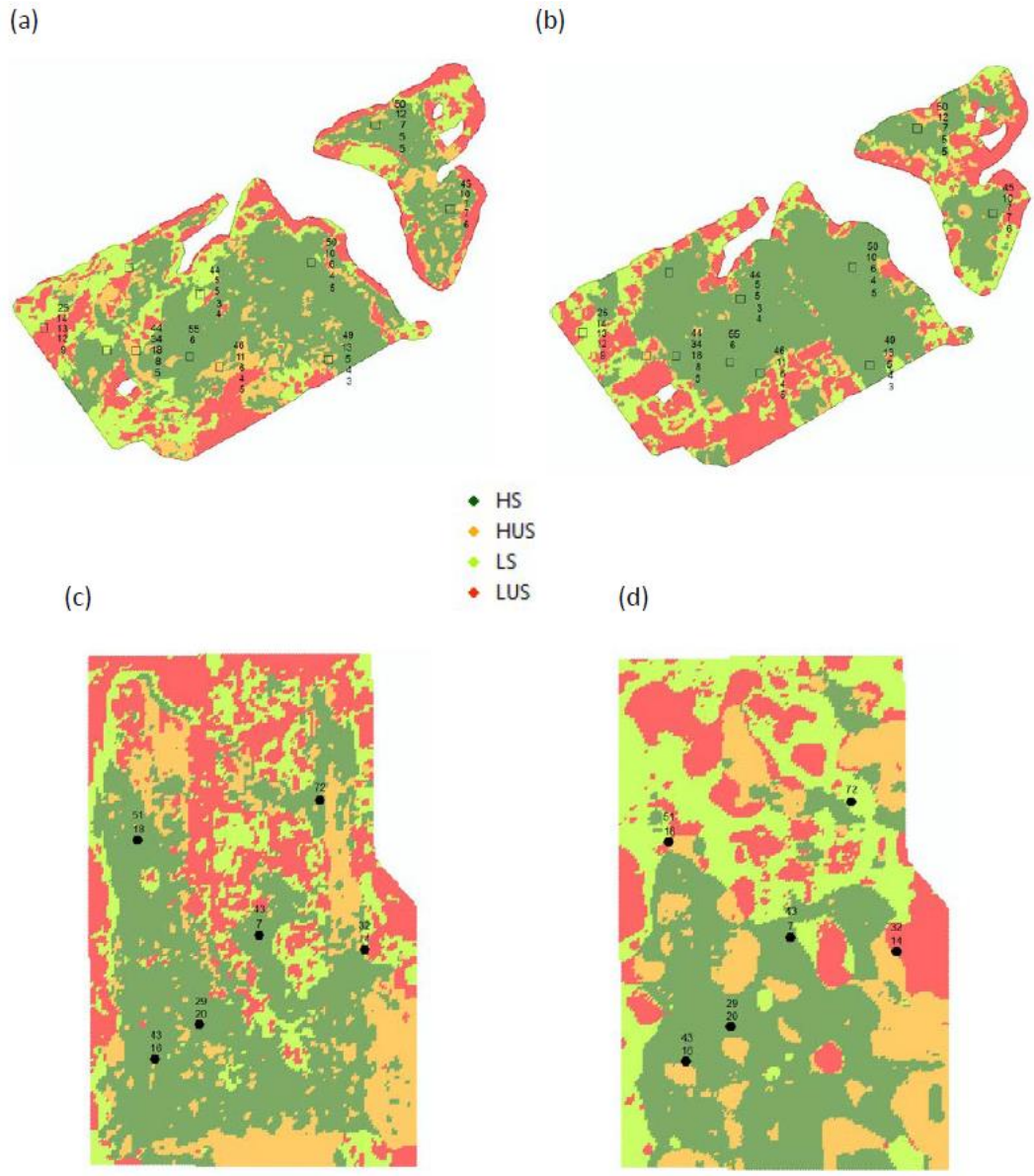


**FIGURE 7.12:** MAPS OF (A) "MILROY" PADDOCK M41 CROP PHASE, (B) PASTURE PHASE, (C) "GRANDVIEW" PADDOCK GV39 CROP PHASE, AND (D) PASTURE PHASE STABILITY MAPS SHOWING SOIL TEST POINTS AND COLWELL P RESULTS. HS = HIGH AND STABLE YIELDING ZONES, HUS = HIGH AND UNSTABLE, LS = LOW AND STABLE AND LUS = LOW AND UNSTABLE.

**TABLE 7.4:** RESULTS FROM THE KRUSKAL–WALLIS ONE-WAY ANOVA TEST FOR DIFFERENCES BETWEEN THE STABILITY ZONES BASED ON CROP AND PASTURE YIELD OR CV FOR "MILROY" PADDOCKS M25 AND M41. VALUES SHOW THE ZONE MEDIANS CALCULATED BY THE KRUSKAL–WALLIS TEST AND INDICATE WHERE A SIGNIFICANT DIFFERENCE OCCURRED BETWEEN AT LEAST ONE MEDIAN. THE CORRELATION BETWEEN CROP YIELD AND PASTURE TGDM WAS ALSO TESTED WITH SPEARMAN'S RHO. HS = HIGH AND STABLE YIELDING ZONES, HUS = HIGH AND UNSTABLE, LS = LOW AND STABLE AND LUS = LOW AND UNSTABLE. $\chi^2$ IS THE CHI-SQUARED TEST STATISTIC FOR EACH KRUSKAL–WALLIS TEST, ρ IS THE SPEARMAN'S CORRELATION COEFFICIENT AND P IS THE RELATED PROBABILITY. N IS THE NUMBER OF POINTS IN THE SAMPLE.

| PADDOCK | HS | HUS | LS | LUS | $\chi^2$ | P | ρ | P |
|---|---|---|---|---|---|---|---|---|
| **"MILROY" M25** | (N=199) | | | | | | | |
| Correlation: crop yld x pasture yld | | | | | | | 0.25 | **0.004** |
| Crop yield | $116.2^{a}$† | $113.4^{a}$ | $88.1^{b}$ | $73.3^{c}$ | 151.8 | **<0.001** | | |
| Pasture yield | $103.4^{ns}$ | $102.3^{ns}$ | $97.4^{ns}$ | $96.7^{ns}$ | 7.7 | **0.053** | | |
| Crop CV | $7.1^{a}$ | $26.9^{b}$ | $9.3^{a}$ | $34.8^{b}$ | 137.9 | **<0.001** | | |
| Pasture CV | $16.9^{ns}$ | $16.1^{ns}$ | $16.5^{ns}$ | $18.7^{ns}$ | 0.96 | 0.81 | | |
| Crop yld–Pasture yld | $19.4^{a}$ | $19.3^{ab}$ | $12.6^{a}$ | $24.1^{b}$ | 10.35 | **0.02** | | |
| Crop CV–Pasture CV | $13.1^{a}$ | $12.0^{a}$ | $10.0^{a}$ | $19.5^{b}$ | 9.8 | **0.02** | | |
| **"MILROY" M41** | (N=262) | | | | | | | |
| Correlation: crop yld x pasture yld | | | | | | | 0.66 | **<0.001** |
| Crop yield | $110.5^{a}$ | $112.7^{a}$ | $85.6^{b}$ | $78.3^{b}$ | 193.18 | **<0.001** | | |
| Pasture yield | $116.8^{a}$ | $105.9^{a}$ | $91.3^{b}$ | $82.8^{b}$ | 99.29 | **<0.001** | | |
| Crop CV | $5.2^{a}$ | $18.7^{b}$ | $5.8^{a}$ | $25.2^{c}$ | 177.09 | **<0.001** | | |
| Pasture CV | $4.9^{a}$ | $7.3^{b}$ | $11.0^{bc}$ | $14.9^{c}$ | 53.17 | **<0.001** | | |
| Crop yld–Pasture yld | $10.0^{a}$ | $7.5^{a}$ | $15.6^{b}$ | $17.2^{b}$ | 25.68 | **<0.001** | | |
| Crop CV–Pasture CV | $3.2^{a}$ | $11.4^{bc}$ | $6.6^{c}$ | $14.8^{b}$ | 54.81 | **<0.001** | | |

† Median values with different letters indicate that the SI zone medians are significantly different. ns = not significant.

**TABLE 7.5:** RESULTS FROM THE KRUSKAL–WALLIS ONE-WAY ANOVA TEST FOR DIFFERENCES BETWEEN THE STABILITY ZONES BASED ON CROP AND PASTURE YIELD OR CV FOR "GRANDVIEW" PADDOCKS GV8 AND GV39. VALUES SHOW THE ZONE MEDIANS CALCULATED BY THE KRUSKAL–WALLIS TEST AND INDICATE WHERE A SIGNIFICANT DIFFERENCE OCCURRED BETWEEN AT LEAST ONE MEDIAN. THE CORRELATION BETWEEN CROP YIELD AND PASTURE TGDM WAS ALSO TESTED WITH SPEARMAN'S RHO. HS = HIGH AND STABLE YIELDING ZONES, HUS = HIGH AND UNSTABLE, LS = LOW AND STABLE AND LUS = LOW AND UNSTABLE. $\chi^2$ IS THE CHI-SQUARED TEST STATISTIC FOR EACH KRUSKAL–WALLIS TEST, ρ IS THE SPEARMAN'S CORRELATION COEFFICIENT AND P THE RELATED PROBABILITY. N IS THE NUMBER OF POINTS IN THE SAMPLE.

| PADDOCK | HS | HUS | LS | LUS | $\chi^2$ | P | ρ | P |
|---|---|---|---|---|---|---|---|---|
| **"GRANDVIEW"** | **GV8** | (N=253) | | | | | | |
| Correlation:crop yld x pasture yld | | | | | | | 0.57 | **<0.001** |
| Crop yield | $108.5^{a}$† | $109.4^{a}$ | $94.5^{b}$ | $88.7^{b}$ | 176.89 | **<0.001** | | **<0.001** |
| Pasture yield | $104.9^{a}$ | $106.8^{a}$ | $86.1^{b}$ | $94.7^{b}$ | 37.64 | **<0.001** | | **<0.001** |
| Crop CV | $6.7^{a}$ | $15.0^{b}$ | $9.7^{c}$ | $20.6^{d}$ | 181.98 | **<0.001** | | **<0.001** |
| Pasture CV | $6.0^{a}$ | $12.2^{b}$ | $13.5^{b}$ | $12.5^{b}$ | 26.74 | **<0.001** | | **<0.001** |
| Crop yld–Pasture yld | $8.5^{a}$ | $7.2^{a}$ | $10.8^{ab}$ | $12.9^{b}$ | 8.51 | **<0.001** | | **<0.001** |
| Crop CV–Pasture CV | $4.2^{a}$ | $7.5^{b}$ | $9.7^{b}$ | $11.3^{b}$ | 36.76 | **<0.001** | | **<0.001** |
| **"GRANDVIEW"** | **GV39** | (N=192) | | | | | | |
| Correlation:crop yld x pasture yld | | | | | | | 0.66 | **<0.001** |
| Crop yield | $114.8^{a}$ | $119.2^{a}$ | $77.2^{b}$ | $74.3^{b}$ | 138.9 | **<0.001** | | **<0.001** |
| Pasture yield | $112.1^{a}$ | $105.9^{a}$ | $88.4^{b}$ | $86.4^{b}$ | 57.84 | **<0.001** | | **<0.001** |
| Crop CV | $12.0^{a}$ | $29.4^{b}$ | $16.7^{c}$ | $30.5^{b}$ | 143.09 | **<0.001** | | **<0.001** |
| Pasture CV | $7.8^{ns}$ | $12.2^{ns}$ | $7.6^{ns}$ | $10.4^{ns}$ | 7.34 | 0.06 | | **<0.001** |
| Crop yld–Pastureyld | $10.1^{a}$ | $13.8^{ab}$ | $14.9^{b}$ | $17.3^{b}$ | 11.36 | **0.01** | | **<0.001** |
| Crop CV–Pasture CV | $6.3^{a}$ | $19.1^{b}$ | $12.3^{c}$ | $17.2^{bd}$ | 54.45 | **<0.001** | | **<0.001** |

† Median values with different letters indicate that the SI zone medians are significantly different. ns = not significant.

**TABLE 7.6:** RESULTS FROM THE KRUSKAL–WALLIS ONE-WAY ANOVA TEST FOR DIFFERENCES BETWEEN THE EMI READINGS BY STABILITY ZONES FOR "MILROY" PADDOCKS M25 AND M41 AND "GRANDVIEW" PADDOCKS GV8 AND GV39. VALUES SHOW THE ZONE MEDIANS CALCULATED BY THE KRUSKAL–WALLIS TEST AND INDICATE WHERE A SIGNIFICANT DIFFERENCE OCCURRED BETWEEN AT LEAST ONE MEDIAN. HS = HIGH AND STABLE YIELDING ZONES, HUS = HIGH AND UNSTABLE, LS = LOW AND STABLE AND LUS = LOW AND UNSTABLE. $\chi^2$ IS THE CHI-SQUARED TEST STATISTIC FOR EACH KRUSKAL–WALLIS TEST AND P THE RELATED PROBABILITY. N IS THE NUMBER OF POINTS IN THE SAMPLE.

| PADDOCK | HS | HUS | LS | LUS | $\chi^2$ | P |
|---|---|---|---|---|---|---|
| **"MILROY"** | | | | | | |
| **M25** | (N=199) | | | | | |
| EM 0–50 cm | 6.7†$^{ns}$ | 7.3$^{ns}$ | 5.6$^{ns}$ | 6.4$^{ns}$ | 3.79 | 0.28 |
| EM 0–100 cm | 19.1$^{ns}$ | 24.9$^{ns}$ | 15.9$^{ns}$ | 20.2$^{ns}$ | 5.45 | 0.14 |
| **M41** | (N=262) | | | | | |
| EM 0–50 cm | 5.2$^{a}$ | 6.6$^{c}$ | 5.8$^{a,b}$ | 9.0$^{c}$ | 28.38 | **<0.001** |
| EM 0–100 cm | 10.2$^{a}$ | 11.5$^{a,c}$ | 6.5$^{b}$ | 12.2$^{a,c}$ | 11.80 | **<0.01** |
| **"GRANDVIEW"** | | | | | | |
| **GV8** | (N=253) | | | | | |
| EM 0–38 cm | 42.4$^{a,b}$ | 37.7$^{a}$ | 45.2$^{c,d}$ | 42.3$^{b,d}$ | 12.29 | **<0.01** |
| EM 0–75 cm | 103.2$^{a}$ | 94.6$^{b}$ | 110.2$^{c}$ | 106.9$^{a,c}$ | 18.41 | **<0.001** |
| **GV39** | (N=192) | | | | | |
| EM 0–38 cm | 12.3$^{a}$ | 15.1$^{a,b}$ | 23.8$^{b}$ | 17.3$^{b}$ | 14.48 | **<0.01** |
| EM 0–38 cm | 76.9$^{a}$ | 78.8$^{a}$ | 84.6$^{b}$ | 82.7$^{b}$ | 36.36 | **<0.001** |

† Median values with different letters indicate that the SI zone medians are significantly different.
ns = not significant.

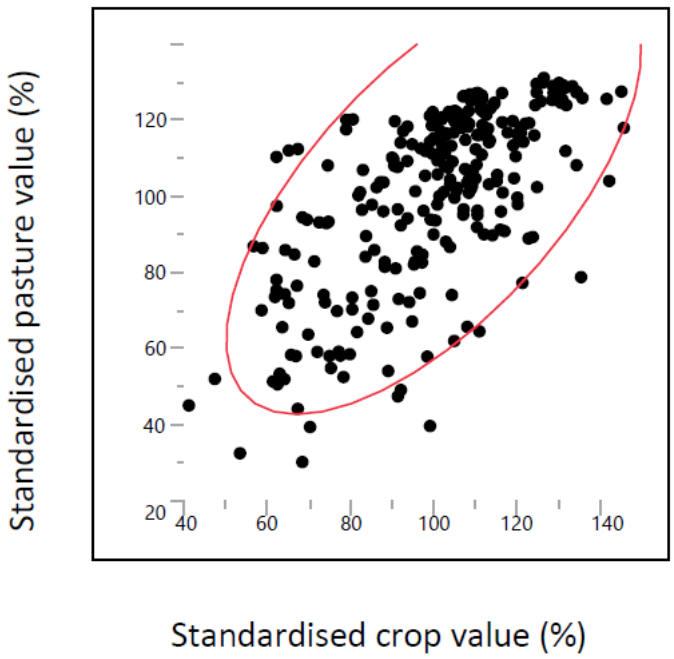


**FIGURE 7.13:** SCATTERPLOT MATRIX OF SPEARMAN'S RHO FOR STANDARDISED CROP YIELD VS. PASTURE TGDM VALUES AT RANDOMISED DATA POINTS IN "MILROY" PADDOCK M41 (P=0.66, P<0.0001, N=262). THE DENSITY ELLIPSE (RED LINE) ENCLOSES APPROXIMATELY 95% OF THE POINTS.

## 7.4 DISCUSSION

This chapter has outlined a methodology for calculating spatial variation and temporal stability for both crop and pasture yields within a paddock. Much of the crop, pasture and soil data acquired in Chapters 5 and 6 has been combined in a novel way to test Hypothesis 3 (Chapter 2, p. 36) that, "*data acquired using PA technologies can be used to create a single index of paddock productivity that describes the spatial variation in, and temporal stability of, crop and pasture production over time*".

Previous attempts to create paddock stability zones have been restricted to either crop or grassland paddocks but have never been combined for paddocks that include a sequence of both crop and pasture in a mixed farming system. Blackmore (2000), Blackmore et al. (2003), Marques da Silva (2006), Marques da Silva et al. (2008) and Xu et al. (2006) have described the creation of stability zones in either crop or pasture paddocks. However, all struggled to find a valid method to

determine a 'threshold' value for temporal variability. Blackmore (2000) used an arbitrary CV value of 30% for the stability threshold but found that this left 97% of the experimental paddock classified as stable and concluded that the threshold figure was far too high and the unstable area too insignificant to be worthwhile managing. Xu et al. (2006) in grassland used threshold figures of CV < 15% for stable, 15 < CV < 25% for moderately stable, and CV > 25% for unstable.

In the work described here, the stability threshold value was determined as the CV distribution mean for crop and pasture yield for each paddock. None of the authors mentioned above attempted to statistically test the stability zones they created. If the stability zone categories as tested by the Kruskal–Wallis test (Tables 7.4 and 7.5) correctly reflect spatial variability in yield across a paddock for crop and pasture phases, then it would be expected that the medians of the high-yielding areas in both crop and pasture phases (HS and HUS) would not significantly differ (i.e. areas that are high yielding in crop are also high yielding in pasture), as would the medians for low-yielding areas (LS and LUS). For temporal stability, the expectation was that the medians for stable areas in the paddock for both crop and pasture phases (HS and LS) would not significantly differ (i.e. irrespective of being high or low yielding, areas that are stable in crop yield are also stable in pasture yield), as would the medians for unstable areas (HUS and LUS). Table 7.7 summarises the results from the Kruskal–Wallis test data shown in Tables 7.4 and 7.5. With the exception of the M25 pasture yield, all medians for spatial variation in yield at both "Milroy" and "Grandview" are differentiated into high yielding (HS and HUS) and low yielding (LS and LUS) zones at P<0.001. The M25 pasture yield spatial variation medians, although not significantly different at P=0.05, were still grouped into high- and low-yielding zones. This provides strong evidence to support the validity of the methodology used to split the yield spatial variability data among zones. That is, the methodology partitioned both crop and pasture yields in the same areas in each paddock.

The Kruskal–Wallis test for the temporal stability aspect (CV) of the stability zones did not always show a significant difference between the medians of the stable and unstable categories (Table 7.7). The crop CV medians were consistent, with both

"Milroy" paddocks having significantly different medians between the stable and unstable yields. Although not showing a significant difference at P=0.05, the "Grandview" crop CV medians were grouped into stable and unstable categories. For example, at "Grandview" GV8, the crop CV medians were 6.7 and 9.7 for the stable yields (HS and LS) and distant from the medians in the unstable zones (HUS and LUS), which were also close to each other (15.0 and 20.6) (Table 7.5). The results for pasture phase temporal stability were much less consistent. There were no paddocks where the pasture CV medians differed significantly at P=0.05 and "Grandview" GV39 was the only paddock where the medians were grouped into stable and unstable categories.

There are many factors in the pasture phase which confound temporal stability in comparison to the cropping phase. In effect, a highly managed monoculture in the cropping phase is being compared to a largely unmanaged, highly diverse and complex sward of pasture species with uncontrolled animal impact. These factors combine to affect the spatial heterogeneity of a paddock during the pasture–livestock phase compared to when the paddock is in crop. Pasture stability is also affected by factors such as animal grazing and diet selection impact, stocking rate decisions by managers, pasture regrowth, and often highly variable species composition within swards. These effects can result in significant variations over time in species dominance in different parts of a paddock. For example Figure 6.26 (p. 203) shows variation in species distribution in "Milroy" paddock M41 between 2012 and 2013 and the increasing dominance of broadleaf weeds (in this case, capeweed, *Arctotheca calendula* L.). Similarly, Figure 6.27 (p. 204) shows an increase in legumes and reduction in grasses in "Grandview" paddock GV39 between 2012 and 2013. Figures 6.14 (p. 193) and 6.15 (p. 194) also show the changes in TGDM distribution at "Milroy" and "Grandview", respectively, across the 2012 and 2013 seasons.

It is, therefore, difficult in the short term to differentiate between variations in temporal stability of pasture growth brought about by rainfall, soil moisture and soil nutrient supply from those caused by grazing. The overall spatial and temporal

utilisation of a paddock by livestock is unclear without acquiring data through GPS tracking (Trotter and Lamb, 2008).

It was anticipated that the stability zones might be useful for identifying potential nutrient variations across a paddock and providing the opportunity to better manage decisions around fertiliser strategy. Nutrients enter and leave the soil and farm system via several pathways, including exports of grain, animal products, fodder, leaching and run-off, and variations in soil retention. The amounts lost through leaching are not readily or accurately known, and the distributions brought about through manure and urine deposition by grazing animals is highly variable and can influence the spatial distribution of nutrients across a paddock.

It was expected that the 'high and stable' zones would show lower nutrient levels than the low and unstable areas, as greater nutrient removal would occur from the high and stable areas in the form of crop and animal product exports compared to low and stable areas. The levels of nutrients exported by both crops and animal products have been quantified (Price, 2006). Soils require a certain level of phosphorus to maintain their current P status. This is largely determined by the particular soil type and its associated PBI value (Gourley et al., 2007). Maintaining paddock P at levels higher than that necessary for production is costly because additional P inputs are required to build and maintain high levels of soil fertility because of phosphorous 'tie up' in soil (Simpson et al., 2010). The higher the PBI value and the greater the Colwell P level, the greater the amount of P required to maintain the *status quo*. Therefore, parts of a paddock that have different soil nutrient levels and PBIs can have differing maintenance fertiliser requirements and might benefit from differential fertiliser treatment.

Although only a small number of soil tests were conducted in the research paddocks, when the paddock stability index maps were overlaid on the soil test results, some broad trends were apparent. The levels of P in all paddocks varied considerably but were generally above critical levels. In "Milroy" paddock M25 (Figure 7.12), the high production areas (HS, HUS) had lower levels of P than the low-producing areas, indicating that nutrient export may have been occurring from the high production areas. This also appeared to be the case in "Grandview"

paddock GV39 (Figure 7.12). Unfortunately, the soil tests were conducted before the stability zones were identified. With the benefit of hindsight, it would be of great benefit to conduct further soil testing now that the stability zones have been identified. Currently, variable rate fertiliser P decisions at "Grandview" are based solely on P removal in grain during the cropping phase. The pastures receive a blanket rate of P.

**TABLE 7.7:** SUMMARY OF KRUSKAL–WALLIS TEST RESULTS FOR YIELD AND STABILITY.

| PADDOCK | CROP YIELD | PASTURE YIELD | CROP CV | PASTURE CV |
|---|---|---|---|---|
| **"MILROY"** | | | | |
| M25 | Sig. difference between high & low yield medians | Median differences between high and low yield not significant but grouped H & L | Sig. difference between stable and unstable medians | No significant difference between medians nor groupings S & US |
| M41 | Sig. difference between high & low yield medians | Sig. difference between high & low yield medians | Sig. difference between stable and unstable medians | No significant difference between medians nor groupings S & US |
| **"GRANDVIEW"** | | | | |
| GV8 | Sig. difference between high & low yield medians | Sig. difference between high & low yield medians | Median differences between stable and unstable yield not significant but grouped S & US | No significant difference between medians nor groupings S & US |
| GV39 | Sig. difference between high & low yield medians | Sig. difference between high & low yield medians | Median differences between stable and unstable yield not significant but grouped S & US | Median differences between stable and unstable yield not significant but grouped S & US |

H = high yield, L = low yield, S = stable yield, US = unstable yield.

The analysis of the relationships between EMI data and the stability zones was inconclusive, and there were no clear associations with either yield or stability. At "Milroy", the ECa median values for both the (HS and HUS) and (LS and LUS) zones in paddock M41 differed, i.e. the medians were differentiating on temporal stability (5.2, 5.8) and (6.6, 9.0) rather than spatial variation in yield (H or L). The effect was not as pronounced at greater depth (0–100 cm). In "Grandview" paddock GV8, differences in the medians of ECa 0–38 cm appear to be associated with spatial variation in yield i.e. (HS and HUS) and (LS and LUS), although the medians for HS and LUS did not differ. At 0–75 cm, the high yield zones differentiate on temporal stability (i.e. the medians of HS and HUS differ), which may be the influence of sodic subsoils. For paddock GV39, the medians appeared grouped on spatial variation in yield (HS and HUS) and (LS and LUS) with significant differences between the medians of (HS and LS) and (HS and LUS), indicating that soil conductivity might be influencing spatial variation in yield rather than yield temporal stability. At 0–75 cm, there was a similar result, with the medians again aligning on yield. There is not enough data to draw any definitive conclusions, but this is an area that warrants further investigation.

Previous attempts at creating stability analyses have tried to use the analysis (unsuccessfully) to predict future crop yields (Blackmore, 2000; Blackmore et al., 2003; Robinson et al., 2009). This is not the intention here. The index has been created as a whole-of-farm management tool, integrating high-resolution data from both crop and pasture phases to form a rolling sequence of data to inform longer-term management decisions.

On the basis of the results discussed here, there are grounds to conclude that Hypothesis 3, "*data acquired using PA technologies can be used to create a single index of paddock productivity that describes the spatial variation in, and temporal stability of, crop and pasture production over time*" has been proven. There are some exceptions and uncertainties revolving around the measurement of spatial variation and temporal stability in pasture phases. There was limited capacity for replication because of the timeframes associated with the research. These constraints are not insurmountable and do not lessen the value of the concepts

behind the stability index which, given the complexity of temporal stability in pasture, still appears to be a resilient tool. Proximal sensing has been successfully used to identify crop and pasture production at high spatial resolution as well as variations in soil physical properties. These are significant steps forward in creating an integrated whole-farm management system based on precision technology.

## 7.5 CONCLUSION

This chapter has described the creation of paddock stability maps and a stability index that identifies and combines the spatial and temporal variation for both crop and pasture phases in a mixed farming system into four productivity zones: high and stable, high and unstable, low and stable, and low and unstable. Production in each zone was analysed statistically for consistency and relevance between crop and pasture phases.

A combined spatial and temporal index of production was created for each paddock as a whole. This stability index takes the crop yield and pasture TGDM data acquired and analysed in Chapters 5 and 6 and reduces it to a single variable: SI (stability index) for each paddock. EMI data was analysed in terms of the stability zones, but the results were inconclusive.

The combined paddock stability maps created in this chapter are visually similar, in both the extent and location of the zones, to the potential management zones identified from k-means clustering of pasture and crop yields with ECa and elevation data that were created in Chapter 6 (Figures 6.28–6.31). This is especially the case for “Milroy” paddock M41, but also for “Milroy” M25 and the “Grandview” paddocks. Although created from an entirely different analysis and use of data, the paddock stability maps developed here, where zones of common spatial and temporal ‘behaviour’ of crop and pasture are overlaid, bear a strong resemblance to the potential management classes identified in Chapter 6 (Section 6.3.6) using *k*-means clustering that included EMI data.

There is still a great deal of work required to refine the definition of pasture SI zones. Additional soil test data based on the SI zones would have been invaluable to help identify and possibly better characterise zone differences. The soil test data

was gathered before the stability zone work was commenced and unfortunately do not match the stability zone boundaries. As a result, the interpretive value of the soil test data was limited. Future work will also need to address the impact of grazing on pasture TGDM estimation and decisions about productive stability. These are both areas where there are significant knowledge gaps that were unable to be taken into account in the work described here. This is evident in the Kruskal–Wallis tests, where there were a number of non-significant results associated with the pasture CVs. It is not always going to be clear if a particular part of a paddock happened to be low in pasture TGDM production because nothing much grew there, or because it was eaten off. Meta-analysis of data from livestock fitted with GPS tracking collars and accelerometers could identify spatial preference and distribution of animals within a paddock at particular times of day, week, month or by season and of livestock social networks. It could also identify foraging patterns, time spent grazing, resting and ruminating. This applies to the grazing of a crop in a 'grain & graze' system (Price and Hacker, 2009) as well as when the paddock is in pasture. The use of tracking data combined with modelling of grazing with software packages such as Grass Gro (Donnelly et al., 2002) or Ausfarm (Moore et al., 2007) could further refine the accuracy of the pasture data. Notwithstanding these reservations, this work has shown the paddock stability index to be a robust methodology that can identify significant areas of a paddock that exhibit similar productive behaviour, whether in crop or pasture, year in year out.

While highly mobile nutrients like nitrogen need to be managed in-season during cropping phases in response to in-season soil moisture and rainfall (Basso et al., 2012), less mobile nutrients such as P, K and S can be managed with a longer-term view, based on the temporal variance reflected in stability zones. In this way, the different outcomes required from a crop (maximising grain yield) and pasture (maximising digestible biomass) phase can be managed and monitored at the sub-paddock scale. The stability zones can also be used to create 'gross margin' maps of each paddock to assist in optimising financial inputs and returns.

The work described here is unique but needs further testing. There are sufficient grounds to conclude that Hypothesis 3 has been proven. The methodology can be

of great benefit to a farm manager, not only in terms of future expectations of production but also in terms of decisions regarding variable rate applications of seed and fertiliser and even future land uses.

## 7.6 REFERENCES

Basso, B., Fiorentino, C., Cammarano, D., Cafiero, G., & Dardanelli, J. (2012). Analysis of rainfall distribution on spatial and temporal patterns of wheat yield in mediterranean environment. *European Journal of Agronomy, 41*, 52–65.

Blackmore, S. (2000). The interpretation of trends from multiple yield maps. *Computers and Electronics in Agriculture, 26*(1), 37–51.

Blackmore, S., Godwin, R. J., & Fountas, S. (2003). The analysis of spatial and temporal trends in yield map data over six years. *Biosystems Engineering, 84*(4), 455–466.

Cook, S., & Bramley, R. G. V. (2001). *Is agronomy being left behind by precision agriculture?* Paper presented at the Proceedings of the 10th Australian agronomy conference Hobart, Tasmania.

Dobermann, A., Ping, J., Adamchuk, V., Simbahan, G., & Ferguson, R. (2003). Classification of crop yield variability in irrigated production fields. *Agronomy Journal, 95*(5), 1105–1120.

Donnelly, J. R., Freer, M., Salmon, L., Moore, A. D., Simpson, R. J., Dove, H., & Bolger, T. P. (2002). Evolution of the GRAZPLAN decision support tools and adoption by the grazing industry in temperate Australia. *Agricultural Systems, 74*(1), 115–139.

Gourley, C. J. P., Peverill, K. I., & Dougherty, W. J. (2007). *Making better fertiliser decisions for grazed pastures in Australia, accounting for nutrients and fertcare*. Paper presented at the Australian Fertilizer Industry Conference, Hamilton Island, Queensland.

Kruskal, W. H., & Wallis, W. A. (1952). Use of ranks in one-criterion variance analysis. *Journal of the American Statistical Association, 47*(260), 583–621.

Lawes, R. A., Oliver, Y. M., & Robertson, M. J. (2009). Capturing the in-field spatial–temporal dynamic of yield variation. *Crop and Pasture Science, 60*(9), 834–843. doi:10.1071/CP08346

Marques da Silva, J. R. (2006). Analysis of the spatial and temporal variability of irrigated maize yield. *Biosystems Engineering, 94*(3), 337–349.

Marques Da Silva, J. R., Peça, J. O., Serrano, J. M., De Carvalho, M. J., & Palma, P. M. (2008). Evaluation of spatial and temporal variability of pasture based on topography and the quality of the rainy season. *Precision Agriculture, 9*(4), 209–229.

McBratney, A. B., Whelan, B. M., & Shatar, T. M. (1997). Variability and uncertainty in spatial, temporal and spatiotemporal crop-yield and related data. *Ciba Foundation Symposium*, *210*, 141–160.

Moore, A. D., Holzworth, D. P., Herrmann, N. I., Huth, N. I., & Robertson, M. J. (2007). The Common Modelling Protocol: a hierarchical framework for simulation of agricultural and environmental systems. *Agricultural Systems, 95*(1–3), 37–48. doi: 10.1016/j.agsy.2007.03.006

Nuttall, J., & Armstrong, R. (2006). *Are flip-flop yields of crops on alkaline soils in the Victorian Mallee related to subsoil physicochemical constraints?* Paper presented at the Proceedings of the 13th Australian Agronomy Conference. Perth, Western Australia.

Plant, R. (2001). Site-specific management: the application of information technology to crop production. *Computers and Electronics in Agriculture, 30*(1), 9–29.

Price, G. (2006). *Australian Soil Fertility Manual* (3rd ed.). Collingwood Victoria: CSIRO Publishing.

Price, R. J., & Hacker, R. B. (2009). Grain and Graze: an innovative triple bottom line approach to collaborative and multidisciplinary mixed-farming systems research, development and extension. *Animal Production Science, 49*(10), 729–735. doi:10.1071/EA08306

Robinson, N. J., Rampant, P. C., Callinan, A. P. L., Rab, M. A., & Fisher, P. D. (2009). Advances in precision agriculture in south-eastern Australia. II. Spatio-temporal prediction of crop yield using terrain derivatives and proximally sensed data. *Crop and Pasture Science, 60*(9), 859–869. doi:10.1071/CP08348

Serrano, J. M., Peça, J. O., Marques da Silva, J. R., & Shahidian, S. (2011). Spatial and temporal stability of soil phosphate concentration and pasture dry matter yield. *Precision Agriculture, 12*(2), 214–232.

Simpson, R. J., Stefanski, A., Marshall, D. J., Moore, A. D., & Richardson, A. E. (2010). *The farm-gate phosphorus balance of sheep grazing systems maintained at three contrasting soil fertility levels*. Paper presented at the Food Security from Sustainable Agriculture. Proceedings of the 15th Australian Agronomy Conference, Lincoln, New Zealand.

Taylor, J. A., McBratney, A. B., & Whelan, B. M. (2007). Establishing management classes for broadacre agricultural production. *Agronomy Journal, 99*(5), 1366–1376. doi: 10.2134/agronj2007.0070

Trotter, M., & Lamb, D. (2008). *GPS tracking for monitoring animal, plant and soil interactions in livestock systems*. Paper presented at the 9th International Conference on Precision Agriculture, Denver, Colorado, USA.

Turner, N., & Asseng, S. (2005). Productivity, sustainability, and rainfall-use efficiency in Australian rainfed mediterranean agricultural systems. *Crop and Pasture Science, 56*(11), 1123–1136.

Wong, M. T. F., & Asseng, S. (2006). Determining the causes of spatial and temporal variability of wheat yields at sub-field scale using a new method of upscaling a crop model. *Plant and Soil, 283*(1–2), 203–215.

Xu, H., Wang, K., Bailey, J., Jordan, C., & Withers, A. (2006). Temporal stability of sward dry matter and nitrogen yield patterns in a temperate grassland. *Pedosphere, 16*(6), 735–744.

# CHAPTER 8. GENERAL DISCUSSION, CONCLUSIONS AND FUTURE WORK

**“The future is already here–it's just not evenly distributed”.**

***William Gibson, The Economist, 4 December 2003***

While the applications and benefits of precision agriculture (PA) technologies in cropping systems have been widely discussed in the literature, the use of these technologies as a whole-of-farm management strategy in mixed farming systems has received far less attention. Relatively little is known about the nature, extent or temporal stability of the spatial variability of pasture production in mixed farming systems and whether it is feasible to manage this overall variability in a site-specific way. Given that at any time in a mixed farming system somewhere between 20 and 40% of the farm area will be in pasture, there is significant potential for PA technologies to enhance mixed farm management practices.

This study explored some themes around the use of PA technologies in mixed farming systems, based on the measurement and management of spatial variation in mixed farming systems. Technologies explored included satellite-based remote sensing and 'on-the-go' proximal sensors.

The research described here has been successful in working towards providing both researchers and producers with methodology and information to incorporate pasture phase information into a precision management system. A criterion when planning this work was that it had to benefit farmers, not just research 'curiosity'. This meant that the PA technologies used had to be relatively user-friendly and affordable, and ideally, already in use on-farm. This would encourage farmer uptake and comfort with the concepts and approaches taken, e.g. being able to measure pasture biomass with an instrument.

The following hypotheses were tested:

**HYPOTHESIS 1:** *Spatial variation in biomass production over time is correlated between the cropping and pasture phases of mixed farming enterprises*.

**HYPOTHESIS 2:** *Spatial variation of production in the crop and pasture phases of a mixed farming system can be identified and quantified at high resolution using PA technologies.*

**HYPOTHESIS 3:** *Data acquired using PA technologies can be used to create a single index of paddock productivity that describes the spatial variation in, and temporal stability of, crop and pasture production over time*.

The literature review (Chapter 2) discussed the applications of satellite-based remote sensing to precision agriculture, including the use of vegetation indices. Chapters 3 and 4 investigated the use of low-resolution MODIS NDVI data to test Hypothesis 1. The results from Chapters 3 and 4 provided sufficient evidence, albeit at a very coarse resolution, to support this hypothesis. A clear outcome of the work described in Chapters 3 and 4 is that resolution matters: comparisons between crop and pasture productivity need to be carried out at a spatial resolution that is fine enough to reflect the spatial variability observed from yield mapping data. Yield monitor data was collected at 10 m spacings (the width of the header front), EMI and GR scans were conducted at 30–35 m spacings, and Crop Circle™ data was collected on 40 m transects. These transects fall within the optimal spacings determined by O'Leary et al. (2005). Resolutions of 30–40 m are also compatible with most seeder bars, the requirements of controlled-traffic operations, and appear to be on a scale that growers can manage variability with their current machinery. While 30 m resolution NDVI data is available at no cost from Landsat 7 and 8, the satellite-based remote sensing approach is still limited by the availability of cloud-free images for the peak growing months between July and November.

Chapter 5 explored the use of 'on-the-go' soil sensors to quantify and map soil variability at much higher spatial resolution, supported with traditional physical and chemical soil analysis. The results demonstrated the capacity of EMI and GR sensing to provide accurate and reliable detail on within-paddock variation in soil textures and some soil chemical properties. In regions with highly weathered soils, such as "Milroy", the integration of GR data improved the characterisation of sub-paddock soil properties compared with using an EMI sensor alone. The data acquired and processed in this chapter was then used to test Hypotheses 2 and 3.

The work in Chapter 6 demonstrated that 'yield' maps showing the spatial variation in mixed species pasture green dry biomass can be produced as accurately as paddock sampling using exclusion cages and pasture cuts, or pasture disc meters, but far more rapidly and at much higher spatial resolution. Once pasture cuts have been taken and the weights are calibrated to NDVI readings, ongoing scans of a 100 ha paddock can be completed in less than two hours. This is the first time that high-

resolution pasture and crop yield data has been combined to identify potential management classes for a paddock. The results from Chapter 6 confirmed Hypothesis 2 that, "*spatial variation of production in the crop and pasture phases of a mixed farming system can be identified and quantified at high resolution using precision agriculture technologies"*. They also demonstrated that there was significant spatial variability within a year in both the crop and pasture phases.

At the conclusion of Chapter 6, some of the data was used to identify potential management zones using *k*-means clustering to identify areas within a paddock that might be suitable for site-specific management. There were two further outcomes worth noting from this work:

1) The pasture data did not substantially change the shape or size of the management classes (Figures 6.28–6.31) in any of the paddocks studied. This provides additional evidence to support Hypothesis 1.
2) At "Milroy", moving from two to three management classes partitioned the low yield class into two sub-classes, rather than creating three new classes across the dataset. The original low class was divided into one class of low mean yields containing the infertile deep sands and gravels, and a second class of low mean yields containing saline soils. This is potentially a valuable method for identifying and categorising problem soils for targeted management.

Chapter 7 successfully tested Hypothesis 3 that, "*data acquired using PA technologies can be used to create a single index of paddock productivity that describes the spatial variation in, and temporal stability of, crop and pasture production over time*". Spatial trends in yield were defined by the average value of crop or pasture production at each point in a paddock over time. The temporal variance maps showed how each part of a paddock performed over time, relative to the mean, by using a modified standard deviation function. The creation of the stability index described a methodology for turning spatial and temporal data into management information. Classified management maps based on stability indices were created to show the spatial and temporal trends simultaneously and to identify potential management zones. These maps were derived from a different set

of data from the management class maps in Chapter 6, but there are strong similarities between them. The stability index still has some limitations and areas of uncertainty in its current form but is certainly worthy of further research. Notwithstanding these reservations, this is the first time a pasture stability index has been created for mixed farming systems. The work described in this thesis has shown that the paddock stability index is a robust methodology that can identify areas within a paddock that exhibit similar productive behaviour, whether in crop or pasture, year in year out. It has the potential to inform decisions regarding fertiliser use and application as well as grazing management in whole-farm planning. It enables the capturing of precision data, not just in cropping years, but in every year of production. This is potentially a breakthrough in farming systems management into the future.

## 8.1 CONSTRAINTS

There were some constraints in this study. First were the typical constraints imposed by the nature of a PhD research project—there was a limited budget for travel and field work (field sites were some 3000 km apart).

Livestock grazing had a considerable effect on the spatial heterogeneity of the pasture, and it was not always clear if a particular part of a paddock happened to be low in pasture TGDM production because nothing much grew there, or because it was eaten off. Fixed cameras in paddocks and/or dung counts were considered possible means of identifying paddock spatial usage by stock, but again time became a constraining factor.

Secondly, the corruption of crop yield datasets from both farms limited the amount of yield data available. Corruption was generally due to equipment malfunctions during harvest or not calibrating multiple harvesters. This meant that statistical analysis of data was based on a smaller number of datasets than would be ideal. The very nature of mixed farming rotations also affects available data, as within a ten-year period there may be a maximum of five or six possible cropping years. Budget constraints restricted the amount of soil testing that could be done. Despite CSBP very kindly performing the soil analysis work at no cost at the “Grandview”

sites, and Precision SoilTech at the supplementary "Milroy" sites, the EMI and GR sensing and soil sampling were a significant cost. In hindsight, it would have been valuable to conduct further soil sampling after the delineation of the management classes described in Chapters 6 and 7. This would have helped to identify soil properties which may have been driving differences between zones.

If the work was to continue without constraints, it would have been invaluable to carry out further soil analysis and measure plant available water capacity, both of which have a significant influence on crop and pasture productivity and their correlations with the stability index zones (Armstrong et al., 2009; Oliver et al., 2006; Rab et al., 2009). Prior to identifying test sites, it would also be beneficial to map paddock utilisation by livestock to identify potential nutrient transfer sites. Ideally, there would be sufficient data to create soil fertility and pH maps.

## 8.2 FURTHER WORK

Future work will need to address the impact of grazing on pasture TGDM estimation and decisions about productive stability.

There is a great deal of work required to refine the definition of pasture stability index zones. For example, the impact of grazing on pasture TGDM estimation and decisions about productive stability is an area with significant knowledge gaps that were not accountable in the work described here. This is evident in the Kruskal–Wallis tests, where there were some non-significant results associated with the pasture CVs.

Meta-analysis of data from livestock fitted with GPS tracking collars and accelerometers could identify spatial preference and distribution of animals within a paddock at particular times of the day, week, month or by season and of livestock social networks. It could also identify foraging patterns, time spent grazing, resting and ruminating. This applies to the grazing of a crop in a 'grain & graze' system (Price and Hacker, 2009) as well as when the paddock is in pasture. The use of tracking data combined with modelling of grazing with software packages such as 'Grass Gro' or 'Ausfarm' could further refine the accuracy of the pasture data. Notwithstanding these reservations, this work has shown that the paddock stability

index is a robust methodology that can identify significant areas of a paddock that exhibit similar productive behaviour, whether in crop or pasture, year in year out.

Virtual fencing is a technology that is not far from becoming economically viable, especially for cattle. Virtual fencing based on the stability index zones would further enhance livestock/pasture management flexibility in a mixed farming system. Both farm owners had commented on the difficulty they have in managing stock in paddocks that need to be large enough for efficient cropping–livestock management.

## 8.3 CONCLUDING REMARKS

The dominant influences on yield variability in rainfed farming systems are climate/rainfall and variation in soil physical characteristics such as soil texture and water holding capacity. A key challenge for managers of these farming systems, therefore, is managing the risk associated with low and variable rainfall on highly variable soils. The work described here provides farm owners, managers and researchers with a methodology for monitoring spatial variation in both crop and pasture phases. It is hoped that this work provides a valuable contribution to the challenges of managing from a whole-farm perspective to minimising the costs and risks of moving between cropping and livestock phases.

Although there is still much to do to develop the stability index into a viable management tool, feedback from the participants in this research has been positive:

*“This stability index stuff is more important—it will be valuable for our N strategy and predicting yield potentials and yield targets. This is particularly good”.* Adam Inchbold, “Grandview” 2016.

*“Really interesting—I never thought about variable rate fertiliser in our pastures. We can do it with the stability indices.”* Adam Inchbold, 2015, “Grandview”.

*"Pastures are a significant share of production land area in a mixed farming system, the research described here utilising currently available Precision technologies shows how we can enhance crop productivity, pasture availability and animal feed*

*regimes. This can save costs, leading to better profits.*" Murray Hall, 2015, "Milroy", Brookton, WA.

*"This is excellent, you are cementing in what's going on in the paddock by combining sets of data, rather than looking at just one factor."* Peter Baines, 2016, local agronomist, Albury, NSW.

## 8.4 REFERENCES

Armstrong, R. D., Fitzpatrick, J., Rab, M. A., Abuzar, M., Fisher, P. D., & O'Leary, G. J. (2009). Advances in precision agriculture in south-eastern Australia. III. Interactions between soil properties and water use help explain spatial variability of crop production in the Victorian Mallee. *Crop and Pasture Science, 60*(9), 870–884. doi:10.1071/CP08349

O'Leary, G. J., Grinter, V., & Mock, I. (2005). *Optimal transect spacing for EM38 mapping for dryland agriculture in the Murray Mallee, Australia*. Paper presented at the 4th International Crop Science Congress, Brisbane, Queensland.

Oliver, Y. M., Wong, M. T. F., Robertson, R., & Wittwer, K. (2006). *PAWC determines spatial variability in grain yield and nitrogen requirement by interacting with rainfall on northern WA sandplain*. Paper presented at the 13th Australian Agronomy Conference, Perth, Western Australia.

Price, R. J., & Hacker, R. B. (2009). Grain and Graze: an innovative triple bottom line approach to collaborative and multidisciplinary mixed-farming systems research, development and extension. *Animal Production Science, 49*(10), 729–735. doi: 10.1071/EA08306

Rab, M. A., Fisher, P. D., Armstrong, R. D., Abuzar, M., Robinson, N. J., & Chandra, S. (2009). Advances in precision agriculture in south-eastern Australia. IV. Spatial variability in plant-available water capacity of soil and its relationship with yield in site-specific management zones. *Crop and Pasture Science, 60*(9), 885–900. doi: 10.1071/CP08350

Every reasonable effort has been made to acknowledge the owners of copyright material. I would be pleased to hear from any copyright owner who has been omitted or incorrectly acknowledged.

# APPENDICES

**APPENDIX 1:** MODIS PIXELS FOR "MILROY" PADDOCK M25 (A), M41 (B) AND M45 (C).

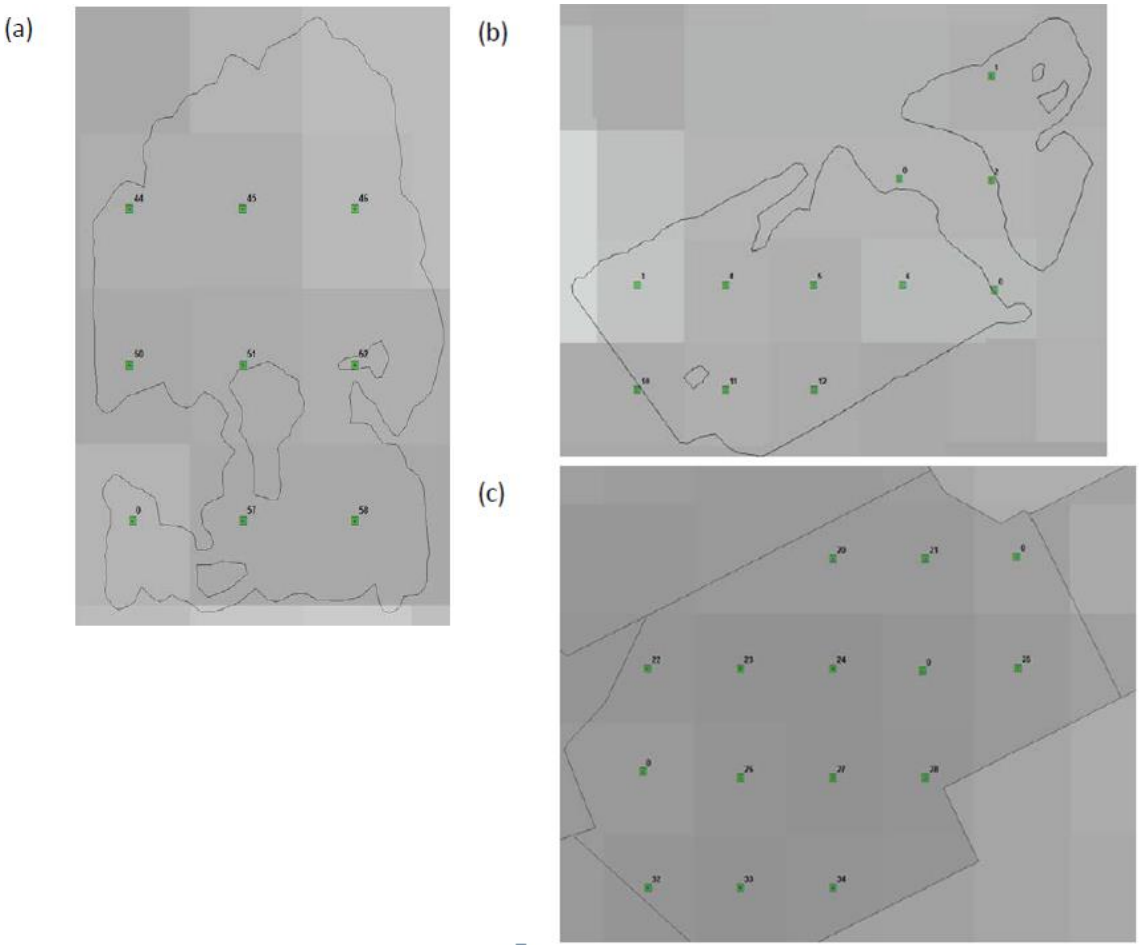

**APPENDIX 2:** MODIS PIXELS FOR ACCUMULATED NDVI FOR "GRANDVIEW" PADDOCKS GV4 (A) GV8 (B) AND GV39 (C).

(a)

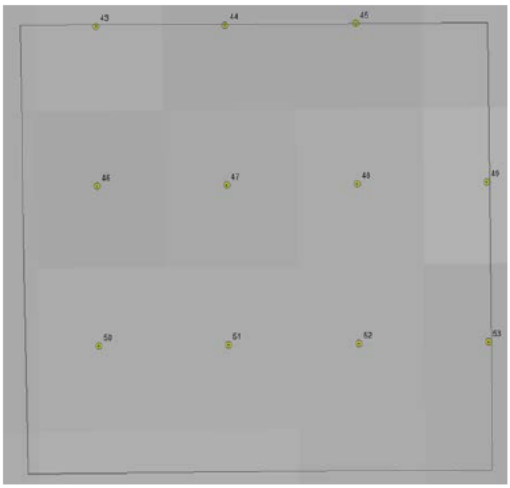


(b)


(c)

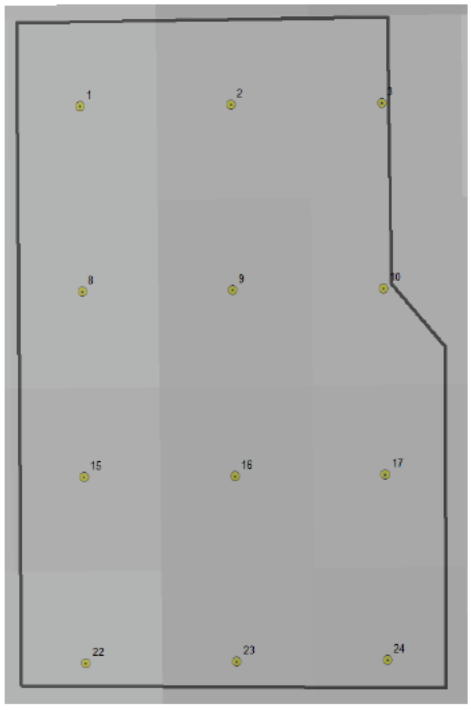

**APPENDIX 3:** CORRELATION MATRIX FOR ACCUMULATED NDVI FOR "MILROY" PADDOCK M25 (A) AND M41 (B).

(a)

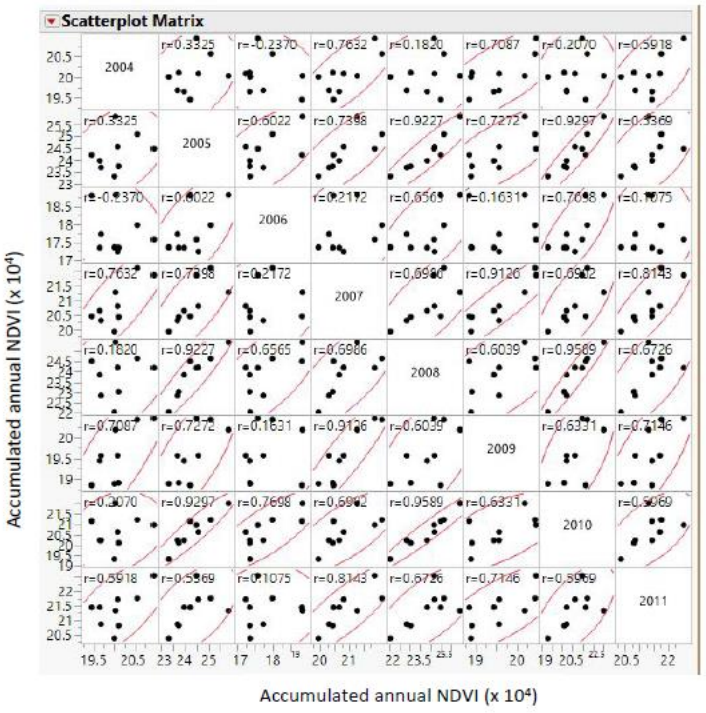


(b)

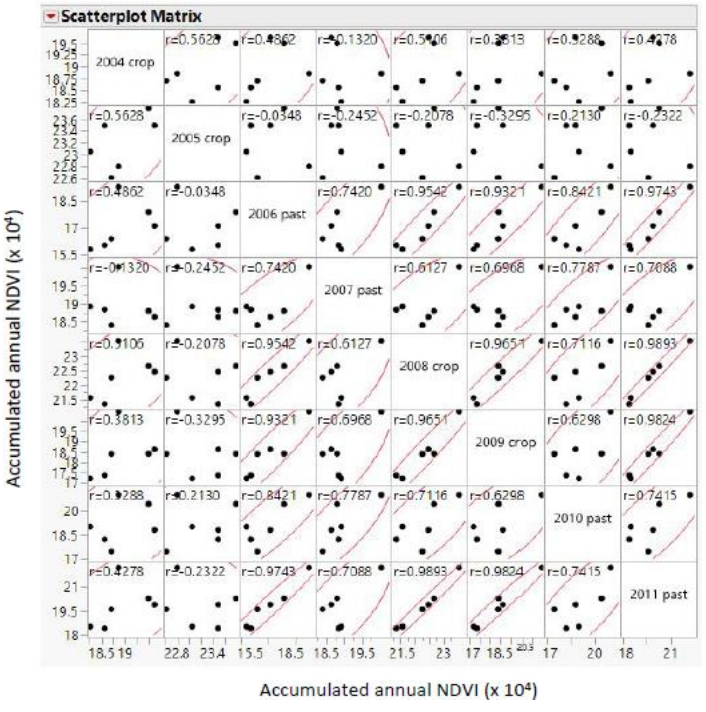

**APPENDIX 4:** CORRELATION MATRIX FOR ACCUMULATED NDVI FOR "GRANDVIEW" PADDOCK GV4 (A) GV8 (B) AND GV39 (C).

(a)

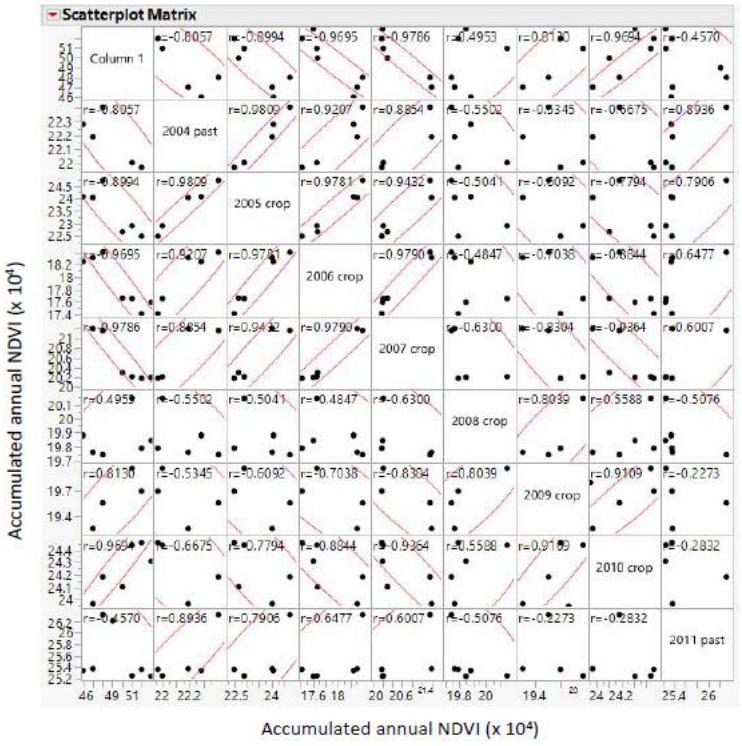


(b)

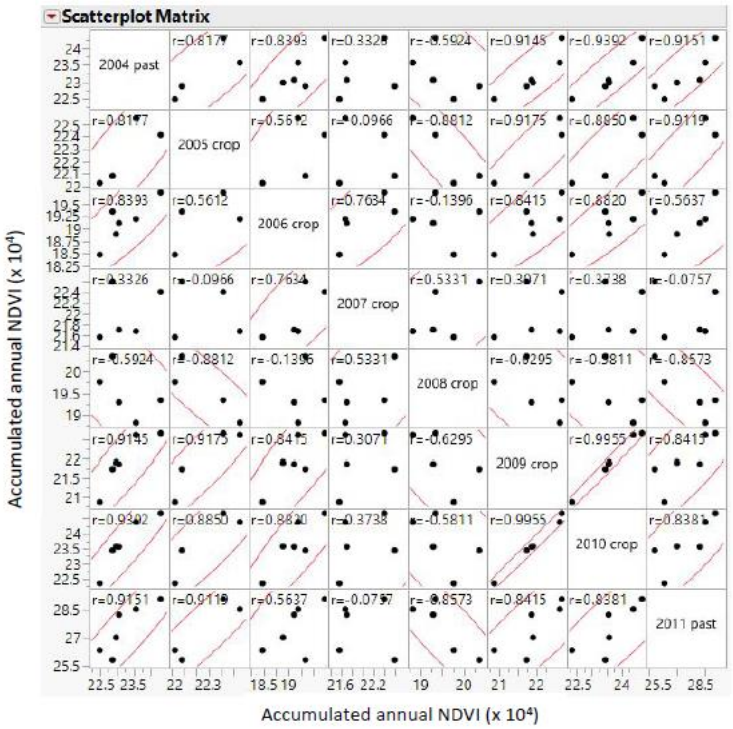

(c)

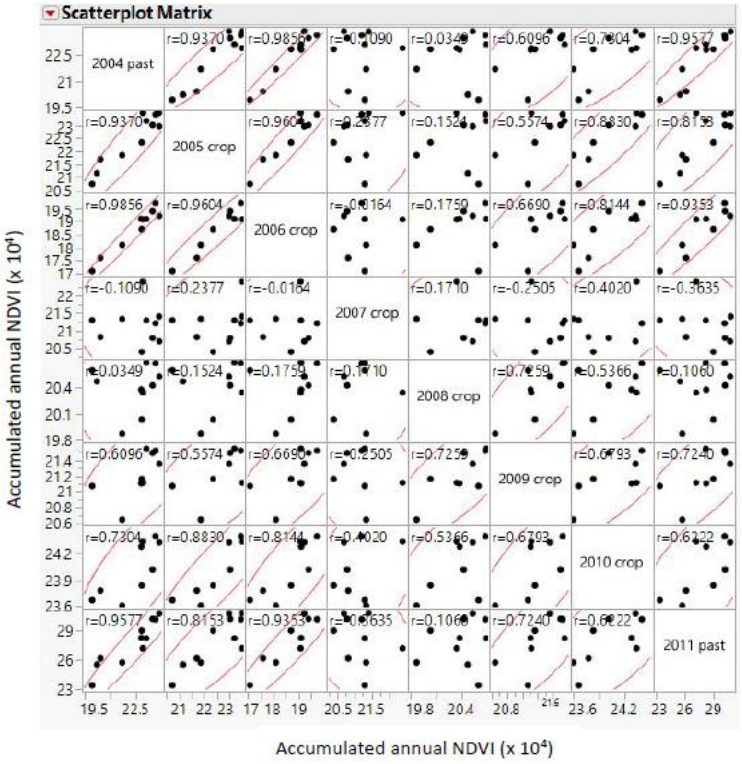
Scatterplot Matrix
2004 past
2005 crop
2006 crop
2007 crop
2008 crop
2009 crop
2010 crop
2011 past
Accumulated annual NDVI (x 10⁴)
Accumulated annual NDVI (x 10⁴)

**APPENDIX 5:** EMI MAPS FOR "MILROY" PADDOCK M45 (A) 0–50 CM, (B) 0–100 CM AND "GRANDVIEW" PADDOCKS GV3 (C) 0–38 CM AND (D) 0–75 CM) AND GV4 (E) 0–38 CM AND (F) 0–75 CM.

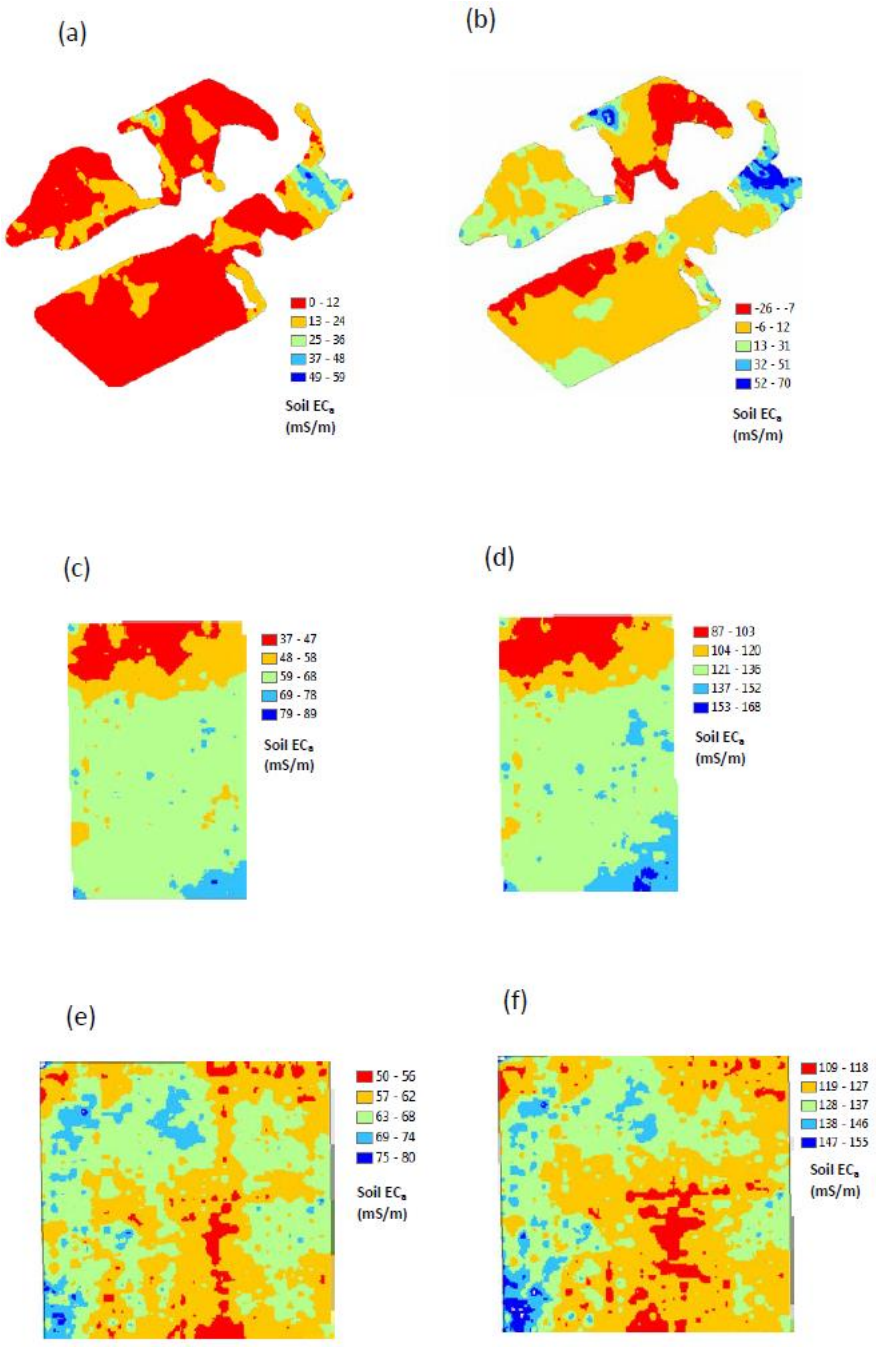

**APPENDIX 6:** GAMMA RADIOMETRIC MAPS FOR "MILROY" PADDOCK M45 (A) GAMMA TC, (B) GAMMA K (C) GAMMA TH AND (D) GAMMA U.

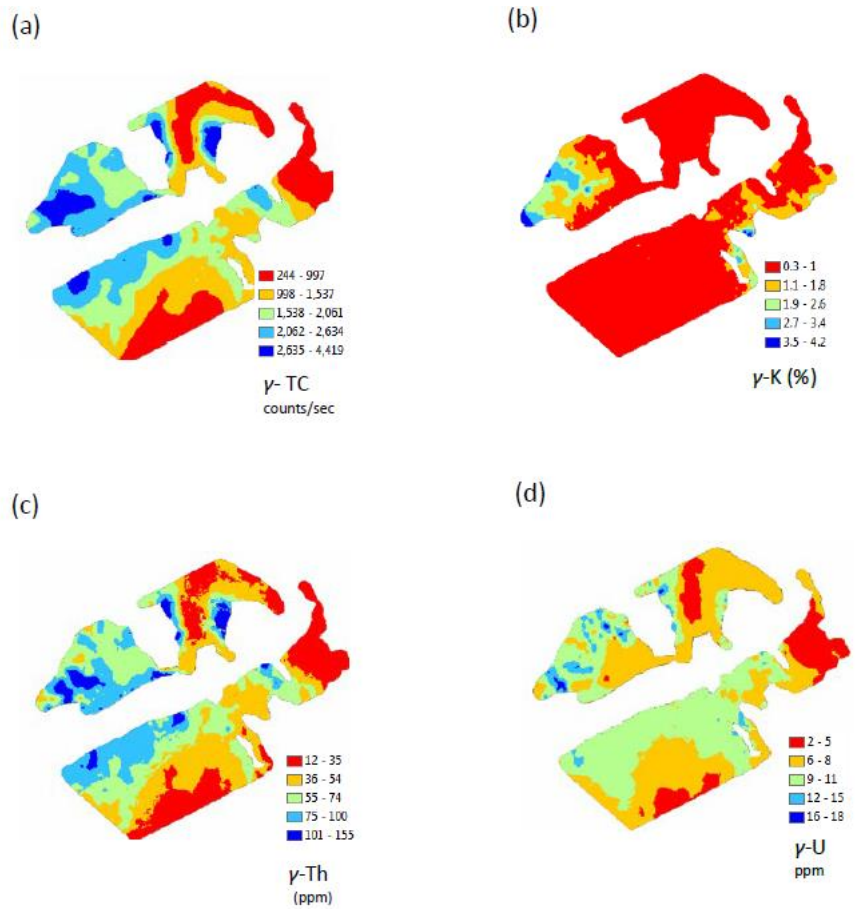

**APPENDIX 7:** SOIL TEST RESULTS FOR "MILROY" PADDOCKS M25.

| Paddock | Site | Depth | $NO_3$ | $NH_4$ | Colwell P | Colwell K | S (ppm) | OC% | EC (mS/m) | pH ($CaCl_2$) | Al ($CaCl_2$) ppm | PBI |
|---|---|---|---|---|---|---|---|---|---|---|---|---|
| M25 | EM3 | 0–10 | 1.0 | 9.0 | 31.0 | 82.0 | 4.6 | 2.2 | 4.4 | 4.7 | | 39 |
| | | 10–30 | | | 13.0 | 40.0 | | | 2.0 | 4.9 | 0.6 | |
| | | 30–60 | | | | | | | 1.7 | 5.5 | 0.2 | |
| | EM5 | 0–10 | 5.0 | 18.0 | 28.0 | 233.0 | 4.9 | 2.8 | 5.6 | 4.7 | | 69 |
| | | 10–30 | | | 5.0 | 159.0 | | | 7.1 | 5.8 | 0.2 | |
| | | 30–60 | | | | | | | 11.8 | 6.6 | 0.2 | |
| | Th4 | 0–10 | | | | | | | 6.0 | 4.7 | 2.7 | 29.8 |
| | | 10–30 | | | | | | | 0 | 0 | 0 | |
| | | 30–60 | | | | | | | 2.0 | 1.57 | 0.89 | |
| | K4 | 0–10 | | | 23.0 | 29.0 | | | 5.4 | 4.9 | 2.1 | 30.9 |
| | | 10–30 | | | 9.0 | 15.0 | | | 2.2 | 4.8 | 1.5 | |
| | | 30–60 | | | 14.0 | 20.0 | | | 3.3 | 4.83 | 1.66 | |

**APPENDIX 8:** SOIL TEST RESULTS FOR "MILROY" PADDOCK M41.

| Paddock | Site | Depth | $NO_3$ | $NH_4$ | Colwell P | Colwell K | S (ppm) | OC% | EC (mS/m) | pH ($CaCl_2$) | Al ($CaCl_2$) ppm | PBI |
|---|---|---|---|---|---|---|---|---|---|---|---|---|
| M41 | EM2 | 0–10 | 2.0 | 12.0 | 55.0 | 86.0 | 3.8 | 1.5 | 2.7 | 4.8 | | 60 |
| | | 10–30 | | | 6.0 | 49.0 | | | 1.5 | 4.9 | 0.3 | |
| | | 30–60 | | | | | | | 2.5 | 5.9 | 0.2 | |
| | Th1 | 0–10 | | | | | | | 2.1 | 4.7 | 3.1 | 22.6 |
| | | 10–30 | | | | | | | 2.0 | 4.4 | 8.4 | |
| | | 30–60 | | | | | | | 2.0 | 4.5 | 6.6 | |
| | K3 | 0–10 | | | 48.0 | 43.0 | | | 2.8 | 4.8 | 2.8 | 39 |
| | | 10–30 | | | 12.0 | 20.0 | | | 1.1 | 4.7 | 2.0 | |
| | | 30–60 | | | 24.0 | 28.0 | | | 1.7 | 4.73 | 2.23 | |
| | 1 | 0–10 | 1 | 3 | 25 | 47 | 4.7 | 0.78 | 3.4 | 4.8 | | 11.5 |
| | | 10–20 | 1 | <1 | 14 | <15 | 1.4 | 0.17 | <1 | 4.6 | | 3.8 |
| | | 20–30 | <1 | <1 | 13 | <15 | 1.9 | 0.14 | <1 | 4.6 | | 10.0 |
| | | 30–40 | 1 | <1 | 12 | 17 | 1.9 | 0.12 | <1 | 4.7 | | 11.6 |
| | | 40–50 | 1 | <1 | 9 | 20 | 2.1 | 0.28 | <1 | 4.6 | | 18.5 |
| | 2 | 0–10 | 1 | 7 | 44 | 79 | 4.1 | 1.02 | 5.3 | 4.8 | | 23.9 |
| | | 10–20 | 1 | <1 | 34 | 18 | 2.8 | 0.30 | 1.3 | 4.7 | | 19.5 |
| | | 20–30 | 1 | <1 | 18 | 15 | 3.0 | 0.18 | 1.0 | 4.8 | | 19.2 |
| | | 30–40 | <1 | <1 | 8 | 19 | 2.5 | 0.10 | 1.3 | 4.9 | | 13.6 |
| | | 40–50 | <1 | <1 | 5 | 22 | 1.9 | 0.06 | <1.0 | 5.1 | | 10.6 |
| | 3 | 0–10 | 2 | 14 | 44 | 277 | 10 | 2.1 | 11.7 | 4.9 | | 124.3 |
| | | 10–20 | 2 | <1 | 5 | 111 | 10.5 | 0.57 | 2.5 | 5.5 | | 148.7 |
| | | 20–30 | 1 | <1 | 5 | 53 | 14.2 | 0.34 | 2.7 | 5.8 | | 161.0 |
| | | 30–40 | 1 | <1 | 3 | 38 | 15.6 | 0.30 | 2.7 | 6.0 | | 189.7 |
| | | 40–50 | 1 | <1 | 4 | 35 | 16.1 | 0.31 | 2.5 | 5.9 | | 180.9 |

| Paddock | Site | Depth | $NO_3$ | $NH_4$ | Colwell P | Colwell K | S (ppm) | OC% | EC (mS/m) | pH ($CaCl_2$) | Al ($CaCl_2$) ppm | PBI |
|---|---|---|---|---|---|---|---|---|---|---|---|---|
| M41 | 4 | 0–10 | 2 | 9 | 50 | 133 | 14.1 | 2.56 | 7.7 | 5.0 | | 100.5 |
| | | 10–20 | 2 | 1 | 12 | 50 | 10.2 | 0.83 | 2.6 | 5.2 | | 114.7 |
| | | 20–30 | 2 | 1 | 7 | 36 | 8.8 | 0.43 | 2.8 | 5.6 | | 106.1 |
| | | 30–40 | 1 | 1 | 5 | 32 | 13.6 | 0.39 | 2.9 | 5.7 | | 162.8 |
| | | 40–50 | 1 | 2 | 5 | 28 | 30.4 | 0.38 | 4.2 | 5.8 | | 188.5 |
| | 5 | 0–10 | 2 | 8 | 50 | 184 | 7.7 | 2.13 | 5.2 | 5.1 | | 77.9 |
| | | 10–20 | 2 | <1 | 10 | 120 | 4.5 | 0.6 | 2.2 | 5.4 | | 69.6 |
| | | 20–30 | 2 | <1 | 6 | 90 | 6.1 | 0.36 | 2.2 | 5.9 | | 76.4 |
| | | 30–40 | 1 | <1 | 4 | 69 | 6.9 | 0.23 | 2.1 | 6.1 | | 83.3 |
| | | 40–50 | 1 | <1 | 5 | 69 | 7.7 | 0.29 | 2.3 | 6.1 | | 99.2 |
| | 6 | 0–10 | 5 | 8 | 49 | 127 | 7.4 | 1.37 | 5.4 | 4.9 | | 35.9 |
| | | 10–20 | 2 | 2 | 13 | 25 | 3.4 | 0.26 | 1.7 | 4.9 | | 28.3 |
| | | 20–30 | 1 | <1 | 5 | 23 | 4.2 | 0.17 | 1.4 | 5.4 | | 35.0 |
| | | 30–40 | <1 | <1 | 4 | 20 | 7.0 | 0.18 | 2.1 | 5.5 | | 49.4 |
| | | 40–50 | 1 | 2 | 3 | 21 | 21.8 | 0.20 | 4.4 | 5.7 | | 105.5 |
| | 7 | 0–10 | 8 | 3 | 46 | 71 | 9.8 | 1.6 | 6.0 | 4.9 | | 57.7 |
| | | 10–20 | 2 | 2 | 11 | 31 | 6.7 | 0.7 | 2.4 | 5.1 | | 80.2 |
| | | 20–30 | 1 | 1 | 6 | 27 | 4.8 | 0.55 | 1.6 | 5.5 | | 83.2 |
| | | 30–40 | 2 | <1 | 4 | 18 | 4.0 | 0.32 | 2.2 | 5.7 | | 59.7 |
| | | 40–50 | <1 | 2 | 5 | 17 | 5.6 | 0.22 | 2.4 | 5.8 | | 59.8 |
| | 8 | 0–10 | 15 | 5 | 45 | 120 | 20.6 | 2.57 | 11.8 | 4.9 | | 124.5 |
| | | 10–20 | 2 | 3 | 10 | 33 | 16.4 | 0.95 | 4.3 | 5.1 | | 170.1 |
| | | 20–30 | 1 | 2 | 7 | 29 | 22.6 | 0.6 | 4.5 | 5.3 | | 174.6 |
| | | 30–40 | 1 | 2 | 7 | 26 | 21.1 | 0.72 | 3.6 | 5.3 | | 205.7 |
| | | 40–50 | 1 | <1 | 6 | 26 | 24.6 | 0.59 | 3.9 | 5.3 | | 206.2 |

**APPENDIX 9:** SOIL TEST RESULTS FOR "MILROY" PADDOCK M45.

| Paddock | Site | Depth | $NO_3$ | $NH_4$ | Colwell P | Colwell K | S (ppm) | OC% | EC (mS/m) | pH ($CaCl_2$) | Al ($CaCl_2$) ppm | PBI |
|---|---|---|---|---|---|---|---|---|---|---|---|---|
| M45 | EM4 | 0–10 | 4.0 | 13.0 | 38.0 | 179.0 | 11 | 3.6 | 4.5 | 4.8 | | 172 |
| | | 10–30 | | | 9.0 | 144.0 | | | 2.9 | 5.2 | 0.3 | |
| | | 30–60 | | | | | | | 2.8 | 5.9 | 0.2 | |
| | K2 | 0–10 | | | 13.0 | 75.0 | | | 4.0 | 4.8 | 1.8 | 103.8 |
| | | 10–30 | | | 4.0 | 42.0 | | | 2.5 | 4.8 | 1.5 | |
| | | 30–60 | | | 7.0 | 53.0 | | | 3.0 | 4.8 | 1.57 | |
| | Th3 | 0–10 | | | | | | | 8.4 | 4.7 | 2.0 | 153.9 |
| | | 10–30 | | | | | | | 4.0 | 5.6 | 1.6 | |
| | | 30–60 | | | | | | | 5.5 | 5.3 | 1.04 | |
| | 1 | 0–10 | 7 | 9 | 28 | 250 | 14.8 | 3.61 | 11.2 | 5.1 | | 108.2 |
| | | 10–20 | 3 | 4 | 11 | 109 | 8.3 | 1.45 | 8.0 | 5.4 | | 122.6 |
| | | 20–30 | 3 | 3 | 11 | 132 | 13.5 | 1.58 | 9.6 | 5.5 | | 126.9 |
| | | 30–40 | 2 | 2 | 7 | 129 | 23.5 | 1.33 | 12.2 | 5.5 | | 121.4 |
| | 2 | 0–10 | 4 | 7 | 26 | 371 | 13.0 | 3.3 | 6.6 | 5.2 | | 228.6 |
| | | 10–20 | 2 | 2 | 6 | 216 | 9.8 | 1.69 | 2.2 | 5.5 | | 333.3 |
| | | 20–30 | 1 | <1 | 3 | 222 | 9.4 | 1.11 | 3.2 | 5.6 | | 385.3 |
| | | 30–40 | 1 | 1 | 3 | 180 | 11.0 | 1.32 | 2.6 | 5.9 | | 451.5 |
| | | 40–50 | 2 | <1 | 4 | 142 | 10.2 | 1.19 | 3.4 | 5.9 | | 482.1 |
| | 3 | 0–10 | 3 | 6 | 21 | 180 | 8.8 | 2.17 | 3.2 | 5.3 | | 95.9 |
| | | 10–20 | 2 | <1 | 4 | 107 | 5.8 | 0.68 | 1.7 | 5.3 | | 104.3 |
| | | 20–30 | 1 | <1 | 2 | 100 | 4.8 | 0.34 | 1.3 | 5.7 | | 109.8 |
| | | 30–40 | 1 | 1 | <2 | 69 | 4.6 | 0.22 | 1.4 | 5.8 | | 124.3 |
| | | 40–50 | <1 | <1 | <2 | 50 | 4.6 | 0.27 | 1.1 | 5.9 | | 116.9 |
| | 4 | 0–10 | 2 | 12 | 44 | 380 | 20.1 | 3.29 | 10.3 | 5.1 | | 159.2 |

| Paddock | Site | Depth | $NO_3$ | $NH_4$ | Colwell P | Colwell K | S (ppm) | OC% | EC (mS/m) | pH ($CaCl_2$) | Al ($CaCl_2$) ppm | PBI |
|---|---|---|---|---|---|---|---|---|---|---|---|---|
| | | 10–20 | 2 | <1 | 10 | 182 | 10.0 | 1.07 | 3.5 | 5.7 | | 170.2 |
| | | 20–30 | 1 | 1 | 5 | 115 | 14.3 | 0.40 | 3.1 | 6.1 | | 169.1 |
| | | 30–40 | 1 | <1 | 5 | 97 | 13.9 | 0.21 | 2.3 | 6.2 | | 171.4 |
| | | 40–50 | 1 | <1 | 4 | 67 | 10.6 | 0.35 | 3.1 | 6.3 | | 165.0 |
| M45 | 5 | 0–10 | 1 | 7 | 46 | 126 | 10.8 | 1.93 | 3.7 | 4.5 | | 89.8 |
| | | 10–20 | 2 | <1 | 10 | 76 | 12.5 | 0.85 | 1.8 | 4.5 | | 100.9 |
| | | 20–30 | 1 | <1 | 5 | 48 | 12.8 | 0.45 | 1.4 | 4.8 | | 105.5 |
| | | 30–40 | 1 | <1 | 7 | 24 | 12.5 | 0.34 | 1.6 | 5.0 | | 25.8 |
| | | 40–50 | 1 | <1 | 5 | 26 | 13.1 | 0.33 | 1.9 | 5.1 | | 111.4 |
| | 6 | 0–10 | 1 | 6 | 46 | 130 | 13.3 | 1.89 | 5.2 | 4.6 | | 129.5 |
| | | 10–20 | 1 | <1 | 9 | 50 | 11.7 | 0.62 | 2.0 | 4.6 | | 132.6 |
| | | 20–30 | 1 | <1 | 6 | 25 | 11.5 | 0.36 | 2.5 | 5.2 | | 143.4 |
| | | 30–40 | 1 | <1 | 4 | 23 | 14.8 | 0.34 | 2.0 | 5.3 | | 151.1 |
| | | 40–50 | 1 | <1 | 7 | 31 | 13.6 | 0.5 | 2.3 | 5.4 | | 162.2 |
| | 7 | 0–10 | 13 | 6 | 58 | 126 | 16.2 | 2.15 | 7.0 | 4.7 | | 50.5 |
| | | 10–20 | 3 | 1 | 28 | 40 | 6.1 | 1.21 | 1.6 | 4.6 | | 54.3 |
| | | 20–30 | 2 | <1 | 10 | 34 | 3.8 | 0.42 | 1.4 | 5.1 | | 30.2 |
| | | 30–40 | <1 | <1 | 7 | 22 | 3.4 | 0.27 | <1.0 | 5.2 | | 101.0 |
| | | 40–50 | 1 | <1 | 5 | 27 | 3.5 | 0.3 | 1.2 | 5.4 | | 26.2 |

**APPENDIX 10:** SOIL TEST RESULTS FOR "GRANDVIEW" PADDOCKS GV3 AND GV4.

| Paddock | Site | Depth | $NO_3$ (mg/kg) | $NH_4$ (mg/kg) | kg N/ha 0–50 cm | Colwell P (mg/kg) | Colwell K (mg/kg) | S (mg/kg) | OC% | EC (mS/m) | pH ($CaCl_2$) | Al ($CaCl_2$) (meq/100 g) | ESP (%) |
|---|---|---|---|---|---|---|---|---|---|---|---|---|---|
| GV3 | Low 1 | 0–10 | 5 | 2 | | 84 | 330 | 7.6 | 2.32 | 5.7 | 5.1 | 0.067 | 2 |
| | Low 2 | 0–10 | 6 | 3 | | 57 | 374 | 7 | 2.7 | 6.4 | 5.2 | 0.077 | 1 |
| | | 20–50 | 1 | 1 | 16.9 | <2 | 232 | 8.5 | 0.56 | 8.2 | 6.9 | 0.189 | 4 |
| | Low 3 | 0–10 | 5 | 3 | | 36 | 252 | 7.9 | 1.27 | 5.0 | 4.8 | 0.198 | 3 |
| | High 1 | 0–10 | 3 | 4 | | 49 | 254 | 7.8 | 1.43 | 9.6 | 6.4 | 0.095 | 7 |
| | | 20–50 | <1 | 1 | 14.3 | 3 | 146 | 26.2 | 0.56 | 21.4 | 7.5 | 0.087 | 4 |
| | High 2 | 0–10 | 5 | 5 | | 52 | 276 | 7.3 | 3.24 | 5.3 | 5.8 | 0.080 | 5 |
| | | 20–50 | 1 | <1 | 18.2 | <2 | 240 | 26.6 | 0.58 | 20.2 | 7.5 | 0.128 | 13 |
| | High 3 | 0–10 | 4 | 4 | | 23 | 326 | 8.8 | 1.68 | 11.2 | 6.2 | 0.077 | 8 |
| | | 20–50 | <1 | <1 | | <2 | 254 | 40.1 | 0.66 | 38.2 | 7.7 | 0.103 | 18 |
| GV4 | Med 1 | 0–10 | 6 | 3 | | 53 | 311 | 5.6 | 1.71 | 6.5 | 6.0 | 0.040 | 5 |
| | | 10–50 | 2 | 2 | 22.1 | 3 | 273 | 13.1 | 0.71 | 17.3 | 7.3 | 0.103 | 13 |
| | Med 2 | 0–10 | 5 | 4 | | 44 | 283 | 6.0 | 1.82 | 8.3 | 6.0 | 0.072 | 5 |
| | | 10–50 | 2 | 2 | 22.1 | 5 | 183 | 13.9 | 0.65 | 11.6 | 6.7 | 0.107 | 13 |
| | Med 3 | 0–10 | 9 | 2 | | 67 | 399 | 5.3 | 1.93 | 7.8 | 6.0 | 0.036 | 3 |
| | | 10–50 | 3 | 2 | | 24 | 216 | 6.0 | 0.83 | 6.0 | 6.0 | 0.078 | 9.2 |
| | High 1 | 0–10 | 5 | 2 | | 62 | 368 | 5.8 | 1.70 | 10.5 | 7.2 | 0.088 | 5 |
| | | 10–50 | 2 | <1 | 19.5 | <2 | 342 | 30.8 | 0.44 | 39.5 | 8.0 | 0.113 | 16 |
| | High 2 | 0–10 | 4 | 4 | | 66 | 228 | 9.1 | 2.02 | 6.8 | 5.9 | 0.060 | 6 |
| | | 10–50 | <1 | 2 | 20.8 | 7 | 140 | 16.1 | 0.74 | 17.4 | 6.6 | 0.122 | 14 |
| | High 3 | 0–10 | 7 | 3 | | 79 | 298 | 5.1 | 2.99 | 10.3 | 6.1 | 0.065 | 4 |
| | | 10–50 | 2 | 3 | 28.6 | 3 | 194 | 20.2 | 0.73 | 21.0 | 7.1 | 0.119 | 14 |

**APPENDIX 11:** SOIL TEST RESULTS FOR "GRANDVIEW" PADDOCKS GV8 AND GV39.

| Paddock | Site | Depth | $NO_3$ (mg/kg) | $NH_4$ (mg/kg) | kg N/ha 0–50 cm | Colwell P (mg/kg) | Colwell K (mg/kg) | S (mg/kg) | OC% | EC (mS/m) | pH ($CaCl_2$) | Al ($CaCl_2$) (meq/100 g) | ESP (%) |
|---|---|---|---|---|---|---|---|---|---|---|---|---|---|
| GV8 | Med 1 | 0–10 | 17 | 2 | | 43 | 306 | 6.4 | 1.9 | 0.64 | 4.9 | 0.105 | 4 |
| | | 10–50 | 3 | <1 | 27.3 | 6 | 254 | 5.0 | 0.6 | 0.58 | 6.4 | 0.128 | 10 |
| | Med 2 | 0–10 | 15 | 10 | | 57 | 213 | 9.1 | 2.8 | 1.1 | 5.0 | 0.102 | 8 |
| | | 10–50 | 3 | 2 | 42.9 | <2 | 206 | 14.9 | 0.69 | 2.4 | 7.2 | 0.130 | 15 |
| | Med 3 | 0–10 | 20 | 4 | | 30 | 403 | 9.8 | 2.15 | 1.0 | 4.9 | 0.106 | 3 |
| | | 10–50 | 4 | 3 | 46.8 | 13 | 239 | 7.5 | 1.06 | 0.41 | 4.8 | 0.223 | 6 |
| | Low 1 | 0–10 | 25 | 7 | | 74 | 506 | 8.5 | 3.98 | 1.58 | 5.2 | 0.071 | 5 |
| | Low 2 | 0–10 | 26 | 3 | | 47 | 302 | 9.5 | 3.14 | 1.16 | 4.5 | 0.389 | 6 |
| | | 10–50 | 3 | 1 | 42.9 | 9 | 186 | 10.2 | 0.88 | 0.73 | 5.7 | 0.099 | 12 |
| | Low 3 | 0–10 | 18 | 7 | | 58 | 240 | 7.4 | 2.97 | 0.94 | 5.2 | 0.061 | 5 |
| | | 10–50 | 4 | 3 | | 23 | 140 | 5.6 | 1.76 | 0.64 | 4.9 | 0.171 | 9.7 |
| GV39 | Low 1 | 0–10 | 15 | 3 | | 51 | 631 | 15.4 | 3.7 | 0.98 | 5.9 | 0.024 | 1 |
| | | 10–50 | 3 | 2 | 33.8 | 18 | 399 | 3.1 | 1.7 | 0.29 | 5.1 | 0.072 | 1 |
| | Low 2 | 0–10 | 9 | 3 | | 29 | 427 | 4.0 | 2.37 | 0.62 | 5.7 | 0.025 | 0 |
| | | 10–50 | 3 | 2 | 26 | 20 | 334 | 4.9 | 1.94 | 0.42 | 5.4 | 0.060 | 2 |
| | Low 3 | 0–10 | 15 | 12 | | 43 | 612 | 11.4 | 4.06 | 1.2 | 6.1 | 0.027 | 0 |
| | | 10–50 | 4 | 1 | | 16 | 523 | 4.3 | 2.37 | 0.4 | 5.3 | 0.060 | 0.5 |
| | High 1 | 0–10 | 7 | 4 | | 72 | 467 | 28.1 | 3.49 | 1.2 | 6.3 | 0.045 | 3 |
| | High 2 | 0–10 | 7 | 6 | | 43 | 420 | 7.3 | 3.13 | 1.0 | 5.2 | 0.059 | 5 |
| | | 10–50 | 3 | 4 | 37.7 | 7 | 325 | 8.2 | 1.11 | 0.96 | 6.4 | 0.064 | 12 |
| | High 3 | 0–10 | 16 | 4 | | 32 | 468 | 5.6 | 3.26 | 0.76 | 5.2 | 0.055 | 4 |
| | | 10–50 | 4 | 4 | 46.8 | 14 | 324 | 4.1 | 1.91 | 0.58 | 4.8 | 0.443 | 10 |

**APPENDIX 12:** YIELD MAPS FOR "MILROY" PADDOCK M45 (A) 2007, (B) 2008 AND (C) 2010.

(a)

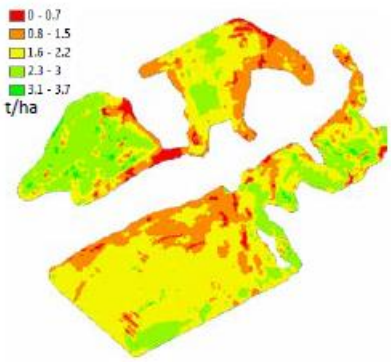


(b)

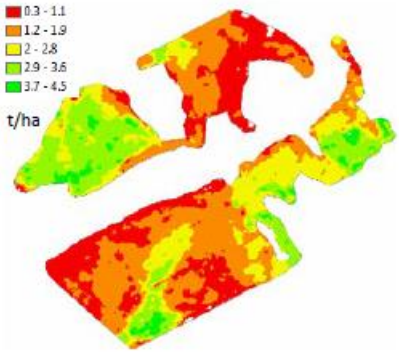


(c)

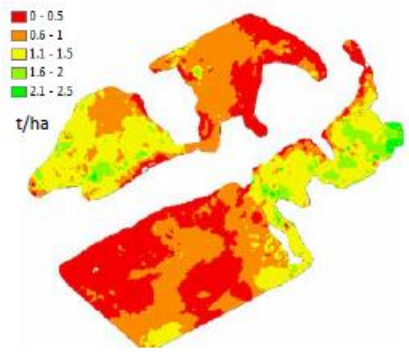

**APPENDIX 13:** YIELD MAPS FOR "GRANDVIEW" GV3 (A) 2005, (B) 2007, (C) 2009, (D) 2010 AND GV4 (E) 2007, (F) 2009 AND (G) 2010.

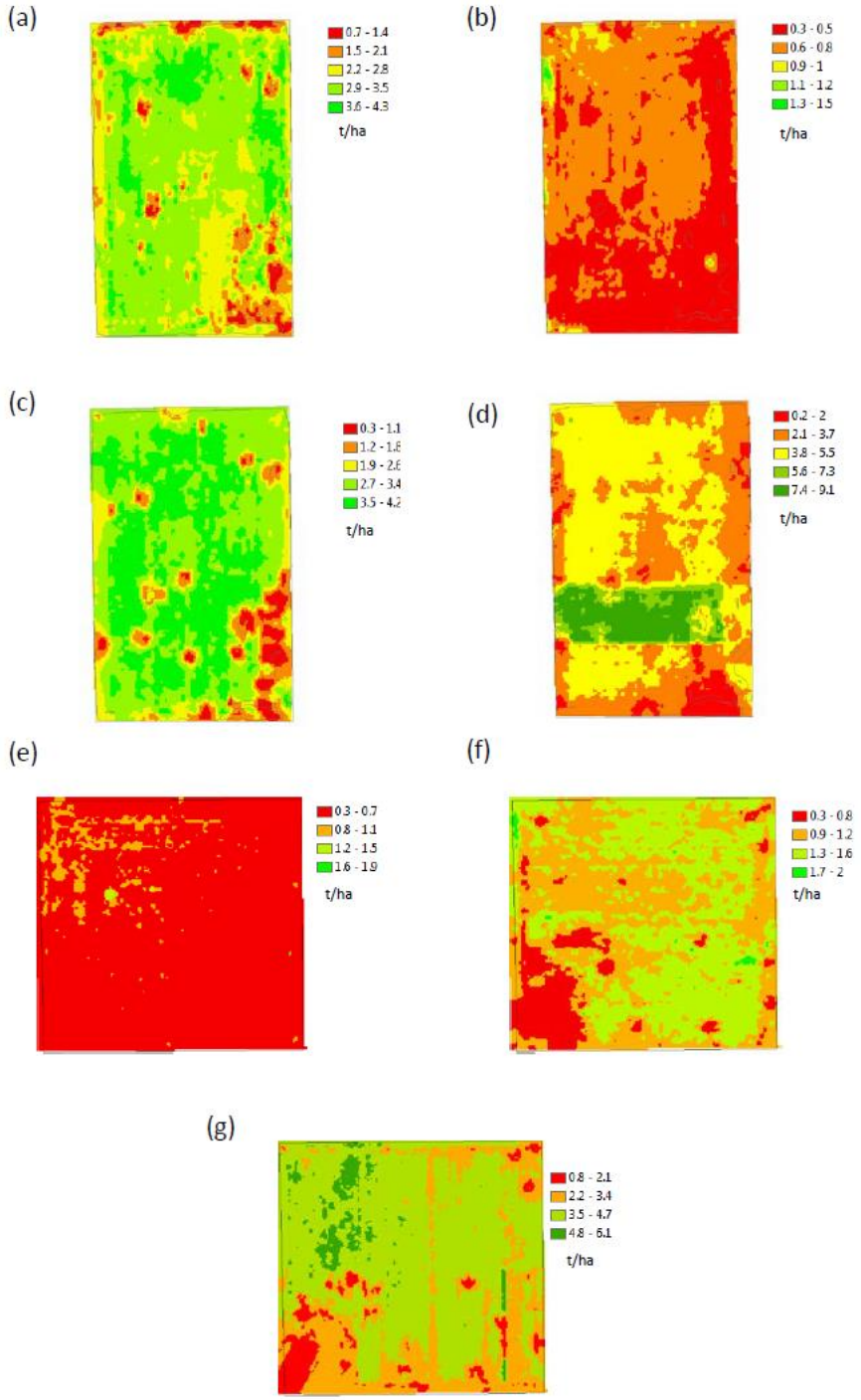

**APPENDIX 14:** MAPS OF NDVI SCANS FOR "MILROY" PADDOCK M45 IN (A) JULY 2012, (B) AUGUST (2012) AND (C) SEPTEMBER 2012.

(a)

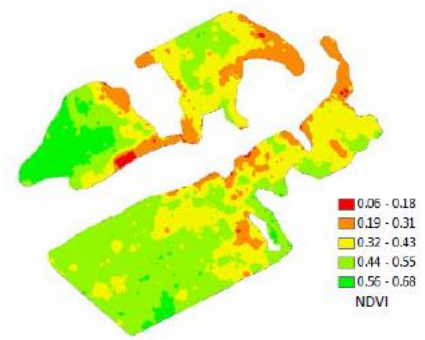


(b)

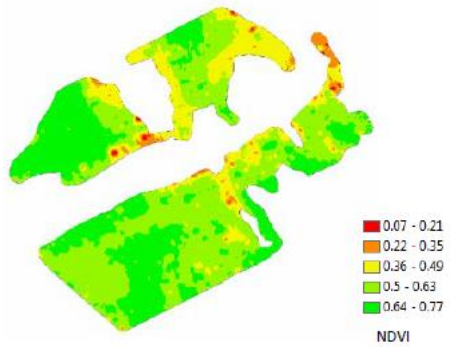


(c)

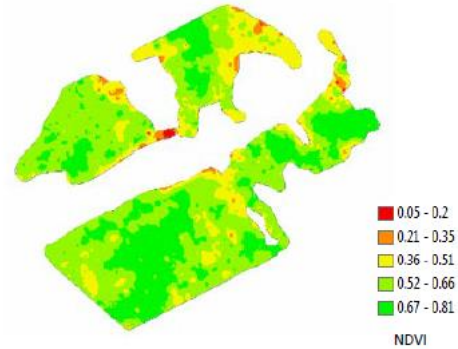

**APPENDIX 15:** R SCRIPT FOR LEAVE ONE OUT CROSS VALIDATION.

```
##LEAVE ONE OUT CROSS VALIDATION of EXPONENTIAL DATA#####
library(boot)
data <- read.delim("C:/R/Biomass_LOOCV/Pete_WA.txt")
attach(data,pos = 2)
head(data)
trick.glm <- glm(Green.kg.ha~NDVI, family = gaussian(link = 'identity'))
coeff.ests<-log(trick.glm$coefficients)
print(coeff.ests)
####MUST SET START LIST TO COEFFICIENTS PRINTED, NaN = 0######
dez.glm <- glm(Green.kg.ha~NDVI, family = gaussian(link = 'log'), start = c(0,12))
plot(Green.kg.ha~NDVI, pch = 16)
pred.seq <- data.frame('NDVI' = sort(NDVI))
preds.glm <- predict(dez.glm,pred.seq,type = 'response')
lines(y = preds.glm, x = pred.seq$NDVI, lty = 2, col = 'red')
#### TOTAL ERROR OF FIT!!! ####
pred.fit <- fitted.values(dez.glm)
RMSE <- (mean((pred.fit-NDVI)^2))^0.5
print(RMSE)
#### LOOCV ERROR BAR ####
dez.cv <- cv.glm(data,dez.glm, K = length(data))
cv.RMSE.raw.error <- dez.cv$delta[1]^0.5
cv.RMSE.adj.error <- dez.cv$delta[2]^0.5
print(cv.RMSE.raw.error)
print(cv.RMSE.adj.error)
detach(data,pos = 2)
```

**APPENDIX 16:** REGRESSION OF CROP CIRCLE NORMALISED DIFFERENCE VEGETATION INDEX (NDVI) VALUES AGAINST TOTAL GREEN DRY MATTER (TGDM) FOR (A) "MILROY" M45 IN 2012, (B) "GRANDVIEW" GV3 IN 2012 AND GV4 IN 2012.

(a)

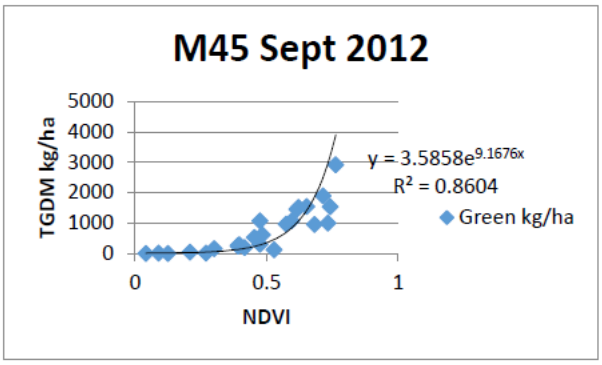


(b)

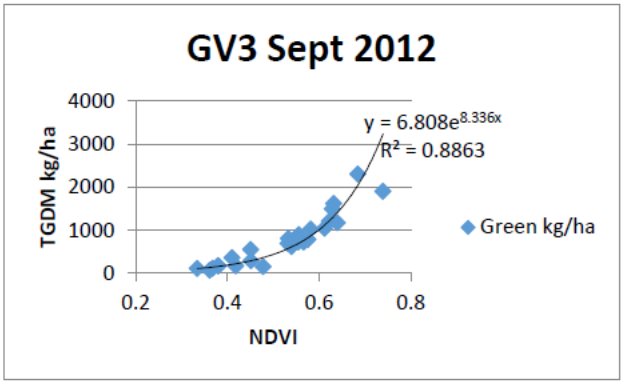


(c)

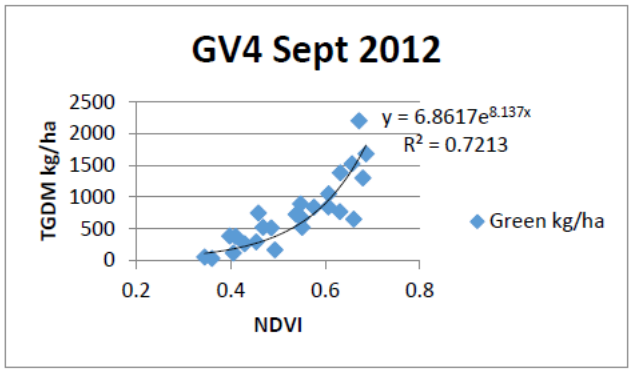

**APPENDIX 17:** MAPS OF NDVI SCANS FOR "GRANDVIEW" PADDOCKS GV3 IN (A) AUGUST 2012, (B) SEPTEMBER (2012), GV4 IN (C) AUGUST 2012, (B) SEPTEMBER (2012), GV8 IN AUGUST 2012 AND GV39 IN AUGUST 2012.

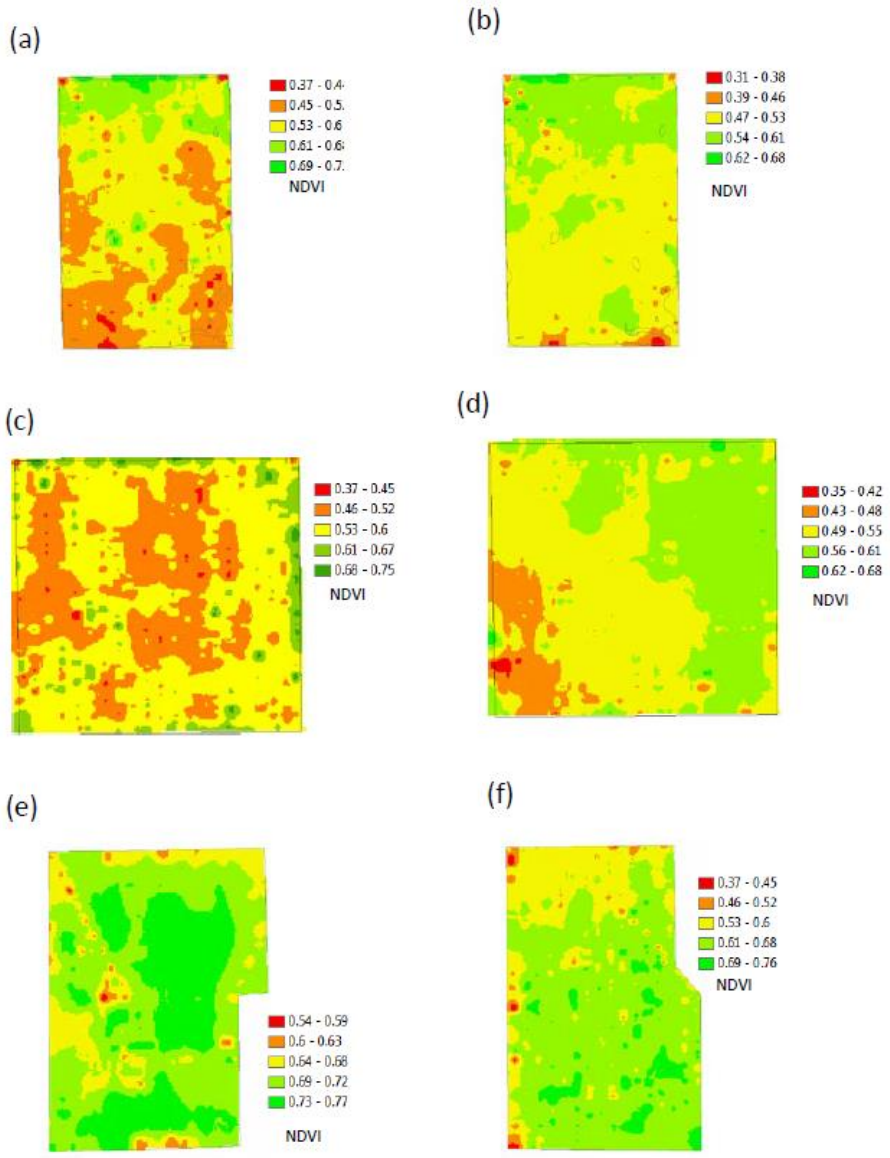

**APPENDIX 18:** MAPS OF TGDM FOR "MILROY" PADDOCK M45 IN SEPTEMBER 2012 (A) AND "GRANDVIEW" PADDOCK GV3 IN SEPTEMBER 2012 (B) AND GV4 IN SEPTEMBER 2012 (C).

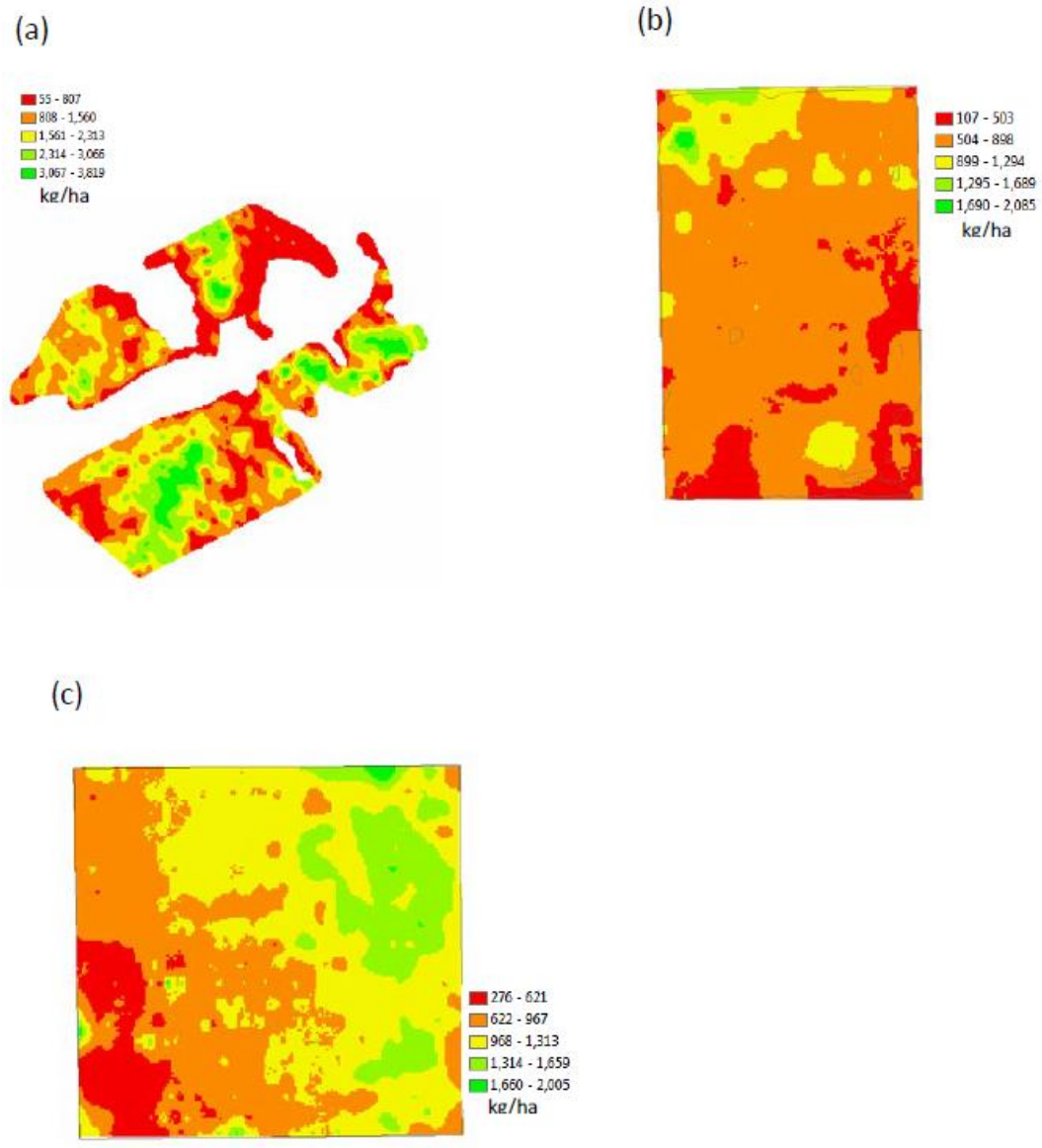

**APPENDIX 19:** R SCRIPT FOR ANOVA AND KRUSKAL–WALLIS ANALYSIS.

```
 N <- sum(grp.sizes <- table(groups))
 S.2 <- 1/(N–1) * (sum(rank(y)^2)–N/4 * (N + 1)^2)
 R <- tapply(rank(y), groups, sum)
 K <- 1/S.2 * (sum(R^2/grp.sizes)–N/4 * (N + 1)^2)
 ret.val <- list(statistic = K, parameters = length(grp.sizes)–1,
              alternative = "two.sided", method =
               "Kruskal–Wallis rank sum test", data.name =
paste(deparse(substitute(y)), " and ", deparse(substitute(groups)), sep =""))
 ret.val$p.value <- 1–pchisq(ret.val$statistic, ret.val$parameters)
 names(ret.val$statistic) <- "Kruskal–Wallis chi-square"
 names(ret.val$parameters) <- "df"
 ret.val <- ret.val[c("statistic", "parameters", "p.value","alternative", "method",
"data.name")]
 number.of.observations <- table(groups)
 grps <- length(grp.sizes)
 group.medians <- round(tapply(y, groups, median,na.rm=T), 3)
 names(group.medians) <- names(table(groups))
 if(ret.val$p.value < alpha) {
   Mult <- qt(1–alpha/2, N–grps) * sqrt((S.2 *
                                  (N–1–K))/(N–grps))
   LHS <- abs(rep((R/grp.sizes), rep(grps, grps))–rep((R/
                                        grp.sizes), grps))
   RHS <- Mult * sqrt(rep((1/grp.sizes), rep(grps, grps))
                + rep((1/grp.sizes), grps))
   pairwise.comparisons <- matrix(LHS > RHS, nrow = grps,
                           dimnames = list(names(table(groups)),
                                    names(table(groups))))
 }
 attr(ret.val, "class") <- "htest"
  if(ret.val$p.value >= alpha)
 {
   pairwise.comparisons<-"NIL. Kruskall-Wallis Test not significant"
 }
 pairwise.significance.comparisons<-pairwise.comparisons
 names(number.of.observations)<-levels(factor(groups))
 return(list(number.of.observations=number.of.observations,
group.medians=group.medians, ret.val=ret.val,
pairwise.significance.comparisons=pairwise.significance.comparisons))
}
```

**APPENDIX 20:** "MILROY" M25 SOIL TEST RESULTS OVER STABILITY ZONES: COLWELL K (A)CROP, (B) PASTURE, COLWELL P (C) CROP, (D) PASTURE, EC (E) CROP, (F) PASTURE, PH CROP (G), PASTURE (H), PBI (I) CROP, (J) PASTURE AND TOTAL N (K) CROP AND (L) PASTURE.

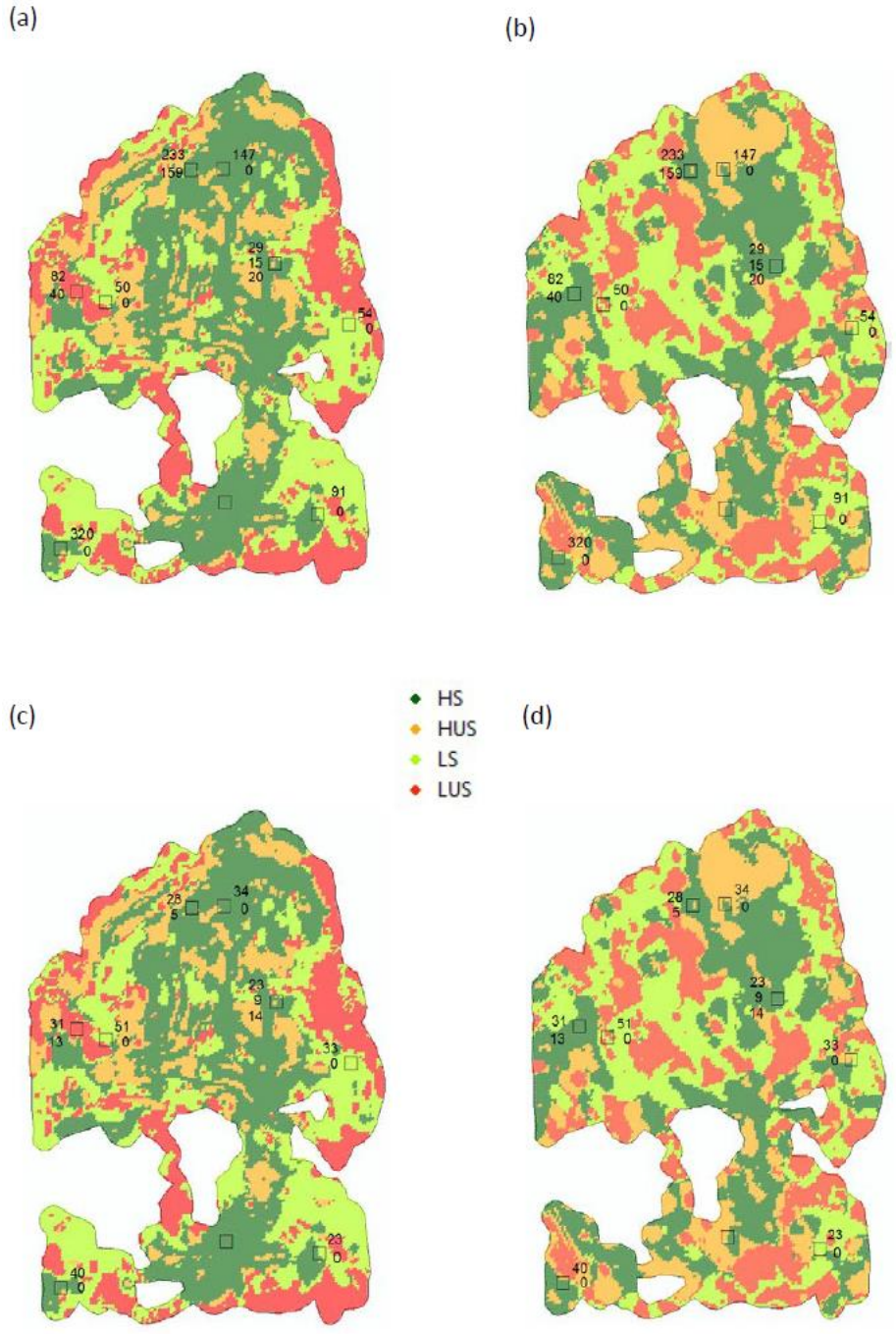

(e)

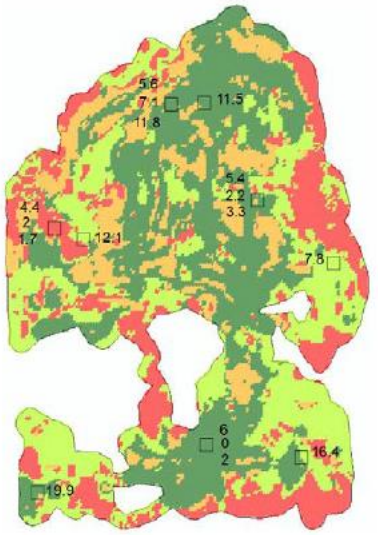


(f)

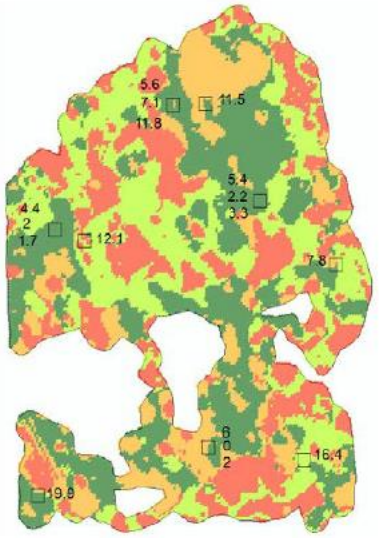


- HS
- HUS
- LS
- LUS

(g)

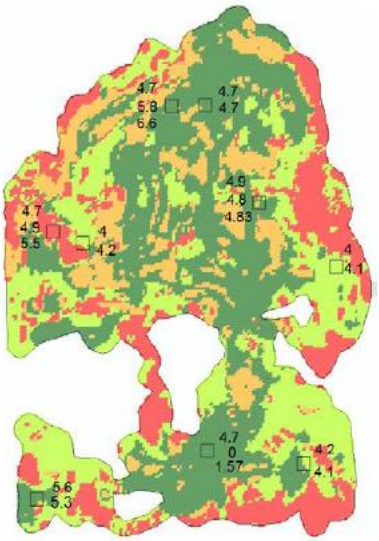


(h)

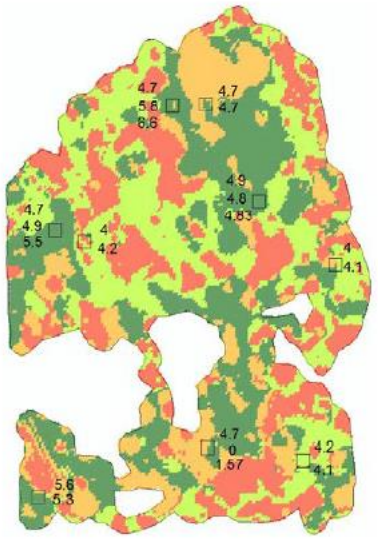

(i)

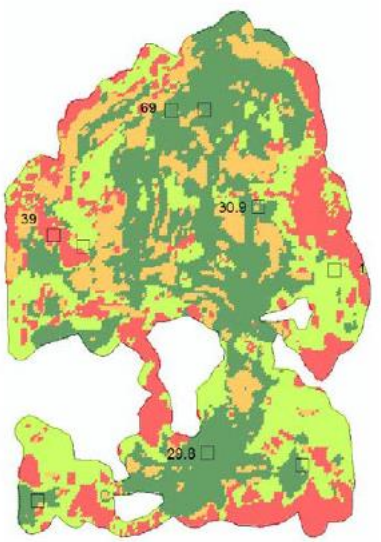


(j)

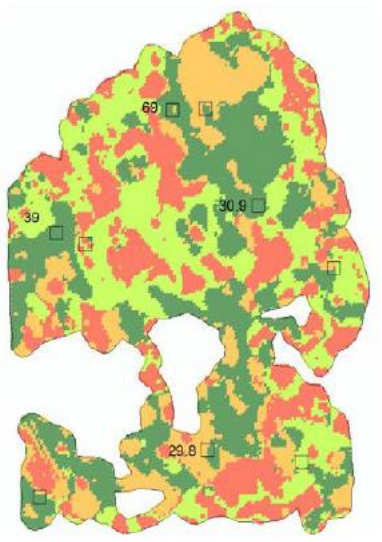


HS
HUS
LS
LUS

(k)

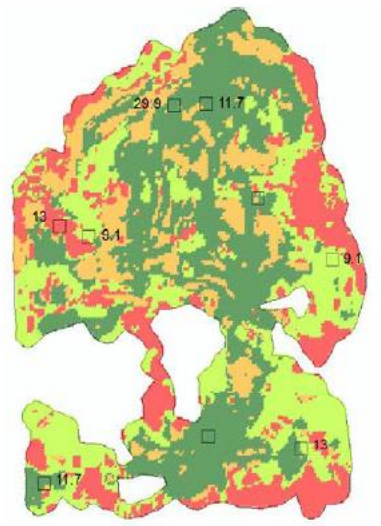


(l)

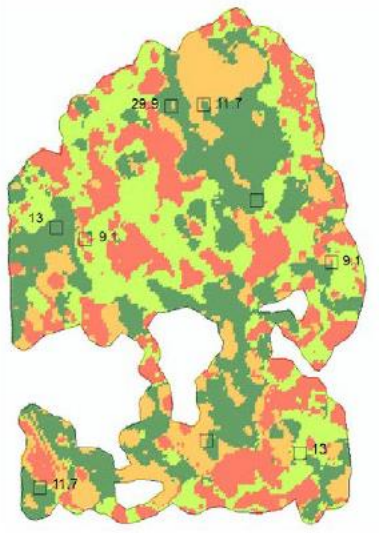

**APPENDIX 21:** "MILROY" M25 SOIL TEST RESULTS OVER STABILITY ZONES: COLWELL K (A)CROP, (B) PASTURE, COLWELL P (C) CROP, (D) PASTURE, EC (E) CROP, (F) PASTURE, PH CROP (G), PASTURE (H), PBI (I) CROP, (J) PASTURE AND TOTAL N (K) CROP AND (L) PASTURE.

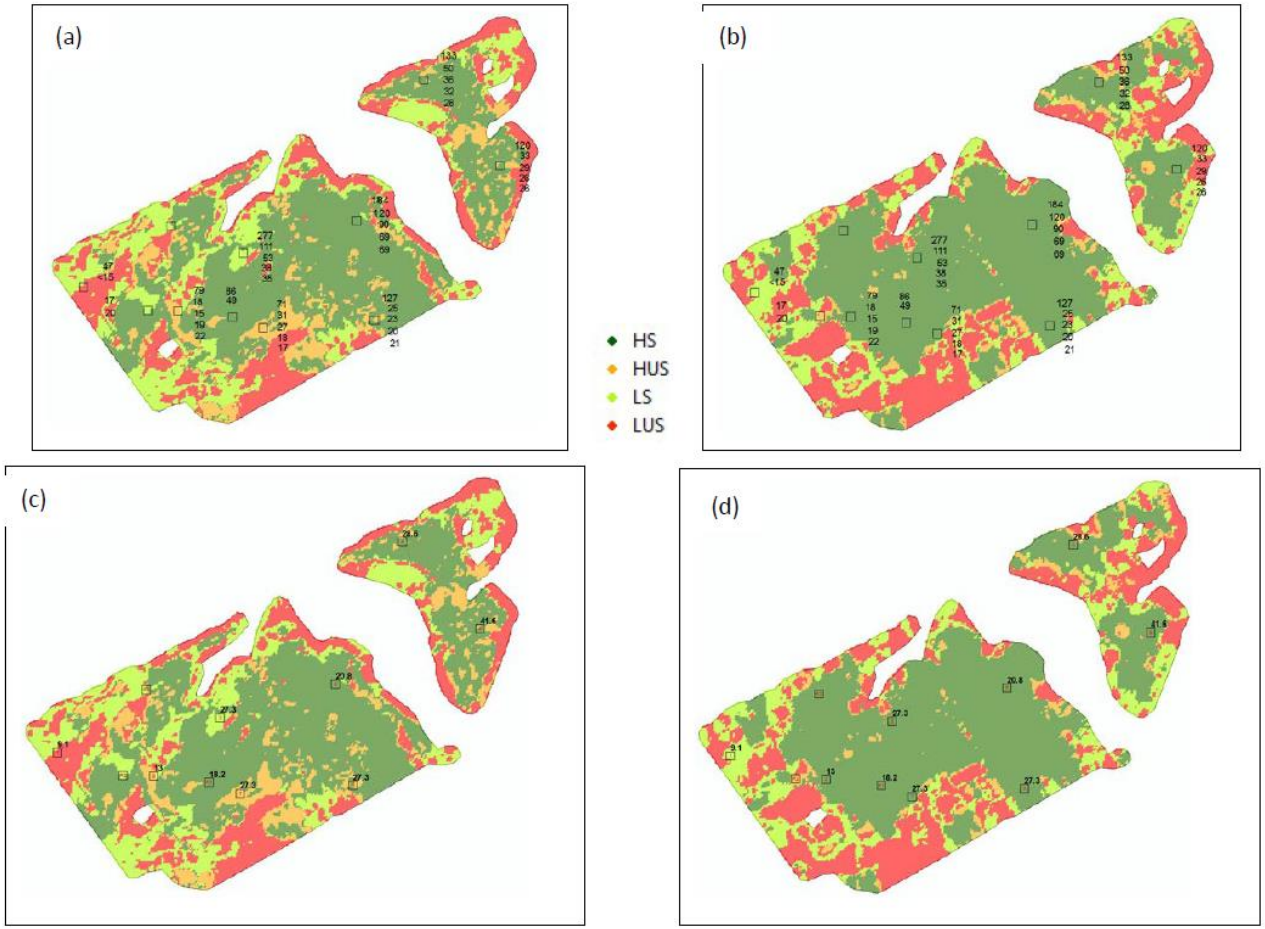

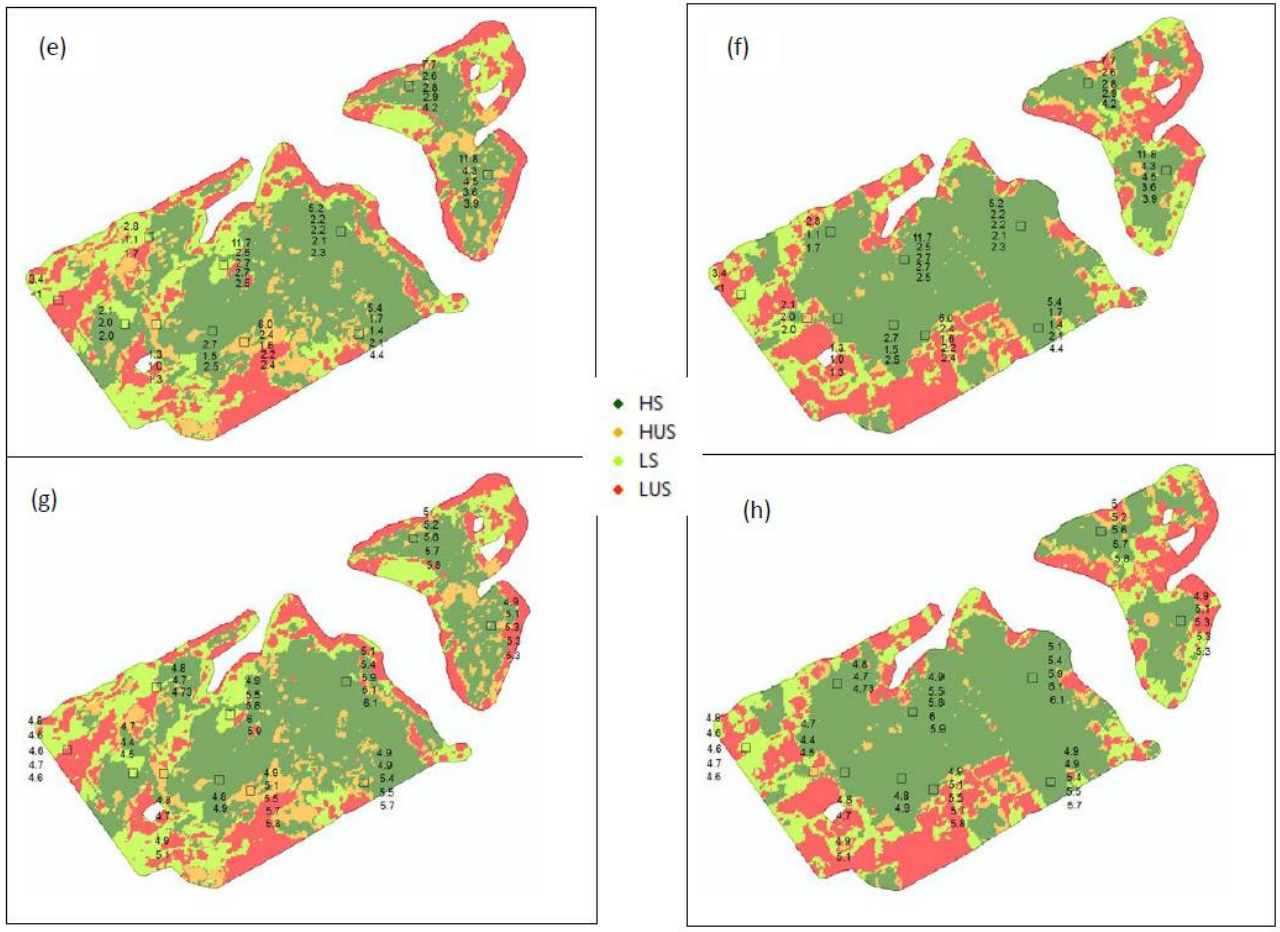
(e)
(f)
(g)
(h)
HS
HUS
LS
LUS


(i)
(j)
HS
HUS
LS
LUS

**APPENDIX 22:** "GRANDVIEW" GV8 SOIL TEST RESULTS OVER STABILITY ZONES: COLWELL P (A)CROP, (B) PASTURE, TOTAL N (C) CROP, (D) PASTURE, ESP (E) CROP, (F) PASTURE, AND S CROP (G), PASTURE (H).

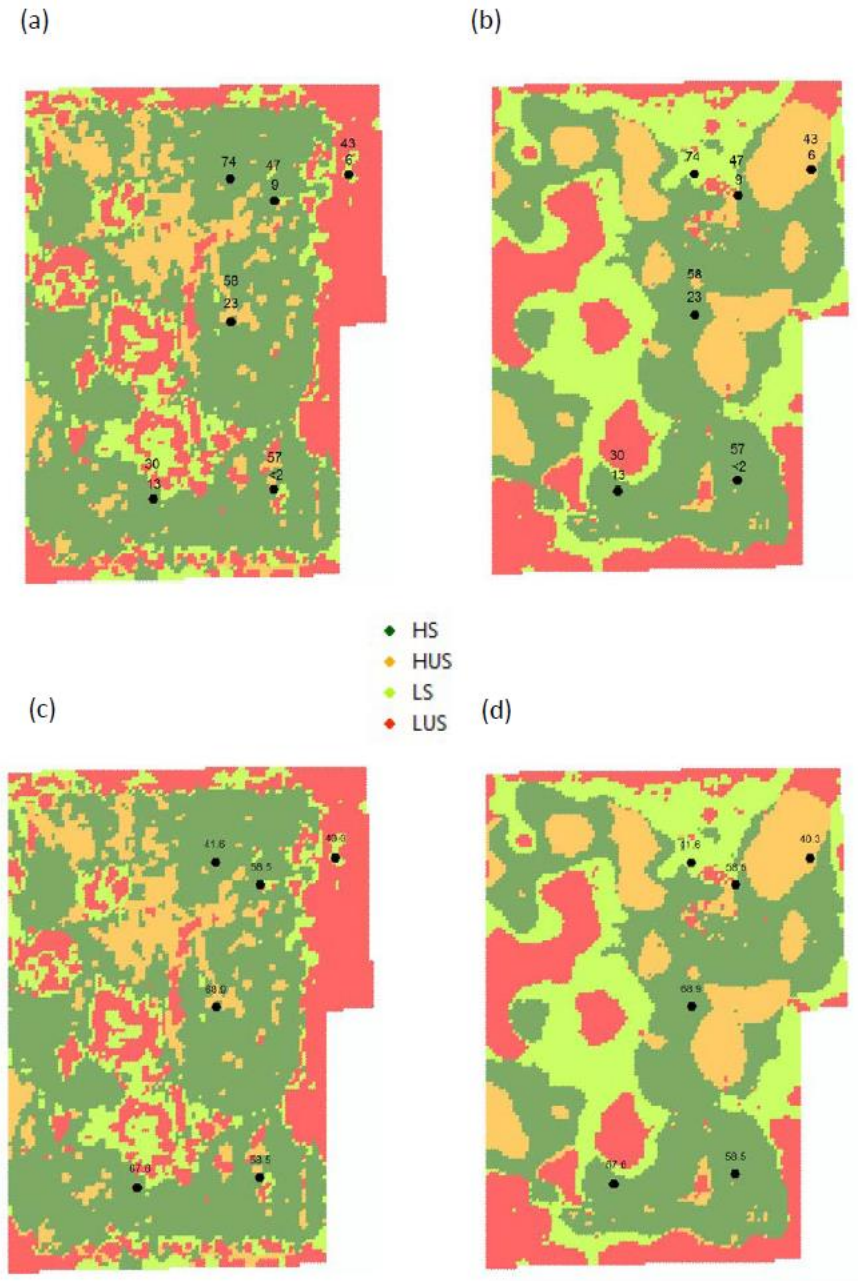

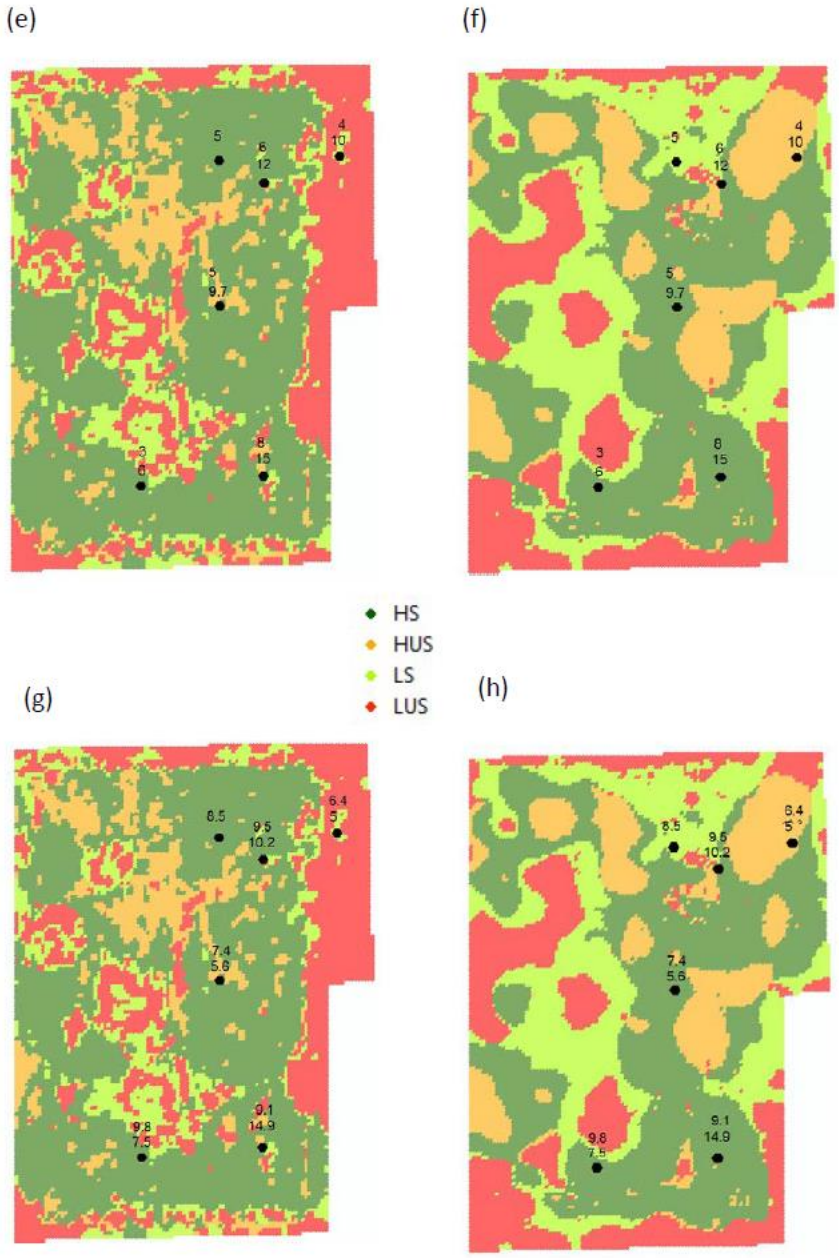
(e)
(f)
HS
HUS
LS
LUS
(g)
(h)

**APPENDIX 23:** "GRANDVIEW" GV39 SOIL TEST RESULTS OVER STABILITY ZONES: COLWELL P (A)CROP, (B) PASTURE, TOTAL N (C) CROP, (D) PASTURE, ESP (E) CROP, (F) PASTURE, AND S CROP (G), PASTURE (H).

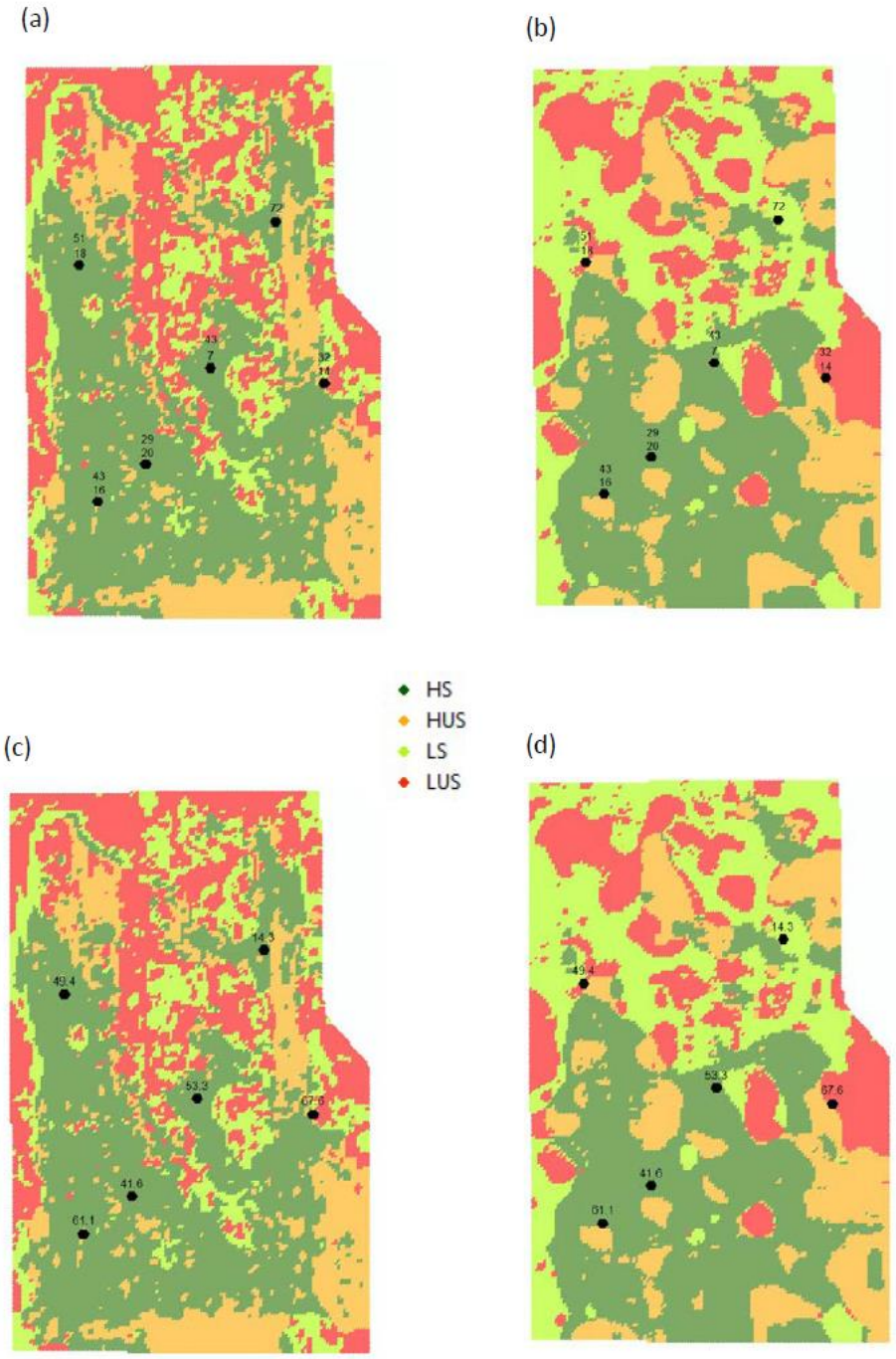

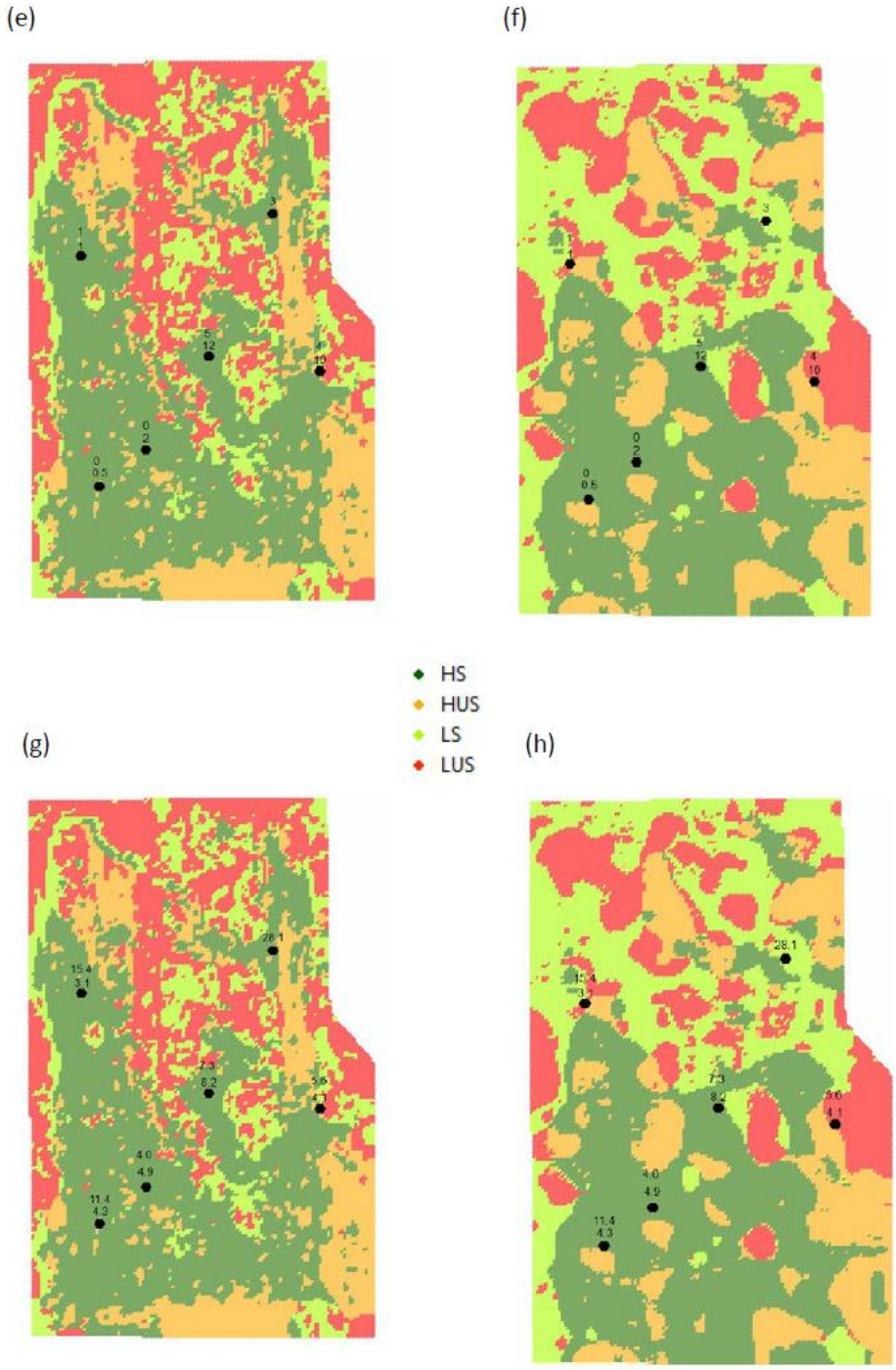
(e)
(f)
HS
HUS
LS
LUS
(g)
(h)